TRANSCRIPTIONAL REGULATION OF STEM CELL SELF-RENEWAL

by

Shenghui He

A dissertation submitted in partial fulfillment
of the requirements for the degree of
Doctor of Philosophy
(Cellular and Molecular Biology)
in The University of Michigan
2010

Doctoral Committee:

Professor Sean J. Morrison, Chair
Professor Andrzej A. Dlugosz
Professor Deborah L. Gumucio
Associate Professor Thomas M. Glaser

ACKNOWLEDGEMENTS

I wish to most sincerely thank my mentor Sean Morrison, for his intellectual and financial support throughout my graduate training. His passion for the hunt for new knowledge and his dedication to rigorously answering every scientific question in the finest detail will be a great source of inspiration throughout my scientific career.

I wish to thank Anna Molofsky and Ricardo Pardal for training me to study central and peripheral nervous system neural stem cells. They initiated the project on the function of *Bmi-1* in regulating neural stem cell self-renewal and contributed to the majority of the work described in Chapter 2 of this dissertation.

I wish to thank Mark Kiel for his support and friendship. He has taught me all the skills to study mouse hematopoietic stem cells (HSCs), and has been the driving force leading the project testing immortal strand segregation and label retention in HSCs (described in Chapter 5).

I wish to thank Daisuke Nakada, Jack Mosher, Melih Acar, Jeff Megee, Injune Kim and Lei Ding for their technical assistance and intellectual contribution to my work at various stages of my training. I also wish to thank all former and current members of the Morrison lab for their support and friendship, which made the pursuit of my degree an enjoyable experience.

I wish to thank my program director Jessica Schwartz and administrator Cathy Mitchell for their support during my entire graduate training, and for ensuring that I would graduate on time.

I wish to thank the members of my thesis committee, Andrzej Dlugosz, Deborah Gumucio and Thomas Glaser for their support and guidance during the pursuit of my degree.

I wish to thank the Rackham School of Graduate Studies for providing the financial support for my first year of graduate training, and for providing travel grants allowing me the opportunity for scientific travel to Vancouver and Toronto.

Lastly, I wish to thank my parents and my wife Jing Xu, without whose support none of the work described here would be possible.

The work described in this dissertation was supported by grants from the Howard Hughes Medical Institute and the National Institutes of Health.

PREFACE

The work described in this thesis comprises most of the work I have performed in the Morrison laboratory since January, 2004.

Most of the contents described in Chapter 1 (Introduction) were published in *Annual Reviews of Cell and Developmental Biology. 2009;25:377-406.* Daisuke Nakada and I contributed equally to this work.

Chapter 2 describes the identification of *Ink4a* and *Arf* as the two major downstream target genes mediating the depletion of central and peripheral nervous system (CNS and PNS) stem cells in the absence of *Bmi-1*. Anna Molofsky and Ricardo Pardal initiated this project. Anna collected all the data for the CNS neural stem cells, Ricardo and I collected all the data from the PNS as well as the growth and survival data of *Bmi-1*, *Ink4a*, *Arf* compound mice. This work was published in *Genes and Development. 2005, 19:1432-7*; and a modified version of this chapter was included in Anna Molofsky's thesis as chapter three.

Chapter 3 describes the effects of *Bmi-1* overexpression on CNS stem cell self-renewal and neural development, and was originally published in *Developmental Biology. 2009, 328:257-72*. I conducted most of the experiments described in this chapter. Toshihide Iwashita generated the original *Nestin-Bmi-1-IRES-GFP* transgenic mice. Anna Molofsky performed southern blotting on the transgenic mouse founders and

generated the MSCV-Bmi-1 retrovirus vector. Johanna Buchtaller analyzed Bmi-1 expression in human brain tumor samples with help from Dafydd Thomas.

Chapter 4 demonstrates that *Sox17* overexpression in adult hematopoietic stem and/or progenitor cells is sufficient to confer certain fetal characteristics including enhanced self-renewal potential and fetal specific gene expression. This work has not yet been published. I conducted all the experiments and collected all the data described in this chapter. Injune Kim generated the $Sox17^{GFP}$ knock-in mice that were used in this study. Megan Lim helped with the pathological evaluation of the *Sox17* overexpression induced leukemia.

Chapter 5 demonstrates that adult mouse bone marrow hematopoietic stem cells (HSCs) do not asymmetrically segregate their chromosomes during cell division, and BrdU label retention cannot be used as a reliable marker for identifying HSCs. Mark Kiel initiated this project and collected most of the data. I participated in the design and interpretation of all the experiments testing immortal strand segregation of HSCs, and collected the chromosome segregation data from *in vitro* cultured HSCs. This work was originally published in *Nature. 2007, 449:238-42*, and a modified version of this chapter was included in Mark Kiel's thesis as chapter 5.

In additional work which will not be included in this dissertation, I have performed experiments to optimize the purification of fetal and adult mouse enteric neural crest stem cells, and compared the gene expression profiles of these cells with help from Melih Acar. I have also studied the *in vivo* differentiation of adult mouse enteric neural crest stem cells under both physiological and pathological condition in collaboration with Nancy Joseph and Elsa Quintana.

TABLE OF CONTENTS

LIST OF FIGURES

ABSTRACT

Self-renewal is a defining feature that distinguishes stem cells from transiently amplifying progenitors. Regulation of stem cell self-renewal involves precise control of cell cycle progression, suppression of premature differentiation, as well as maintenance of stem cell genomic integrity.

The polycomb group protein Bmi-1 is essential for the postnatal self-renewal of mouse neural stem cells. We show that the depletion of neural stem cells in the absence of *Bmi-1* is partially due to the derepression of two cell cycle inhibitors, $p16^{Ink4a}$ and $p19^{Arf}$. Deletion of *Ink4a* and *Arf* from *Bmi-1* deficient mice is sufficient to partially rescue the self-renewal defects of neural stem cells, indicating *Bmi-1* regulates adult neural stem cell self-renewal mainly, but not exclusively by repressing the expression of *Ink4a* and *Arf*. Conversely, overexpression of *Bmi-1* is sufficient to enhance the self-renewal potential of CNS neural stem cells *in vitro* by suppressing culture-induced *Ink4a* and *Arf* expression, but has little effect on stem cell number or SVZ proliferation *in vivo*, where *Ink4a* and *Arf* are not normally expressed. Together, our data demonstrate that stem cell self-renewal capacity is modulated by factors affecting their cell cycle progression.

The Sry-related HMG box transcription factor *Sox17* is specifically expressed by fetal, but not adult, hematopoietic stem cells (HSCs), and is essential for their maintenance. We demonstrate that Sox17 overexpression is sufficient to confer adult

hematopoietic progenitors with certain fetal characteristics, and bias adult hematopoiesis to resemble fetal hematopoiesis. This is achieved at least partially by upregulating fetal HSC-specific gene expression, and suppressing differentiation-associated genes, raising the possibility that Sox17 may maintain fetal HSC identity by repressing differentiation or lineage commitment.

The immortal strand hypothesis has been proposed as a mechanism to protect the genomic integrity of stem cells by asymmetrically segregating old and newly synthesized chromosomes during cell division. Using HSCs as a model system, we demonstrate that asymmetric chromosome segregation does not occur at a significant frequency in HSCs *in vivo* or in culture. Therefore "immortal strand" segregation cannot be a universal mechanism protecting stem cells from accumulating genetic mutations.

CHAPTER 1

MECHANISM OF STEM CELL SELF-RENEWAL[1]

SUMMARY

Self-renewal is the process by which stem cells divide to make more stem cells, perpetuating the stem cell pool throughout life. Self-renewal is division with maintenance of the undifferentiated state. This requires cell cycle control and maintenance of multipotency or pluripotency, depending on the stem cell. Self-renewal programs involve networks that balance proto-oncogenes (promoting self-renewal), gate-keeping tumor suppressors (limiting self-renewal) and care-taking tumor suppressors (maintaining genomic integrity). These cell-intrinsic mechanisms are regulated by cell-extrinsic signals from the niche, the microenvironment that maintains stem cells and regulates their function in tissues. In response to changing tissue demands stem cells undergo changes in cell cycle status and developmental potential over time, requiring different self-renewal programs at different stages of life. Reduced stem cell function and tissue regenerative capacity during aging are caused by changes in self-renewal programs that augment tumor suppression. Cancer arises from mutations that inappropriately activate self-renewal programs.

[1] Originally published in *Annual Reviews of Cell and Developmental Biology. 2009;25:377-406* with authors listed as ***He, S.**, *Nakada, D. and Morrison, S.J. (*equal contribution)

INTRODUCTION

Self-renewal is the process by which a stem cell divides asymmetrically or symmetrically to generate one or two daughter stem cells that have a developmental potential similar to the mother cell. The ability to self-renew is essential for stem cells to expand their numbers during development, for their maintenance within adult tissues, and to restore the stem cell pool after injury. Defects in self-renewal mechanisms can lead to developmental defects, premature aging phenotype, and cancer. Thus, the elucidation of stem cell self-renewal mechanisms offers the potential for fundamental insights into development, cancer, and aging.

Studying stem cell self-renewal requires the precise identification of stem cells using anatomical, phenotypic, or functional criteria. Invertebrate stem cells are usually defined by position and marker expression, in accordance to fate mapping experiments that place them at the top of a cell hierarchy. For example, male germline stem cells (GSCs) in Drosophila are identified based on marker expression as well as based on their position surrounding hub cells, which constitute the niche (Fuller and Spradling, 2007). This makes it possible to image the self-renewing divisions of many invertebrate stem cell populations in the niche *in vivo* (Cheng et al., 2008). In contrast, mammalian stem cells are mainly identified based on functional assays or marker expression among dissociated cells because anatomical criteria are often less useful in large and complex mammalian tissues. It has been impossible to image the self-renewing divisions of many mammalian stem cells within the niche. Rather mammalian stem cell self-renewal is generally inferred based on changes in stem cell numbers in functional assays performed *in vitro* or *in vivo*. Nonetheless, important insights have been gained by imaging the

divisions of undifferentiated cells in the skin, nervous system, and muscle (Huttner and Kosodo, 2005; Kuang et al., 2007; Lechler and Fuchs, 2005). As a result of these technical differences among invertebrate and mammalian stem cell systems we often have different types of information regarding the regulation of self-renewal in these systems.

Self-renewal is not the same as proliferation, although both processes depend on cell division. Proliferation is a more general term that incorporates all types of stem and progenitor cell divisions, self-renewing and otherwise. Self-renewal requires that at least one of the daughter cells has a developmental potential that is similar to the mother cell. For most mammalian stem cells, like hematopoietic stem cells and neural stem cells, this means that self-renewal is division with maintenance of multipotency. As a result, molecular mechanisms that regulate stem cell self-renewal include mechanisms that regulate the ability of stem cells to divide while remaining multipotent. For stem cells that make a single type of daughter cell, like spermatogonial stem cells, self-renewal involves mechanisms that regulate the ability of stem cells to divide while remaining undifferentiated. Some of these mechanisms might overlap with mechanisms that generically regulate the proliferation of many cells, though a surprising number of stem cell self-renewal mechanisms preferentially regulate stem cell self-renewal (Molofsky et al., 2003; Nishino et al., 2008).

Self-renewal is not uniquely a property of stem cells. Some types of restricted progenitors and differentiated cells, such as restricted glial progenitors and lymphocytes, can also undergo self-renewing divisions. Indeed, self-renewal mechanisms in lymphocytes share at least some mechanistic similarities to stem cell self-renewal, such

as a common dependence on *Bmi-1* (Luckey et al., 2006; van der Lugt et al., 1994a). Nonetheless, the extensive self-renewal potential of stem cells can generally be quantitatively distinguished from the limited self-renewal potential of restricted progenitors. The mechanistic differences that distinguish stem cell self-renewal from the more limited self-renewal of restricted progenitors and differentiated cells largely remain to be identified.

Although stem cells have extensive self-renewal potential, this does not necessarily mean that these cells actually self-renew extensively under physiological conditions. For example, individual hematopoietic stem cells have the potential to undergo extensive self-renewing divisions upon serial transplantation in irradiated mice (Harrison and Astle, 1982); however, under physiological conditions *in vivo*, most hematopoietic stem cells are quiescent most of the time and may undergo a limited number of self-renewing divisions in normal adult mouse (Cheshier et al., 1999b; Foudi et al., 2008; Wilson et al., 2008). Neural crest stem cells likely undergo a limited number of self-renewing divisions *in vivo* before differentiating (Fraser et al., 1991; Morrison et al., 1999), despite having the potential for massive self-renewal upon serial subcloning in culture (Kruger et al., 2002). Thus stem cells may be fated *in vivo* to execute many fewer divisions than they have the potential to undergo. This may have evolved to endow stem cells with the potential to repair tissues after injuries that involve much higher regenerative demands than are encountered under normal physiological conditions.

THE REGULATION OF PLURIPOTENT STEM CELL SELF-RENEWAL

Embryonic stem (ES) cells are derived from the inner cell mass of the blastocyst prior to implantation. They possess indefinite self-renewal potential as well as the ability to generate all cell types within the body (pluripotency). These characteristics distinguish ES cells from somatic stem cells, which have extensive, though limited, self-renewal potential and more limited developmental potentials. The unlimited self-renewal potential and pluripotency of ES cells appear to be conferred by unique transcriptional and cell cycle regulation (Jaenisch and Young, 2008; Niwa, 2007; Silva and Smith, 2008) (Figure 1.1).

Maintenance of ES cell pluripotency

The self-renewal of pluripotent stem cells is regulated by a transcriptional network involving *Oct4*, *Sox2* and *Nanog* (Jaenisch and Young, 2008). The POU domain transcription factor *Oct4* is critical for the pluripotency of both the inner cell mass *in vivo* and ES cells in culture (Nichols et al., 1998; Niwa et al., 2000). Reducing *Oct4* expression in ES cells leads them to differentiate into trophectoderm, while overexpression leads to differentiation into primitive endoderm and mesoderm, indicating ES cell pluripotency depends upon an optimal level of *Oct4* expression (Niwa et al., 2000). The SRY-related HMG-box transcription factor *Sox2* is also required for the maintenance of pluripotency in the embryo and in ES cells in culture (Avilion et al., 2003; Masui et al., 2007). *Sox2* cooperates with Oct4 to activate the expression of a number of genes that regulate pluripotency, including *Oct4* and *Nanog* ((Masui et al., 2007) and references therein). The homeodomain protein Nanog is required for the maintenance of pluripotency in the inner cell mass *in vivo* (Mitsui et al., 2003).

Overexpression of *Nanog* can bypass the requirement of leukemia inhibitory factor (LIF) in maintaining ES cell pluripotency, while *Nanog*-deficient ES cells are prone to spontaneous differentiation (Chambers et al., 2003; Mitsui et al., 2003). However, rather than being absolutely required for pluripotency, *Nanog* appears to stabilize the pluripotent state (Chambers et al., 2007). These three factors form the core of a transcriptional regulatory network that promotes the expression of genes that maintain pluripotency while repressing genes that induce differentiation (Fujikura et al., 2002; Niwa et al., 2005).

Ectopic expression of *Oct4* together with various combinations of other transcription factors including *Sox2* and *Nanog* can reprogram differentiated mouse and human cells into ES-like induced pluripotent stem (iPS) cells (Okita et al., 2007; Park et al., 2008; Takahashi et al., 2007; Takahashi and Yamanaka, 2006; Wernig et al., 2007; Yu et al., 2007). This demonstrates that these factors can restore pluripotency to cells that are epigenetically quite different from ES cells.

To maintain the pluripotency of ES cells, the *Oct4*-*Sox2*-*Nanog* network needs to be fine-tuned by positive and negative regulation, as slight hyper- or hypo-activation of some of these factors can disrupt pluripotency (Niwa et al., 2000). These three transcription factors interact physically with each other, and co-occupy regulatory regions in many target genes coordinately regulating the pluripotent state (Boyer et al., 2005; Loh et al., 2006; Masui et al., 2007; Wang et al., 2006). *Oct4*, *Sox2*, and *Nanog* also regulate their own expression as well as each other's expression, forming a positive feedback circuit that maintains pluripotency (Figure 1.1). Since overexpression of *Oct4* leads to

trophectodermal differentiation of ES cells, this circuit also requires negative feedback (reviewed by (Niwa, 2007)).

Maintenance of ES cell pluripotency is aided by epigenetic regulators that balance gene repression and activation. Polycomb and Trithorax proteins modulate the expression of numerous developmental genes through histone modification and chromatin remodeling (Schuettengruber et al., 2007). Polycomb complexes trimethylate histone H3 at lysine 27 (H3K27) and then assemble complexes that promote chromatin compaction on this methylation mark. Trithorax proteins oppose polycomb repression by methylating histone H3 at lysine 4 (H3K4), promoting transcription by recruiting nucleosome remodeling enzymes and histone acetylases (Ruthenburg et al., 2007). Polycomb and trithorax complexes segregate the pluripotent genome into stably repressed domains marked by H3K27 methylation as well as activated domains marked by H3K4 methylation (Mikkelsen et al., 2007). However, polycomb and trithorax complexes also coincide at "bivalent domains" within genes in ES cells that bear regions containing both marks (Bernstein et al., 2006; Zhao et al., 2007). It appears that such domains repress the expression of genes involved in fate determination and differentiation, while poising such genes for activation upon exit from the pluripotent state (Azuara et al., 2006; Bernstein et al., 2006; Boyer et al., 2006; Lee et al., 2006b). Loss of certain polycomb complex components from ES cells leads to the inappropriate activation of some of these developmental regulators, rendering ES cells prone to spontaneous differentiation (Azuara et al., 2006; Boyer et al., 2006; Lee et al., 2006b; Marson et al., 2008).

There are also other critical transcription factors beyond *Oct4*, *Nanog* and *Sox2*. The zinc finger DNA-binding protein Ronin is necessary and sufficient for maintaining

ES cell pluripotency (Dejosez et al., 2008). Overexpression of Ronin maintains ES cell pluripotency in the absence of LIF or *Oct4* (Dejosez et al., 2008). Ronin suppresses ES cell differentiation by directly binding and suppressing the transcription of many differentiation-inducing genes, including *GATA4* and *GATA6*. Upon induction of differentiation, Ronin (Dejosez et al., 2008) and Nanog (Fujita et al., 2008) are inactivated by Caspase-3 proteolysis to allow differentiation. The requirement for Ronin emphasizes the critical role that factors that block differentiation play in the promoting self-renewal.

Like other stem cells, ES cell self-renewal is also under cell-extrinsic controls (Figure 1.1). LIF is a key factor that blocks the differentiation of mouse ES cells in culture (Williams et al., 1988). LIF receptor consists of a heterodimer of LIFR and gp130 which activates the JAK/Stat3 pathway (Niwa et al., 1998). The targets of JAK/Stat3 pathway are largely unknown but have been suggested to include c-myc, a known promoter of pluripotency (Cartwright et al., 2005; Takahashi and Yamanaka, 2006). Maintaining the pluripotency of ES cells also requires Bone Morphogenetic Proteins (BMPs) that signal through SMAD proteins to promote the expression of Inhibitor of differentiation (Id) transcriptional regulators, helix-loop-helix domain proteins that dimerize with and inhibit the function of other helix-loop-helix transcription factors (Ying et al., 2003). LIF/JAK/Stat3 and BMP/Id signaling pathways work together to prevent the differentiation of ES cells in culture by inhibiting the consequences of mitogen-activated protein kinase (MAPK) pathway signaling, which tends to promote differentation (Ying et al., 2008). These studies demonstrate that the inhibition of differentiation is a key mechanism to promote self-renewal. Regulatory networks act in a

concerted manner in pluripotent stem cells to do this at the level of signal transduction, chromatin structure, and transcriptional regulation

Cell Cycle Regulation in ES Cells

ES cell self-renewal is facilitated by rapid proliferation and unique cell cycle kinetics. Mouse ES cells have a very short G1 phase of the cell cycle, marked by little or no hypophosphorylated Rb (Burdon et al., 2002; Stead et al., 2002). The lack of Rb activity renders the cells insensitive to cyclin D/cyclin-dependent kinase (CDK) regulation and to the cyclin-dependent kinase inhibitor, $p16^{Ink4a}$ (Burdon et al., 2002; Savatier et al., 1996). Unlike tissue stem cells, ES cells also do not undergo p53-dependent cell cycle arrest in response to DNA damage (Aladjem et al., 1998). ES cells have high levels of constitutively active CDK2-cyclin A/cyclin E, allowing rapid S phase entry (Stead et al., 2002). In contrast, when ES cells differentiate, G1 phase lengthens and the rate of cell division slows (White et al., 2005), mitogen-induced cyclin D-CDK4/6 activity becomes required for progression through G1 phase of the cell cycle and cyclin E-CDK2 activity becomes cell cycle regulated (Savatier et al., 1996). As a result of these differences, ES cells are not subject to many of the cell cycle checkpoints that regulate tissue stem cells. Reprogramming of somatic cells to pluripotency confers similar cell cycle regulation as in mouse ES cells (Jaenisch and Young, 2008), suggesting that the pluripotent state is tightly linked to the rapid and relatively unregulated cell cycle.

CELL INTRINSIC REGULATION OF TISSUE STEM CELL SELF-RENEWAL

In contrast to ES cells, tissue-specific stem cells possess extensive, but limited, self-renewal potential and they are multipotent rather than pluripotent. The emergence of tissue specific stem cells within the embryo marks the requirement for a new set of tissue-specific self-renewal programs that allow more elaborate cell cycle control. In many cases, these programs must perpetuate stem cells throughout life, responding to developmental changes in the regenerative requirements of tissues, while avoiding transformation to cancer. These programs must maintain multipotency while restricting developmental potential to avoid fates that are inappropriate to the tissue of origin. These are different problems than ES cells must confront and require self-renewal mechanisms that are not active in ES cells.

Cell cycle regulation of tissue specific stem cells

To self-renew throughout life, tissue stem cells need mechanisms that confer the potential for repeated periods of quiescence and cell cycle re-entry. This distinguishes tissue stem cells from ES cells and most other types of progenitors. To control this potential, tissue stem cells are subject to more complex cell cycle regulation, more checkpoints, and perhaps more cell extrinsic control than ES cells. Mechanisms regulating the transition from quiescence to G1 to S phase are necessary for long-term stem cell maintenance as well as homeostasis in many tissues.

Ink4-CDK4/6-Rb pathway

Rb family proteins are major regulators of the G1-S cell cycle transition (Figure 1.2). Rb family proteins Rb, p107, and p130 inhibit E2F transcription factors, which induce genes required for DNA replication and S-phase entry (reviewed by (Giacinti and

Giordano, 2006)). Rb appears to be relatively inactive in ES cells, rendering them less dependent upon mitogens to stimulate cell cycle entry via cyclin D-CDK4/6 complex activation (reviewed by (Burdon et al., 2002)). However, as embryogenesis progresses, tissue-specific stem cells become dependent upon mitogens that activate cyclin D-CDK4/6 so that Rb can be inactivated (reviewed by (Sherr and Roberts, 2004)). Rb family proteins redundantly promote quiescence. Deletion of a single *Rb* gene in hematopoietic cells only modestly affects HSC homeostasis (Daria et al., 2008; Walkley and Orkin, 2006; Walkley et al., 2007). However, deletion of all three *Rb* family genes leads to the proliferation and mobilization of HSCs as well as to myeloproliferative disease (Viatour et al., 2008). Additional studies will be required to determine whether HSCs are able to maintain themselves in the complete absence of Rb function.

Cyclin D-CDK4/6 promotes cell cycle entry by phosphorylating and inactivating Rb proteins, and by sequestering $p21^{Cip1}$/$p27^{Kip1}$ cyclin-dependent kinase inhibitors, thereby facilitating the activation of cyclin E-CDK2 (Figure 1.2). Deletion of all three D cyclins is embryonic lethal (likely due to heart defect and and hematopoiesis failure) but not until late gestation (E14.5-E17.5) (Kozar et al., 2004). In the absence of D cyclins, HSCs are unable to divide normally and become depleted (Kozar et al., 2004). Similarly, mice lacking both CDK4 and CDK6 die with defective hematopoiesis, but not until late gestation (Malumbres et al., 2004). These studies demonstrates that cell cycle progression in the early embryo is remarkably independent of D cyclin and CDK4/6 activity, consistent with the relative inactivity of Rb in ES cells, but that tissue stem cells become G1 phase regulated by Rb, cyclins and CDKs. This reversible activation and inactivation

of Rb in response to cell extrinsic signals may be a fundamental difference in cell cycle control between ES cells and tissue stem cells.

The activity of the cyclin D-CDK4/6 complex is regulated by the Ink4 (*In*hibitor of cyclin dependent *k*inase) family proteins. The Ink4 family consists of $p16^{Ink4a}$, $p15^{Ink4b}$, $p18^{Ink4c}$ and $p19^{Ink4d}$ in mice, all of which function by binding and inactivating the cyclin D-CDK4/6 complex (reviewed by (Sherr and Roberts, 2004)). $p16^{Ink4a}$ is encoded by the *Cdkn2a* locus in mice, which encodes a second unrelated protein, $p19^{Arf}$, using an alternative reading frame. Combined deletion of both $p16^{Ink4a}$ and $p19^{Arf}$ at the *Cdkn2a* locus in young animals has only a modest effect on hematopoietic stem cell frequency or self-renewal, suggesting that these proteins have little function under normal conditions in young mice (Stepanova and Sorrentino, 2005). However, $p16^{Ink4a}$ and $p19^{Arf}$ expression increase with age, and at least $p16^{Ink4a}$ expression reduces stem cell frequency and function in a variety of aging tissues (Janzen et al., 2006; Krishnamurthy et al., 2006; Molofsky et al., 2006). The function of $p19^{Arf}$ in aging tissues has not yet been tested, and there is some evidence that its expression may be regulated differently in mice and humans, because $p19^{Arf}$ expression may not increase with age in humans. $p18^{Ink4c}$ deficiency also increases hematopoietic stem cell frequency and enhances the repopulating capacity of hematopoietic stem cells in transplantation assays, though the function of $p18^{Ink4c}$ is observed even in stem cells from young mice (Yuan et al., 2004). These results suggest that Ink4 family proteins negatively regulate stem cell self-renewal by slowing cell division, though the exact effect of these proteins on the cell cycle in stem cells (do they prevent or just slow division, etc.) remains untested.

$p19^{Arf}$-p53-$p21^{Cip1}$ pathway

The $p19^{Arf}$-p53-$p21^{Cip1}$ pathway also regulates cell division and quiescence in a variety of mammalian stem cells. p53 is a transcription factor that negatively regulates stem cell frequency under steady state conditions. *p53* deficiency modestly increases stem cell frequency and self-renewal in adult mouse neural stem cells and HSCs (Meletis et al., 2006; TeKippe et al., 2002), perhaps by reducing quiescence (Liu et al., 2009b). p53 function is increased above steady-state levels by a variety of stresses including DNA damage and oncogenic stimuli and sometimes by induction of $p19^{Arf}$ expression. $p19^{Arf}$ is a tumor suppressor that increases p53 levels by relieving p53 from Mdm2-mediated degradation (reviewed by (Sherr, 2001a)). Elevated p53 levels can promote DNA repair but can also induce cell cycle arrest and apoptosis (Sherr, 2001a). The function of p53 in some stem cells may be mediated partly by its ability to promote the transcription of the $p21^{Cip1}$ CDK inhibitor (Kippin et al., 2005; Qiu et al., 2004)(Figure 1.2). Although p53 generally functions to restrict stem cell self-renewal, it likely also contributes to the long-term maintenance of stem cells by maintaining the integrity of the genome.

Developmental regulation of Rb and p53 pathway in tissue stem cells

Over-activation of the Rb and p53 tumor suppressor pathways can lead to senescence and premature depletion of the stem cell pool, at least in HSCs and neural stem cells (Levi and Morrison, 2009). This is avoided in part by overlapping transcriptional mechanisms that repress *Ink4a* and *Arf* in normal stem cells (Figure 1.2). In fetal and young adult mice this is accomplished partly through the high mobility group transcriptional regulator, Hmga2, which regulates chromatin structure (Nishino et al., 2008). In the absence of *Hmga2*, $p16^{Ink4a}$ and $p19^{Arf}$ expression modestly increase and

stem cell frequency and self-renewal potential modestly decline. A more powerful repressor of the *Ink4a/Arf* locus is the polycomb repressor complex. Bmi-1 is one component of the polycomb repressor complex 1 that appears to repress *Ink4a/Arf* by binding to trimethylated H3K27 at this locus (Bracken et al., 2007; Kotake et al., 2007). Bmi-1 is not necessary *in vivo* for *Ink4a/Arf* locus repression during fetal development but becomes critical postnatally (Jacobs et al., 1999a; Molofsky et al., 2003). *Bmi-1*-deficient mice exhibit profound stem cell self-renewal defects and progressive stem cell depletion in multiple tissues (Lessard and Sauvageau, 2003a; Molofsky et al., 2003; Park et al., 2003b). *Bmi-1*-deficient mice generally die within a month after birth with severe growth retardation, hematopoietic failure, and neurological abnormalities (van der Lugt et al., 1994a). Deletion of $p16^{Ink4a}$ and/or $p19^{Arf}$ and/or *p53* partially rescues the stem cell defects in *Bmi-1* deficient mice (Akala et al., 2008; Bruggeman et al., 2005; Molofsky et al., 2005; Molofsky et al., 2003; Oguro et al., 2006). Repression of $p16^{Ink4a}/p19^{Arf}$ is critical for appropriate regulation of the Rb and p53 pathways in stem cells and for the maintenance of stem cells throughout life.

Under-activation of the Rb pathway can lead to stem cell hyperproliferation and cancer (Levi and Morrison, 2009). This is avoided in stem cells by the function of JunB, an AP-1 family transcription factor which promotes $p16^{Ink4a}$ expression (Passegue and Wagner, 2000). *JunB*-deficiency in the hematopoietic system leads to reduced $p16^{Ink4a}$ expression, expansion of primitive hematopoietic progenitors, and eventually to myeloproliferative disease (Passegue et al., 2004). Thus stem cells have both positive and negative transcriptional regulators of $p16^{Ink4a}$ and $p19^{Arf}$ expression that are balanced to promote stem cell maintenance while avoiding neoplastic proliferation.

Stem cell self-renewal versus progenitor proliferation

Stem cell self-renewal is mechanistically distinct from the proliferation of many downstream progenitors. *Bmi-1* and *Hmga2* are required for multipotent neural stem cell self-renewal but not for the proliferation of many restricted neuronal or glial progenitors (Molofsky et al., 2003; Nishino et al., 2008). Nonetheless, this is not a black and white difference as granule precursor cells in the cerebellum and lymphocytes in the hematopoietic system also require *Bmi-1* for their proliferation (Leung et al., 2004; van der Lugt et al., 1994a). The trithorax protein Mll is required for the maintenance of HSCs but not required for the maintenance of committed lymphoid and myeloid progenitors (Jude et al., 2007; McMahon et al., 2007). Sox17 is required for the maintenance of fetal and neonatal hematopoietic stem cells but is expressed by less than 1% of cells in the hematopoietic system and therefore must not be required for the function of many downstream hematopoietic progenitors (Kim et al., 2007). Conversely, $p27^{Kip1}$ is required for the limited self-renewal of transit amplifying cells and the proliferation of restricted progenitors in the hematopoietic and nervous systems but not stem cells in these tissues (Cheng et al., 2000; Doetsch et al., 2002). These results demonstrate that some mechanisms preferentially regulate stem cell self-renewal while other mechanisms preferentially regulate restricted progenitor proliferation.

The p53 and Rb pathways may be required to exit the stem cell state. When certain members of the p53 and Rb tumor-suppressor pathways are mutated, some types of progenitors can regain self-renewal capacity and behave like stem cells. For example, transiently self-renewing multipotent hematopoietic progenitors can regain long-term self-renewal potential when *p53, Ink4a,* and *Arf* are deleted (Akala et al., 2008).

Similarly, the deletion of *Ink4a* and *Arf* in astrocyte progenitors allows these cells to dedifferentiate in culture into neural stem cell like cells (Bachoo et al., 2002). Remarkably, deleting five out six *Rb* family alleles in terminally differentiated retinal neurons allows these cells to resume division (Ajioka et al., 2007). These observations suggest that Rb and p53 pathways reinforce the ability of progenitors to exit the stem cell state, although the mechanisms by which they do so remain unknown.

Maintaining stem cell self-renewal by suppressing lineage commitment

Tissue stem cell self-renewal requires maintenance of multipotency in addition to the ability to divide. Stem cells maintain their undifferentiated state by repressing the expression of genes that restrict developmental potential or specify differentiation (Figure 1.3). In *Caenorbabditis elegans*, the PUF RNA-binding proteins FBF-1 and FBF-2 are specifically expressed in undifferentiated germ-line stem cells and maintain stem-cell identity by repressing the translation of two critical regulators of meiotic cell-cycle entry, *gld-1* and *gld-3* (Kimble and Crittenden, 2007). In the absence of *fbf-1* and *fbf-2*, germ-line stem cells enter meiosis, committing to differentiation. Similarly, in the Drosophila ovary, Pumilio and its binding partner Nanos are essential in germ-line stem cells to prevent premature differentiation by inhibiting the translation of proteins that promote differentiation (Wong et al., 2005)(Figure 1.3A).

Mammalian tissue stem cells have analogous mechanisms that prevent differentiation, as illustrated by neural stem cells. The bZIP transcription factor ATF5 maintains neural stem cells by suppressing both neuronal and glial differentiation (Angelastro et al., 2003; Angelastro et al., 2005). SoxB1 family proteins (including Sox1, 2, 3) suppress neuronal differentiation and maintain neural stem cell identity during the

neurogenic phase of cortical development, avoiding premature differentiation (Avilion et al., 2003; Graham et al., 2003). The orphan nuclear receptor Tailless (Tlx) and the nuclear co-receptor N-coR suppress the differentiation of postnatal neural stem cells into astrocytes, thereby preventing the premature depletion of the stem cell pool (Hermanson et al., 2002; Shi et al., 2004). The maintenance of neural stem cell identity appears to depend on the function of many transcription factors avoid premature differentiation at various times during development (Figure 1.3B).

Premature lineage commitment is also suppressed by epigenetic mechanisms (Figure 1.3C). The promoter regions of many astrocyte-specific genes, including *gfap*, are preferentially methylated in cortical neural progenitors during neurogenesis, rendering them refractory to gliogenic signals (Takizawa et al., 2001). Consistent with this, *DNA methyltransferase 1* (*Dnmt1*)-deficient neural progenitors show precocious astrocytic differentiation (Fan et al., 2005). Hematopoietic stem cells deficient in *Dnmt1*, or *Dnmt3a* and *Dnmt3b* lack long-term repopulating ability (Broske et al., 2009; Tadokoro et al., 2007; Trowbridge et al., 2009), raising the possibility that DNA methylation is also required to prevent the spontaneous differentiation of HSCs.

Chromatin structure is also regulated to avoid premature differentiation. Stem cells lacking *Bmi-1* exhibit little self-renewal potential (Lessard and Sauvageau, 2003a; Molofsky et al., 2003; Park et al., 2003b) and can prematurely differentiate in at least certain circumstances (Pietersen et al., 2008). Polycomb complexes therefore promote stem cell self-renewal by suppressing differentiation in addition to repressing cell cycle inhibitors.

Some stem cells may rely on a balance between the activities of lineage specification genes, rather than their outright repression, to maintain multipotency. No stem-cell specific factor that can suppress lineage determination has so far been identified in hematopoietic stem cells. Instead, many lineage specification genes are expressed at low levels in hematopoietic stem cells (Ye et al., 2003). This phenomenon has been described as lineage priming and has been proposed to be characteristic of the multipotent state (Orkin and Zon, 2008). However, it is unclear how multipotency is maintained in the presence of these lineage specification factors. One possibility is that the function of these factors is suppressed through yet to be identified mechanisms, or that the expression levels in hematopoietic stem cells are too low to influence fate. Alternatively, opposing lineage specification factors may act antagonistically and the balance may maintain multipotency (Figure 1.3D). Pairs of lineage specification factors in the hematopoietic system are known to be mutually antagonistic (Laslo et al., 2008). Furthermore, the multipotency and self-renewal capacity of hematopoietic stem cells are compromised when one component of these paired transcription factors, such as PU.1, is deleted (Iwasaki et al., 2005; Kim et al., 2004). Thus hematopoietic stem cell multipotency may be maintained by counterbalanced lineage specification genes. However, for this model to be true, hematopoietic stem cells would have to have mechanisms that avoid the differentiation of the entire stem cell pool upon exposure to an extrinsic differentiation signal that tips the balance in favor of a particular lineage specification gene.

Asymmetric stem cell division

Strategies by which stem cells regulate the symmetry of division (Morrison and Kimble, 2006) and molecular mechanisms regulating asymmetric division have been reviewed in detail elsewhere (Gonczy, 2008; Knoblich, 2008; Lin, 2008). Many stem cell populations likely undergo both symmetric and asymmetric divisions, either stochastically or in response to environmental cues. Symmetric divisions predominate in circumstances in which stem cells must expand in number, such as during development and after injury. Under steady-state conditions, asymmetric divisions allow stem cells to generate a stem cell daughter as well as a daughter fated to differentiate, maintaining the balance between stem cells and differentiated cells.

Intrinsically asymmetric divisions allow stem cells to regulate self-renewal by asymmetrically segregating fate determinants into daughter cells (Figure 1.3E). For example, *Drosophila* neuroblasts divide asymmetrically to segregate atypical Protein Kinase C to daughters fated to remain as stem cells and Numb, Prospero and Brat to daughters fated to differentiate (Knoblich, 2008). Mutations that affect the expression or the asymmetric segregation of these cell fate determinants can lead to either symmetric self-renewing divisions that create stem cell tumors or to symmetric differentiating divisions that prematurely deplete the stem cell pool (Knoblich, 2008; Lee et al., 2006a). Mammalian stem cells employ similar mechanisms to self-renew asymmetrically in the central nervous system, in the basal layer of the epidermis, in skeletal muscle and in other tissues (Huttner and Kosodo, 2005; Kuang et al., 2007; Lechler and Fuchs, 2005).

Alternative, asymmetric divisions need not be intrinsically asymmetric, as polarized divisions can lead daughter cells to acquire different fates as a result of ending

up in different environment. Mitotic spindle orientation can determine the positions of the daughter cells with respect to the stem cell niche, thereby determining daughter cell fate (Figure 1.3F). For example, Drosophila spermatogonial stem cells self-renew asymmetrically with the spindle oriented perpendicularly to the hub cells that constitute the niche, such that one daughter cell ends up adjacent to the niche and the other daughter cells is displaced from the niche (Fuller and Spradling, 2007). Spindle orientation is determined by centrosome orientation (Yamashita et al., 2003), where the mother centrosome is located apically (close to the hub), whereas the daughter centrosome is located basally (away from the hub)(Yamashita et al., 2007). Indeed, spermatogonial stem cells have a spindle orientation checkpoint in which they are unable to divide until one centrosome aligns apically and the other aligns basally (Cheng et al., 2008; Yamashita et al., 2007). It remains uncertain whether mammalian stem cell divisions are also regulated by the orientation and asymmetric segregation of centrosomes.

MAINTAINING GENOMIC INTEGRITY IN STEM CELLS

As the longest-lived, mitotically active cells in the body, stem cells are particularly sensitive to the accumulation of genetic lesions. Preserving genomic integrity is not only important for maintaining normal function but also prevents carcinogenesis. This is more important in stem cells than in other cells because stem cells pass mutations on to large numbers of progeny, amplifying the risk of cancer. Many mechanisms protect stem cells from endogenous and exogenous mutagens and enhance their capacity to repair the damages that has already occurred. In cases where the damage is too extensive to be repaired, stem cells may undergo apoptosis or senescence.

Reactive Oxygen Species

Reactive oxygen species (ROS) are toxic byproducts of oxidative energy metabolism (Balaban et al., 2005). Although important for certain physiological processes such as intracellular signal transduction and combating infection, excessive level of ROS within cells can damage lipids, proteins, RNA and DNA, thus impairing cellular function. To persist throughout adult life, stem cells must minimize ROS damage.

FoxO family transcription factors are tumor suppressors that protect stem cells and other cells from oxidative damage, reducing mutagenesis and extending cellular lifespan (Paik et al., 2007). In response to oxidative stress, FoxO transcription factors increase the expression of genes required for detoxification of ROS including superoxide dismutase and catalase as well as genes that promote quiescence (Tothova and Gilliland, 2007). FoxO function is negatively regulated by PI-3kinase pathway signaling as Akt phosphorylates FoxOs, causing their translocation out of the nucleus. Deletion of three members of the *FoxO* family, *FoxO1*, *3* and *4* in mouse HSCs leads to increased levels of ROS, increased proliferation, and stem cell depletion (Tothova et al., 2007). These defects can be at least partially rescued by treating the mice with antioxidant N-acetyl-L-cysteine (NAC). Disruption of *FoxO3* alone also increases ROS levels in hematopoietic stem cells and leads to their depletion, though to a lesser extent than in the triple knock-out (Miyamoto et al., 2007). Enzymes involved in ROS metabolism including superoxide dismutase and catalase were reduced in *FoxO*-deficient HSCs, providing a potential mechanism for ROS accumulation.

ATM, a kinase that is activated in response to DNA damage, is required for normal DNA repair and to avoid oxidative stress (Barzilai et al., 2002). *Atm*-deficient HSCs are depleted due to their accumulation of ROS, which activates p38 MAPK and induces $p16^{Ink4a}$ (Ito et al., 2004; Ito et al., 2006). Neural stem cells also require *Atm* to avoid genomic instability, abnormal proliferation, and depletion (Allen et al., 2001). These defects can be partially rescued by treating the mice with NAC or a p38 inhibitor. Although it remains unclear precisely why ROS accumulates in the absence of ATM, these data demonstrate a link between DNA repair, ROS levels, and stem cell maintenance.

Telomere maintenance

Mammalian telomeres are repetitive DNA sequences (thousands of TTAGGG repeats) along with specialized protein complexes that are located at the ends of each chromosome (Gilson and Geli, 2007). Telomeres are required to protect chromosomes from fusing to each other, from exonuclease activity, and from the loss of coding sequence due to the "end replication problem". That is, based on the way in which DNA replication occurs, 50-150 base pairs of sequence are lost from each end of the chromosomes during each round of replication (Gilson and Geli, 2007). As a result, telomeres become progressively shorter with each round of replication in most cells that lack telomerase (Gilson and Geli, 2007). This telomere attrition ultimately leads to cellular senescence when telomeres reach a critical length, limiting the number of divisions that a cell can undergo in a lifetime. Cells that escape senescence exhibit genomic instability due to aberrant chromosome fusions (Counter et al., 1992). Some cells, including stem cells and many cancer cells, express telomerase, an enzyme that can

lengthen telomeres by adding new TTAGGG repeats (Gilson and Geli, 2007). This allows stem cells to escape the replication limits imposed by telomere length. Some cells also use alternative mechanisms for lengthening telomeres (Bryan et al., 1997). Thus, telomere maintenance is critical for ensuring genetic stability and for maintaining the proliferative capacity of cells.

Many stem cells express telomerase, reducing the rate at which telomeres erode and increasing replicative capacity (Lee et al., 1998; Morrison et al., 1996a; Vaziri et al., 1994). Deletion of the RNA or the catalytic component of the telomerase reverse transcriptase enzyme accelerates telomere loss (particularly in highly replicative tissues), leading to genomic instability and carcinogenesis (Blasco et al., 1997; Rudolph et al., 1999). Loss of telomerase activity also reduces the self-renewal potential of hematopoietic stem cells upon serial transplantation (Allsopp et al., 2003), their functional capacity during aging (Rossi et al., 2007a) and the regenerative capacity of other tissues (Herrera et al., 1999; Lee et al., 1998). Adult neural stem cells lacking telomerase activity also have less proliferative capacity, and increased genomic instability *in vitro* and *in vivo* (Ferron et al., 2004). These results highlight the importance of telomere maintenance for maintaining the genomic integrity and self-renewal potential of stem cells.

DNA Damage Response

DNA repair mechanisms are critical for maintaining genomic integrity in all cells, but they are particularly important for maintaining the replicative capacity of stem cells (Rossi et al., 2008; Sharpless and DePinho, 2007). DNA damage occurs during normal DNA replication or upon exposure to ionizing irradiation, chemical mutagens, or ROS.

DNA damage in stem cells can lead to senescence, apoptosis, reduced self-renewal potential, or cancer, all of which will ultimately deplete the stem cell pool and reduce tissue regenerative capacity. DNA damage accumulates in stem cells during aging (Rossi et al., 2007a), but the rate at which it accumulates is limited by DNA mismatch repair, nucleotide excision repair, double-strand break repair and DNA damage checkpoints. Conditional deletion of the DNA damage response gene, *ATR*, in all tissues of adult mice leads to widespread stem cell depletion, defects in tissue regenerative capacity, and phenotypes that resemble premature aging (Ruzankina et al., 2007). A variety of other DNA repair/damage response factors are also required for the maintenance of normal hematopoiesis and hematopoietic stem cell function, including the DNA repair protein Brca2 (Navarro et al., 2006), the non-homologous end-joining proteins Lig4 (Nijnik et al., 2007) and Ku80 (Rossi et al., 2007a), the mismatch repair protein MSH2 (Reese et al., 2003), the nucleotide excision repair proteins XPD (Rossi et al., 2007a), Ercc1, and XPA (Prasher et al., 2005), and the double strand break-repair proteins Rad50 (Bender et al., 2002) and ATM (Ito et al., 2004). Although the roles of these pathways have mainly been studied in the hematopoietic system, they are likely to have similar functions in stem cells from other tissues.

CELL EXTRINSIC REGULATION OF STEM CELL SELF-RENEWAL

To maintain homeostasis within complex tissues, metazoans have evolved sophisticated mechanisms to externally control the survival, self-renewal and differentiation of stem cells by both local and systemic signals.

Most stem cells in metazoans reside within specialized microenvironments known as "niches" (Fuchs et al., 2004; Morrison and Spradling, 2008). These niches contain supporting cells that promote stem cell maintenance and regulate stem cell function. Niches accomplish these functions by providing an anchorage site for stem cells as well as by producing membrane bound and secreted signals that regulate stem cell survival, cell cycle status, and differentiation. In many cases, the size and availability of niches physically limits the number of stem cells within tissues. Displacement of cells from the niche fates these cells to differentiate as these cells lose access to niche signals required to remain undifferentiated.

Niche signals regulate stem cell maintenance

The primary function of the niche is to maintain undifferentiated stem cells. In the *Drosophila* germline an average of 9 spermatogonial stem cells adhere to the hub, a cluster of 12 somatic cells that secrete a factor called Unpaired (Fuller and Spradling, 2007) (Figure 1.4A). Unpaired is required for the maintenance of spermatogonial stem cells and is concentrated in the extracellular matrix surrounding hub cells, so the stem cells can only be maintained immediately adjacent to the hub (Kiger et al., 2001; Tulina and Matunis, 2001). The stem cells divide asymmetrically such that one daughter cell remains adjacent to the hub and retains stem cell identity, whereas the other daughter cell is displaced from the niche and is fated to differentiate. Because the niche is constrained by the need for contact with the hub, this physically limits the number of stem cells that can reside within the tissue and ensures that half of the progeny of stem cells are displaced from the niche and fated to differentiate.

In the *C. elegans* germline, stem cells are found in the distal half of the mitotic region within the gonad, in contact with the distal tip cell (Kimble and Crittenden, 2007) (Figure 1.4B). In contrast to fly germline, there is no evidence that germline stem cells undergo asymmetric division in the worm germ line (Morrison and Kimble, 2006). Rather, the distal tip cell expresses the GLP-1/Notch ligand Lag-2, which promotes mitosis and suppresses differentiation (entry into meiosis) by activating GLP-1/Notch signaling within the germline stem cells (Kimble and Crittenden, 2007). Ablation of the distal tip cell or loss of GLP-1 signaling causes the germline stem cells to prematurely enter meiosis. In contrast, constitutive GLP-1 signaling in the stem cells blocks differentiation and causes uncontrolled mitosis, resulting in tumorigenesis (Berry et al., 1997). Comparison of mechanisms employed by the fly and worm germlines suggests that one key element of stem cell niches is the expression of factors that maintain undifferentiated stem cells.

In germline niches, stem cell progeny that are initially fated to differentiate can de-differentiate to re-occupy the niche in certain circumstances. If Drosophila germline stem cells are ablated, the daughter cell that is normally destined to differentiate can reoccupy the open space in the niche to maintain homeostasis (Brawley and Matunis, 2004; Kai and Spradling, 2003). Under physiological circumstances, this appears to be a mechanism by which the fly spermatogonial stem cell pool is maintained during aging, as de-differentiated spermatogonial stem cells accumulate with age. Adult mouse spermatogonial cells have also been suggested to contribute to the stem cell pool through de-differentiation (Barroca et al., 2008; Nakagawa et al., 2007). These results suggest that

in addition to maintaining undifferentiated stem cells, germ line niches also have mechanisms that can reprogram differentiating cells to restore stem cell identity.

The identity of mammalian stem cell niches and the mechanisms by which these niches regulate stem cell maintenance are not as well understood as in the fly and worm germ lines. Part of the problem is that we generally do not have the ability to identify and image stem cells or niche cells with certainty in vast mammalian tissues (Morrison and Spradling, 2008). In addition, not as much has been done in mammalian tissues to test genetically for which factors are required for stem cell maintenance, and which cells produce these factors. As a result, models of mammalian stem cell niche are often provisional as key questions remain to be answered.

In the mammalian hematopoietic system, some of the key factors required for stem cell maintenance have been identified but the cells that produce these factors and create the niche remain uncertain (Kiel and Morrison, 2008) (Figure 1.4C). Hematopoietic stem cells are maintained primarily in the bone marrow during steady-state adult hematopoiesis. Bone marrow hematopoietic stem cell niches have been proposed to be created by endosteal (bone-lining) cells, perivascular cells, or a collaboration between these cell types, but direct evidence is lacking for each of these possibilities (Kiel and Morrison, 2008). It remains unclear precisely which bone marrow cells are the physiological sources of the factors that regulate HSC maintenance. The chemokine CXCL12 (SDF-1) is required for the maintenance of bone marrow HSCs and is expressed by both perivascular and endosteal cells (Kollet et al., 2006; Sacchetti et al., 2007; Sugiyama et al., 2006). Angiopoietin-1, a factor proposed to regulate HSC quiescence (Arai et al., 2004), has been suggested to be expressed by both osteoblasts at

the endosteum (Arai et al., 2004) and by perivascular mesenchymal progenitors (Sacchetti et al., 2007). So far, none of the factors that are thought to regulate HSC maintenance have been conditionally deleted from specific cell types to determine which cell is the physiologically important source. Similar results have been obtained in multiple other mammalian systems such as hair follicles (Blanpain and Fuchs, 2006) and forebrain subventricular zone (Riquelme et al., 2008) (Figure 1.4D) where some of the factors that regulate stem cell maintenance have been identified but the sources of such factors generally have not.

Niche signals maintain mammalian stem cell quiescence

Adult mammalian stem cell niches often promote stem cell quiescence. For unknown reasons, many mammalian stem cells appear to require intermittent periods of quiescence for their maintenance. Genetic manipulations that reduce their ability to remain quiescent also tend to deplete the stem cell pool (Ficara et al., 2008; Jude et al., 2007; McMahon et al., 2007; Yilmaz et al., 2006). Nonetheless, quiescence is not a defining feature of stem cells as mouse gut epithelial stem cells appear to divide frequently (Barker et al., 2007) and many invertebrate stem cells divide at a rate comparable to their more differentiated progeny and show no sign of quiescence (Crittenden et al., 2006; Wallenfang et al., 2006).

The maintenance of stem cell quiescence is regulated at least partly through the niche. The quiescence of mouse hematopoietic stem cells depends upon a series of stem cell-extrinsic factors in the bone marrow including Steel factor (McCarthy et al., 1977; Thoren et al., 2008), CXCL12 (Nie et al., 2008; Sugiyama et al., 2006), Thrombopoietin (Qian et al., 2007; Yoshihara et al., 2007), and Angiopoietin-1 (Arai et al., 2004; Puri and

Bernstein, 2003). Loss of signaling by the receptors for any of these factors leads to increased hematopoietic stem cells proliferation and stem cell depletion. BMP signaling is similarly required to maintain the quiescence of mouse hair follicle stem cells (Horsley et al., 2008; Kobielak et al., 2007). In the absence of BMP signaling these stem cells over-proliferate and form tumors (Kobielak et al., 2007). Therefore, mammalian stem cell maintenance depends on niche signals that promote quiescence.

Long-range and systemic signals regulate stem cell function

In addition to being regulated by local niche signals, stem cell self-renewal can also be modulated by long-range signals, such as circulating hormones, cytokines and/or neural activity. One mechanism by which a long-range signal can regulate stem cells is by directly activating receptors on the stem cells. The rate of cell division in *Drosophila* ovary stem cells is regulated by *Drosophila* insulin-like peptides (DILPs) secreted by cells in the brain (Drummond-Barbosa and Spradling, 2001; LaFever and Drummond-Barbosa, 2005). This provides a mechanism by which the rate of egg production can be regulated by the nutritional status of the fly. Systemic signals can also modulate stem cell activity through niche-mediated (indirect) mechanisms. For unknown reasons, HSCs are regularly mobilized from the bone marrow through the circulation (Wright et al., 2001) according to circadian rhythms (Mendez-Ferrer et al., 2008). This is accomplished by adrenergic signals that come from the innervation of cells in the HSC (Mendez-Ferrer et al., 2008). These signals are thought to reduce CXCL12 expression within the niche, allowing the stem cells to go into cycle and to be released from the bone marrow. The observation that many long-range signals can modulate CXCL12 expression level in the bone marrow raises the possibility that this maybe a common mechanism by which

hematopoietic stem cell activation and mobilization are tied to physiological variables such as stress level and circadian time (Spiegel et al., 2008). Unlike local niche signals, systemic signals do not generally appear to be specifically required for stem cell maintenance (with the possible exception of Thrombopoietin, which may regulate hematopoietic stem cells after being secreted by the liver). Rather system signals appear to dynamically modulate stem cell activity according to physiological demands.

STEM CELL AND THEIR SELF-RENEWAL MECHANISMS CHANGE OVER TIME

Developmental changes of stem cell self-renewal

Many stem cells undergo cell-intrinsic changes in their developmental potential over time. For example, *Drosophila* neuroblasts and mammalian cortical and retinal neural stem cells undergo temporal restrictions in the types of neurons they can make during development (Desai and McConnell, 2000; Livesey and Cepko, 2001; Pearson and Doe, 2003; Shen et al., 2006). Neural crest stem cells from the fetal and postnatal gut undergo similar restrictions in neuronal subtype potential, even while remaining self-renewing and multipotent (Kruger et al., 2002). Even HSCs change their developmental potential throughout life. Fetal hematopoietic stem cells have the potential to make certain subtypes of B and T lymphocytes that adult stem cells cannot generate (even when transplanted into the fetal environment) (Hayakawa et al., 1985; Ikuta et al., 1990; Kantor et al., 1992). During aging, hematopoietic stem cells undergo intrinsic changes that bias them toward the myelopoiesis and away from lymphopoiesis (Rossi et al., 2005). Thus, multipotent stem cells persist throughout life in the nervous and

hematopoietic systems, but they undergo restrictions in the cell type they can produce. Therefore self-renewing divisions perpetuate undifferentiated multipotent stem cells throughout life but do not necessarily generate daughter cells that are identical to the mother cell.

To meet the changing demands of tissue growth and regeneration during development and aging, many tissue stem cells undergo dynamic changes in their cell cycle status. For instance, fetal liver hematopoietic stem cells appear to undergo daily symmetric self-renewing divisions to expand the stem cell pool (Morrison et al., 1995). In contrast, adult hematopoietic stem cells are quiescent most of the time (Cheshier et al., 1999b). Most adult mouse hematopoietic stem cells asynchronously go into cycle once every 12 days, but a more slowly dividing subset of HSCs divides only once every 55 days or so (Foudi et al., 2008; Kiel et al., 2007; Wilson et al., 2008). The rate at which adult hematopoietic stem cells divide further changes during aging (de Haan et al., 1997; Morrison et al., 1996b). These changes in stem-cell cell cycle status and developmental potential require developmental changes in self-renewal programs.

Although multiple transcriptional regulators are required by both fetal and adult hematopoietic stem cells, there are also mechanistic differences in the self-renewal of these stem cells (Levi and Morrison, 2009) (Figure 1.5). Fetal HSC maintenance depends on AML1 and Sox17, but these transcription factors are not required for the maintenance of adult HSCs (Ichikawa et al., 2004; Kim et al., 2007; Okuda et al., 1996b). Conversely, adult hematopoietic stem cell maintenance depends on several transcriptional regulators that are dispensable for the maintenance of fetal hematopoietic stem cells, including Bmi-1 (Park et al., 2003b), Gfi-1 (Hock et al., 2004a) and Tel/Etv6 (Hock et al., 2004b). These

changes in the transcriptional regulation of self-renewal between fetal and adult HSCs at least partially reflect changes in cell cycle regulation. Sox17 is turned off as neonatal stem cells make the transition to a more slowly dividing adult phenotype (Kim et al., 2007), and Gfi-1 is required in adult hematopoietic stem cells to maintain quiescence (Hock et al., 2004a) (Figure 1.5).

Neural stem cells exhibit similar changes in the transcriptional regulation of self-renewal between the fetal and adult stages (Figure 1.5). Fetal and young adult neural stem cells depend on Hmga2 for self-renewal (Nishino et al., 2008). Hmga2 negatively regulates the expression of $p16^{Ink4a}$ and $p19^{Arf}$ in these cells, increasing stem cell frequency and self-renewal potential. However, Hmga2 expression is extinguished in old adult neural stem cells (Nishino et al., 2008). Bmi-1 also promotes neural stem cell self-renewal by repressing the expression of $p16^{Ink4a}$ and $p19^{Arf}$ (Bruggeman et al., 2005; Molofsky et al., 2005; Molofsky et al., 2003); however, Bmi-1 is not required *in vivo* during fetal development to repress $p16^{Ink4a}$ and $p19^{Arf}$, rather it is required throughout adulthood. These studies demonstrate that stem cells employ overlapping transcriptional regulators to repress $p16^{Ink4a}$/$p19^{Arf}$ expression throughout life.

Stem cell self-renewal, aging and cancer

Stem cells from diverse tissues exhibit changes in their self-renewal capability during aging. The frequency, self-renewal potential, mitotic activity, and rate of neurogenesis of neural stem/progenitor cells in the forebrain subventricular zone decline with age (Maslov et al., 2004; Molofsky et al., 2006). In the hematopoietic system, stem cells also change their frequency and cell cycle status with age, but in a strain-dependent manner: stem cell frequency increases with age in long-lived strains and decreases with

age in short-lived mouse strains (de Haan et al., 1997; de Haan and Van Zant, 1999; Morrison et al., 1996b). Aging HSCs also exhibit increased myelopoiesis and decreased lymphopoiesis (Rossi et al., 2005) as well as decreased capacity to home to the bone marrow upon intravenous injection (Liang et al., 2005; Morrison et al., 1996b). These data indicate that stem cells properties change with age, though the nature of the changes varies depending on tissue and genetic background.

Age-related changes in stem cell properties are determined by both cell-intrinsic and cell-extrinsic changes. Cell-intrinsic changes in the transcriptional regulation of self-renewal involve changes in $p16^{Ink4a}$ expression. $p16^{Ink4a}$ is not expressed by most types of stem cells in fetal and young adult animals (partly due to Hmga2 and Bmi-1 mediated repression), but its expression is upregulated with age in multiple tissues (Krishnamurthy et al., 2004) including in HSCs (Janzen et al., 2006) and neural stem cells (Molofsky et al., 2006) (Figure 1.5). Deletion of $p16^{Ink4a}$ from these tissues partially rescues the age-related decline in stem cell frequency and self-renewal potential (Janzen et al., 2006; Krishnamurthy et al., 2006; Molofsky et al., 2006). The increased $p16^{Ink4a}$ expression in aging stem cells is at least partially attributable to the decline in Hmga2 expression, which is caused by increased *let-7* microRNA expression during aging (Nishino et al., 2008) (Figure 1.5). This demonstrates that by having overlapping transcriptional regulators, stem cells achieve fine-gain control over the expression of tumor suppressors that limit self-renewal potential. By maintaining Bmi-1-mediated repression and eliminating Hmga2-mediated repression during aging, stem cells can modestly increase $p16^{Ink4a}$ expression to achieve tumor suppression while maintaining a reduced level of stem cell function (Figure 1.6A).

Cell extrinsic changes that regulate changes in stem cell function during aging have best been studied in muscle, where Notch ligand expression declines with age, reducing Notch activation in satellite cells and muscle regenerative capacity (Conboy et al., 2003). Parabiosis of old mice to young mice and exposure of old satellite cells to young serum increases Notch ligand expression, muscle satellite cell proliferation, and muscle regenerative capacity, thereby demonstrating that local cues are regulated by circulating systemic factors (Conboy et al., 2005). It appears that such circulating factors include Wnts as canonical Wnt pathway activation increases with age in muscle satellite cells and inhibitors of this pathway can restore myogensis and suppress fibrogenesis by satellite cells (Brack et al., 2007). The premature aging of Klotho mutant mice have also been associated with increased Wnt signaling, and serum Klotho levels decline with age (Liu et al., 2007). These systemic changes in the environment of aging tissues may cause the cell intrinsic changes in tumor suppressor expression that have been observed in aging stem cells as increased Wnt and TGFß in the aging environment appear to counteract the effects of Notch ligands on muscle satellite cells, promoting the expression of CDK inhibitors including $p16^{Ink4a}$.

It is not clear whether there is any relationship between stem cell aging and lifespan. On one hand, the changes in stem cell function that occur during aging appear to reduce tissue regenerative capacity and the accumulation of genetic damage in stem cells likely contributes to increased cancer incidence during aging (Rossi et al., 2008; Sharpless and DePinho, 2007). On the other hand, the effects of aging on fully differentiated cells are likely a major and independent contributor to age-related morbidity, cancer incidence, and degenerative disease. It remains unclear whether the

changes that occur in stem cells during aging are a major or minor contributor to age-related morbidity and lifespan. Notably, the transgenic overexpression of *p15*^{Ink4d}/*p16*^{Ink4a}/*p19*^{Arf} and *p53* increases mouse lifespan (Matheu et al., 2007) even though loss of *p16*^{Ink4a} rescues stem cell function in multiple tissues during aging (Janzen et al., 2006; Krishnamurthy et al., 2006; Molofsky et al., 2006). These observations raise the possibility that tumor suppressors may have anti-aging effects in some cells, and that lifespan may reflect a convoluted mixture of pro-aging and anti-aging effects by tumor suppressors on stem cells and differentiated cells.

Tumor suppressors regulate stem cell self-renewal and aging

Tumor-suppressor genes can be largely divided into care-taking tumor suppressors and gate-keeping tumor suppressors (Campisi, 2005; Kinzler and Vogelstein, 1997). Gate-keeping tumor suppressors, like p53, p16^{Ink4a}, and p19^{Arf} serve as fail-safe mechanisms to prevent uncontrolled cell proliferation. As indicated above, these genes tend to negatively regulate self-renewal by slowing cell division, or by inducing senescence or apoptosis when activated by DNA damage, stress, or oncogenic stimuli. In contrast, care-taking tumor suppressors, like the DNA damage response proteins ATM and ATR, maintain cellular integrity and therefore promote the maintenance of stem cells. As discussed above, ROS detoxification, telomere maintenance, and DNA repair by care-taking tumor suppressors are all required to maintain genomic integrity in stem cells. A loss of care-taking tumor suppressor function resembles premature aging phenotype marked by stem cell depletion and reduced tissue regenerative capacity (Lombard et al., 2005) (Figure 1.6C). This functional distinction of tumor suppressors is not clear-cut and some genes, such as p53 and Pten have both care-taking and gate-keeping functions.

Care-taking tumor suppressors are unable to completely prevent the accumulation of damage in stem cells during aging. To compensate for this, cellular stress or damage activates gate-keeping tumor suppressor mechanisms to ensure that stem cells are not transformed into cancer cells. For example, critical levels of telomere attrition lead to p53 activation, inducing cell death or cell senescence (Chin et al., 1999). p53 deficiency reduces the cell death and senescence observed in response to telomere dysfunction but also accelerates cancer development in these cells. Together, these results illustrate how DNA damage activates gate-keeping tumor suppressors that reduce normal stem cell function as a consequence of their efforts to prevent cancer (Figure 1.6C). Although these mechanisms operate in many cells, they are particularly important in stem cells to prevent the propagation of DNA damage throughout tissues and to avoid stem cell transformation, which might occur more easily than the transformation of their post-mitotic progeny.

Cancer cells hijack normal self-renewal mechanisms

Cancer cells proliferate out of control by inappropriately activating normal self-renewal pathways either through mutations that constitutively activate oncogenes or through mutations that inactivate tumor suppressors (Pardal et al., 2005) (Figure 1.6D). Like normal stem cells, cancer cells rely on mechanisms that promote proliferation and suppress differentiation. In many cases, self-renewal regulators have surprisingly similar functions in cancer cells and in normal stem cells. For example, the proto-oncogene *Bmi-1* is required to maintain the proliferative potential of leukemic stem cells (Lessard and Sauvageau, 2003a) and brain tumor cells (Bruggeman et al., 2007) just as it is required to maintain the self-renewal potential of normal hematopoietic and neural stem cells

(without being generically required for the proliferation of all cells) (Molofsky et al., 2003; Park et al., 2003b). Hedgehog signaling is not only required for normal neural stem cell maintenance, but also for brain tumor cell proliferation (Balordi and Fishell; Balordi and Fishell, 2007; Ruiz i Altaba et al., 2002). These are only a few of many examples. Therefore, by identifying the mechanisms that regulate normal stem cell self-renewal we can also gain insights into the regulation of cancer cell proliferation; however it is difficult to target these mechanisms in the context of cancer without also impairing normal stem cell function and tissue regenerative capacity. This contributes to the toxicity of cancer therapy.

It is possible, however, to identify mechanistic differences between stem cell self-renewal and cancer cell proliferation, even cancer stem cell proliferation. The PI-3kinase pathway is essential for the regulation of normal stem cell self-renewal and is frequently hyper-activated by mutations in cancer (Yuan and Cantley, 2008). Pten, a tumor suppressor that attenuates signaling through this pathway, is one of the most frequently deleted loci in cancer. In some tissues, the consequences of Pten function appear to be very similar in cancer cells and normal stem cells. For example, *Pten* is frequently deleted in brain tumors and Pten also negatively regulates the self-renewal of normal neural stem cells (Groszer et al., 2006; Groszer et al., 2001). However, the situation in the hematopoietic system is more complicated. Widespread deletion of *Pten* in the hematopoietic system does lead to leukemogenesis, as expected (Yilmaz et al., 2006); however, deletion in hematopoietic stem cells leads to the depletion of these cells, rather than their expansion (Yilmaz et al., 2006; Zhang et al., 2006). In the absence of *Pten*, hematopoietic stem cells lose their ability to remain quiescent, and go into cycle within

days, transiently expanding the stem cell pool. However, within weeks, the stem cells become depleted through mechanisms that are just being elucidated now, but which depend upon hyper-activation of mTor. Treatment of these mice with the mTor inhibitor rapamycin not only reduces leukemogenesis but also rescues normal stem cell function, (Yilmaz et al., 2006), providing proof-of-principle that it is possible to identify chemotherapies that are more effective against cancer while exhibiting less toxicity to normal stem cells.

Since normal stem cells employ different self-renewal programs at different ages, one prediction is that cancers will require different mutations at different ages to hijack these self-renewal programs. This remains to be tested but offers a potential explanation for the differences that are observed in mutation spectrum between the childhood and adult versions of certain cancers (Gilliland et al., 2004).

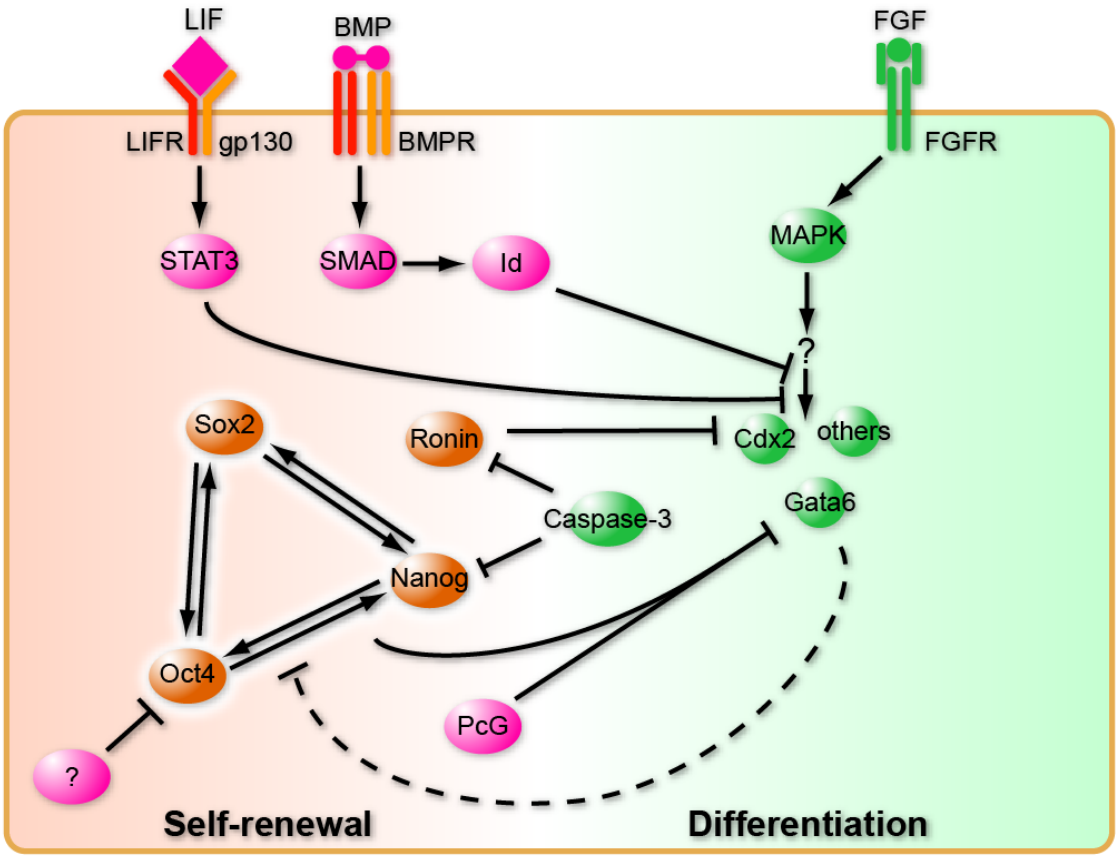

Figure 1.1: The regulation of pluripotency.
ES cell self-renewal is maintained by the Oct4-Sox2-Nanog transcriptional regulatory network, which forms a positive feedback loop that negatively regulates the expression of differentiationpromoting genes. Polycomb family (PcG) proteins aid in this process by suppressing the expression of genes associated with differentiation. Leukemia inhibitory factor (LIF) and bone morphogenetic protein (BMP) signaling suppress differentiation by inhibiting MAPK pathway signaling, which is activated by autocrine fibroblast growth factor (FGF) signaling. Thus ES cells self-renew by inhibiting differentiation (Ying et al. 2008). Self-renewal is possible in culture conditions that lack differentiation inducing stimuli, but ES cells spontaneously differentiate when they achieve high densities in culture as FGF builds up and LIF/BMP become depleted.

Figure 1.2: Differences in cell-cycle regulation among stem cells at different stages of life.
A) ES cells have constitutive cyclin E-CDK2 activity which hyperphosphorylates and inactivates Rb. This leads to a short G1 phase of the cell cycle, with rapid G1-S transition, and little dependence upon mitogenic signals or D cyclins for S phase entry. B) In fetal stem cells, mitogens promote a relatively rapid G1-S transition through cooperative action of cyclin D-CDK4/6 and cyclin E-CDK2 to inactivate Rb family proteins. $p16^{Ink4a}$ and $p19^{Arf}$ expression are inhibited by Hmga2-dependent chromatin regulation. C) Many young adult stem cells are quiescent most of the time. In the absence of mitogenic signals, cyclin-CDKs and the G1-S transition are suppressed by cell-cycle inhibitors, including Ink4 and Cip/Kip family proteins. As a result, Rb is hypophosphorylated and inhibits E2F, promoting quiescence in G0-phase of the cell cycle. Mitogen stimulation mobilizes these cells into cycle by activating cyclin D expression. D) In old adult stem cells, let-7 microRNA expression increases, reducing Hmga2 levels and increasing $p16^{Ink4a}$ and $p19^{Arf}$ levels (Nishino et al., 2008). This reduces the sensitivity of stem cells to mitogenic signals by inhibiting cyclin-CDK complexes. As a result, stem cells either cannot enter the cell cycle, or cell division slows. Red ovals indicate proto-oncogene products and blue ovals indicate tumor suppressors. P denotes phosphorylation, R denotes the cell cycle restriction point. Ovals with more intense color indicate gene products that are functionally important in these cells while ovals with less intense color are less expressed/active.

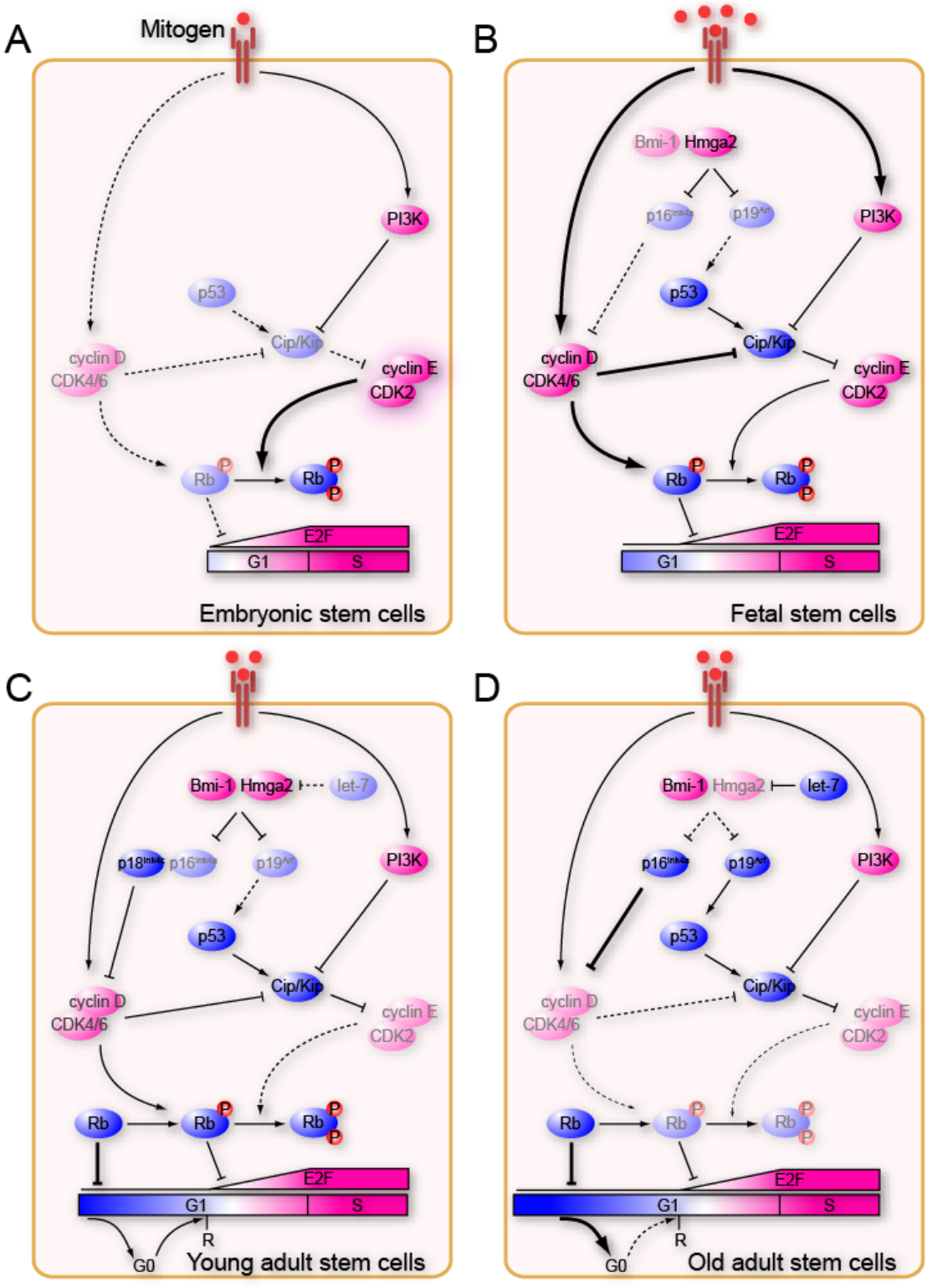
A
Mitogen
PI3K
p53
Cip/Kip
cyclin D
CDK4/6
cyclin E
CDK2
Rb
P
E2F
G1
S
Embryonic stem cells
B
Bmi-1
Hmga2
p16Ink4a
p19Arf
PI3K
p53
Cip/Kip
cyclin D
CDK4/6
cyclin E
CDK2
Rb
P
E2F
G1
S
Fetal stem cells
C
Bmi-1
Hmga2
let-7
p18Ink4c
p16Ink4a
p19Arf
PI3K
p53
Cip/Kip
cyclin D
CDK4/6
cyclin E
CDK2
Rb
P
E2F
G1
S
R
G0
Young adult stem cells
D
Bmi-1
Hmga2
let-7
p16Ink4a
p19Arf
PI3K
p53
Cip/Kip
cyclin D
CDK4/6
cyclin E
CDK2
Rb
P
E2F
G1
S
R
G0
Old adult stem cells

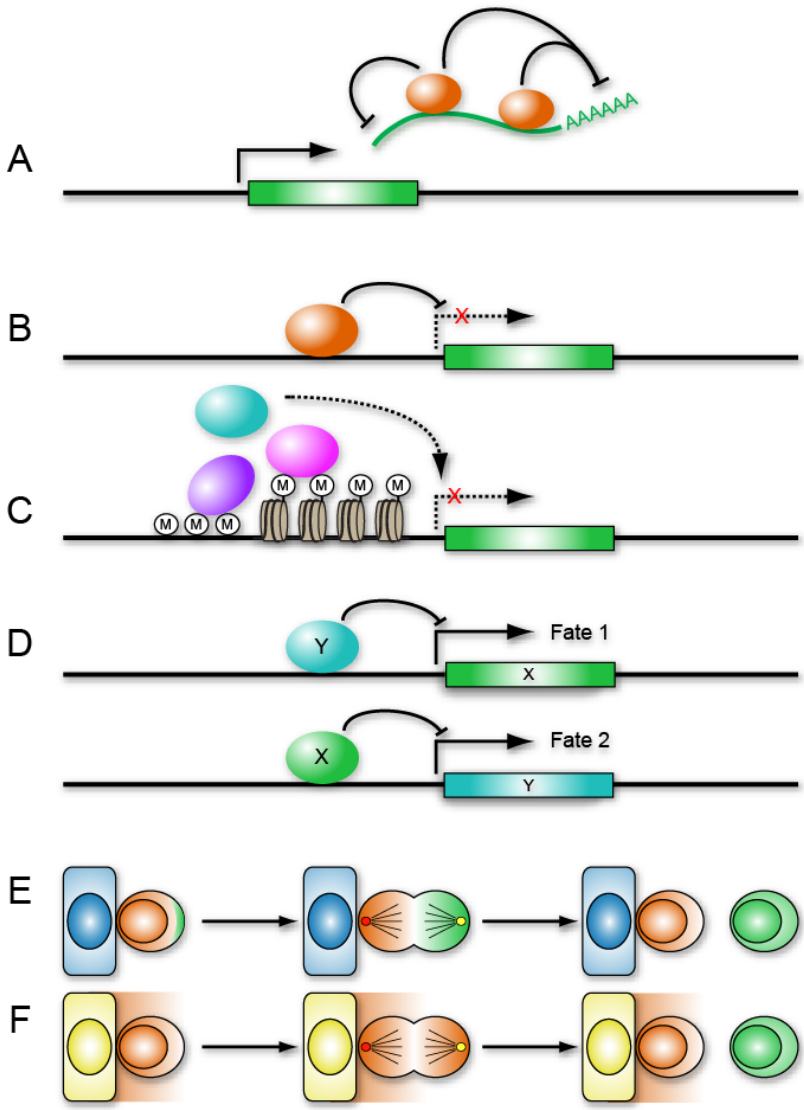

Figure 1.3: Mechanisms suppressing stem cell differentiation.
A) In some systems, such as the *C. elegans* germline, differentiation is blocked by RNA-binding proteins that post-transcriptionally block the function of differentiation-inducing gene product. B) Expression of lineage specification genes can be repressed by stem cell-specific transcription factors (orange oval). C) Epigenetic modifications can also contribute to the repression of these genes by recruiting chromatin modifiers and transcriptional repressors. D) A balance among lineage specification genes that promote alternative fates may suppress differentiation by mutual inhibition (Shin et al., 2008). E) Intrinsically asymmetric divisions can ensure that one daughter remains a stem cell by asymmetrically segregating factors that promote stem-cell identity (Lee et al., 2006a) or that inhibit differentiation (Seydoux et al., 1996) to one daughter (orange). F) Asymmetric divisions can also suppress differentiation by ensuring that one daughter cell remains within the niche (yellow), and exposed to factors that promote stem-cell maintenance (orange), while the other daughter cell is displaced from the niche (green) similar to *Drosophila* spermatogonial stem cells (Fuller and Spradling, 2007).

Figure 1.4: Niche regulation of stem cell self-renewal
A) In *Drosophila* testis, germ-line stem cells (GSCs) are anchored to the hub cells (niche) through DE-cadherin and β-catenin/armadillo (Arm) mediated adherens junctions. Hub cells also secrete Upaired and Gbb/Dpp to activate JAK-STAT and BMP signaling in the GSCs which suppress GSC differentiation by repressing Bam expression. The mother centrosome in GSCs (red circle) is tethered to the adherens junction by the Adenomatous Polyposis Coli (APC2) complex, while the daughter centrosome (yellow circle) migrates to the other pole of the cell. This determines spindle orientation and the polarity of division, such that stem cells divide asymmetrically to generate one daughter that remains a stem cell within the niche and another daughter that is displaced from the niche and fated to differentiate. B) In the *C.elegans* germ line, the distal tip cell (DTC) expresses the Notch ligand LAG-2, which binds to and activates GLP-1 on GSCs to induce Notch signaling. GLP-1/Notch activation induces the expression of the RNA-binding protein FBF-1 and FBF-2 which suppress GSC differentiation by repressing the translation of the meiosis-inducing transcripts, gld-1 and gld-3. C) Models for the HSC niche. Endosteal and perivascular cells have been implicated in the regulation of HSC maintenance, though the cell type(s) that produce the factors that maintain HSCs remain uncertain, and diverse models remain compatible with existing evidence: a, Spatially distinct but redundant endosteal and perivascular niches may maintain HSCs through similar mechanisms. b, Spatially and functionally distinct endosteal and perivascular niches may maintain HSCs through different mechanisms. c, Endosteal and perivascular cells may work together to form a common niche influenced by both cell types. d, As yet identified cells may create niches or "zones" of HSC maintenance. These models are not mutually exclusive and are not the only models consistent with existing evidence. D, The subventricular zone niche. Neural stem cells (type B-cells) generate transiently amplifying (type C) cells, which then form (type A) neuroblasts. Neural stem cell maintenance is regulated by factors produced by ependymal cells (E) as well as perivascular cells. Neural stem cells contact the ventricle through a short apical process and a blood vessel through a long basal process (Mirzadeh et al., 2008).

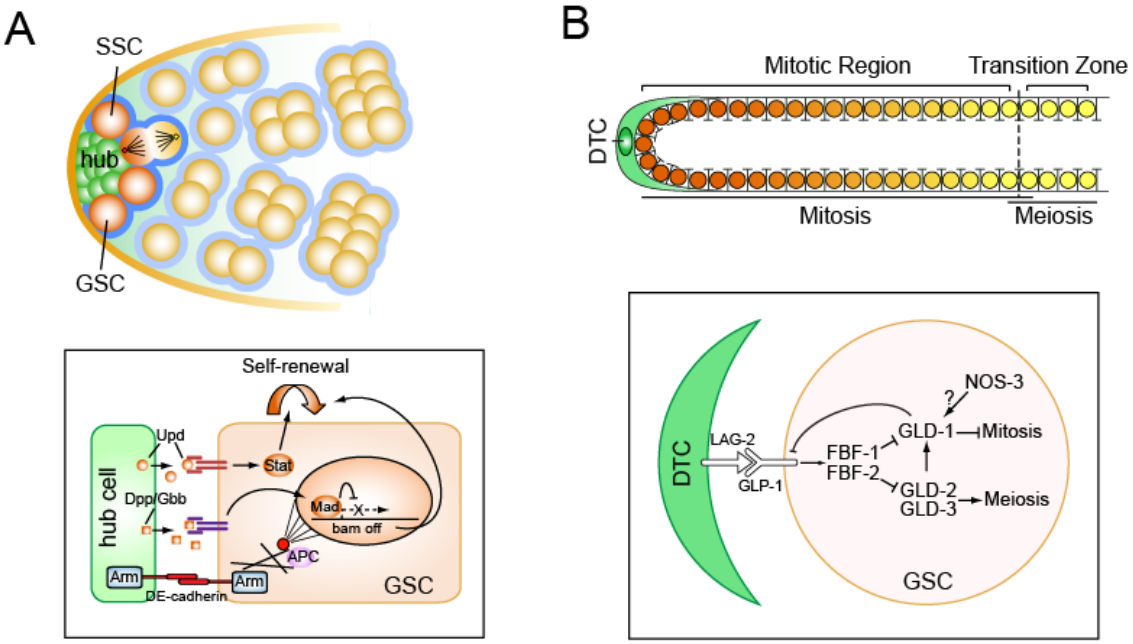
A
SSC
hub
GSC
Self-renewal
hub cell
Upd
Stat
Dpp/Gbb
Mad
-X-
bam off
APC
Arm
Arm
DE-cadherin
GSC
B
Mitotic Region
Transition Zone
DTC
Mitosis
Meiosis
NOS-3
?
GLD-1
Mitosis
LAG-2
FBF-1
FBF-2
GLP-1
GLD-2
GLD-3
Meiosis
DTC
GSC
C
Endosteal cells
Mesenchymal progenitor
a
b
HSC
Sinusoid
Osteoclast
Megakaryocyte
c
d
D
Lateral ventricle
Blood vessel
B
E
A
C

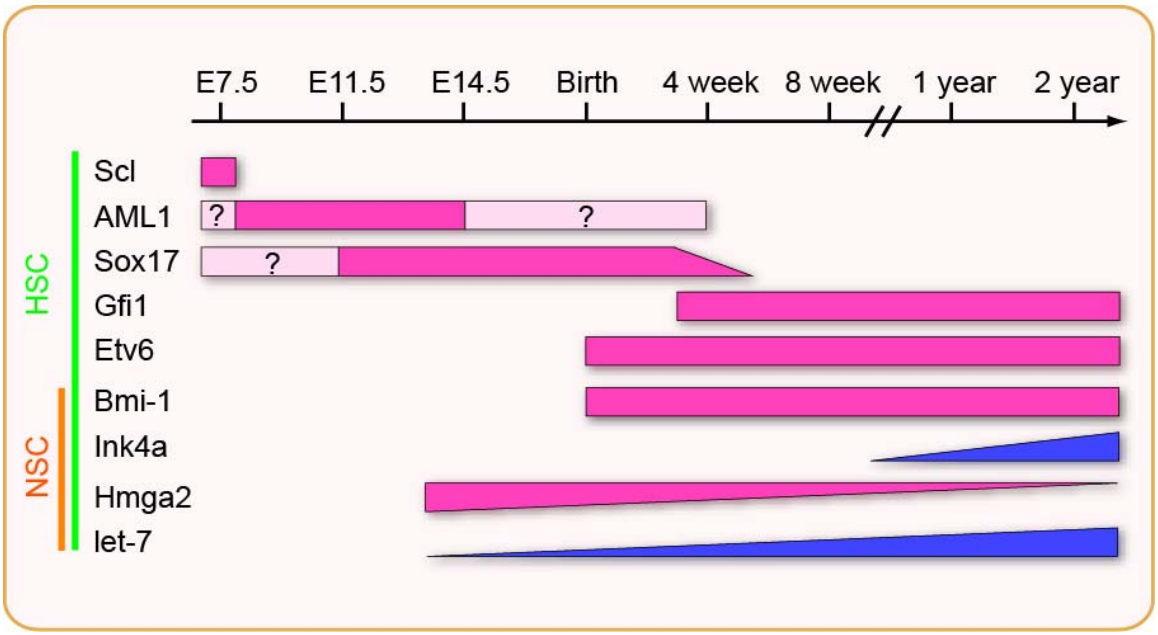

Figure 1.5: Distinct factors regulate hematopoietic stem cell (HSC) and neural stem cell (NSC) self-renewal at different ages.
Schematic representation of stage-specific regulators of HSC and NSC self-renewal. The functional importance of each factor at each developmental stage is depicted by the color shading of bar graph (red indicates a positive regulator of self-renewal; blue indicates a negative regulator of self-renewal).

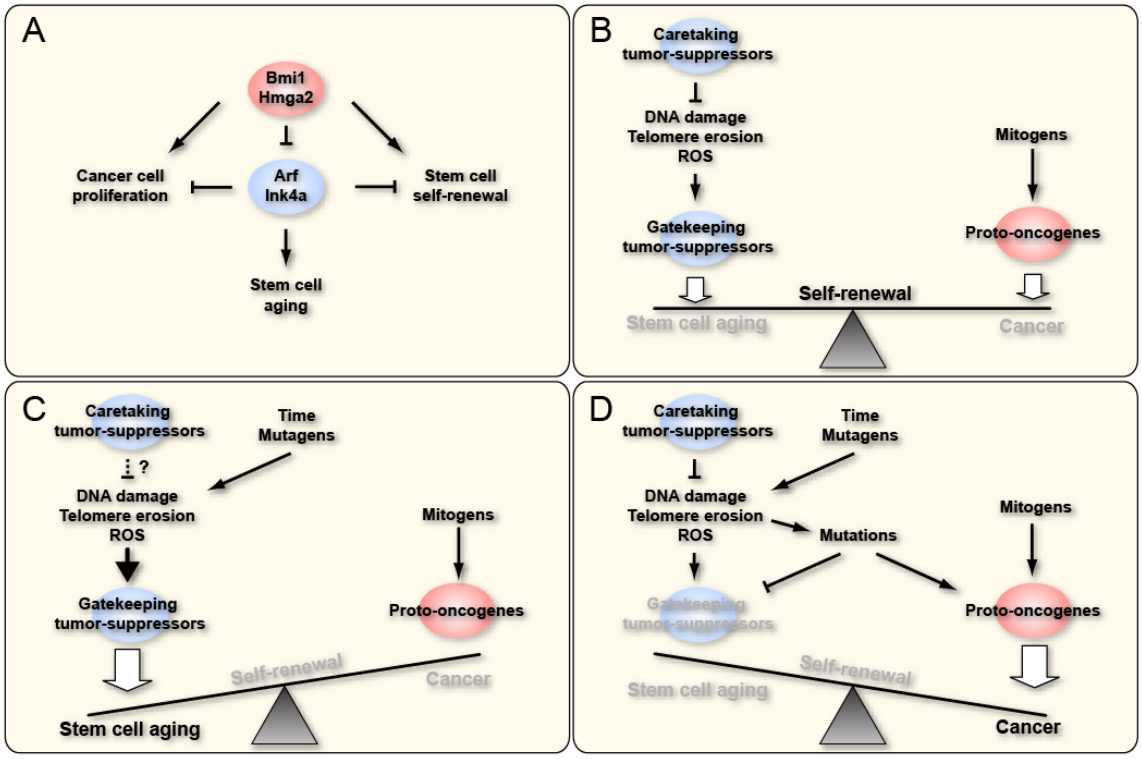

Figure 1.6: Stem cell self-renewal, stem cell aging and cancer cell proliferation are regulated by common networks of proto-oncogenes and tumor suppressors.
A,B) Stem cell self-renewal is maintained by a balance between proto-oncogenes and gate-keeping tumor suppressors. Proto-oncogenes promote stem cell self-renewal and cancer cell proliferation, while gate-keeping tumor suppressors negatively regulate self-renewal and promote stem cell aging. C) As organisms age, DNA damage accumulates and telomeres erode, activating gate-keeping tumor suppressors and leading to reduced stem cell function and tissue regenerative capacity. D) DNA damage can also activate oncogenes and inactivate gate-keeping tumor suppressors, disrupting the balance in their activities and leading to cancer.

BIBLIOGRAPHY

Ajioka, I., Martins, R.A., Bayazitov, I.T., Donovan, S., Johnson, D.A., Frase, S., Cicero, S.A., Boyd, K., Zakharenko, S.S., and Dyer, M.A. (2007). Differentiated horizontal interneurons clonally expand to form metastatic retinoblastoma in mice. Cell *131*, 378-390.

Akala, O.O., Park, I.K., Qian, D., Pihalja, M., Becker, M.W., and Clarke, M.F. (2008). Long-term haematopoietic reconstitution by Trp53-/-p16Ink4a-/-p19Arf-/- multipotent progenitors. Nature *453*, 228-232.

Aladjem, M.I., Spike, B.T., Rodewald, L.W., Hope, T.J., Klemm, M., Jaenisch, R., and Wahl, G.M. (1998). ES cells do not activate p53-dependent stress responses and undergo p53-independent apoptosis in response to DNA damage. Curr Biol *8*, 145-155.

Allen, D.M., van Praag, H., Ray, J., Weaver, Z., Winrow, C.J., Carter, T.A., Braquet, R., Harrington, E., Ried, T., Brown, K.D.*, et al.* (2001). Ataxia telangiectasia mutated is essential during adult neurogenesis. Genes Dev *15*, 554-566.

Allsopp, R.C., Morin, G.B., DePinho, R., Harley, C.B., and Weissman, I.L. (2003). Telomerase is required to slow telomere shortening and extend replicative lifespan of HSCs during serial transplantation. Blood *102*, 517-520.

Angelastro, J.M., Ignatova, T.N., Kukekov, V.G., Steindler, D.A., Stengren, G.B., Mendelsohn, C., and Greene, L.A. (2003). Regulated expression of ATF5 is required for the progression of neural progenitor cells to neurons. J Neurosci *23*, 4590-4600.

Angelastro, J.M., Mason, J.L., Ignatova, T.N., Kukekov, V.G., Stengren, G.B., Goldman, J.E., and Greene, L.A. (2005). Downregulation of activating transcription factor 5 is required for differentiation of neural progenitor cells into astrocytes. J Neurosci *25*, 3889-3899.

Arai, F., Hirao, A., Ohmura, M., Sato, H., Matsuoka, S., Takubo, K., Ito, K., Koh, G.Y., and Suda, T. (2004). Tie2/angiopoietin-1 signaling regulates hematopoietic stem cell quiescence in the bone marrow niche. Cell *118*, 149-161.

Avilion, A.A., Nicolis, S.K., Pevny, L.H., Perez, L., Vivian, N., and Lovell-Badge, R. (2003). Multipotent cell lineages in early mouse development depend on SOX2 function. Genes Dev *17*, 126-140.

Azuara, V., Perry, P., Sauer, S., Spivakov, M., Jorgensen, H.F., John, R.M., Gouti, M., Casanova, M., Warnes, G., Merkenschlager, M.*, et al.* (2006). Chromatin signatures of pluripotent cell lines. Nat Cell Biol *8*, 532-538.

Bachoo, R.M., Maher, E.A., Ligon, K.L., Sharpless, N.E., Chan, S.S., You, M.J., Tang, Y., DeFrances, J., Stover, E., Weissleder, R.*, et al.* (2002). Epidermal growth factor receptor and Ink4a/Arf: convergent mechanisms governing terminal differentiation and transformation along the neural stem cell to astrocyte axis. Cancer Cell *1*, 269-277.

Balaban, R.S., Nemoto, S., and Finkel, T. (2005). Mitochondria, oxidants, and aging. Cell *120*, 483-495.

Balordi, F., and Fishell, G. Mosaic Removal of Hedgehog Signaling in the Adult SVZ Reveals That the Residual Wild-Type Stem Cells Have a Limited Capacity for Self-Renewal. J Neurosci *27*, 14248-14259.

Balordi, F., and Fishell, G. (2007). Hedgehog signaling in the subventricular zone is required for both the maintenance of stem cells and the migration of newborn neurons. J Neurosci *27*, 5936-5947.

Barker, N., van Es, J.H., Kuipers, J., Kujala, P., van den Born, M., Cozijnsen, M., Haegebarth, A., Korving, J., Begthel, H., Peters, P.J., *et al.* (2007). Identification of stem cells in small intestine and colon by marker gene Lgr5. Nature.

Barroca, V., Lassalle, B., Coureuil, M., Louis, J.P., Le Page, F., Testart, J., Allemand, I., Riou, L., and Fouchet, P. (2008). Mouse differentiating spermatogonia can generate germinal stem cells in vivo. Nat Cell Biol.

Barzilai, A., Rotman, G., and Shiloh, Y. (2002). ATM deficiency and oxidative stress: a new dimension of defective response to DNA damage. DNA repair *1*, 3-25.

Bender, C.F., Sikes, M.L., Sullivan, R., Huye, L.E., Le Beau, M.M., Roth, D.B., Mirzoeva, O.K., Oltz, E.M., and Petrini, J.H. (2002). Cancer predisposition and hematopoietic failure in Rad50(S/S) mice. Genes Dev *16*, 2237-2251.

Bernstein, B.E., Mikkelsen, T.S., Xie, X., Kamal, M., Huebert, D.J., Cuff, J., Fry, B., Meissner, A., Wernig, M., Plath, K., *et al.* (2006). A Bivalent Chromatin Structure Marks Key Developmental Genes in Embryonic Stem Cells. Cell *125*, 315-326.

Berry, L.W., Westlund, B., and Schedl, T. (1997). Germ-line tumor formation caused by activation of glp-1, a Caenorhabditis elegans member of the Notch family of receptors. Development *124*, 925-936.

Blanpain, C., and Fuchs, E. (2006). Epidermal stem cells of the skin. Annu Rev Cell Dev Biol *22*, 339-373.

Blasco, M.A., Lee, H.W., Hande, M.P., Samper, E., Lansdorp, P.M., DePinho, R.A., and Greider, C.W. (1997). Telomere shortening and tumor formation by mouse cells lacking telomerase RNA. Cell *91*, 25-34.

Boyer, L.A., Lee, T.I., Cole, M.F., Johnstone, S.E., Levine, S.S., Zucker, J.P., Guenther, M.G., Kumar, R.M., Murray, H.L., Jenner, R.G., *et al.* (2005). Core transcriptional regulatory circuitry in human embryonic stem cells. Cell *122*, 947-956.

Boyer, L.A., Plath, K., Zeitlinger, J., Brambrink, T., Medeiros, L.A., Lee, T.I., Levine, S.S., Wernig, M., Tajonar, A., Ray, M.K., *et al.* (2006). Polycomb complexes repress developmental regulators in murine embryonic stem cells. Nature *441*, 349-353.

Brack, A.S., Conboy, M.J., Roy, S., Lee, M., Kuo, C.J., Keller, C., and Rando, T.A. (2007). Increased Wnt signaling during aging alters muscle stem cell fate and increases fibrosis. Science (New York, NY *317*, 807-810.

Bracken, A.P., Kleine-Kohlbrecher, D., Dietrich, N., Pasini, D., Gargiulo, G., Beekman, C., Theilgaard-Monch, K., Minucci, S., Porse, B.T., Marine, J.C., *et al.* (2007). The Polycomb group proteins bind throughout the INK4A-ARF locus and are disassociated in senescent cells. Genes Dev *21*, 525-530.

Brawley, C., and Matunis, E. (2004). Regeneration of male germline stem cells by spermatogonial dedifferentiation in vivo. Science (New York, NY *304*, 1331-1334.

Broske, A.M., Vockentanz, L., Kharazi, S., Huska, M.R., Mancini, E., Scheller, M., Kuhl, C., Enns, A., Prinz, M., Jaenisch, R., *et al.* (2009). DNA methylation protects hematopoietic stem cell multipotency from myeloerythroid restriction. Nat Genet *41*, 1207-1215.

Bruggeman, S.W., Hulsman, D., Tanger, E., Buckle, T., Blom, M., Zevenhoven, J., van Tellingen, O., and van Lohuizen, M. (2007). Bmi1 controls tumor development in an Ink4a/Arf-independent manner in a mouse model for glioma. Cancer Cell *12*, 328-341.

Bruggeman, S.W., Valk-Lingbeek, M.E., van der Stoop, P.P., Jacobs, J.J., Kieboom, K., Tanger, E., Hulsman, D., Leung, C., Arsenijevic, Y., Marino, S., *et al.* (2005). Ink4a and Arf differentially affect cell proliferation and neural stem cell self-renewal in Bmi1-deficient mice. Genes Dev *19*, 1438-1443.

Bryan, T.M., Englezou, A., Dalla-Pozza, L., Dunham, M.A., and Reddel, R.R. (1997). Evidence for an alternative mechanism for maintaining telomere length in human tumors and tumor-derived cell lines. Nat Med *3*, 1271-1274.

Burdon, T., Smith, A., and Savatier, P. (2002). Signalling, cell cycle and pluripotency in embryonic stem cells. Trends in Cell Biology *12*, 432-438.

Campisi, J. (2005). Senescent cells, tumor suppression, and organismal aging: good citizens, bad neighbors. Cell *120*, 513-522.

Cartwright, P., McLean, C., Sheppard, A., Rivett, D., Jones, K., and Dalton, S. (2005). LIF/STAT3 controls ES cell self-renewal and pluripotency by a Myc-dependent mechanism. Development *132*, 885-896.

Chambers, I., Colby, D., Robertson, M., Nichols, J., Lee, S., Tweedie, S., and Smith, A. (2003). Functional expression cloning of Nanog, a pluripotency sustaining factor in embryonic stem cells. Cell *113*, 643-655.

Chambers, I., Silva, J., Colby, D., Nichols, J., Nijmeijer, B., Robertson, M., Vrana, J., Jones, K., Grotewold, L., and Smith, A. (2007). Nanog safeguards pluripotency and mediates germline development. Nature *450*, 1230-1234.

Cheng, J., Turkel, N., Hemati, N., Fuller, M.T., Hunt, A.J., and Yamashita, Y.M. (2008). Centrosome misorientation reduces stem cell division during ageing. Nature *456*, 599-604.

Cheng, T., Rodrigues, N., Dombkowski, D., Stier, S., and Scadden, D.T. (2000). Stem cell repopulation efficiency but not pool size is governed by p27(kip1). Nat Med *6*, 1235-1240.

Cheshier, S.H., Morrison, S.J., Liao, X., and Weissman, I.L. (1999). In vivo proliferation and cell cycle kinetics of long-term self-renewing hematopoietic stem cells. Proc Natl Acad Sci U S A *96*, 3120-3125.

Chin, L., Artandi, S.E., Shen, Q., Tam, A., Lee, S.L., Gottlieb, G.J., Greider, C.W., and DePinho, R.A. (1999). p53 deficiency rescues the adverse effects of telomere loss and cooperates with telomere dysfunction to accelerate carcinogenesis. Cell *97*, 527-538.

Conboy, I.M., Conboy, M.J., Smythe, G.M., and Rando, T.A. (2003). Notch-mediated restoration of regenerative potential to aged muscle. Science (New York, NY *302*, 1575-1577.

Conboy, I.M., Conboy, M.J., Wagers, A.J., Girma, E.R., Weissman, I.L., and Rando, T.A. (2005). Rejuvenation of aged progenitor cells by exposure to a young systemic environment. Nature *433*, 760-764.

Counter, C.M., Avilion, A.A., LeFeuvre, C.E., Stewart, N.G., Greider, C.W., Harley, C.B., and Bacchetti, S. (1992). Telomere shortening associated with chromosome instability is arrested in immortal cells which express telomerase activity. The EMBO journal *11*, 1921-1929.

Crittenden, S.L., Leonhard, K.A., Byrd, D.T., and Kimble, J. (2006). Cellular analyses of the mitotic region in the Caenorhabditis elegans adult germ line. Mol Biol Cell *17*, 3051-3061.

Daria, D., Filippi, M.D., Knudsen, E.S., Faccio, R., Li, Z., Kalfa, T., and Geiger, H. (2008). The retinoblastoma tumor suppressor is a critical intrinsic regulator for hematopoietic stem and progenitor cells under stress. Blood *111*, 1894-1902.

de Haan, G., Nijhof, W., and Van Zant, G. (1997). Mouse strain-dependent changes in frequency and proliferation of hematopoietic stem cells during aging: correlation between lifespan and cycling activity. Blood *89*, 1543-1550.

de Haan, G., and Van Zant, G. (1999). Dynamic changes in mouse hematopoietic stem cell numbers during aging. Blood *93*, 3294-3301.

Dejosez, M., Krumenacker, J.S., Zitur, L.J., Passeri, M., Chu, L.-F., Songyang, Z., Thomson, J.A., and Zwaka, T.P. (2008). Ronin Is Essential for Embryogenesis and the Pluripotency of Mouse Embryonic Stem Cells. Cell *133*, 1162-1174.

Desai, A.R., and McConnell, S.K. (2000). Progressive restriction in fate potential by neural progenitors during cerebral cortical development. Development *127*, 2863-2872.

Doetsch, F., Verdugo, J.M., Caille, I., Alvarez-Buylla, A., Chao, M.V., and Casaccia-Bonnefil, P. (2002). Lack of the cell-cycle inhibitor p27Kip1 results in selective increase of transit-amplifying cells for adult neurogenesis. J Neurosci *22*, 2255-2264.

Drummond-Barbosa, D., and Spradling, A.C. (2001). Stem cells and their progeny respond to nutritional changes during Drosophila oogenesis. Dev Biol *231*, 265-278.

Fan, G., Martinowich, K., Chin, M.H., He, F., Fouse, S.D., Hutnick, L., Hattori, D., Ge, W., Shen, Y., Wu, H.*, et al.* (2005). DNA methylation controls the timing of astrogliogenesis through regulation of JAK-STAT signaling. Development *132*, 3345-3356.

Ferron, S., Mira, H., Franco, S., Cano-Jaimez, M., Bellmunt, E., Ramirez, C., Farinas, I., and Blasco, M.A. (2004). Telomere shortening and chromosomal instability abrogates proliferation of adult but not embryonic neural stem cells. Development *131*, 4059-4070.

Ficara, F., Murphy, M.J., Lin, M., and Cleary, M.L. (2008). Pbx1 regulates self-renewal of long-term hematopoietic stem cells by maintaining their quiescence. Cell Stem Cell *2*, 484-496.

Foudi, A., Hochedlinger, K., Van Buren, D., Schindler, J.W., Jaenisch, R., Carey, V., and Hock, H. (2008). Analysis of histone 2B-GFP retention reveals slowly cycling hematopoietic stem cells. Nat Biotechnol.

Fraser, S.E., Bronner-Fraser, M., and Division of Biology, B.I.C.I.o.T.P. (1991). Migrating neural crest cells in the trunk of the avian embryo are multipotent. Development *112(4)*, 913-920.

Fuchs, E., Tumbar, T., and Guasch, G. (2004). Socializing with the neighbors: stem cells and their niche. Cell *116*, 769-778.

Fujikura, J., Yamato, E., Yonemura, S., Hosoda, K., Masui, S., Nakao, K., Miyazaki Ji, J., and Niwa, H. (2002). Differentiation of embryonic stem cells is induced by GATA factors. Genes Dev *16*, 784-789.

Fujita, J., Crane, A.M., Souza, M.K., Dejosez, M., Kyba, M., Flavell, R.A., Thomson, J.A., and Zwaka, T.P. (2008). Caspase Activity Mediates the Differentiation of Embryonic Stem Cells. Cell Stem Cell *2*, 595-601.

Fuller, M.T., and Spradling, A.C. (2007). Male and female Drosophila germline stem cells: two versions of immortality. Science (New York, NY *316*, 402-404.

Giacinti, C., and Giordano, A. (2006). RB and cell cycle progression. Oncogene *25*, 5220-5227.

Gilliland, D.G., Jordan, C.T., and Felix, C.A. (2004). The molecular basis of leukemia. Hematology Am Soc Hematol Educ Program, 80-97.

Gilson, E., and Geli, V. (2007). How telomeres are replicated. Nat Rev Mol Cell Biol *8*, 825-838.

Gonczy, P. (2008). Mechanisms of asymmetric cell division: flies and worms pave the way. Nat Rev Mol Cell Biol *9*, 355-366.

Graham, V., Khudyakov, J., Ellis, P., and Pevny, L. (2003). SOX2 functions to maintain neural progenitor identity. Neuron *39*, 749-765.

Groszer, M., Erickson, R., Scripture-Adams, D.D., Dougherty, J.D., Le Belle, J., Zack, J.A., Geschwind, D.H., Liu, X., Kornblum, H.I., and Wu, H. (2006). PTEN negatively regulates neural stem cell self-renewal by modulating G0-G1 cell cycle entry. Proc Natl Acad Sci U S A *103*, 111-116.

Groszer, M., Erickson, R., Scripture-Adams, D.D., Lesche, R., Trumpp, A., Zack, J.A., Kornblum, H.I., Liu, X., and Wu, H. (2001). Negative regulation of neural stem/progenitor cell proliferation by the Pten tumor suppressor gene in vivo. Science (New York, NY *294*, 2186-2189.

Harrison, D.E., and Astle, C.M. (1982). Loss of stem cell repopulating ability upon transplantation. Effects of donor age, cell number, and transplantation procedure. J Exp Med *156*, 1767-1779.

Hayakawa, K., Hardy, R.R., Hertzenberg, L.A., and Herzenberg, L.A. (1985). Progenitors for Ly-1 B cells are distinct from progenitors for other B cells. J Exp Med *161*, 1554-1568.

Hermanson, O., Jepsen, K., and Rosenfeld, M.G. (2002). N-CoR controls differentiation of neural stem cells into astrocytes. Nature *419*, 934-939.

Herrera, E., Samper, E., Martin-Caballero, J., Flores, J.M., Lee, H.W., and Blasco, M.A. (1999). Disease states associated with telomerase deficiency appear earlier in mice with short telomeres. The EMBO journal *18*, 2950-2960.

Hock, H., Hamblen, M.J., Rooke, H.M., Schindler, J.W., Saleque, S., Fujiwara, Y., and Orkin, S.H. (2004a). Gfi-1 restricts proliferation and preserves functional integrity of haematopoietic stem cells. Nature *431*, 1002-1007.

Hock, H., Meade, E., Medeiros, S., Schindler, J.W., Valk, P.J., Fujiwara, Y., and Orkin, S.H. (2004b). Tel/Etv6 is an essential and selective regulator of adult hematopoietic stem cell survival. Genes Dev *18*, 2336-2341.

Horsley, V., Aliprantis, A.O., Polak, L., Glimcher, L.H., and Fuchs, E. (2008). NFATc1 balances quiescence and proliferation of skin stem cells. Cell *132*, 299-310.

Huttner, W.B., and Kosodo, Y. (2005). Symmetric versus asymmetric cell division during neurogenesis in the developing vertebrate central nervous system. Current opinion in cell biology *17*, 648-657.

Ichikawa, M., Asai, T., Saito, T., Yamamoto, G., Seo, S., Yamazaki, I., Yamagata, T., Mitani, K., Chiba, S., Hirai, H., *et al.* (2004). AML-1 is required for megakaryocytic maturation and lymphocytic differentiation, but not for maintenance of hematopoietic stem cells in adult hematopoiesis. Nat Med *10*, 299-304.

Ikuta, K., Kina, T., Macneil, I., Uchida, N., Peault, B., Chien, Y.H., and Weissman, I.L. (1990). A developmental switch in thymic lymphocyte maturation potential occurs at the level of hematopoietic stem cells. Cell *62*, 863-874.

Ito, K., Hirao, A., Arai, F., Matsuoka, S., Takubo, K., Hamaguchi, I., Nomiyama, K., Hosokawa, K., Sakurada, K., Nakagata, N., *et al.* (2004). Regulation of oxidative stress by ATM is required for self-renewal of haematopoietic stem cells. Nature *431*, 997-1002.

Ito, K., Hirao, A., Arai, F., Takubo, K., Matsuoka, S., Miyamoto, K., Ohmura, M., Naka, K., Hosokawa, K., Ikeda, Y., *et al.* (2006). Reactive oxygen species act through p38 MAPK to limit the lifespan of hematopoietic stem cells. Nat Med *12*, 446-451.

Iwasaki, H., Somoza, C., Shigematsu, H., Duprez, E.A., Iwasaki-Arai, J., Mizuno, S., Arinobu, Y., Geary, K., Zhang, P., Dayaram, T., *et al.* (2005). Distinctive and indispensable roles of PU.1 in maintenance of hematopoietic stem cells and their differentiation. Blood *106*, 1590-1600.

Jacobs, J.J., Kieboom, K., Marino, S., DePinho, R.A., and van Lohuizen, M. (1999). The oncogene and Polycomb-group gene bmi-1 regulates cell proliferation and senescence through the ink4a locus. Nature *397*, 164-168.

Jaenisch, R., and Young, R. (2008). Stem cells, the molecular circuitry of pluripotency and nuclear reprogramming. Cell *132*, 567-582.

Janzen, V., Forkert, R., Fleming, H.E., Saito, Y., Waring, M.T., Dombkowski, D.M., Cheng, T., DePinho, R.A., Sharpless, N.E., and Scadden, D.T. (2006). Stem-cell ageing modified by the cyclin-dependent kinase inhibitor p16INK4a. Nature *443*, 421-426.

Jude, C.D., Climer, L., Xu, D., Artinger, E., Fisher, J.K., and Ernst, P. (2007). Unique and independent roles for MLL in adult hematopoietic stem cells and progenitors. Cell Stem Cell *1*, 324-337.

Kai, T., and Spradling, A. (2003). An empty Drosophila stem cell niche reactivates the proliferation of ectopic cells. Proc Natl Acad Sci U S A *100*, 4633-4638.

Kantor, A.B., Stall, A.M., Adams, S., Herzenberg, L.A., and Herzenberg, L.A. (1992). Differential development of progenitor activity for three B-cell lineages. Proceedings of the National Academy of Sciences USA *89*, 3320-3324.

Kiel, M.J., He, S., Ashkenazi, R., Gentry, S.N., Teta, M., Kushner, J.A., Jackson, T.L., and Morrison, S.J. (2007). Haematopoietic stem cells do not asymmetrically segregate chromosomes or retain BrdU. Nature *449*, 238-242.

Kiel, M.J., and Morrison, S.J. (2008). Uncertainty in the niches that maintain haematopoietic stem cells. Nat Rev Immunol *8*, 290-301.

Kiger, A.A., Jones, D.L., Schulz, C., Rogers, M.B., and Fuller, M.T. (2001). Stem cell self-renewal specified by JAK-STAT activation in response to a support cell cue. Science (New York, NY *294*, 2542-2545.

Kim, H.G., de Guzman, C.G., Swindle, C.S., Cotta, C.V., Gartland, L., Scott, E.W., and Klug, C.A. (2004). The ETS family transcription factor PU.1 is necessary for the maintenance of fetal liver hematopoietic stem cells. Blood *104*, 3894-3900.

Kim, I., Saunders, T.L., and Morrison, S.J. (2007). Sox17 dependence distinguishes the transcriptional regulation of fetal from adult hematopoietic stem cells. Cell *130*, 470-483.

Kimble, J., and Crittenden, S.L. (2007). Controls of Germline Stem Cells, Entry into Meiosis, and the Sperm/Oocyte Decision in Caenorhabditis elegans. Annu Rev Cell Dev Biol *23*, 405-433.

Kinzler, K.W., and Vogelstein, B. (1997). Cancer-susceptibility genes. Gatekeepers and caretakers. Nature *386*, 761, 763.

Kippin, T.E., Martens, D.J., and van der Kooy, D. (2005). p21 loss compromises the relative quiescence of forebrain stem cell proliferation leading to exhaustion of their proliferation capacity. Genes Dev *19*, 756-767.

Knoblich, J.A. (2008). Mechanisms of Asymmetric Stem Cell Division. Cell *132*, 583-597.

Kobielak, K., Stokes, N., de la Cruz, J., Polak, L., and Fuchs, E. (2007). Loss of a quiescent niche but not follicle stem cells in the absence of bone morphogenetic protein signaling. Proc Natl Acad Sci U S A *104*, 10063-10068.

Kollet, O., Dar, A., Shivtiel, S., Kalinkovich, A., Lapid, K., Sztainberg, Y., Tesio, M., Samstein, R.M., Goichberg, P., Spiegel, A.*, et al.* (2006). Osteoclasts degrade endosteal components and promote mobilization of hematopoietic progenitor cells. Nat Med *12*, 657-664.

Kotake, Y., Cao, R., Viatour, P., Sage, J., Zhang, Y., and Xiong, Y. (2007). pRB family proteins are required for H3K27 trimethylation and Polycomb repression complexes binding to and silencing p16INK4alpha tumor suppressor gene. Genes Dev *21*, 49-54.

Kozar, K., Ciemerych, M.A., Rebel, V.I., Shigematsu, H., Zagozdzon, A., Sicinska, E., Geng, Y., Yu, Q., Bhattacharya, S., Bronson, R.T.*, et al.* (2004). Mouse development and cell proliferation in the absence of D-cyclins. Cell *118*, 477-491.

Krishnamurthy, J., Ramsey, M.R., Ligon, K.L., Torrice, C., Koh, A., Bonner-Weir, S., and Sharpless, N.E. (2006). p16INK4a induces an age-dependent decline in islet regenerative potential. Nature *443*, 453-457.

Krishnamurthy, J., Torrice, C., Ramsey, M.R., Kovalev, G.I., Al-Regaiey, K., Su, L., and Sharpless, N.E. (2004). Ink4a/Arf expression is a biomarker of aging. J Clin Invest *114*, 1299-1307.

Kruger, G.M., Mosher, J.T., Bixby, S., Joseph, N., Iwashita, T., and Morrison, S.J. (2002). Neural crest stem cells persist in the adult gut but undergo changes in self-renewal, neuronal subtype potential, and factor responsiveness. Neuron *35*, 657-669.

Kuang, S., Kuroda, K., Le Grand, F., and Rudnicki, M.A. (2007). Asymmetric self-renewal and commitment of satellite stem cells in muscle. Cell *129*, 999-1010.

LaFever, L., and Drummond-Barbosa, D. (2005). Direct control of germline stem cell division and cyst growth by neural insulin in Drosophila. Science (New York, NY *309*, 1071-1073.

Laslo, P., Pongubala, J.M., Lancki, D.W., and Singh, H. (2008). Gene regulatory networks directing myeloid and lymphoid cell fates within the immune system. Seminars in immunology *20*, 228-235.

Lechler, T., and Fuchs, E. (2005). Asymmetric cell divisions promote stratification and differentiation of mammalian skin. Nature *437*, 275-280.

Lee, C.Y., Robinson, K.J., and Doe, C.Q. (2006a). Lgl, Pins and aPKC regulate neuroblast self-renewal versus differentiation. Nature *439*, 594-598.

Lee, H.W., Blasco, M.A., Gottlieb, G.J., Horner, J.W., 2nd, Greider, C.W., and DePinho, R.A. (1998). Essential role of mouse telomerase in highly proliferative organs. Nature *392*, 569-574.

Lee, T.I., Jenner, R.G., Boyer, L.A., Guenther, M.G., Levine, S.S., Kumar, R.M., Chevalier, B., Johnstone, S.E., Cole, M.F., Isono, K.*, et al.* (2006b). Control of developmental regulators by Polycomb in human embryonic stem cells. Cell *125*, 301-313.

Lessard, J., and Sauvageau, G. (2003). Bmi-1 determines the proliferative capacity of normal and leukaemic stem cells. Nature *423*, 255-260.

Leung, C., Lingbeek, M., Shakhova, O., Liu, J., Tanger, E., Saremaslani, P., Van Lohuizen, M., and Marino, S. (2004). Bmi1 is essential for cerebellar development and is overexpressed in human medulloblastomas. Nature *428*, 337-341.

Levi, B.P., and Morrison, S.J. (2009). Stem Cells Use Distinct Self-renewal Programs at Different Ages. Cold Spring Harb Symp Quant Biol.

Liang, Y., Van Zant, G., and Szilvassy, S.J. (2005). Effects of aging on the homing and engraftment of murine hematopoietic stem and progenitor cells. Blood.

Lin, H. (2008). Cell biology of stem cells: an enigma of asymmetry and self-renewal. J Cell Biol *180*, 257-260.

Liu, H., Fergusson, M.M., Castilho, R.M., Liu, J., Cao, L., Chen, J., Malide, D., Rovira, II, Schimel, D., Kuo, C.J.*, et al.* (2007). Augmented Wnt signaling in a mammalian model of accelerated aging. Science (New York, NY *317*, 803-806.

Liu, Y., Elf, S.E., Miyata, Y., Sashida, G., Huang, G., Di Giandomenico, S., Lee, J.M., Deblasio, A., Menendez, S., Antipin, J.*, et al.* (2009). p53 Regulates Hematopoietic Stem Cell Quiescence. Cell Stem Cell *4*, 37-48.

Livesey, F.J., and Cepko, C.L. (2001). Vertebrate neural cell-fate determination: lessons from the retina. Nature Reviews Neuroscience *2*, 109-118.

Loh, Y.-H., Wu, Q., Chew, J.-L., Vega, V.B., Zhang, W., Chen, X., Bourque, G., George, J., Leong, B., Liu, J., *et al.* (2006). The Oct4 and Nanog transcription network regulates pluripotency in mouse embryonic stem cells. Nat Genet *38*, 431-440.

Lombard, D.B., Chua, K.F., Mostoslavsky, R., Franco, S., Gostissa, M., and Alt, F.W. (2005). DNA repair, genome stability, and aging. Cell *120*, 497-512.

Luckey, C.J., Bhattacharya, D., Goldrath, A.W., Weissman, I.L., Benoist, C., and Mathis, D. (2006). Memory T and memory B cells share a transcriptional program of self-renewal with long-term hematopoietic stem cells. Proceedings of the National Academy of Sciences of the United States of America *103*, 3304-3309.

Malumbres, M., Sotillo, R., Santamaria, D., Galan, J., Cerezo, A., Ortega, S., Dubus, P., and Barbacid, M. (2004). Mammalian cells cycle without the D-type cyclin-dependent kinases Cdk4 and Cdk6. Cell *118*, 493-504.

Marson, A., Levine, S.S., Cole, M.F., Frampton, G.M., Brambrink, T., Johnstone, S., Guenther, M.G., Johnston, W.K., Wernig, M., Newman, J., *et al.* (2008). Connecting microRNA genes to the core transcriptional regulatory circuitry of embryonic stem cells. Cell *134*, 521-533.

Maslov, A.Y., Barone, T.A., Plunkett, R.J., and Pruitt, S.C. (2004). Neural stem cell detection, characterization, and age-related changes in the subventricular zone of mice. J Neurosci *24*, 1726-1733.

Masui, S., Nakatake, Y., Toyooka, Y., Shimosato, D., Yagi, R., Takahashi, K., Okochi, H., Okuda, A., Matoba, R., Sharov, A.A., *et al.* (2007). Pluripotency governed by Sox2 via regulation of Oct3/4 expression in mouse embryonic stem cells. Nat Cell Biol *9*, 625-635.

Matheu, A., Maraver, A., Klatt, P., Flores, I., Garcia-Cao, I., Borras, C., Flores, J.M., Vina, J., Blasco, M.A., and Serrano, M. (2007). Delayed ageing through damage protection by the Arf/p53 pathway. Nature *448*, 375-379.

McCarthy, K.F., Ledney, G.D., and Mitchell, R. (1977). A deficiency of hematopoietic stem cells in steel mice. Cell Tissue Kinet *10*, 121-126.

McMahon, K.A., Hiew, S.Y., Hadjur, S., Veiga-Fernandes, H., Menzel, U., Price, A.J., Kioussis, D., Williams, O., and Brady, H.J. (2007). Mll has a critical role in fetal and adult hematopoietic stem cell self-renewal. Cell Stem Cell *1*, 338-345.

Meletis, K., Wirta, V., Hede, S.M., Nister, M., Lundeberg, J., and Frisen, J. (2006). p53 suppresses the self-renewal of adult neural stem cells. Development *133*, 363-369.

Mendez-Ferrer, S., Lucas, D., Battista, M., and Frenette, P.S. (2008). Haematopoietic stem cell release is regulated by circadian oscillations. Nature *452*, 442-447.

Mikkelsen, T.S., Ku, M., Jaffe, D.B., Issac, B., Lieberman, E., Giannoukos, G., Alvarez, P., Brockman, W., Kim, T.-K., Koche, R.P., *et al.* (2007). Genome-wide maps of chromatin state in pluripotent and lineage-committed cells. Nature *448*, 553-560.

Mitsui, K., Tokuzawa, Y., Itoh, H., Segawa, K., Murakami, M., Takahashi, K., Maruyama, M., Maeda, M., and Yamanaka, S. (2003). The homeoprotein Nanog is required for maintenance of pluripotency in mouse epiblast and ES cells. Cell *113*, 631-642.

Miyamoto, K., Araki, K.Y., Naka, K., Arai, F., Takubo, K., Yamazaki, S., Matsuoka, S., Miyamoto, T., Ito, K., Ohmura, M., *et al.* (2007). Foxo3a is essential for maintenance of the hematopoietic stem cell pool. Cell Stem Cell *1*, 101-112.

Molofsky, A.V., He, S., Bydon, M., Morrison, S.J., and Pardal, R. (2005). Bmi-1 promotes neural stem cell self-renewal and neural development but not mouse growth and survival by repressing the p16Ink4a and p19Arf senescence pathways. Genes Dev *19*, 1432-1437.

Molofsky, A.V., Pardal, R., Iwashita, T., Park, I.K., Clarke, M.F., and Morrison, S.J. (2003). Bmi-1 dependence distinguishes neural stem cell self-renewal from progenitor proliferation. Nature *425*, 962-967.

Molofsky, A.V., Slutsky, S.G., Joseph, N.M., He, S., Pardal, R., Krishnamurthy, J., Sharpless, N.E., and Morrison, S.J. (2006). Increasing p16INK4a expression decreases forebrain progenitors and neurogenesis during ageing. Nature *443*, 448-452.

Morrison, S.J., Hemmati, H.D., Wandycz, A.M., and Weissman, I.L. (1995). The purification and characterization of fetal liver hematopoietic stem cells. Proc Natl Acad Sci U S A *92*, 10302-10306.

Morrison, S.J., and Kimble, J. (2006). Asymmetric and symmetric stem-cell divisions in development and cancer. Nature *441*, 1068-1074.

Morrison, S.J., Prowse, K.R., Ho, P., and Weissman, I.L. (1996a). Telomerase activity in hematopoietic cells is associated with self-renewal potential. Immunity *5*, 207-216.

Morrison, S.J., and Spradling, A.C. (2008). Stem cells and niches: mechanisms that promote stem cell maintenance throughout life. Cell *132*, 598-611.

Morrison, S.J., Wandycz, A.M., Akashi, K., Globerson, A., and Weissman, I.L. (1996b). The aging of hematopoietic stem cells. Nature Medicine *2*, 1011-1016.

Morrison, S.J., White, P.M., Zock, C., and Anderson, D.J. (1999). Prospective identification, isolation by flow cytometry, and in vivo self-renewal of multipotent mammalian neural crest stem cells. Cell *96*, 737-749.

Nakagawa, T., Nabeshima, Y., and Yoshida, S. (2007). Functional identification of the actual and potential stem cell compartments in mouse spermatogenesis. Dev Cell *12*, 195-206.

Navarro, S., Meza, N.W., Quintana-Bustamante, O., Casado, J.A., Jacome, A., McAllister, K., Puerto, S., Surralles, J., Segovia, J.C., and Bueren, J.A. (2006). Hematopoietic dysfunction in a mouse model for Fanconi anemia group D1. Mol Ther *14*, 525-535.

Nichols, J., Zevnik, B., Anastassiadis, K., Niwa, H., Klewe-Nebenius, D., Chambers, I., Scholer, H., and Smith, A. (1998). Formation of pluripotent stem cells in the mammalian embryo depends on the POU transcription factor Oct4. Cell *95*, 379-391.

Nie, Y., Han, Y.-C., and Zou, Y.-R. (2008). CXCR4 is required for the quiescence of primitive hematopoietic cells. J Exp Med, jem.20072513-jem.20072513.

Nijnik, A., Woodbine, L., Marchetti, C., Dawson, S., Lambe, T., Liu, C., Rodrigues, N.P., Crockford, T.L., Cabuy, E., Vindigni, A.*, et al.* (2007). DNA repair is limiting for haematopoietic stem cells during ageing. Nature *447*, 686-690.

Nishino, J., Kim, I., Chada, K., and Morrison, S.J. (2008). Hmga2 promotes neural stem cell self-renewal in young but not old mice by reducing p16Ink4a and p19Arf Expression. Cell *135*, 227-239.

Niwa, H. (2007). How is pluripotency determined and maintained? Development *134*, 635-646.

Niwa, H., Burdon, T., Chambers, I., and Smith, A. (1998). Self-renewal of pluripotent embryonic stem cells is mediated via activation of STAT3. Genes Dev *12*, 2048-2060.

Niwa, H., Miyazaki, J., and Smith, A.G. (2000). Quantitative expression of Oct-3/4 defines differentiation, dedifferentiation or self-renewal of ES cells. Nat Genet *24*, 372-376.

Niwa, H., Toyooka, Y., Shimosato, D., Strumpf, D., Takahashi, K., Yagi, R., and Rossant, J. (2005). Interaction between Oct3/4 and Cdx2 determines trophectoderm differentiation. Cell *123*, 917-929.

Oguro, H., Iwama, A., Morita, Y., Kamijo, T., van Lohuizen, M., and Nakauchi, H. (2006). Differential impact of Ink4a and Arf on hematopoietic stem cells and their bone marrow microenvironment in Bmi1-deficient mice. The Journal of experimental medicine *203*, 2247-2253.

Okita, K., Ichisaka, T., and Yamanaka, S. (2007). Generation of germline-competent induced pluripotent stem cells. Nature *448*, 313-317.

Okuda, T., van Deursen, J., Hiebert, S.W., Grosveld, G., and Downing, J.R. (1996). AML1, the target of multiple chromosomal translocations in human leukemia, is essential for normal fetal liver hematopoiesis. Cell *84*, 321-330.

Orkin, S.H., and Zon, L.I. (2008). Hematopoiesis: an evolving paradigm for stem cell biology. Cell *132*, 631-644.

Paik, J.H., Kollipara, R., Chu, G., Ji, H., Xiao, Y., Ding, Z., Miao, L., Tothova, Z., Horner, J.W., Carrasco, D.R., *et al.* (2007). FoxOs are lineage-restricted redundant tumor suppressors and regulate endothelial cell homeostasis. Cell *128*, 309-323.

Pardal, R., Molofsky, A.V., He, S., and Morrison, S.J. (2005). Stem cell self-renewal and cancer cell proliferation are regulated by common networks that balance the activation of proto-oncogenes and tumor suppressors. Cold Spring Harb Symp Quant Biol *70*, 177-185.

Park, I.H., Zhao, R., West, J.A., Yabuuchi, A., Huo, H., Ince, T.A., Lerou, P.H., Lensch, M.W., and Daley, G.Q. (2008). Reprogramming of human somatic cells to pluripotency with defined factors. Nature *451*, 141-146.

Park, I.K., Qian, D., Kiel, M., Becker, M.W., Pihalja, M., Weissman, I.L., Morrison, S.J., and Clarke, M.F. (2003). Bmi-1 is required for maintenance of adult self-renewing haematopoietic stem cells. Nature *423*, 302-305.

Passegue, E., and Wagner, E.F. (2000). JunB suppresses cell proliferation by transcriptional activation of p16(INK4a) expression. The EMBO journal *19*, 2969-2979.

Passegue, E., Wagner, E.F., and Weissman, I.L. (2004). JunB deficiency leads to a myeloproliferative disorder arising from hematopoietic stem cells. Cell *119*, 431-443.

Pearson, B.J., and Doe, C.Q. (2003). Regulation of neuroblast competence in Drosophila. Nature *425*, 624-628.

Pietersen, A.M., Evers, B., Prasad, A.A., Tanger, E., Cornelissen-Steijger, P., Jonkers, J., and van Lohuizen, M. (2008). Bmi1 regulates stem cells and proliferation and differentiation of committed cells in mammary epithelium. Curr Biol *18*, 1094-1099.

Prasher, J.M., Lalai, A.S., Heijmans-Antonissen, C., Ploemacher, R.E., Hoeijmakers, J.H., Touw, I.P., and Niedernhofer, L.J. (2005). Reduced hematopoietic reserves in DNA interstrand crosslink repair-deficient Ercc1-/- mice. The EMBO journal *24*, 861-871.

Puri, M.C., and Bernstein, A. (2003). Requirement for the TIE family of receptor tyrosine kinases in adult but not fetal hematopoiesis. Proc Natl Acad Sci U S A *100*, 12753-12758.

Qian, H., Buza-Vidas, N., Hyland, C.D., Jensen, C.T., Antonchuk, J., Mansson, R., Thoren, L.A., Ekblom, M., Alexander, W.S., and Jacobsen, S.E. (2007). Critical role of thrombopoietin in maintaining adult quiescent hematopoietic stem cells. Cell Stem Cell *1*, 671-684.

Qiu, J., Takagi, Y., Harada, J., Rodrigues, N., Moskowitz, M.A., Scadden, D.T., and Cheng, T. (2004). Regenerative response in ischemic brain restricted by p21cip1/waf1. The Journal of experimental medicine *199*, 937-945.

Reese, J.S., Liu, L., and Gerson, S.L. (2003). Repopulating defect of mismatch repair-deficient hematopoietic stem cells. Blood *102*, 1626-1633.

Riquelme, P.A., Drapeau, E., and Doetsch, F. (2008). Brain micro-ecologies: neural stem cell niches in the adult mammalian brain. Philosophical transactions of the Royal Society of London *363*, 123-137.

Rossi, D.J., Bryder, D., Seita, J., Nussenzweig, A., Hoeijmakers, J., and Weissman, I.L. (2007). Deficiencies in DNA damage repair limit the function of haematopoietic stem cells with age. Nature *447*, 725-729.

Rossi, D.J., Bryder, D., Zahn, J.M., Ahlenius, H., Sonu, R., Wagers, A.J., and Weissman, I.L. (2005). Cell intrinsic alterations underlie hematopoietic stem cell aging. Proc Natl Acad Sci U S A *102*, 9194-9199.

Rossi, D.J., Jamieson, C.H., and Weissman, I.L. (2008). Stems cells and the pathways to aging and cancer. Cell *132*, 681-696.

Rudolph, K.L., Chang, S., Lee, H.W., Blasco, M., Gottlieb, G.J., Greider, C., and DePinho, R.A. (1999). Longevity, stress response, and cancer in aging telomerase-deficient mice. Cell *96*, 701-712.

Ruiz i Altaba, A., Sanchez, P., and Dahmane, N. (2002). Gli and hedgehog in cancer: tumours, embryos and stem cells. Nat Rev Cancer *2*, 361-372.

Ruthenburg, A.J., Allis, C.D., and Wysocka, J. (2007). Methylation of lysine 4 on histone H3: intricacy of writing and reading a single epigenetic mark. Molecular cell *25*, 15-30.

Ruzankina, Y., Pinzon-Guzman, C., Asare, A., Ong, T., Pontano, L., Cotsarelis, G., Zediak, V.P., Velez, M., Bhandoola, A., and Brown, E.J. (2007). Deletion of the developmentally essential gene ATR in adult mice leads to age-related phenotypes and stem cell loss. Cell Stem Cell *1*, 113-126.

Sacchetti, B., Funari, A., Michienzi, S., Di Cesare, S., Piersanti, S., Saggio, I., Tagliafico, E., Ferrari, S., Robey, P.G., Riminucci, M., *et al.* (2007). Self-renewing osteoprogenitors in bone marrow sinusoids can organize a hematopoietic microenvironment. Cell *131*, 324-336.

Savatier, P., Lapillonne, H., van Grunsven, L.A., Rudkin, B.B., and Samarut, J. (1996). Withdrawal of differentiation inhibitory activity/leukemia inhibitory factor up-regulates D-type cyclins and cyclin-dependent kinase inhibitors in mouse embryonic stem cells. Oncogene *12*, 309-322.

Schuettengruber, B., Chourrout, D., Vervoort, M., Leblanc, B., and Cavalli, G. (2007). Genome regulation by polycomb and trithorax proteins. Cell *128*, 735-745.

Sharpless, N.E., and DePinho, R.A. (2007). How stem cells age and why this makes us grow old. Nat Rev Mol Cell Biol *8*, 703-713.

Shen, Q., Wang, Y., Dimos, J.T., Fasano, C.A., Phoenix, T.N., Lemischka, I.R., Ivanova, N.B., Stifani, S., Morrisey, E.E., and Temple, S. (2006). The timing of cortical neurogenesis is encoded within lineages of individual progenitor cells. Nature neuroscience *9*, 743-751.

Sherr, C.J. (2001). The INK4a/ARF network in tumour suppression. Nat Rev Mol Cell Biol *2*, 731-737.

Sherr, C.J., and Roberts, J.M. (2004). Living with or without cyclins and cyclin-dependent kinases. Genes Dev *18*, 2699-2711.

Shi, Y., Chichung Lie, D., Taupin, P., Nakashima, K., Ray, J., Yu, R.T., Gage, F.H., and Evans, R.M. (2004). Expression and function of orphan nuclear receptor TLX in adult neural stem cells. Nature *427*, 78-83.

Silva, J., and Smith, A. (2008). Capturing Pluripotency. Cell *132*, 532-536.

Spiegel, A., Kalinkovich, A., Shivtiel, S., Kollet, O., and Lapidot, T. (2008). Stem cell regulation via dynamic interactions of the nervous and immune systems with the microenvironment. Cell Stem Cell *3*, 484-492.

Stead, E., White, J., Faast, R., Conn, S., Goldstone, S., Rathjen, J., Dhingra, U., Rathjen, P., Walker, D., and Dalton, S. (2002). Pluripotent cell division cycles are driven by ectopic Cdk2, cyclin A/E and E2F activities. Oncogene *21*, 8320-8333.

Stepanova, L., and Sorrentino, B.P. (2005). A limited role for p16Ink4a and p19Arf in the loss of hematopoietic stem cells during proliferative stress. Blood *106*, 827-832.

Sugiyama, T., Kohara, H., Noda, M., and Nagasawa, T. (2006). Maintenance of the hematopoietic stem cell pool by CXCL12-CXCR4 chemokine signaling in bone marrow stromal cell niches. Immunity *25*, 977-988.

Tadokoro, Y., Ema, H., Okano, M., Li, E., and Nakauchi, H. (2007). De novo DNA methyltransferase is essential for self-renewal, but not for differentiation, in hematopoietic stem cells. The Journal of experimental medicine *204*, 715-722.

Takahashi, K., Tanabe, K., Ohnuki, M., Narita, M., Ichisaka, T., Tomoda, K., and Yamanaka, S. (2007). Induction of pluripotent stem cells from adult human fibroblasts by defined factors. Cell *131*, 861-872.

Takahashi, K., and Yamanaka, S. (2006). Induction of pluripotent stem cells from mouse embryonic and adult fibroblast cultures by defined factors. Cell *126*, 663-676.

Takizawa, T., Nakashima, K., Namihira, M., Ochiai, W., Uemura, A., Yanagisawa, M., Fujita, N., Nakao, M., and Taga, T. (2001). DNA methylation is a critical cell-intrinsic determinant of astrocyte differentiation in the fetal brain. Dev Cell *1*, 749-758.

TeKippe, M., Harrison, D.E., and Chen, J. (2002). Expansion of hematopoietic stem cell phenotype and activity in Trp53-null mice. Experimental Hematology *31*, 521-527.

Thoren, L.A., Liuba, K., Bryder, D., Nygren, J.M., Jensen, C.T., Qian, H., Antonchuk, J., and Jacobsen, S.E. (2008). Kit regulates maintenance of quiescent hematopoietic stem cells. J Immunol *180*, 2045-2053.

Tothova, Z., and Gilliland, D.G. (2007). FoxO transcription factors and stem cell homeostasis: insights from the hematopoietic system. Cell Stem Cell *1*, 140-152.

Tothova, Z., Kollipara, R., Huntly, B.J., Lee, B.H., Castrillon, D.H., Cullen, D.E., McDowell, E.P., Lazo-Kallanian, S., Williams, I.R., Sears, C.*, et al.* (2007). FoxOs are critical mediators of hematopoietic stem cell resistance to physiologic oxidative stress. Cell *128*, 325-339.

Trowbridge, J.J., Snow, J.W., Kim, J., and Orkin, S.H. (2009). DNA methyltransferase 1 is essential for and uniquely regulates hematopoietic stem and progenitor cells. Cell Stem Cell *5*, 442-449.

Tulina, N., and Matunis, E. (2001). Control of stem cell self-renewal in Drosophila spermatogenesis by JAK-STAT signaling. Science (New York, NY *294*, 2546-2549.

van der Lugt, N.M., Domen, J., Linders, K., van Roon, M., Robanus-Maandag, E., te Riele, H., van der Valk, M., Deschamps, J., Sofroniew, M., van Lohuizen, M.*, et al.* (1994). Posterior transformation, neurological abnormalities, and severe hematopoietic defects in mice with a targeted deletion of the bmi-1 proto-oncogene. Genes Dev *8*, 757-769.

Vaziri, H., Dragowska, W., Allsopp, R.C., Thomas, T.E., Harley, C.B., and Lansdorp, P.M. (1994). Evidence for a mitotic clock in human hematopoietic stem cells: loss of telomeric DNA with age. Proc Natl Acad Sci U S A *91*, 9857-9860.

Viatour, P., Somervaille, T.C., Venkatasubrahmanyam, S., Kogan, S., McLaughlin, M.E., Weissman, I.L., Butte, A.J., Passegue, E., and Sage, J. (2008). Hematopoietic stem cell quiescence is maintained by compound contributions of the retinoblastoma gene family. Cell Stem Cell *3*, 416-428.

Walkley, C.R., and Orkin, S.H. (2006). Rb is dispensable for self-renewal and multilineage differentiation of adult hematopoietic stem cells. Proceedings of the National Academy of Sciences *103*, 9057-9062.

Walkley, C.R., Shea, J.M., Sims, N.A., Purton, L.E., and Orkin, S.H. (2007). Rb regulates interactions between hematopoietic stem cells and their bone marrow microenvironment. Cell *129*, 1081-1095.

Wallenfang, M.R., Nayak, R., and DiNardo, S. (2006). Dynamics of the male germline stem cell population during aging of Drosophila melanogaster. Aging Cell *5*, 297-304.

Wang, J., Rao, S., Chu, J., Shen, X., Levasseur, D.N., Theunissen, T.W., and Orkin, S.H. (2006). A protein interaction network for pluripotency of embryonic stem cells. Nature *444*, 364-368.

Wernig, M., Meissner, A., Foreman, R., Brambrink, T., Ku, M., Hochedlinger, K., Bernstein, B.E., and Jaenisch, R. (2007). In vitro reprogramming of fibroblasts into a pluripotent ES-cell-like state. Nature *448*, 318-324.

White, J., Stead, E., Faast, R., Conn, S., Cartwright, P., and Dalton, S. (2005). Developmental activation of the Rb-E2F pathway and establishment of cell cycle-regulated cyclin-dependent kinase activity during embryonic stem cell differentiation. Mol Biol Cell *16*, 2018-2027.

Williams, R.L., Hilton, D.J., Pease, S., Willson, T.A., Stewart, C.L., Gearing, D.P., Wagner, E.F., Metcalf, D., Nicola, N.A., and Gough, N.M. (1988). Myeloid leukaemia inhibitory factor maintains the developmental potential of embryonic stem cells. Nature *336*, 684-687.

Wilson, A., Laurenti, E., Oser, G., van der Wath, R.C., Blanco-Bose, W., Jaworski, M., Offner, S., Dunant, C.F., Eshkind, L., Bockamp, E.*, et al.* (2008). Hematopoietic Stem Cells Reversibly Switch from Dormancy to Self-Renewal during Homeostasis and Repair. Cell.

Wong, M.D., Jin, Z., and Xie, T. (2005). Molecular mechanisms of germline stem cell regulation. Annu Rev Genet *39*, 173-195.

Wright, D.E., Wagers, A.J., Gulati, A.P., Johnson, F.L., and Weissman, I.L. (2001). Physiological migration of hematopoietic stem and progenitor cells. Science (New York, NY *294*, 1933-1936.

Yamashita, Y.M., Jones, D.L., and Fuller, M.T. (2003). Orientation of asymmetric stem cell division by the APC tumor suppressor and centrosome. Science (New York, NY *301*, 1547-1550.

Yamashita, Y.M., Mahowald, A.P., Perlin, J.R., and Fuller, M.T. (2007). Asymmetric inheritance of mother versus daughter centrosome in stem cell division. Science (New York, NY *315*, 518-521.

Ye, M., Iwasaki, H., Laiosa, C.V., Stadtfeld, M., Xie, H., Heck, S., Clausen, B., Akashi, K., and Graf, T. (2003). Hematopoietic stem cells expressing the myeloid lysozyme gene retain long-term, multilineage repopulation potential. Immunity *19*, 689-699.

Yilmaz, O.H., Valdez, R., Theisen, B.K., Guo, W., Ferguson, D.O., Wu, H., and Morrison, S.J. (2006). Pten dependence distinguishes haematopoietic stem cells from leukaemia-initiating cells. Nature *441*, 475-482.

Ying, Q.-L., Wray, J., Nichols, J., Batlle-Morera, L., Doble, B., Woodgett, J., Cohen, P., and Smith, A. (2008). The ground state of embryonic stem cell self-renewal. Nature *453*, 519-523.

Ying, Q.L., Nichols, J., Chambers, I., and Smith, A. (2003). BMP induction of Id proteins suppresses differentiation and sustains embryonic stem cell self-renewal in collaboration with STAT3. Cell *115*, 281-292.

Yoshihara, H., Arai, F., Hosokawa, K., Hagiwara, T., Takubo, K., Nakamura, Y., Gomei, Y., Iwasaki, H., Matsuoka, S., Miyamoto, K.*, et al.* (2007). Thrombopoietin/MPL

signaling regulates hematopoietic stem cell quiescence and interaction with the osteoblastic niche. Cell Stem Cell *1*, 685-697.

Yu, J., Vodyanik, M.A., Smuga-Otto, K., Antosiewicz-Bourget, J., Frane, J.L., Tian, S., Nie, J., Jonsdottir, G.A., Ruotti, V., Stewart, R., *et al.* (2007). Induced pluripotent stem cell lines derived from human somatic cells. Science (New York, NY *318*, 1917-1920.

Yuan, T.L., and Cantley, L.C. (2008). PI3K pathway alterations in cancer: variations on a theme. Oncogene *27*, 5497-5510.

Yuan, Y., Shen, H., Franklin, D.S., Scadden, D.T., and Cheng, T. (2004). In vivo self-renewing divisions of haematopoietic stem cells are increased in the absence of the early G1-phase inhibitor, p18INK4C. Nat Cell Biol *6*, 436-442.

Zhang, J., Grindley, J.C., Yin, T., Jayasinghe, S., He, X.C., Ross, J.T., Haug, J.S., Rupp, D., Porter-Westpfahl, K.S., Wiedemann, L.M., *et al.* (2006). PTEN maintains haematopoietic stem cells and acts in lineage choice and leukaemia prevention. Nature *441*, 518-522.

Zhao, X.D., Han, X., Chew, J.L., Liu, J., Chiu, K.P., Choo, A., Orlov, Y.L., Sung, W.-K., Shahab, A., Kuznetsov, V.A., *et al.* (2007). Whole-Genome Mapping of Histone H3 Lys4 and 27 Trimethylations Reveals Distinct Genomic Compartments in Human Embryonic Stem Cells. Cell Stem Cell *1*, 286-298.

CHAPTER 2

BMI-1 PROMOTES NEURAL STEM CELL SELF-RENEWAL AND NEURAL DEVELOPMENT BUT NOT GROWTH AND SURVIVAL BY SUPPRESSING THE $P16^{INK4A}$ AND $P19^{ARF}$ SENESCENCE PATHWAYS[1]

SUMMARY

Bmi-1 is required for the postnatal maintenance of stem cells in multiple tissues including the central (CNS) and peripheral (PNS) nervous systems. Deletion of *Ink4a* or *Arf* from *Bmi-1*$^{-/-}$ mice partially rescued stem cell self-renewal, and stem cell frequency in the CNS and PNS as well as forebrain proliferation and gut neurogenesis. *Arf* deficiency, but not *Ink4a* deficiency, partially rescued cerebellum development, demonstrating regional differences in the sensitivity of progenitors to $p16^{Ink4a}$ and $p19^{Arf}$. Deletion of both *Ink4a* and *Arf* did not affect the growth or survival of *Bmi-1*$^{-/-}$ mice or completely rescue neural development. Bmi-1 thus prevents the premature senescence of neural stem cells by repressing *Ink4a* and *Arf* but additional pathways must also function downstream of Bmi-1.

---

[1] Originally published in *Genes and Development. 2005;19:1432-7* with authors listed as Molofsky, A.V., **He, S.**, Bydon, M.; Morrison, S.J. and Pardal, R.

INTRODUCTION

Stem cells must persist throughout adult life in numerous tissues in order to replace the mature cells that are lost to turnover, injury, or disease. The mechanism by which stem cells persist throughout life involves self-renewal - stem cell divisions that generate one or two daughter stem cells (Molofsky et al., 2004; Morrison et al., 1997a). Stem cells self-renew postnatally in numerous tissues, including the CNS (Maslov et al., 2004), PNS (Kruger et al., 2002), and hematopoietic system (Harrison, 1979; Morrison et al., 1996b).

The polycomb family transcriptional repressor Bmi-1 is required for the self-renewal and postnatal maintenance of hematopoietic stem cells (Lessard and Sauvageau, 2003b; Park et al., 2003a), and neural stem cells from the CNS and PNS (Molofsky et al., 2003). In each tissue *Bmi-1*$^{-/-}$ stem cells form in normal numbers and appear to differentiate normally, but exhibit a postnatal self-renewal defect that leads to their depletion by early adulthood. *Bmi-1* tends to be turned off as cells differentiate (Lessard et al., 1998) and is not required for the proliferation of all cells (Molofsky et al., 2003). Bmi-1 functions as part of a protein complex that maintains gene silencing by regulating chromatin structure (Valk-Lingbeek et al., 2004). Except for a mild skeletal transformation, *Bmi-1*$^{-/-}$ mice are normal in size and appearance at birth (van der Lugt et al., 1994b). However, they exhibit progressive postnatal growth retardation and die by early adulthood with signs of hematopoietic failure (hypocellular bone marrow) and neurological abnormalities (seizures and ataxia) (van der Lugt et al., 1994b).

Bmi-1$^{-/-}$ mice develop several specific neural abnormalities. The rate of proliferation in the forebrain subventricular zone (SVZ; where CNS stem cells undergo

neurogenesis) is reduced by postnatal day 30 (P30) when stem cell depletion becomes severe (Molofsky et al., 2003). The cerebellum also fails to develop normally, partly because *Bmi-1* is required for the proliferation of granule precursor cells (Leung et al., 2004). Finally, adult *Bmi-1*$^{-/-}$ mice exhibit fewer neurons in the myenteric plexus of the gut as the neural crest stem cells (NCSCs) in this region of the postnatal PNS become depleted (Molofsky et al., 2003). These defects indicate that the pathways regulated by Bmi-1 have important consequences for neural development.

Bmi-1 represses transcription at the *Ink4a-Arf* locus (Jacobs et al., 1999b; Jacobs et al., 1999c) which encodes two inhibitors of cell proliferation (Sherr, 2001b). *Ink4a* encodes p16^{Ink4a}, a cyclin-dependent kinase inhibitor that promotes Rb activation. *Arf* encodes p19^{Arf}, which promotes p53 activation. p16^{Ink4a} and p19^{Arf} are induced in cultured primary cells and can cause these cells to senesce (reviewed in (Lowe and Sherr, 2003)). Bmi-1 overexpression can prevent senescence and extend the replicative lifespan of primary cells by reducing p16^{Ink4a} and p19^{Arf} expression (Dimri et al., 2002; Itahana et al., 2003; Jacobs et al., 1999b). Deletion of *Ink4a-Arf* from *Bmi-1*$^{-/-}$ mice rescues the ability of mouse embryonic fibroblasts to proliferate in culture and at least partially rescues defects in cerebellum development (Jacobs et al., 1999b). p16^{Ink4a} expression is elevated in *Bmi-1*$^{-/-}$ neural stem cells and deletion of *Ink4a* from *Bmi-1*$^{-/-}$ mice partially rescues neural stem cell self-renewal in culture (Molofsky et al., 2003).

To test whether *Ink4a* deletion rescues stem cell frequency or neural development in *Bmi-1*$^{-/-}$ mice, and whether p19^{Arf} also mediates part of the effect of Bmi-1 on stem cell function or neural development we have generated compound mutant mice that lack *Bmi-1* (van der Lugt et al., 1994b) and/or *Ink4a* (Sharpless et al., 2001), *Arf* (Kamijo et al.,

1997), or *Ink4a-Arf* (Serrano et al., 1996). Our results indicate that the repression of *Ink4a* and *Arf* each represent major mechanisms by which Bmi-1 promotes neural stem cell self-renewal and neural development. The postnatal maintenance of neural stem cells depends upon the repression of senescence pathways that otherwise cause the premature depletion of stem cells.

RESULTS AND DISCUSSION

Like $p16^{Ink4a}$ (Molofsky et al., 2003), $p19^{Arf}$ expression increased in the absence of *Bmi-1*. $p19^{Arf}$ was not detected in the wild-type SVZ or cerebellum, but was detected in these tissues in the absence of *Bmi-1* (Figure 2.1A). $p19^{Arf}$ was upregulated in *Bmi-1*$^{-/-}$ CNS neurospheres cultured from the SVZ (Figure 2.1B) and *Bmi-1*$^{-/-}$ PNS neurospheres cultured from the adult gut wall (data not shown), though $p19^{Arf}$ was also detected at lower levels in wild-type neurospheres. The detection of both $p16^{Ink4a}$ (Molofsky et al., 2003) and $p19^{Arf}$ in cultured neurospheres despite not detecting these proteins *in vivo* suggests that *Ink4a* and *Arf* are induced in wild-type cells in culture, though not to the extent as in *Bmi-1*$^{-/-}$ cells. This is consistent with our failure to detect *Ink4a* or *Arf* by PCR in uncultured wild-type NCSCs isolated by flow-cytometry (Molofsky et al., 2003).

Arf deficiency significantly increased self-renewal within both *Bmi-1*$^{+/+}$ and *Bmi-1*$^{-/-}$ neurospheres from the CNS and PNS (Figure 2.1C, D). The ability of *Arf* deficiency to increase the self-renewal of *Bmi-1*$^{+/+}$ neural stem cells in culture presumably reflects the fact that primary neurospheres were subcloned after 10 days in culture, well after $p19^{Arf}$ was induced in these cells. Since only about half as much self-renewal was observed within *Bmi-1*$^{-/-}$*Arf* $^{-/-}$ neurospheres as compared to *Bmi-1*$^{+/+}$*Arf* $^{-/-}$ neurospheres

in the CNS and PNS, *Arf* deficiency appeared to only partially rescue the self-renewal of *Bmi-1*$^{-/-}$ neurospheres. Consistent with this, *Arf* deficiency also significantly increased the size of neurospheres (Figure 2.2B), and the percentage of cells within *Bmi-1*$^{-/-}$ neurospheres that could form secondary neurospheres (Figure 2.3B).

Deletion of *Ink4a* and *Arf* (*Ink4a-Arf* $^{-/-}$) significantly increased self-renewal within *Bmi-1*$^{+/+}$ and *Bmi-1*$^{-/-}$ neurospheres from the CNS and PNS (Figure 2.1E,F). The rates of self-renewal suggested that *Ink4a-Arf* deficiency rescued most but not all of the *Bmi-1*$^{-/-}$ CNS self-renewal defect and about half of the PNS self-renewal defect (compare *Bmi-1*$^{-/-}$*Ink4a-Arf* $^{-/-}$ versus *Bmi-1*$^{+/+}$*Ink4a-Arf* $^{-/-}$, Figure 2.1E,F). More self-renewal was observed in Figure 2.1F than in Figure 2.1D because the neurospheres were cultured longer before subcloning. *Ink4a-Arf* deficiency also significantly increased the size of neurospheres (Figure 2.2C,D), and the percentage of cells within *Bmi-1*$^{-/-}$ neurospheres that could form secondary neurospheres (Figure 2.3C).

Ink4a, Arf, or *Ink4a-Arf* deficiency partially rescue *Bmi-1*$^{-/-}$ neural stem cell frequency

To test whether *Ink4a* deficiency could also rescue stem cell frequency *in vivo*, we cultured dissociated forebrain SVZ cells from 4 to 8 week old mice to determine the frequency of freshly dissociated cells that could form multipotent neurospheres. Cells were plated at clonal density, cultured for 10 days, then replated to adherent cultures for 3 to 5 days and stained for neurons, astrocytes, and oligodendrocytes. As observed previously, a significantly lower percentage of cells from the *Bmi-1*$^{-/-}$ SVZ formed multipotent neurospheres (Figure 2.4). *Ink4a* deficiency significantly increased the percentage of *Bmi-1*$^{-/-}$ but not *Bmi-1*$^{+/+}$ SVZ cells that formed multipotent neurospheres

(Figure 2.4A). This is consistent with $p16^{Ink4a}$ expression in *Bmi-1*$^{-/-}$ but not in *Bmi-1*$^{+/+}$ SVZ cells in vivo (Molofsky et al., 2003). The magnitude of the increase suggested that *Ink4a* deficiency partially rescued stem cell frequency in the *Bmi-1*$^{-/-}$ SVZ.

We also cultured dissociated cells from the outer gut wall where NCSCs persist throughout adult life (Kruger et al., 2002). Cells were plated at clonal density, cultured for 10 days, then replated to adherent cultures for 5 days and stained for neurons, glia, and myofibroblasts. *Ink4a* deficiency significantly increased the percentage of *Bmi-1*$^{-/-}$ but not *Bmi-1*$^{+/+}$ cells that formed multipotent neurospheres (Figure 2.4B). The magnitude of the increase again suggested that *Ink4a* deficiency partially rescued stem cell frequency in the *Bmi-1*$^{-/-}$ gut.

To confirm the partial rescue in neural stem cell frequency *in vivo*, we exploited our ability to prospectively identify uncultured NCSCs by flow-cytometry based on their expression of high levels of the p75 neurotrophin receptor ($p75^+$ cells) (Bixby et al., 2002; Kruger et al., 2002). In these experiments, 30 to 50% of $p75^+$ cells of all genotypes formed NCSC colonies in culture (data not shown), a 30 to 300-fold enrichment for NCSCs relative to unfractionated cells (0.1 to 1.4% of unfractionated gut cells, depending on genotype, formed stem cell colonies in culture; Figure 2.4). The frequency of $p75^+$ cells was significantly reduced in the absence of Bmi-1 (Figure 2.5A,B). *Ink4a* deficiency had no effect on the frequency of $p75^+$ cells from *Bmi-1*$^{+/+}$ mice, but did significantly increase the frequency of $p75^+$ cells in *Bmi-1*$^{-/-}$ mice (Figure 2.5C-E). The magnitude of the increase again suggested a partial rescue of *Bmi-1*$^{-/-}$ stem cell depletion. This analysis of prospectively identified, uncultured NCSCs was thus consistent with results from the

functional assays in culture in indicating that Bmi-1 promotes the postnatal maintenance of neural stem cells partly by repressing *Ink4a*.

Arf deficiency (Figure 2.4C, D) and *Ink4a-Arf* deficiency (Figure 2.4E,F) also partly rescued the depletion of CNS and PNS stem cells in *Bmi-1*$^{-/-}$ mice, significantly increasing the percentage of freshly dissociated SVZ cells and outer gut wall cells from *Bmi-1*$^{-/-}$ but not *Bmi-1*$^{+/+}$ mice that formed multipotent neurospheres in culture. The percentages of SVZ and gut cells from *Bmi-1*$^{-/-}$*Ink4a-Arf* $^{-/-}$ and *Bmi-1*$^{+/+}$*Ink4a-Arf* $^{-/-}$ mice that formed multipotent neurospheres suggest that *Ink4a-Arf* deficiency rescued most of the CNS stem cell maintenance defect and about half of the *Bmi-1*$^{-/-}$ PNS stem cell maintenance defect. These results demonstrate that increased expression of $p16^{Ink4a}$ and $p19^{Arf}$ in the absence of Bmi-1 are responsible for much but not all of the neural stem cell self-renewal and maintenance defects observed in *Bmi-1*$^{-/-}$ mice.

Ink4a, Arf, or *Ink4a-Arf* deficiency partially rescue neural development in *Bmi-1*$^{-/-}$ mice

In the absence of Bmi-1 there was a significant decline in the rate of proliferation (the percentage of cells that incorporated a pulse of BrdU) in the adult SVZ, where neurogenesis occurs in the forebrain (Figure 2.6A). *Ink4a* deficiency had no effect on proliferation in the *Bmi-1*$^{+/+}$ forebrain (data not shown) but significantly increased proliferation in the *Bmi-1*$^{-/-}$ forebrain, suggesting a partial rescue of this phenotype (Figure 2.6A). The number of myenteric plexus neurons per cross-section of the adult small intestine was significantly reduced in the absence of *Bmi-1* (Figure 2.6B). *Ink4a* deficiency significantly increased the number of neurons per section through the *Bmi-1*$^{-/-}$

intestine (Figure 2.6B). Thus *Ink4a* deficiency partially rescued proliferation/neurogenesis in the forebrain and enteric nervous system of *Bmi-1*$^{-/-}$ mice.

Arf deficiency (Figure 2.6C) or *Ink4a-Arf* deficiency (Figure 2.6E) also significantly increased proliferation in the *Bmi-1*$^{-/-}$ but not *Bmi-1*$^{+/+}$ SVZ, suggesting partial rescue of this defect. *Arf* deficiency appeared to increase the number of neurons per section through the *Bmi-1*$^{-/-}$ small intestine, though the effect was not statistically significant (Figure 2.6D). *Ink4a-Arf* deficiency significantly increased the number of neurons per section through the *Bmi-1*$^{-/-}$ but not *Bmi-1*$^{+/+}$ small intestine (Figure 2.6F) to a degree consistent with a complete rescue. That some phenotypes (e.g. gut neurogenesis) appeared to be completely rescued by deleting *Ink4a* and *Arf*, while other phenotypes (e.g. SVZ proliferation) were only partially rescued indicates that the importance of other pathways downstream of Bmi-1 differs between regions of the nervous system.

Arf, or *Ink4a-Arf* deficiency partially rescue cerebellum development in *Bmi-1*$^{-/-}$ mice

Bmi-1$^{-/-}$ mice exhibit morphologically smaller cerebellums, including significantly thinner granular and molecular cell layers, and reduced cell density in the molecular layer (Figure 2.7A-C) (Leung et al., 2004; van der Lugt et al., 1994b). *Ink4a-Arf* deficiency partially rescues cerebellum development in *Bmi-1*$^{-/-}$ mice (Jacobs et al., 1999b), though the relative importance of *Ink4a* and *Arf* in cerebellum development was not tested. Consistent with this prior report, we found that *Ink4a-Arf* deficiency had no effect on cerebellum development in *Bmi-1*$^{+/+}$ mice (data not shown), but did increase the overall cerebellum size in *Bmi-1*$^{-/-}$ mice, including significantly increasing the thickness of the granular and molecular layers, as well as cell density in the molecular layer (Figure

2.7C). Nonetheless, all of these parameters remained significantly less than observed in wild-type littermates, indicating a partial rescue of cerebellum growth (Figure 2.7C).

Ink4a deficiency had no effect on cerebellum development in *Bmi-1*$^{-/-}$ mice (Figure 2.7A), despite the increased expression of p16^{Ink4a} in the *Bmi-1*$^{-/-}$ cerebellum (Figure 2.8). This suggests that progenitors from some regions of the nervous system can be insensitive to p16^{Ink4a} expression. *Arf* deficiency had no effect on cerebellum development in *Bmi-1*$^{+/+}$ mice (data not shown) but increased the overall cerebellum size in *Bmi-1*$^{-/-}$ mice, in addition to significantly increasing the thickness of the granular and molecular layers, and cell density in the molecular layer (Figure 2.7B) to a similar degree as observed from *Ink4a-Arf* deficiency (compare to Figure 2.7C). The observation that *Arf* deficiency had a greater effect than *Ink4a* deficiency on cerebellum development in *Bmi-1*$^{-/-}$ mice indicates that the relative importance of p16^{Ink4a} and p19^{Arf} differs between progenitor populations and regions of the nervous system.

Ink4a, Arf, or *Ink4a-Arf* deficiency do not rescue the growth or survival of *Bmi-1*$^{-/-}$ mice

Although *Ink4a* deficiency, *Arf* deficiency, or *Ink4a-Arf* deficiency each partially rescued aspects of neural stem cell function and neural development in *Bmi-1*$^{-/-}$ mice, they did not affect the overall growth of *Bmi-1*$^{-/-}$ mice, which were significantly smaller than wild-type littermates (Figure 2.9). *Ink4a* deficiency or *Arf* deficiency also did not significantly affect brain mass in *Bmi-1*$^{-/-}$ mice (Figure 2.10A,B). *Ink4a-Arf* deficiency on the other hand did significantly increase brain mass in adult *Bmi-1*$^{-/-}$ mice, though only slightly (Figure 2.10C). The ability of *Ink4a* deficiency, *Arf* deficiency, and *Ink4a-Arf* deficiency to substantially rescue neural stem cell function while having little or no effect

on brain growth in *Bmi-1*$^{-/-}$ mice indicates that the effects of Bmi-1 on neural stem cells can be uncoupled from effects on tissue growth.

Ink4a deficiency, *Arf* deficiency, or *Ink4a-Arf* deficiency also did not rescue the survival of *Bmi-1*$^{-/-}$ mice, which usually died by postnatal day 30 (Figure 2.9), despite being born in nearly expected numbers (data not shown). *Ink4a-Arf* deletion did not prevent *Bmi-1*$^{-/-}$ mice from exhibiting ataxia (data not shown). Abnormalities in other tissues, such as the hematopoietic system, are also not completely rescued by *Ink4a-Arf* deletion and may exhibit less of a rescue than observed in the nervous system (see companion paper from van Lohuizen and colleagues). It is likely that *Bmi-1*$^{-/-}$ mice have uncharacterized defects in the maintenance of other tissues that could also affect viability. Thus the early death of these mice is likely to derive from complex combinations of defects in multiple tissues.

It is difficult to precisely estimate the fraction of each phenotype rescued by *Ink4a* or *Arf* deletion; however, the extent to which *Ink4a-Arf* deficiency rescued SVZ proliferation (Figure 2.6E) did not appear to be greater than observed from deletion of *Ink4a* (Figure 2.6A) or *Arf* alone (Figure 2.6C). Similarly, the extent to which *Ink4a-Arf* deficiency rescued neural stem cell frequency (Figure 2.4E, F) appeared to be less than the sum of the effects of *Ink4a* deficiency (Figure 2.4A, B) and *Arf* deficiency (Figure 2.4C, D). This suggests that there is cross regulation between the $p16^{Ink4a}$ and $p19^{Arf}$ pathways. A number of mechanisms by which the $p16^{Ink4a}$ and $p19^{Arf}$ pathways influence each other have already been identified (Lowe and Sherr, 2003). For example, since $p21^{cip1}$, like $p16^{Ink4a}$, promotes Rb activation, changes in $p21^{cip1}$ expression affect the levels of $p16^{Ink4a}$ that are required to inhibit proliferation (Lowe and Sherr, 2003).

Consistent with this, we found that *cip1* RNA levels were reduced by *Arf* deficiency and increased by *Bmi-1* deficiency (as would be predicted based on the presumed changes in $p19^{Arf}$ and p53 activity in these cells; Figure 2.11). These changes in *cip1* levels offer one possible source of cross regulation that could account for the less-than-additive effects of *Ink4a* and *Arf* deletion, particularly given that $p21^{cip1}$ regulates neural stem cell self-renewal (Kippin et al., 2005; Qiu et al., 2004).

Ink4a and *Arf* repression represent important mechanisms by which Bmi-1 promotes postnatal stem cell self-renewal, stem cell maintenance, and development in the nervous system. Since induction of $p16^{Ink4a}$ and $p19^{Arf}$ have been associated with cellular senescence (Lowe and Sherr, 2003), neural stem cells appear to undergo premature senescence in the absence of Bmi-1 and become depleted by adulthood. This suggests that the repression of these senescence pathways is a fundamental requirement for the maintenance of neural stem cells throughout life.

MATERIALS AND METHODS

The *Bmi-1*$^{+/-}$, *Arf* $^{+/-}$, and *Ink4a-Arf* $^{+/-}$ mice were backcrossed at least 8 times onto a C57BL background. Initial experiments employed *Ink4a*$^{+/-}$ mice on an FvB background, but all results were subsequently confirmed using *Ink4a*$^{+/-}$ mice backcrossed 5 times onto a C57BL background. All mice were genotyped by PCR using primers described in Suppl. Methods.

Isolation of CNS and PNS progenitors

Adult SVZ was obtained by coronally sectioning brains in ice-cold Opti-MEM medium (Gibco). The lateral walls of the lateral ventricles were removed, minced, then dissociated for 20 min at 37˚C in 0.025% trypsin/0.5mM EDTA (Calbiochem, San Diego, CA) plus 0.001% DNase1 (Roche, Indianapolis, IN). Cells were quenched with staining medium (L15 medium containing 1 mg/ml BSA (Sigma A-3912, St. Louis, MO), 10 mM HEPES (pH 7.4), and 1% penicillin/streptomycin (BioWhittaker, Walkersville, MD)) containing 0.014% soybean trypsin inhibitor (Sigma) and 0.001% DNAse1. After centrifuging, the cells were resuspended in staining medium, triturated, filtered through nylon screen (45 m, Sefar America, Kansas City, MO), counted by hemocytometer, and plated.

For PNS progenitor isolation, adult mouse guts were dissected into ice cold PBS. Outer muscle/plexus layers were peeled free from the underlying epithelium as described (Kruger et al., 2002); then minced, and dissociated for 45 min in 0.025% trypsin/EDTA (Gibco 25300-054, Grand Island, NY) plus 1 mg/ml type 4 collagenase (Worthington) in Ca, Mg-free HBSS at 37°C with agitation every 5 minutes. The dissociated cells were then quenched in staining medium, resuspended and filtered as described above. Dissociated gut cells were sometimes stained with an antibody against p75 (Ab 1554; Chemicon International) as described previously (Bixby et al., 2002). The analysis and sorting of $p75^{+}$ cells was performed by a FACS VantageSE flow-cytometer (Becton-Dickinson).

Cell culture and self-renewal assay

Cells were plated at clonal density (2000 cells per well of a 6-well plate; 1.3

cells/ul of culture medium) on ultra-low binding plates (Corning) to grow neurospheres. Culture medium was based on a 5:3 mixture of DMEM-low glucose: neurobasal medium (Gibco) supplemented with 20 ng/ml human bFGF (R&D Systems, Minneapolis, MN), 1% N2 supplement (Gibco), 2% B27 supplement (Gibco), 50 M 2-mercaptoethanol, and 1% pen/strep (Biowhittaker). CNS cultures also contained 20 ng/ml EGF (R&D Systems) and 10% chick embryo extract (prepared as described (Stemple and Anderson, 1992)). PNS cultures contained 15% chick embryo extract, 35 mg/ml (110 nM) retinoic acid (Sigma), and 20 ng/ml IGF1 (R&D Systems). All cultures were maintained at 37˚C in 6% CO_2/balance air.

To measure self-renewal, individual CNS neurospheres were dissociated by trituration then replated at clonal density in non-adherent cultures. Secondary neurospheres were counted 5-10 days later to determine the number of secondary neurospheres formed per primary neurosphere. Individual PNS neurospheres were replated for 48 h into adherent plates to allow the spheres to spread out over the culture dish. The adherent colonies were then treated with trypsin and collagenase (4 parts 0.05% trypsin-EDTA plus 1 part 10mg/ml collagenase IV) for 5 min at 37°C followed by trituration. 5,000 dissociated cells were replated per well of a 6 well plate and secondary neurospheres were counted 10 days later.

Anti-BrdU antibody staining

For detection of BrdU in the CNS tissue sections, DNA was first denatured in 2M HCl for 30 min at room temperature and neutralized with 0.1M Sodium Borate. Sections were pre-blocked for 1 hr at room temperature in goat serum solution (GSS) (PBS containing 5% goat serum, 1% BSA, and 0.3% Triton X-100 (Sigma)). Primary rat anti-

BrdU (1:200, Accurate Chemical, Westbury, NY) diluted in GSS was incubated overnight at 4˚C, followed by FITC-conjugated anti-rat Fc fragment (Jackson Labs) for 3-4 hrs at room temperature. Slides were counter stained in 2.5µg/ml DAPI for 10 min at RT, then mounted using ProLong antifade solution (Molecular Probes, Eugene, OR). Numbers of BrdU labeled cells were divided by total DAPI-positive nuclei.

Western blots and quantitative RT-PCR

Cells or tissues were resuspended in ice-cold cell lysis buffer (Cell Signaling Technology) with protease inhibitor cocktail (complete mini tablet, Roche), and incubated for 15-30 minutes on ice. Tissues were briefly homogenized, then all samples were sonicated for 1 minute at 20-30% power in a microson ultrasonic cell disruptor, spun down for 5 minutes at 16,000g and the supernatant quantified colorimetrically (BioRad protein assay). 50-100 ug of protein per lane were separated in 12% denaturing SDS-PAGE gels and transferred overnight at 4°C to PVDF membranes (Bio-Rad). The membranes were blocked in Tris buffered saline with 0.1% tween-20 and 5% milk, incubated with primary and secondary antibodies, and washed following standard procedures. Horseradish peroxidase conjugated secondary antibodies were detected by chemiluminescence (ECL Plus; Amersham-Pharmacia). Primary antibodies were mouse monoclonal anti-ß-actin (Ab-1; Oncogene), rabbit polyclonal anti-$p19^{ARF}$ (ab80, Abcam), mouse monoclonal anti $p21^{cip1}$ (Pharmigen) and rabbit polyclonal anti-$p16^{Ink4a}$ (M-156; Santa Cruz Biotechnology).

Quantitative RT-PCR was performed as described previously (Molofsky et al., 2003). Primers used to amplify *Ink4a* were 5'CGAACTCTTTCGGTCGTACCC-3' (sense) and 5'-CGAATCTGCACCGTAGTTGAGC-3' (antisense). These primers

amplified an 89 nucleotide product that spanned an intron and that was identical to *Ink4a* upon sequencing. Primers for *cip1* (*cdkn1a*) were 5-GCAGACCAGCCTGACAGATTTC-3 (sense) and 5-TCCTGACCCACAGCAGAAGAGG-3 (antisense). These primers spanned an intron and yielded a single 109 nucleotide product that was identical to *cip1* upon sequencing.

Immunocytochemistry of cultured cells

CNS neurospheres were tested for multipotency by replating one neurosphere per well into 48-well plates and then culturing adherently for 3 to 5 days prior to triple staining for markers of oligodendrocytes (O4), neurons (TuJ1), and astrocytes (GFAP). Plates were incubated first in anti-O4 antibody, and then in donkey anti-mouse IgM secondary antibody conjugated to horse radish peroxidase (Jackson Immunoresearch) followed by nickel diaminobenzidine staining (Shah et al., 1996). The cultures were then fixed in acid ethanol (5% glacial acetic acid in 100% ethanol) for 20 min at –20°C. After blocking in PBS containing 4% horse serum, 0.4% BSA, 0.05% sodium azide, and 0.1% Igepal (Sigma), the cultures were stained with anti-Tuj1 (1:500, Covance, Princeton, NJ) and anti-GFAP (1:200, Sigma G-3893) primary antibodies followed by FITC-conjugated goat anti mouse IgG1, and PE-conjugated goat anti mouse IgG2a antibodies (Southern Biotech, Birmingham, AL). PNS neurospheres were replated into adherent cultures in which the plates had been coated with poly-D-lysine and human fibronectin as described previously (Bixby et al., 2002). The neurospheres were allowed to differentiate for 7 to 10 days and then fixed in acid ethanol for 20 min at –20°C, washed, blocked, and triply labeled for Peripherin (Chemicon International AB1530), GFAP (Sigma G-3893), and SMA (Sigma A-2547) as described previously (Shah et al., 1996). Cells were stained

for 10 min at room temperature with 10 g/ml DAPI (Sigma D-8417) to visualize nuclei.

Immunohistochemistry of tissue sections

To quantify SVZ proliferation, mice were injected with 50 mg/kg of bromodeoxyuridine (BrdU) (Sigma), and sacrificed one or two hours after BrdU injection, depending on the experiment. Brains were fixed in 4% paraformaldehyde overnight, then cryoprotected in 15% sucrose, embedded in 7.5% gelatin/15% sucrose, and flash frozen. 12 μm sections were cut on a Leica cryostat. See supplementary material for BrdU immunohistochemistry.

For cerebellum histology, 30 um sagital sections were obtained, post-fixed in 10% neutral buffered formalin and stained with hematoxylin and eosin.

To study gut neurogenesis, segments of intestine were fixed in 4% paraformaldehyde overnight, then cryoprotected in 30% sucrose, embedded in OCT (Tissue-Tek) and frozen. 12 μm sections were labeled with the neuronal marker HuC/D, by subjecting the sections to antigen retrieval as recommended by the antibody manufacturer, then pre-blocked for 1 hr at room temperature in modified GSS (PBS containing 5% goat serum, and 0.5% Triton X-100). Primary mouse anti-HuC/D (Molecular Probes, Inc., Eugene, OR) diluted in modified GSS was incubated for 1h at room temperature, followed by Alexa Fluor 555-conjugated goat anti-mouse IgG2b (Molecular Probes, Inc., Eugene, OR) for 30 min at room temperature. Slides were counter stained in 2.5μg/ml DAPI for 10 min at room temperature, then mounted using ProLong antifade solution (Molecular Probes, Eugene, OR). Only HuC/D+ neurons in the myenteric plexus were counted.

Primers used for mouse genotyping

Ink4a genotyping was performed by PCR as described (Sharpless et al., 2001). *Bmi-1* genotyping was performed using the oligonucleotides 5'-CGCCGTGCACAGGGTGTCACGTTGCAAGAC -3' and 5'-CAAGCCAACCACGGCCTCCAGAAG-3' to detect the gene targeted allele, and the oligonucleotides 5'-AGCAGCAATGACTGTGATGCACTTGAG-3' and 5'-GCTCTCCAGCATTCGTCAGTCCATCCC-3' to detect wild-type *Bmi-1*. *Arf* genotyping was performed using the oligonucleotides 5'-CGCTGTTCTCCTCTTCCTCATCTC -3' and 5'-CCAGTCATAGCCGAATAGCCTCTC -3' to detect the gene-targeted allele and the oligonucleotides 5'- GCGTACCGCTAAGGGTTCAAAAC -3' and 5'-TCCTCACAGTGACCAAGAACCTG -3' to detect wild-type *Arf*. *Ink4a-Arf* genotyping (mice targeted to lack the exons common to both *Ink4a* and *Arf*) were genotyped using the oligonucleotides 5'- CTGCTCAACTACGGTGCAGATTC -3' and 5' - GCAAATATCGCACGATGTCTTGATG -3' to detect wild-type *Ink4a-Arf* and the oligonucleotides 5'- CGCTGTTCTCCTCTTCCTCATCTC -3' and 5'-CCAGTCATAGCCGAATAGCCTCTC -3' to detect the gene-targeted allele.

ACKNOWLEDGEMENTS

This work was supported by the National Institutes of Health (R01 NS40750), the James S. McDonnell Foundation, and the Howard Hughes Medical Institute. A.V.M. was supported by a National Research Service Award from NIH (F30 NS048642). R.P. was supported by a postdoctoral fellowship from the Spanish Ministry of Science and

Technology. S.H. was supported by a fellowship from the University of Michigan Cellular and Molecular Biology program. Thanks to David Adams, Anne Marie Deslaurier, and the University of Michigan Flow-Cytometry Core Facility (supported by UM-Comprehensive Cancer NIH CA46592, and UM-Multipurpose Arthritis Center NIH P60-AR20557). Thanks to Elizabeth Smith in the Hybridoma Core Facility (supported through the Michigan Diabetes Research and Training Center, NIH5P60-DK20572, and the Rheumatic Disease Center, P30 AR48310). Thanks to Kelly Yeager for tissue sectioning. Thanks to Maarten van Lohuizen for providing *Bmi-1*$^{+/-}$ mice and for sharing unpublished results, to Charles Sherr for providing *Arf* $^{+/-}$ mice, and to Ronald DePinho for providing *Ink4a*$^{+/-}$ and *Ink4a-Arf* $^{+/-}$ mice.

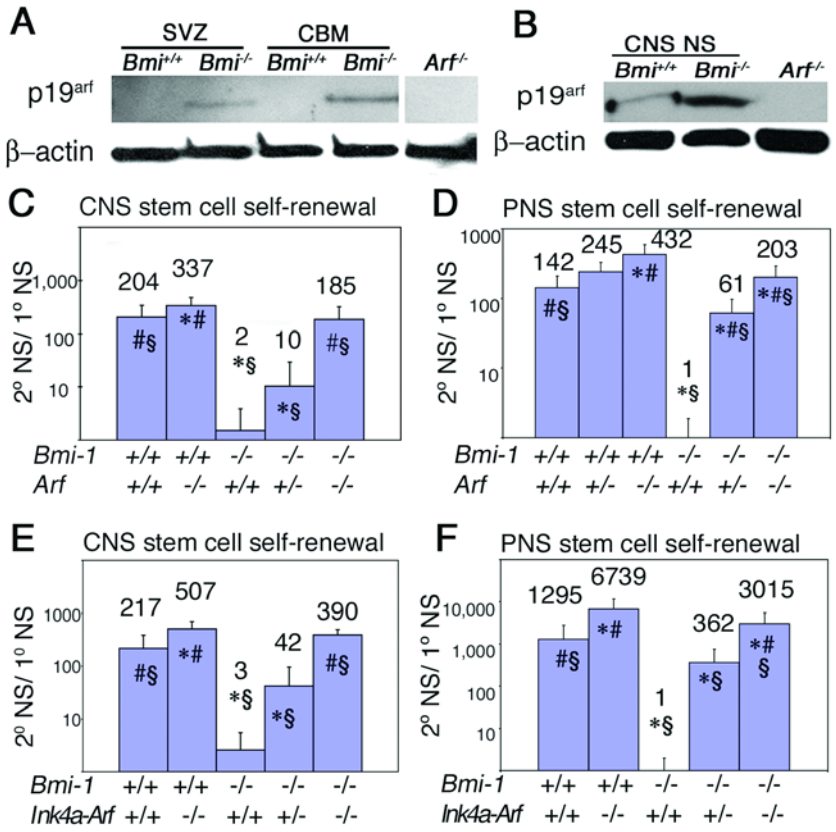

Figure 2.1: p19^{Arf} is upregulated in the absence of *Bmi-1*, and deletion of *Arf* or *Ink4a-Arf* significantly increased the self-renewal of neural stem cells from the SVZ and gut of *Bmi-1*$^{-/-}$ mice.

A) p19^{Arf} was increased in uncultured SVZ and cerebellum of 4 week old *Bmi-1*$^{-/-}$ mice. Western blot of neurosphere cells from *Arf* $^{-/-}$ mice is shown as a negative control. B) p19^{Arf} was increased in *Bmi-1*$^{-/-}$ CNS neurospheres cultured for 13 days. C, D) *Arf* deficiency significantly increased self-renewal (the number of secondary neurospheres generated per subcloned primary neurosphere) within *Bmi-1*$^{+/+}$ and *Bmi-1*$^{-/-}$ CNS neurospheres(C), and PNS neurospheres (D), as well as the percentage of cells from *Bmi-1*$^{-/-}$ (but not *Bmi-1*$^{+/+}$) primary neurospheres that formed secondary neurospheres upon replating (Figure 2.3). CNS data represent mean±SD for 2 to 4 mice per genotype, in 4 independent experiments. PNS data are from 3 to 7 mice per genotype in 4 independent experiments. E, F) *Ink4a-Arf* deficiency significantly increased self-renewal within *Bmi-1*$^{+/+}$ and *Bmi-1*$^{-/-}$ CNS neurospheres (E; mean±SD for 2 to 4 mice per genotype, 4 independent experiments), and PNS neurospheres (F; 3 to 6 mice per genotype, 6 independent experiments) and the percentage of cells from *Bmi-1*$^{-/-}$ (but not *Bmi-1*$^{+/+}$) primary neurospheres that formed secondary neurospheres upon replating (Figure 2.3). indicates significantly ($p<0.05$) different from *Bmi-1*$^{+/+}$*Arf* $^{+/+}$ or *Bmi-1*$^{+/+}$*Ink4a-Arf*$^{+/+}$, # indicates significantly different from *Bmi-1*$^{-/-}$*Arf* $^{+/+}$ or *Bmi-1*$^{-/-}$*Ink4a-Arf* $^{+/+}$, and § indicates significantly different from *Bmi-1*$^{+/+}$*Arf* $^{-/-}$ or *Bmi-1*$^{+/+}$*Ink4a-Arf* $^{-/-}$. All experiments were performed on 4 to 8 week old mice.

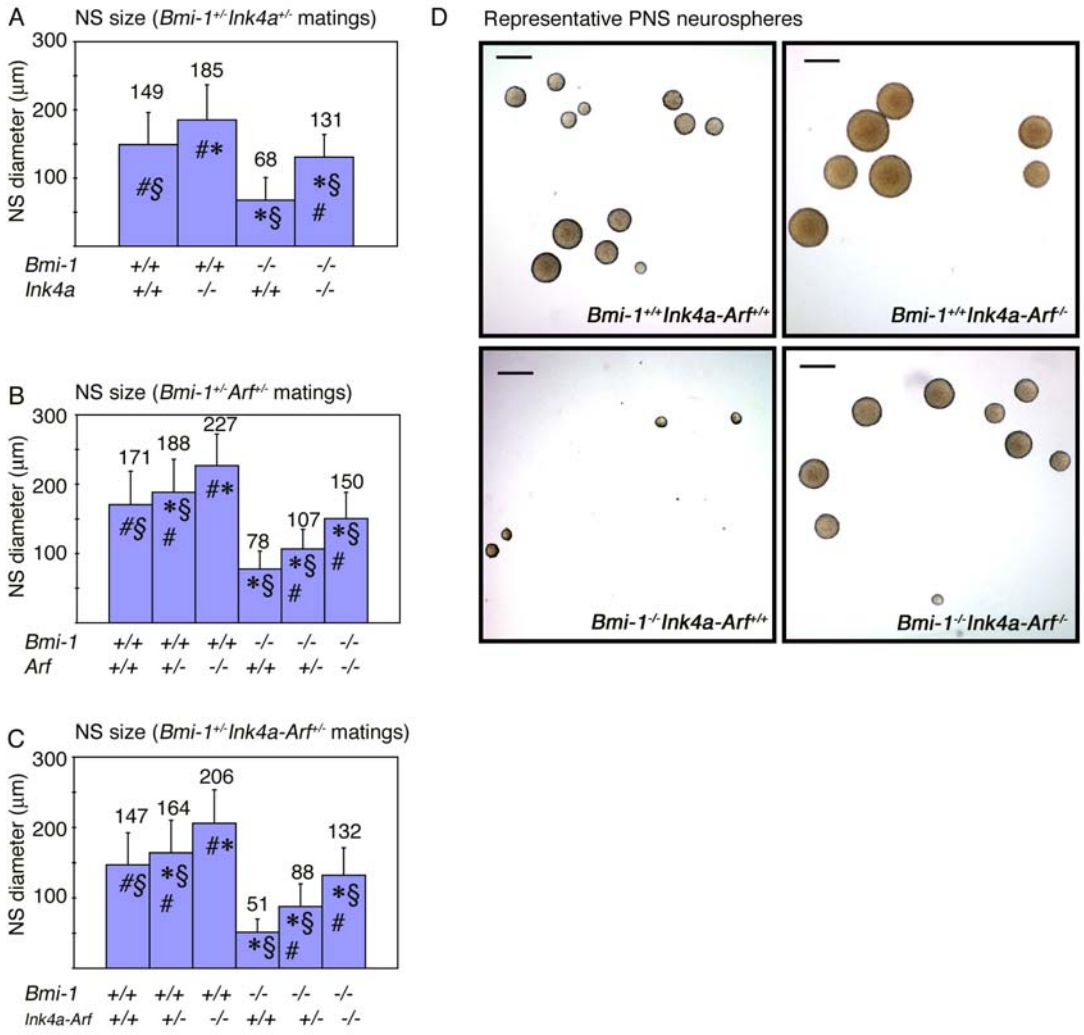

Figure 2.2: *Bmi-1* deficiency significantly reduced the diameter of neurospheres, but this effect was partially rescued by *Ink4a*, *Arf*, or *Ink4a-Arf* deficiency

All data were obtained from PNS neurospheres cultured from the guts of 4 to 8 week old mice; however, similar results were obtained with CNS neurospheres. A) *Ink4a* deficiency significantly increased the diameter of *Bmi-1*$^{-/-}$ and *Bmi-1*$^{+/+}$ neurospheres, consistent with a partial rescue of the proliferation defect within *Bmi-1*$^{-/-}$ neurospheres. indicates significantly different (P<0.05 by T-test) from *Bmi-1*$^{+/+}$*Ink4a*$^{+/+}$, # indicates significantly different from *Bmi-1*$^{-/-}$*Ink4a*$^{+/+}$, and § indicates significantly different from *Bmi-1*$^{+/+}$*Ink4a*$^{-/-}$. B) *Arf* deficiency also significantly increased the diameter of *Bmi-1*$^{-/-}$ and *Bmi-1*$^{+/+}$ neurospheres, consistent with a partial rescue of the proliferation defect within *Bmi-1*$^{-/-}$ neurospheres. C) *Ink4a-Arf* deficiency significantly increased the diameter of *Bmi-1*$^{-/-}$ and *Bmi-1*$^{+/+}$ neurospheres, again suggesting a partial rescue of the *Bmi-1*$^{-/-}$ proliferation defect. The data in each panel represent mean±SD for at least 5 independent experiments. D) Representative photographs of neurospheres cultured from the progeny of *Bmi-1*$^{+/-}$*Ink4a-Arf* $^{+/-}$ matings. These apparent effects of *Ink4a* and/or *Arf* deletion on proliferation within neurospheres were consistent with similar effects on BrdU incorporation in CNS stem cell colonies growing in adherent cultures (data not shown).

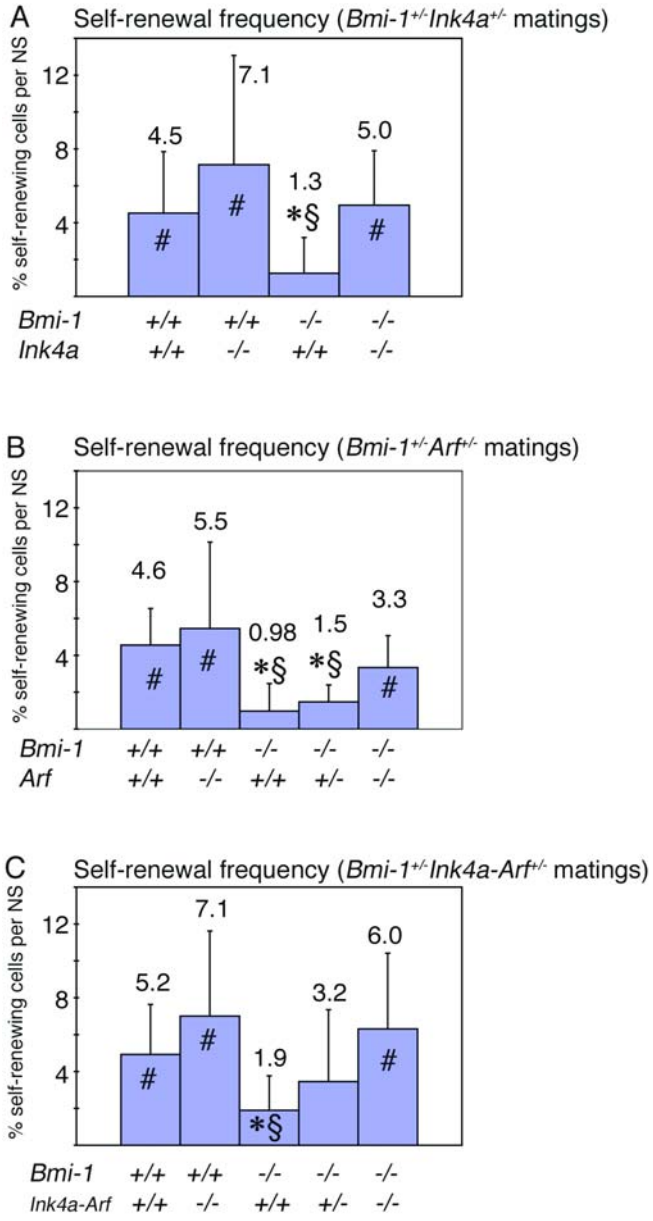

Figure 2.3: *Bmi-1* deficiency significantly reduced the percentage of cells within primary neurospheres capable of forming secondary neurospheres, but *Ink4a*, *Arf*, or *Ink4a-Arf* deficiency significantly increased this percentage.
The frequency of stem cells within primary CNS neurospheres was determined by dividing the number of secondary neurospheres by the number of cells subcloned from primary neurospheres. A) *Bmi-1*$^{+/-}$*Ink4a*$^{+/-}$ matings (mean±SD for 2 mice per genotype in two independent experiments, 6 neurospheres per mouse). B) *Bmi-1*$^{+/-}$*Arf*$^{+/-}$ matings (mean±SD for 2-4 mice per genotype in 4 independent experiments, 4-6 neurospheres per mouse). C) *Bmi-1*$^{+/-}$*Ink4a-Arf*$^{+/-}$ matings (mean±SD for 2-5 mice per genotype in 4 independent experiments, 4-6 neurospheres per mouse). Similar results were obtained using PNS neurospheres (not shown).

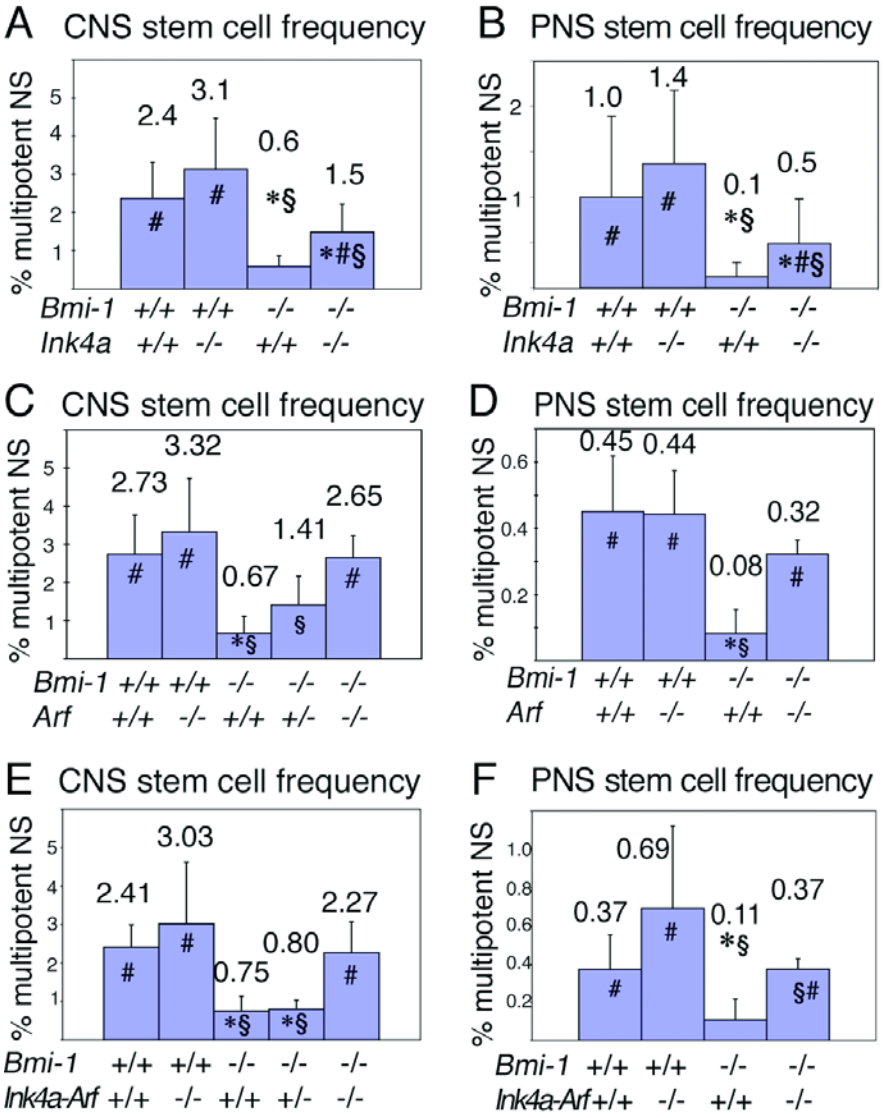

Figure 2.4: Deletion of *Ink4a, Arf,* or *Ink4a-Arf* significantly increased neural stem cell frequency in *Bmi-1*$^{-/-}$ mice.
A,B) *Ink4a* deficiency significantly increased the percentage of SVZ cells (A) or adult gut NCSCs (B) from *Bmi-1*$^{-/-}$ mice that formed multipotent neurospheres in culture (mean±SD for 4 independent experiments). C,D) *Arf* deficiency also significantly increased the percentage of *Bmi-1*$^{-/-}$ cells that formed multipotent neurospheres from the SVZ (C; 3 to 6 mice per genotype, in 6 independent experiments) or gut wall (D; 4 mice per genotype, in 4 independent experiments). E, F) *Ink4a-Arf* deficiency significantly increased the frequency of cells from the *Bmi-1*$^{-/-}$ adult SVZ (E; 2 to 7 mice/genotype, 8 independent experiments) or gut wall (F; 3 to 8 mice per genotype, 3 independent experiments) that formed multipotent neurospheres in culture. indicates significantly different (P<0.05 by T-test) from wild-type, # indicates significantly different from *Bmi-1*$^{-/-}$*Ink4a*$^{+/+}$, *Bmi-1*$^{-/-}$*Arf* $^{+/+}$, or *Bmi-1*$^{-/-}$*Ink4a-Arf* $^{+/+}$, and § indicates significantly different from *Bmi-1*$^{+/+}$*Ink4a*$^{-/-}$, *Bmi-1*$^{+/+}$*Arf* $^{-/-}$, or *Bmi-1*$^{+/+}$*Ink4a-Arf* $^{-/-}$. All experiments employed 4 to 8 week old mice.

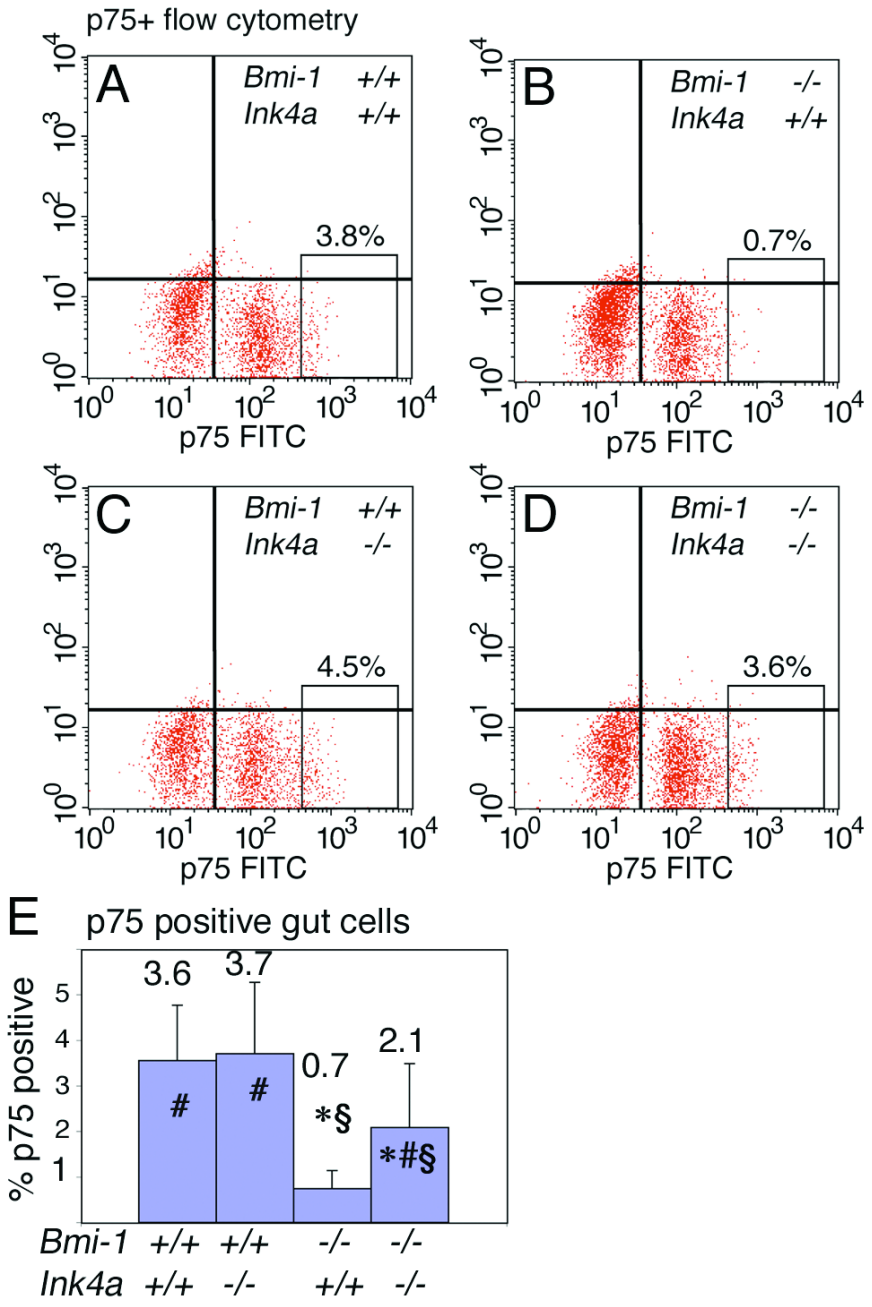

Figure 2.5: *Ink4a* deficiency partially rescued the frequency of uncultured NCSCs in the adult gut.

Ink4a deficiency partially rescued the frequency of $p75^{+}$ cells, which are highly enriched for NCSCs, in the adult gut wall of *Bmi-1*$^{-/-}$ mice. A-D) Representative flow-cytometry plots from the indicated genotypes demonstrating $p75^{+}$ NCSC frequency (boxed region of each plot) among freshly dissociated gut wall cells. E) The frequency of $p75^{+}$ cells was significantly reduced by *Bmi-1* deficiency, and significantly increased by *Ink4a* deficiency. Data in panel E represent mean±SD for 10 independent experiments using 4 to 8 week old mice.

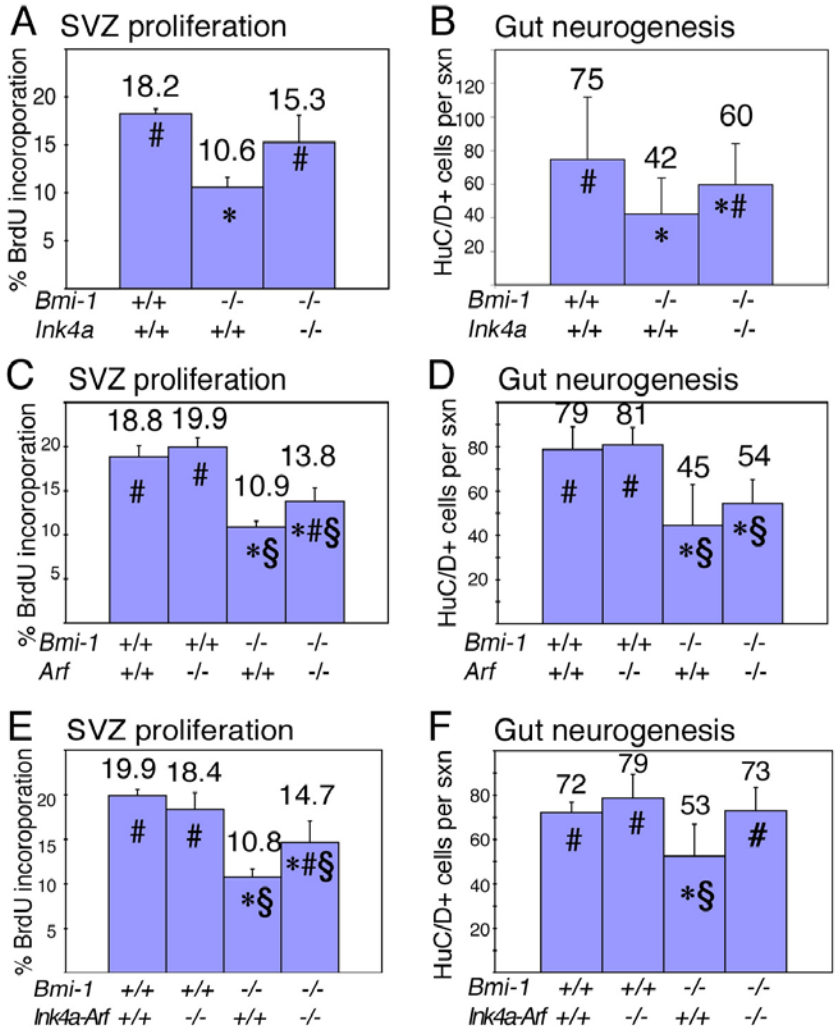

Figure 2.6: Deletion of *Ink4a*, *Arf*, or *Ink4a-Arf* partially rescued SVZ proliferation and gut neurogenesis in 3 to 9 week old *Bmi-1*$^{-/-}$ mice *in vivo*.

A, C, E) The rate of proliferation (percentage of cells that incorporate a pulse of BrdU) in the SVZ of *Bmi-1*$^{-/-}$ mice was significantly increased by *Ink4a* deficiency (A), *Arf* deficiency (C), or combined *Ink4a-Arf* deficiency (E). Note that deletion of these genes had no effect on SVZ proliferation in Bmi-1$^{+/+}$ mice (C, E, and *Ink4a* data not shown; 6 to 8 sections per mouse, 3 to 5 mice per genotype). *Ink4a* deficiency partially rescued the number of myenteric plexus neurons per cross-section through the distal small intestine of *Bmi-1*$^{-/-}$ mice (B; mean±SD for 4 to 7 mice per genotype, 7 to 10 sections per mouse). *Arf* deficiency tended to increase the number of neurons per cross-section in *Bmi-1*$^{-/-}$ mice, though the effect was not statistically significant (D; mean±SD for 4 to 5 mice per genotype and 8 to 10 sections per mouse). *Ink4a-Arf* deficiency significantly increased the number of myenteric plexus neurons per cross-section of *Bmi-1*$^{-/-}$ mice in a way that was consistent with a complete rescue (F; mean±SD for 5 mice per genotype and 6 to 8 sections per mouse). indicates significantly different (P<0.05 by T-test) from wild-type, # indicates significantly different from *Bmi-1*$^{-/-}$*Ink4a*$^{+/+}$, *Bmi-1*$^{-/-}$*Arf*$^{+/+}$, or *Bmi-1*$^{-/-}$ *Ink4a-Arf*$^{+/+}$, and § indicates significantly different from *Bmi-1*$^{+/+}$*Arf*$^{-/-}$, or *Bmi-1*$^{+/+}$*Ink4a-Arf*$^{-/-}$.

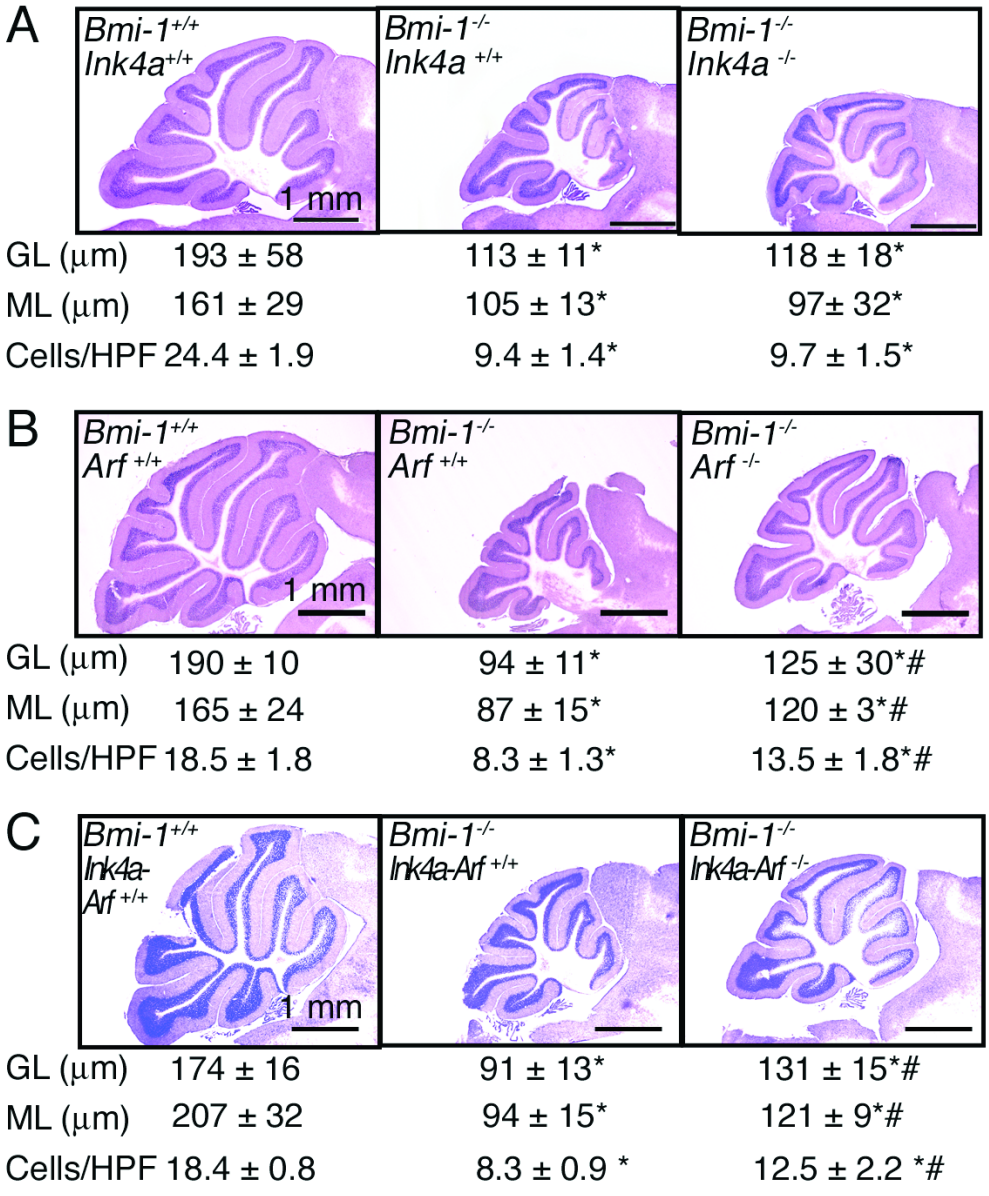

Figure 2.7: Deletion of *Arf* or *Ink4a-Arf*, but not *Ink4a* alone, partially rescues cerebellum development in *Bmi-1*$^{-/-}$ mice.
Hematoxylin and eosin stained saggital sections of adult cerebellum. Measurements of granular layer thickness (GL), molecular layer thickness (ML), and cell density in the molecular layer (cells/High Power Field, HPF is 100 m^2) for each genotype are represented below the corresponding picture. A) *Ink4a* deficiency did not affect cerebellum development in *Bmi-1*$^{-/-}$ mice (mean±SD for 4 mice per genotype, 7 to 25 measurements per mouse). B) *Arf* deficiency partially rescued cerebellum growth in 4 to 8 week old *Bmi-1*$^{-/-}$ mice (mean±SD for 3 to 4 mice per genotype and 10 to 23 measurements per mouse). C) *Ink4a-Arf* deficiency also partially rescued cerebellum growth in *Bmi-1*$^{-/-}$ mice (mean±SD for 3 to 5 mice per genotype, 6 to 32 measurements per mouse). *Ink4a, Arf,* and *Ink4a-Arf* deficiencies did not affect cerebellum growth in *Bmi-1*$^{+/+}$ mice (data not shown).

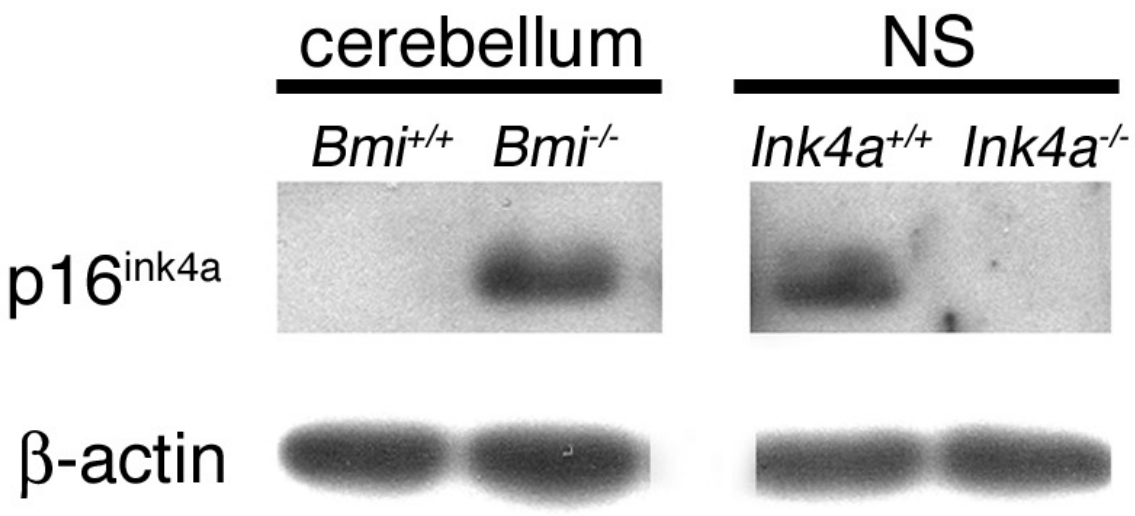

Figure 2.8: p16^{ink4a} is expressed in the cerebellum of adult *Bmi-1*$^{-/-}$ mice.
p16^{ink4a} was not detected in the cerebellum of a four-to-six week old *Bmi-1*$^{+/+}$ mouse but was strongly upregulated in the cerebellum of a littermate *Bmi-1*$^{-/-}$ mouse. Positive and negative controls from the same western blot confirm p16^{ink4a} expression in *Ink4a*$^{+/+}$ neurospheres, as observed previously (Molofsky et al., 2003), and a lack of p16^{ink4a} expression in *Ink4a*$^{-/-}$ neurospheres. At the RNA level, *Ink4a* was also significantly upregulated in the *Bmi-1*$^{-/-}$ cerebellum by quantitative (real-time) PCR (data not shown).

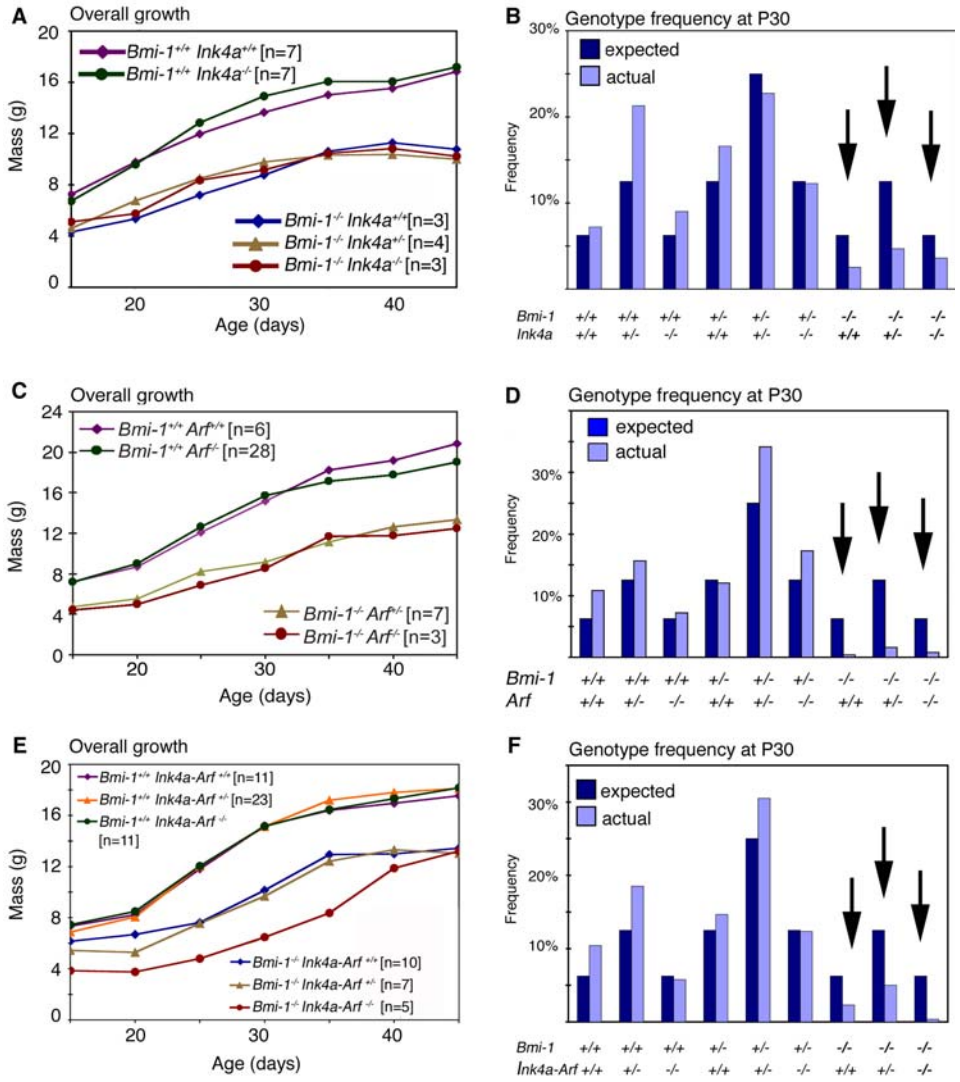

Figure 2.9: *Ink4a, Arf,* or *Ink4a-Arf* deficiency did not rescue the overall growth or survival of *Bmi-1*$^{-/-}$ mice.

A) *Ink4a* deficiency did not significantly affect the growth of either *Bmi-1*$^{+/+}$ or *Bmi-1*$^{-/-}$ mice, though *Bmi-1*$^{-/-}$ mice were significantly ($p<0.05$) smaller than *Bmi-1*$^{+/+}$ mice at all time points. B) *Bmi-1*$^{-/-}$ mice were born at nearly normal frequencies (data not shown) but usually died prior to postnatal day 30. Survival was not significantly increased by *Ink4a* deficiency (arrows; $p=0.306$ by logistic regression analysis). The reduction in the frequency of *Bmi-1*$^{-/-}$ mice was statistically significant ($P<0.001$ for chi^2 test, based on 315 mice). *Arf* deficiency did not significantly affect the growth (C) or survival (D) of either *Bmi-1*$^{+/+}$ or *Bmi-1*$^{-/-}$ mice (see arrows in D; $p=0.552$ by logistic regression analysis). The reduction in the frequency of *Bmi-1*$^{-/-}$ mice was statistically significant ($P<0.001$ for chi^2 based on 249 mice.) E) *Ink4a-Arf* deficiency did not increase the overall growth of either *Bmi-1*$^{+/+}$ or *Bmi-1*$^{-/-}$ mice, though *Bmi-1*$^{-/-}$ mice were significantly ($p<0.01$) smaller than *Bmi-1*$^{+/+}$ mice at all time points after P20. (F) The survival of *Bmi-1*$^{-/-}$ mice was not increased by *Ink4a-Arf* deficiency. The reduction in the frequency of *Bmi-1*$^{-/-}$ mice was statistically significant ($P<0.001$ for chi^2 test based on 259 mice).

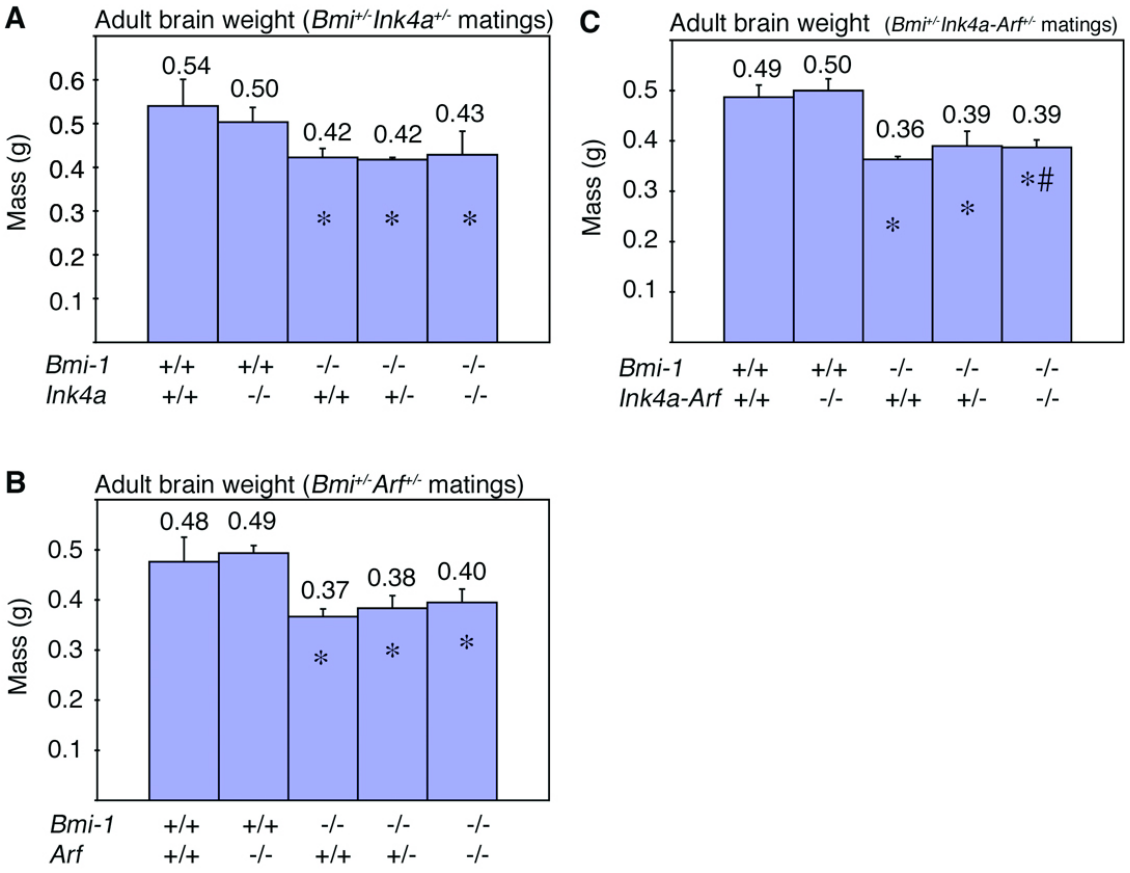

Figure 2.10: The brain masses of adult *Bmi-1*$^{-/-}$ mice were significantly reduced relative to littermate controls regardless of *Ink4a* and/or *Arf* deletion.
A) Brain masses in adult (all mice were 4 to 8 weeks old) *Bmi-1*$^{-/-}$*Ink4a*$^{+/+}$ mice were significantly reduced relative to *Bmi-1*$^{+/+}$*Ink4a*$^{+/+}$ controls (*, $p<0.01$) and *Ink4a* deficiency had no detectable effect on brain mass. Each bar represents mean±SD of 3-7 mice per genotype. B) Brain masses in *Bmi-1*$^{-/-}$*Arf* $^{+/+}$ mice were also significantly smaller than *Bmi-1*$^{+/+}$*Arf* $^{+/+}$ controls (*, $p<0.01$). *Arf* deficiency appeared to be associated with a small recovery in brain mass in *Bmi-1*$^{-/-}$ mice, though this effect was not statistically significant (3-6 mice per genotype). C) Brain masses in *Bmi-1*$^{-/-}$*Ink4a-Arf* $^{+/+}$ mice were significantly smaller than in *Bmi-1*$^{+/+}$*Ink4a-Arf* $^{+/+}$ mice. Deletion of *Ink4a-Arf* from *Bmi-1*$^{-/-}$ mice gave a slight but significant increase in brain mass ($p<0.05$; 4-8 mice per genotype) consistent with its effect on cerebellum development (Figure 2.7).

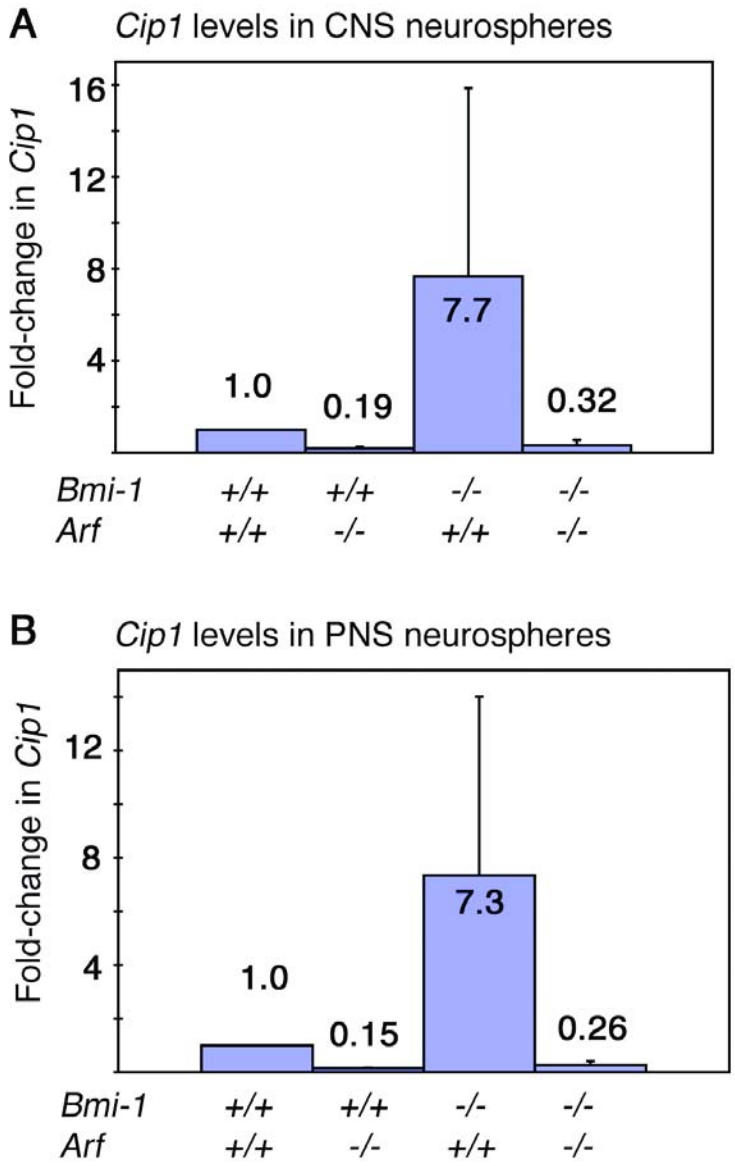

Figure 2.11: *cip1* expression increases in the absence of *Bmi-1* and decreases in the absence of *Arf* in CNS and PNS neurospheres
A) CNS neurospheres, 4 samples per genotype cultured for 10-11 days. B) PNS neurospheres 2-3 samples per genotype, cultured for 12-14 days. These data suggest that *Arf* deletion could indirectly affect Rb activity through its effects on *cip1* expression. As a result, the effects of *Ink4a* deficiency and *Arf* deficiency on neurosphere self-renewal would not be expected to be additive.

BIBLIOGRAPHY

Bixby, S., G.M. Kruger, J.T. Mosher, N.M. Joseph, and S.J. Morrison. 2002. Cell-intrinsic differences between stem cells from different regions of the peripheral nervous system regulate the generation of neural diversity. *Neuron* **35**: 643-56.

Dimri, G.P., J.L. Martinez, J.J. Jacobs, P. Keblusek, K. Itahana, M. Van Lohuizen, J. Campisi, D.E. Wazer, and V. Band. 2002. The Bmi-1 oncogene induces telomerase activity and immortalizes human mammary epithelial cells. *Cancer Res* **62**: 4736-45.

Harrison, D.E. 1979. Proliferative capacity of erythropoietic stem cell lines and aging: an overview. *Mechanisms of Ageing and Development* **9**: 409-426.

Itahana, K., Y. Zou, Y. Itahana, J.-L. Martinez, C. Beausejour, J.J.L. Jacobs, M.v. Lohuizen, V. Band, J. Campisi, and G.P. Dimri. 2003. Control of the replicative life span of human fibroblasts by p16 and the polycomb protein Bmi-1. *Molecular and Cellular Biology* **23**: 389-401.

Jacobs, J.J.L., K. Kieboom, S. Marino, R.A. DePinho, and M.v. Lohuizen. 1999a. The oncogene and polycomb-group gene bmi-1 regulates cell proliferation and senescence through the ink4a locus. *Nature* **397**: 164-168.

Jacobs, J.J.L., B. Scheijen, J.-W. Voncken, K. Kieboom, A. Berns, and M. von Lohuizen. 1999b. Bmi-1 collaborates with c-Myc in tumorigenesis by inhibiting c-Myc-induced apoptosis via INK4a/ARF. *Genes and Development* **13**: 2678-2690.

Kamijo, T., F. Zindy, M.F. Roussel, D.E. Quelle, J.R. Downing, R.A. Ashmun, G. Grosveld, and C.J. Sherr. 1997. Tumor suppression at the mouse INK4a locus mediated by the alternative reading frame product p19ARF. *Cell* **91**: 649-59.

Kippin, T.E., D.J. Martens, and D. van der Kooy. 2005. p21 loss compromises the relative quiescence of forebrain stem cell proliferation leading to exhaustion of their proliferation capacity. *Genes Dev* **19**: 756-67.

Kruger, G.M., J.T. Mosher, S. Bixby, N. Joseph, T. Iwashita, and S.J. Morrison. 2002. Neural crest stem cells persist in the adult gut but undergo changes in self-renewal, neuronal subtype potential, and factor responsiveness. *Neuron* **35**: 657-69.

Lessard, J., S. Baban, and G. Sauvageau. 1998. Stage-specific expression of Polycomb Group genes in human bone marrow cells. *Blood* **91**: 1216-1224.

Lessard, J. and G. Sauvageau. 2003. Bmi-1 determines the proliferative capacity of normal and leukemic stem cells. *Nature* **423**: 255-260.

Leung, C., M. Lingbeek, O. Shakhova, J. Liu, E. Tanger, P. Saremaslani, M. Van Lohuizen, and S. Marino. 2004. Bmi1 is essential for cerebellar development and is overexpressed in human medulloblastomas. *Nature* **428**: 337-41.

Lowe, S.W. and C.J. Sherr. 2003. Tumor suppression by Ink4a-Arf: progress and puzzles. *Current Opinion in Genetics & Development* **13**: 77-83.

Maslov, A.Y., T.A. Barone, R.J. Plunkett, and S.C. Pruitt. 2004. Neural stem cell detection, characterization, and age-related changes in the subventricular zone of mice. *J Neurosci* **24**: 1726-33.

Molofsky, A.V., R. Pardal, T. Iwashita, I.K. Park, M.F. Clarke, and S.J. Morrison. 2003. Bmi-1 dependence distinguishes neural stem cell self-renewal from progenitor proliferation. *Nature* **425**: 962-7.

Molofsky, A.V., R. Pardal, and S.J. Morrison. 2004. Diverse mechanisms regulate stem cell self-renewal. *Curr Opin Cell Biol* **16**: 700-7.

Morrison, S.J., N.M. Shah, and D.J. Anderson. 1997. Regulatory mechanisms in stem cell biology. *Cell* **88**: 287-298.

Morrison, S.J., A.M. Wandycz, K. Akashi, A. Globerson, and I.L. Weissman. 1996. The aging of hematopoietic stem cells. *Nature Medicine* **2**: 1011-1016.

Park, I.-K., D. Qian, M. Kiel, M. Becker, M. Pihalja, I.L. Weissman, S.J. Morrison, and M. Clarke. 2003. Bmi-1 is required for the maintenance of adult self-renewing hematopoietic stem cells. *Nature* **423**: 302-305.

Qiu, J., Y. Takagi, J. Harada, N. Rodrigues, M.A. Moskowitz, D.T. Scadden, and T. Cheng. 2004. Regenerative response in ischemic brain restricted by p21cip1/waf1. *J Exp Med* **199**: 937-45.

Serrano, M., H. Lee, L. Chin, C. Cordon-Cardo, D. Beach, and R.A. DePinho. 1996. Role of the INK4a locus in tumor suppression and cell mortality. *Cell* **85**: 27-37.

Shah, N.M., A. Groves, and D.J. Anderson. 1996. Alternative neural crest cell fates are instructively promoted by TGFß superfamily members. *Cell* **85**: 331-343.

Sharpless, N.E., N. Bardeesy, K.-H. Lee, D. Carrasco, D.H. Castrillon, A.J. Aguirre, E.A. Wu, J.W. Horner, and R.A. DePinho. 2001. Loss of p16Ink4a with retention of p19Arf predisposes mice to tumorigenesis. *Nature* **413**: 86-91.

Sherr, C.J. 2001. The INK4a/ARF network in tumour suppression. *Nature Reviews Molecular Cell Biology* **2**: 731-737.

Stemple, D.L. and D.J. Anderson. 1992. Isolation of a stem cell for neurons and glia from the mammalian neural crest. *Cell* **71**: 973-85.

Valk-Lingbeek, M.E., S.W. Bruggeman, and M. van Lohuizen. 2004. Stem cells and cancer; the polycomb connection. *Cell* **118**: 409-18.

van der Lugt, N.M.T., J. Domen, K. Linders, M. van Roon, E. Robanus-Maandag, H. te Riele, M. van der Valk, J. Deschamps, M. Sofroniew, M. van Lohuizen, and A. Berns. 1994. Posterior transformation, neurological abnormalities, and severe hematopoietic

defects in mice with a targeted deletion of the bmi-1 proto-oncogene. *Genes and Development* **8**: 757-769.

CHAPTER 3

BMI-1 OVEREXPRESSION IN NEURAL STEM/PROGENITOR CELLS INCREASES PROLIFERATION AND NEUROGENESIS IN CULTURE BUT HAS LITTLE EFFECT ON THESE FUNCTIONS *IN VIVO*[1]

SUMMARY

The Polycomb gene *Bmi-1* is required for the self-renewal of stem cells from diverse tissues, including the central nervous system (CNS). Bmi-1 expression is elevated in most human gliomas, irrespective of grade, raising the question of whether Bmi-1 overexpression is sufficient to promote self-renewal or tumorigenesis by CNS stem/progenitor cells. To test this we generated *Nestin-Bmi-1-GFP* transgenic mice. Analysis of two independent lines with expression in the fetal and adult CNS demonstrated that transgenic neural stem cells formed larger colonies, had more self-renewing divisions, and generated more neurons in culture. However, *in vivo*, Bmi-1 overexpression had little effect on CNS stem cell frequency, subventricular zone proliferation, olfactory bulb neurogenesis, or neurogenesis/gliogenesis during development. Bmi-1 transgenic mice were born with enlarged lateral ventricles and a minority developed idiopathic hydrocephalus as adults, but none of the transgenic mice formed detectable CNS tumors, even when aged. The more pronounced effects of Bmi-1 overexpression in culture were largely attributable to its suppression of $p16^{Ink4a}$ and

---

[1] Originally published in *Developmental Biology. 2009;328(2):257-72* with authors listed as **He, S.**, Iwashita, T., Buchstaller, J., Molofsky, A.V., Thomas, D., Morrison, S.J.

p19^{Arf} in culture, cell cycle inhibitors that are generally not expressed by neural stem/progenitor cells in young mice *in vivo*. Bmi-1 overexpression therefore has more pronounced effects in culture and does not appear to be sufficient to induce tumorigenesis *in vivo*.

INTRODUCTION

Bmi-1 is a Polycomb group protein that functions as one component of the repressor complex 1 to modify histones, regulating chromatin structure and repressing transcription (Valk-Lingbeek et al., 2004). *Bmi-1* is required for the postnatal self-renewal of stem cells from diverse tissues including the hematopoietic system (Lessard and Sauvageau, 2003a; Park et al., 2003b) and the CNS (Bruggeman et al., 2005; Molofsky et al., 2005; Molofsky et al., 2003). *Bmi-1* deficient mice exhibit a progressive postnatal depletion of stem cells from these tissues, leading to hematopoietic failure, defects in cerebellum development, neurological abnormalities, and death by early adulthood (Leung et al., 2004; van der Lugt et al., 1994a). Bmi-1 promotes the self-renewal of neural stem cells and other stem cells largely, but not exclusively, by repressing the expression of *Ink4a* and *Arf* (Bruggeman et al., 2005; Jacobs et al., 1999a; Molofsky et al., 2005; Molofsky et al., 2003). *Ink4a* and *Arf* encode the p16^{Ink4a} and p19^{Arf} tumor suppressor proteins that inhibit cell cycle progression and induce cellular senescence (Lowe and Sherr, 2003). Bmi-1 thus promotes the maintenance of CNS stem cells throughout adult life by repressing cell cycle inhibitors associated with cellular senescence.

Bmi-1 was originally identified as a transgene that could co-operate with *myc* to induce hematopoietic malignancies (Haupt et al., 1993; Jacobs et al., 1999c; van Lohuizen et al., 1991). Elevated Bmi-1 expression has been observed in hematopoietic malignancies (Bea et al., 2001), medulloblastomas and gliomas (Bruggeman et al., 2007; Leung et al., 2004), and cancers from other tissues (Song et al., 2006; Tateishi et al., 2006; Vonlanthen et al., 2001; Wang et al., 2007). Indeed, Bmi-1 is necessary for the maintenance of cancer stem cells from acute myeloid leukemias (Lessard and Sauvageau, 2003a) as well as gliomas (Bruggeman et al., 2007). *Bmi-1* is thus necessary for the progression of certain types of cancer and increased Bmi-1 expression may contribute to tumorigenesis in certain contexts.

These observations raise the question of whether overexpression of *Bmi-1* in neural stem/progenitor cells is sufficient to enhance the self-renewal of these cells or to render them tumorigenic. Retroviral overexpression of *Bmi-1* can increase hematopoietic stem cell self-renewal in culture and enhance the ability of these cells to reconstitute irradiated mice (Iwama et al., 2004). However, it is important to distinguish between the effects of Bmi-1 in culture and *in vivo* because the Bmi-1 target genes *Ink4a* and *Arf* are regulated differently in culture: *Ink4a* and *Arf* are rarely expressed by normal cells in fetal or young adult mice *in vivo* but are induced in cultured cells as a stress response to nonphysiological conditions (Lowe and Sherr, 2003; Sherr and DePinho, 2000). Consistent with these observations, Bmi-1 may be necessary for maintaining stem cell self-renewal in culture in a way that is not observed *in vivo* in certain contexts. For example, fetal neural stem cells from *Bmi-1* deficient mice exhibit a self-renewal defect in culture but not *in vivo* (Molofsky et al., 2003). Thus, as a result of increased *Ink4a/Arf*

expression in culture, Bmi-1 can sometimes exhibit functions in culture that are not observed *in vivo*. Nonetheless, Bmi-1 may also promote stem cell self-renewal and cancer cell proliferation through *Ink4a/Arf*-independent mechanisms (Bruggeman et al., 2007; Chagraoui et al., 2006). Resolving the question of whether Bmi-1 overexpression is sufficient for tumorigenesis and increased stem cell self-renewal *in vivo* will be critical to determine whether elevated Bmi-1 expression can be an initiating event in the etiology of brain tumors.

We examined Bmi-1 expression in both high-grade and low-grade human gliomas as well as in normal CNS tissue. Consistent with a recent report (Bruggeman et al., 2007), we observed elevated Bmi-1 expression in most high grade and low grade gliomas. To test whether *Bmi-1* overexpression is sufficient to promote self-renewal of stem/progenitor cells or tumorigenesis in the CNS, we generated *Nestin-Bmi-1-GFP* transgenic mice that express *Bmi-1* throughout CNS stem and progenitor cells. While *Bmi-1* overexpression was sufficient to increase self-renewal potential, overall proliferation, and neuronal differentiation by CNS stem and progenitor cells in culture, we observed little change in neural stem/progenitor cell function, neurogenesis or gliogenesis *in vivo*. A minority of the transgenic mice developed idiopathic hydrocephalus and died early in adulthood, but none of these mice developed CNS tumors at any stage up to two years of age. These results indicate that Bmi-1 overexpression in stem/progenitor cells has more dramatic consequences in culture than *in vivo* and Bmi-1 overexpression is not sufficient to initiate CNS tumorigenesis *in vivo*.

RESULTS

Bmi-1 expression is elevated in a subset of human CNS tumors

We examined the expression of Bmi-1 in normal and diseased human parenchymal brain tissue by performing immunohistochemistry on fixed tissue sections. We did not detect Bmi-1 expression in any of 3 samples of normal brain tissue (Figure 3.1A). We did observe strong Bmi-1 staining in the vast majority of cells within a white matter biopsy from a patient after an epileptic seizure (Figure 3.1B). Bmi-1 staining was also observed in most specimens from patients that exhibited gliosis due to damage (mesial temporal lobe sclerosis) or abscess (4 of 5 specimens; Figure 3.1C). These results demonstrate that Bmi-1 can be upregulated, particularly in glia, after brain injuries.

Similar to what has been reported recently (Bruggeman et al., 2007), we also observed elevated Bmi-1 expression in a subset of human gliomas (Figure 3.1D-F). Strong Bmi-1 expression was observed in most cells from 10 of 30 glioblastoma specimens (Figure 3.1F), while 7 of 30 specimens exhibited detectable, but lower levels of Bmi-1 expression in fewer cells. Variable levels of Bmi-1 expression were detected in some cells in low grade gliomas (1 of 2 specimens, data not shown), pilocytic astrocytomas (3 of 4 specimens; Figure 3.1D), and oligodendrogliomas (4 of 5 specimens; Figure 3.1E). These data indicate that Bmi-1 expression is elevated in most human CNS tumors, though no strong correlation between Bmi-1 expression level and the type or grade of the tumors was observed (Figure 3.1H). These data raise the question of whether elevated Bmi-1 expression is sufficient to drive tumorigenesis in CNS stem/progenitor cells.

Generation of *Nestin-Bmi-1-GFP* transgenic mice

To examine the effects of *Bmi-1* overexpression on neural stem/progenitor cell function and CNS tumorigenesis *in vivo*, we generated transgenic mice in which the human *Nestin* second intron enhancer was used to drive the expression of HA-tagged mouse Bmi-1 protein, as well as a GFP reporter in CNS stem and progenitor cells (Figure 3.2A). Nestin is expressed in CNS stem and progenitor cells (Dahlstrand et al., 1992b; Kawaguchi et al., 2001), as well as in various CNS tumors (Almqvist et al., 2002; Dahlstrand et al., 1992a; Rutka et al., 1999). The human *Nestin* second intron enhancer has been shown to drive transgene expression in mouse CNS stem and progenitor cells during embryonic development and adulthood (Lothian and Lendahl, 1997).

Ten of 77 (13%) pups born after fertilized oocyte injection harbored the *Nestin-Bmi-1-GFP* construct, based on PCR genotyping of tail DNA as well as by observation of GFP expression in the CNS (analyzed by transillumination of the head). Although one transgenic pup died shortly after birth of unknown causes, most of the transgenic offspring appeared healthy and developed normally. Southern blotting was performed on the surviving founders to confirm transgene integration and to determine copy number (Figure 3.3A). Five transgenic lines were established. One line (line B*) exhibited transgene segregation among F1 progeny in a way that suggested the original founder had multiple transgene integration sites (Figure 3.3B). As a result, two sub-lines from line B* were established; line B has ~5 copies of the transgene in a single integration site and line K has >25 copies of the transgene.

To select for lines that exhibited transgene expression in CNS stem/progenitor cells throughout development and adulthood, we analyzed GFP expression in neonatal

and adult F1 transgenic mouse brains by direct observation of GFP fluorescence and by flow cytometric analysis of dissociated cells from various CNS regions. Surprisingly, only the two transgenic lines (lines B and C) with the lowest transgene copy number (approximately 5 copies of the transgene inserted into a single site in the genome) maintained GFP expression in both the newborn and adult brain (Figure 3.4A). All other lines either showed no transgene expression (lines D and K) at either stage, or showed only weak GFP expression at birth that was no longer detectable in the adult brain (lines E and G) (Figure 3.4A). Therefore, for our analysis of the consequences of *Bmi-1* overexpression *in vivo* we studied lines B and C. The transgene was inherited with expected Mendelian frequencies in these lines (Figure 3.5A).

Characterization of transgene expression *in vivo*

Cytoplasmic GFP expression in the transgenic mouse CNS could be detected at all developmental stages in patterns that resembled endogenous Nestin expression (Lothian and Lendahl, 1997) in both lines B and C. At embryonic day (E)14.5, GFP was ubiquitously expressed throughout the developing CNS (Figure 3.2B). In contrast, no GFP fluorescence was observed in tissues outside of the nervous system or in littermate controls (Figure 3.2B). At birth (P0), GFP was still widely expressed in all brain regions of transgenic mice but not littermate controls (Figure 3.2C). The highest levels of expression appeared to be in the ventricular zones throughout the brain as well as in nerve fiber bundles in the corpus callosum and anterior commissure (Figure 3.2C). This widespread transgene expression was also confirmed by analyzing freshly dissociated cells from various neonatal (P0) brain regions by flow-cytometry: most cells from the P0

transgenic lateral ventricle germinal zone (VZ; 90±8%), cerebral cortex (88±9%), and cerebellum (66±11%) expressed GFP (Figure 3.2G).

In contrast, GFP expression in the adult transgenic brain became more spatially restricted. Whole brain GFP fluorescence was greatly reduced as compared with E14.5 or P0 brain (Figure 3.2D), and most of the GFP-expressing cells were localized to brain regions that contain neural stem/progenitor cells, such as the SVZ of the lateral ventricle (Figure 3.2E) and the subgranular cell layer in the dentate gyrus of the hippocampus (Figure 3.2F). Brain layers with differentiated cells showed no detectable GFP expression (Figure 3.2E,F). GFP expression was also not observed in tissue lacking appreciable Nestin expression, such as in adult bone marrow (Figure 3.4B). The enrichment of GFP-expressing cells in adult SVZ was further confirmed by flow-cytometry, which showed that 76±9% of all dissociated SVZ cells were GFP+ (Figure 3.2H). GFP expression thus correlated with the expected pattern of Nestin expression in stem/progenitor cells *in vivo*, throughout development and into adulthood.

To directly confirm that the transgene was indeed expressed by neural stem and progenitor cells, sorted GFP+ and GFP- cells from freshly dissociated neonatal cerebral cortex, VZ, and cerebellum were cultured *in vitro*. The vast majority (>94%) of neurospheres arose from the GFP+ fraction of cells while GFP- cells formed few or no neurospheres (Figure 3.2I). Upon differentiation, some of the GFP+ neurospheres formed multilineage colonies (containing neurons, astrocytes and oligodendrocytes) while other GFP+ neurospheres formed colonies that contained only astrocytes, or neurons and astrocytes. GFP- neurospheres usually did not form multilineage colonies. This indicates that virtually all multipotent cells (>99%) expressed the transgene but that GFP-

expressing cells were functionally heterogeneous and contained both neural stem and progenitor cells.

The transgene was also expressed by neural stem/progenitor cells from the brains of adult transgenic mice. SVZ cells were dissociated from the brains of two- to three-month old transgenic mice and GFP^+ or GFP^- cells were sorted into culture. Over 97% of neurosphere-forming cells were GFP^+ and most of these neurospheres underwent multilineage differentiation (Figure 3.2J,K). Since GFP expression was observed throughout the adult SVZ, and most adult SVZ cells are restricted progenitors that fail to form multipotent colonies in culture, these data suggest that many restricted progenitors in the adult brain also expressed the transgene. These data suggest that newborn and adult mice exhibited transgene expression in neural stem cells as well as in restricted neural progenitors.

The transgene increases Bmi-1 expression in neural stem cells

To assess the level of Bmi-1 overexpression as a result of transgene expression, we performed quantitative (real-time) reverse transcription polymerase chain reaction (qRT-PCR) and western blotting using freshly isolated SVZ cells and cultured neurospheres. In cultured neurospheres from adult SVZ, *Bmi-1* transcript levels were 15-fold and 9-fold higher in line B and Line C transgenic neurospheres, respectively, as compared with neurospheres from littermate controls (Figure 3.6A). Using uncultured tissue, *Bmi-1* transcript levels were 8.5- to 11.1-fold higher in P0 ventricular zone and in the adult SVZ of line B and Line C transgenic mice compared to littermate controls (Figure 3.6A). At the protein level, using anti-HA antibody, we were able to detect the expression of the HA-tagged Bmi-1 in both cultured neurospheres from adult SVZ and in

freshly dissected E14.5 telencephalon tissue and P0 brain from lines B and C (Figure 3.6B-D). Using anti-Bmi-1 antibody, this translated to a significant overall increase in Bmi-1 expression by cultured neurospheres and uncultured telencephalon/P0 brain cells from transgenic mice (Figure 3.6B-D). Furthermore, immunohistochemical staining of Bmi-1 in tissue sections from E15 transgenic and control mouse telencephalon showed significantly increased Bmi-1 expression in most VZ cells in the transgenic mice (Figure 3.6E). Together, these data demonstrate that transgene expression led to Bmi-1 overexpression in neural stem and progenitor cells *in vitro* and *in vivo* throughout CNS development. Moreover, the level of Bmi-1 expression within transgenic mice appeared similar or higher than the level observed within human glioma specimens by both immunohistochemistry (compare Figure 3.6E to Figure 3.1A-F) and western blot (Figure 3.1G).

To test whether the increase in Bmi-1 expression in transgenic mice correlated with increased Bmi-1 function, we assessed the expression of the Bmi-1 target genes *Ink4a* and *Arf*. The Bmi-1-containing polycomb repressor complex 1 represses *Ink4a* and *Arf* expression (Bracken et al., 2007; Bruggeman et al., 2007; Bruggeman et al., 2005; Molofsky et al., 2005). Cultured neurospheres from line B and line C exhibited lower levels of $p16^{Ink4a}$ and $p19^{Arf}$ expression compared to neurospheres cultured from littermate controls (Figure 3.6B). This demonstrated that transgenic Bmi-1 was functionally active and that Bmi-1 overexpression attenuated the induction of $p16^{Ink4a}$ and $p19^{Arf}$ that normally occurs when neurospheres are cultured *in vitro*. Consistent with earlier studies that failed to detect $p16^{Ink4a}$ or $p19^{Arf}$ expression in fetal and young adult mouse brain (Bruggeman et al., 2007; Bruggeman et al., 2005; Molofsky et al., 2005;

Molofsky et al., 2003; Nishino et al., 2008), we were also unable to detect these proteins in transgenic mice or littermate controls at E14.5 (Figure 3.6C) or P0 (Figure 3.6D). The observation that overexpressed Bmi-1 was able to reduce $p16^{Ink4a}$ and $p19^{Arf}$ expression in culture, but that $p16^{Ink4a}$ and $p19^{Arf}$ expression could not be detected *in vivo*, raised the possibility that Bmi-1 overexpression would promote self-renewal/proliferation to a greater degree in culture.

Transgenic neural stem cells show increased self-renewal and neurogenesis in culture

To assess the consequences of Bmi-1 overexpression we compared the frequency that adult SVZ cells from transgenic and control mice formed multipotent neurospheres, as well as the diameter and self-renewal potential of these neurospheres. A modestly (1.7-fold) but significantly ($p<0.05$) higher percentage of dissociated adult SVZ cells from line B and line C transgenic mice formed multipotent neurospheres in culture (Figure 3.7A). However, when multiplied by the total number of dissociated SVZ cells obtained from each mouse, this did not translate into a significant increase in the total number of multipotent neurospheres per SVZ in the transgenic mice (Figure 3.7B). The slight increase in the frequency of multipotent neurospheres could either reflect a slightly increased frequency of stem cells in the SVZ of transgenic mice *in vivo* or slightly increased survival of these cells in culture. The neurospheres formed by transgenic cells were significantly larger than the neurospheres from littermate controls (Figure 3.7C), demonstrating that elevated Bmi-1 expression increased the proliferation capacity of stem/progenitor cells in culture. This is further supported by the significantly increased proliferation rate observed in adherently cultured transgenic neural stem cell colonies

based on BrdU incorporation (Figure 3.7G). To focus on the self-renewal potential of stem cells rather than the overall proliferation of the heterogeneous progenitors that comprise stem cell colonies, we dissociated and subcloned individual primary neurospheres into secondary cultures and counted the number of multipotent secondary neurospheres that arose per primary neurosphere. Stem cells from line B and line C transgenic mice exhibited dramatically increased self-renewal in culture as compared to stem cells from littermate controls (Figure 3.7D).

At the extraordinarily low cell densities used in our experiments (approximately 1 cell/µl) control experiments indicated that most neurospheres were clonally derived (Figure 3.8). Nonetheless, to confirm that Bmi-1 increased the self-renewal of clonal neural stem cell colonies we sorted individual $CD15^{+}CD24^{-}$ SVZ cells from P5 wild type and transgenic mice into different wells of 96 well plates. $CD15^{+}CD24^{-}$ SVZ cells are enriched for neural stem cells (Capela and Temple, 2002). Neurospheres arose in only 10-17% of wells seeded with single $CD15^{+}CD24^{-}$ cells. We found that transgenic neurospheres were significantly larger and had significantly more self-renewal potential than wild-type neurospheres (Figure 3.7E, F). These data demonstrate that elevated Bmi-1 expression increases the proliferation and self-renewal of CNS stem cells in clonal culture.

Loss of *Bmi-1* reduces neuronal differentiation from CNS stem cells in culture (Bruggeman et al., 2007; Zencak et al., 2005). To test whether overexpression of Bmi-1 affects stem cell differentiation, we differentiated primary neurospheres from both transgenic lines to assess their ability to generate Tuj-1+ neurons, GFAP+ astrocytes and O4+ oligodendrocytes in culture. The frequency of oligodendrocytes was comparable in

transgenic and wild type multipotent stem cell colonies (Figure 3.7I; 0.5±0.6% of cells in wild type, 1.0±1.1% of cells in line B transgenic and 1.1±1.0% in line C transgenic respectively). However, transgenic stem cell colonies consistently contained an increased proportion and absolute number of neurons as compared to control colonies (3.9±4.9% in wild type, 23±18% in line B transgenic and 31±17% in line C transgenic respectively) (Figure 3.7H,I;). Transgenic stem cell colonies also contained a modestly reduced frequency of astrocytes compared to wild-type colonies (95±4% in wild type, 76±18% in line B transgenic and 67±17% in line C transgenic respectively). Since multipotent transgenic colonies contained many more cells than multipotent wild type colonies (3,700±2,700 cells/ wild type colony versus 21,000±17,000 cells/ line B colony and 10,000±8,000 cells/ line C colony after 10 days in culture), the reduced frequency of astrocytes in transgenic colonies reflected the dramatic increase in the number of neurons in these colonies, rather than a decrease in the absolute number of astrocytes per colony. Bmi-1 overexpression thus increased the neurogenic capacity of CNS stem cells in culture.

Bmi-1 **overexpression has little effect on neural stem/progenitor cell proliferation** ***in vivo***

To evaluate the effects of Bmi-1 overexpression *in vivo*, we compared various measures of stem/progenitor cell function between control and Bmi-1 transgenic mice. We administered a pulse of BrdU to 2-4 month old transgenic and littermate control mice two hours before they were sacrificed to test whether Bmi-1 overexpression increased the overall proliferation of neural stem and progenitor cells in the SVZ. In contrast to the significantly enhanced proliferation exhibited by cultured transgenic neural

stem/progenitor cells (Figure 3.7G), neither line B nor line C transgenic mice showed a significant difference in the frequency of BrdU+ cells in the SVZ when compared with littermate controls (Figure 3.9A).

To test whether Bmi-1 overexpression could affect neural stem/progenitor cell proliferation during fetal development, we administered BrdU to timed pregnant females to mark dividing cells in the developing telencephalon of wild type and transgenic embryos. After a 15 minute BrdU pulse, many cells in the VZ of both wild type and transgenic embryos became $BrdU^{+}$, indicating rapid proliferation. However, we did not observe any difference in the distribution or frequency of BrdU+ cells between transgenic and control embryos (Figure 3.9B). In addition, the overall thickness of the cerebral cortex and the VZ did not significantly differ between transgenic and wild-type telencephalon (Figure 3.9C). These data suggest that Bmi-1 overexpression does not cause a notable increase in proliferation within the telencephalon during fetal development.

Bmi-1 overexpression has little effect on fetal or adult neurogenesis *in vivo*

To assess whether Bmi-1 overexpression affected the rate of olfactory bulb neurogenesis *in vivo*, we administered BrdU to 1-2 month old transgenic and littermate control mice for one week to mark dividing SVZ progenitors followed by a one month chase without BrdU to allow these cells to migrate into the olfactory bulb and to differentiate into neurons. We then quantified the percentage of NeuN+ neurons that were also BrdU+ by confocal microscopy. Twenty-five random fields of view spanning the whole thickness of the olfactory bulb were imaged and counted. Transgenic mice did not exhibit an increased rate of neurogenesis as compared to littermate controls (Figure

3.10A). Indeed, line B transgenic mice exhibited a significantly lower rate of neurogenesis than littermate controls because a subset (approximately 25%) of these mice were found to be in the process of developing hydrocephalus when sacrificed, and the mice with hydrocephalus tended to have reduced SVZ proliferation and olfactory bulb neurogenesis (data not shown). Thus we could find no evidence of increased SVZ proliferation or neurogenesis in adult transgenic mice *in vivo*, in contrast to what we had observed in culture.

To test whether Bmi-1 overexpression could affect neurogenesis during fetal CNS development, we examined the onset of cortical neurogenesis as well as the organization of the cerebral cortex in the forebrain of transgenic and control mice. Most cortical neurogenesis in mice occurs from E10 to E17, when ventricular zone progenitors give rise to waves of neuronal precursors that migrate toward the pial surface, forming six distinct cortical layers. To examine whether Bmi-1 overexpression affected the onset of cortical neurogenesis, we stained E12 telencephalon with antibody against Tuj1 to label the early born Cajal-Retzius neurons within the marginal zone (Hatten, 1999). We did not observe any difference between transgenic or control mice in terms of the density or localization of these Tuj-1^{+} cells (Figure 3.10B). This suggests that Bmi-1 overexpression did not significantly delay the onset of cortical neurogenesis.

Next we asked whether the overall organization of the cerebral cortex in transgenic mice was altered by *Bmi-1* overexpression. We cut sections through the cerebral cortex of P0 or adult wild-type and transgenic mice and stained with the layer specific neuronal markers Reelin (staining Cajal-Retzius neurons in layer I; (Soriano and Del Rio, 2005)), Cux-1 (staining layer 2-4 neurons; (Nieto et al., 2004)), and FoxP2

(staining layer 6 neurons in the adult brain; (Ferland et al., 2003)). In no case did we detect any difference between transgenic and control littermates in the frequency or localization of Reelin+ neurons at P0 (Figure 3.10C), FoxP2+ neurons in adults (Figure 3.10D) or Cux-1+ neurons at P20 (Figure 3.10F). This suggests that cortical neuronal progenitors acquire normal identities and a normal laminar fate despite *Bmi-1* overexpression.

To assess whether neurons were born according to a normal schedule we pulse labeled wild type and transgenic embryos with the nucleotide analog 5-chloro-2-deoxyuridine (CldU) at E17 (a stage when upper layer neurons are generated (Polleux et al., 1997)), and stained sections cut at P20 with antibodies against CldU and Cux-1. The CldU staining was concentrated in upper cortical layers as expected (Figure 3.10E,F) and there was a similar degree of CldU/Cux-1 co-localization in both wild-type and transgenic mice (Figure 3.10G-I). Therefore, we did not detect any significant change in the timing or pattern of cortical neurogenesis in the transgenic mouse brain, suggesting that *Bmi-1* overexpression did not significantly alter neurogenesis *in vivo*, though we cannot rule out the possibility of subtle changes.

Bmi-1 overexpression has little effect on glial differentiation *in vivo*

While we did not observe significant effects of Bmi-1 overexpression on SVZ proliferation or neurogenesis in embryonic or adult mice, we wondered whether *Bmi-1* overexpression affected gliogenesis since a loss of *Bmi-1* leads to an increase in astrocytes *in vivo* (Zencak et al., 2005). To test this we first examined the expression of the astrocyte marker GFAP and the oligodendrocyte marker MBP in adult mice. We did not observe any difference between line B or line C transgenic mice and littermate

controls in the numbers or positions of GFAP+ cells or MBP+ cells in the corpus callosum or striatum (Figure 3.11A,B). While this suggested that transgenic mice did not have gross changes in gliogenesis, we also examined P4-P5 mice to assess whether there were any early changes. There was no difference between line B or line C transgenic mice and littermate controls in the number or position of BFABP+ glia at P5 (Figure 3.11E). There was also no differences between line C transgenic mice and control littermates in the number or position of GFAP+ astrocytes in the corpus callosum or MBP+ oligodendrocytes in the corpus callosum and striatum at P5 (Figure 3.11C,D). However, we did observe a delay in oligodendrogliogenesis in line B transgenic mice, which have fewer MBP+ oligodendrocytes compared to littermate controls in the P4 corpus callosum and striatum, but a normal frequency of GFAP+ astrocytes (Figure 3.11 F,G). The fact that this delay was not observed in line C mice suggests that it may not be attributable to increased Bmi-1 expression; however, we cannot rule out the possibility that increased Bmi-1 expression delays glial differentiation in some mice under certain circumstances. Overall, our data suggest that elevated Bmi-1 expression has little effect on gliogenesis *in vivo*.

Bmi-1 **overexpression does not further enhance the self-renewal or neurogenic potential of cultured** ***Ink4a-Arf*** $^{-/-}$ **neural stem cells.**

The increased overall proliferation, stem cell self-renewal, and neurogenesis that occurred upon *Bmi-1* overexpression *in vitro* (Figure 3.7) but not *in vivo* (Figure 3.9-11) is correlated with the ability of overexpressed Bmi-1 to reduce $p16^{Ink4a}$ and $p19^{Arf}$ expression *in vitro* but not *in vivo* (Figure 3.6). To test whether the effects of *Bmi-1* overexpression on neural stem cell function in culture were mediated by its ability to

oppose the induction of $p16^{Ink4a}$ and $p19^{Arf}$ expression in culture, we overexpressed *Bmi-1* in neural stem cells cultured from newborn (P2-P6) wild-type and *Ink4a-Arf* deficient mice. This was done using a bicistronic retrovirus (MSCV-Bmi1) expressing both mouse Bmi-1 and GFP. Adherently plated newborn lateral ventricle germinal zone cells from wild type or *Ink4a-Arf*$^{-/-}$ mice were infected with this virus or a control retrovirus bearing only GFP (MSCV-GFP) then replated into non-adherent cultures to generate neurospheres. Infected cells could thus be distinguished from non-infected cells based on GFP expression. qRT-PCR indicated that *Bmi-1* expression was increased 4.0- to 5.5-fold on average by MSCV-Bmi1 infection as compared to neurospheres that were infected with the control virus (Figure 3.12A).

To assess overall proliferation and stem cell self-renewal we measured the diameter of neurospheres and the capacity of multipotent neurospheres to form secondary multipotent neurospheres upon subcloning, respectively. Wild-type neurospheres infected with MSCV-Bmi1 virus were significantly larger than neurospheres infected with MSCV-GFP control virus or uninfected neurospheres (Figure 3.12B), consistent with our previous observations for *Bmi-1* transgenic cells (Figure 3.7C). In contrast, *Ink4a-Arf*$^{-/-}$ neurospheres were significantly larger than wild-type neurospheres, and overexpression of *Bmi-1* in *Ink4a-Arf*$^{-/-}$ neurospheres did not further increase their size (Figure 3.12B). Similar results were observed in the self-renewal assay. While MSCV-Bmi1 infected wild type neurospheres generated significantly more multipotent secondary neurospheres compared to uninfected neurospheres or neurospheres infected with control virus (Figure 3.12C), overexpression of *Bmi-1* in *Ink4a-Arf*$^{-/-}$ neurospheres did not further enhance their self-renewal potential (Figure 3.12C). Finally, *Bmi-1* overexpression or *Ink4a-Arf*

deficiency each increased the amount of neuronal differentiation observed in neural stem cell colonies; however, overexpression of *Bmi-1* in *Ink4a-Arf* deficient neural stem cells did not significantly increase neuronal differentiation beyond that due to *Ink4a-Arf* deficiency alone (Figure 3.12D).

A similar experiment was performed using freshly isolated SVZ cells from adult Bmi-1 transgenic mice crossed onto an *Ink4a-Arf* deficient background. Consistent with the data from retroviral *Bmi-1* overexpression, transgenic *Bmi-1* overexpression in *Ink4a-Arf* deficient mice no longer increased the frequency of multipotent neurospheres, neurosphere diameter, or self-renewal potential (Figure 3.12G-I). Our data suggest that the increased proliferation, self-renewal, and neuronal differentiation of cultured neural stem cells upon *Bmi-1* overexpression are largely attributable to the repressive effects of Bmi-1 on $p16^{Ink4a}$ and $p19^{Arf}$ expression.

A subset of *Bmi-1* transgenic mice developed hydrocephalus but not CNS tumors

Bmi-1 transgenic mice from lines B and C were born at Mendelian frequencies (Figure 3.5A). The mice had a normal appearance at birth and no behavioral abnormalities were noted; however, the transgenic mice consistently exhibited enlarged lateral ventricles (Figure 3.13A). We cut sections throughout lateral ventricles to look for blockages that could prevent the flow of cerebrospinal fluid out of the lateral ventricles but never detected any blockage. Thus it is unclear why *Bmi-1* transgenic mice were born with enlarged lateral ventricles.

Between 4 and 8 weeks of age, a minority of transgenic mice from both transgenic lines (7 of 28 (25%) mice from line B and 14 of 61 (23%) mice from line C) developed hydrocephalus. The mice with hydrocephalus could be distinguished based on

the dome shaped appearance of their heads, severely enlarged lateral ventricles, and behavioral changes that included weight loss, lethargy, and ruffled fur. Hydrocephalus was confirmed in these mice by magnetic resonance imaging (MRI) (Figure 3.13B). MRI images showed that lateral ventricles were most affected in these mice; the third ventricle, sylvius aqueduct, and fourth ventricle appeared relatively normal (Figure 3.13B). However, we could not find any obstruction between the lateral and third ventricles nor any blockage within the third ventricle or the aqueduct that would explain the hydrocephalus phenotype (Figure 3.13C). Nonetheless, it remains possible that a physical blockage exists in the ventricular system *in vivo* that is not readily detected by histology or MRI.

We also assessed other common causes for mouse hydrocephalus such as over-proliferation of choroid plexus, or defects in the ependyma lining the lateral ventricle. No abnormal mass of choroid plexus was observed in the transgenic mice (data not shown). Some transgenic mice with hydrocephalus did exhibit an abnormally folded ependymal cell lining of the lateral ventricle (Figure 3.13D), a similar phenotype was observed in transgenic mice that never developed hydrocephalus. Thus it was unclear whether the ependymal layer abnormality contributed to the development of hydrocephalus. The ependymal cells in young adult mice did not incorporate a two-hour pulse of BrdU (data not shown), so they were not proliferating rapidly as would be expected if these cells were neoplastic. Finally, we also tested whether hydrocephalus was associated with cortical atrophy due to increased apoptosis in the cerebral cortex. However, sections from hydrocephalic transgenic mouse brains did not exhibit increased activated caspase-3 staining relative to littermate controls and little apoptosis was observed in either the

control or transgenic brains (data not shown). Overall, we detected no evidence of lateral ventricle malformations or blockages that could explain why hydrocephalus developed and we never detected any tumors in the brains of these mice by either histology or MRI.

The 75% of transgenic mice that were not affected by hydrocephalus remained healthy and we never detected any abnormalities in appearance or behavior. Line C mice had normal body mass and brain mass while line B mice had slightly but significantly increased brain mass and slightly but significantly decreased body mass by young adulthood (Figure 3.5B,C). We aged these mice for up to 25 months and detected no evidence of premature death or illness as compared to control littermates. To look for evidence of CNS tumors in the transgenic mice, we sacrificed newborn (3 line B and 4 line C), 1-4 month old (5 line B and 16 line C) and 15-24 month old (2 line B and 3 line C) transgenic mice and analyzed serial sections of the whole brain by histology (Figure 3.13E). We also grossly examined the brains from all of the transgenic mice used in earlier experiments (more than 50 mice from each line). We detected no evidence of brain tumors in any mouse at any age (Figure 3.13E). Some transgenic and wild type mice spontaneously developed non-neural neoplasms (mostly hematopoietic) after being aged for more than 20 months; however, none of these neoplasms contained GFP-expressing cells, suggesting that transgene expression did not contribute.

Immunohistochemical staining of Bmi-1 in sections (compare Figure 3.6E to Figure 3.1A-F) and Bmi-1 western blot (Figure 3.1G) suggest that the level of Bmi-1 expression in the transgenic mouse brain is comparable to the level of expression observed in brain tumors, at least in the fetal telencephalon. However, we have been unable to examine levels of Bmi-1 protein expression in the SVZ of adult transgenic mice

because the adult SVZ yielded insufficient material for western blot, and high background staining of the adult SVZ by immunohistochemistry (the anti-Bmi-1 antibody was made in mouse) made this difficult to interpret. Nonetheless, *Bmi-1* transcript levels were elevated in the transgenic adult SVZ by 8.5- to 11-fold relative to control SVZ (Figure 3.6A). As a result, available data suggest that Bmi-1 expression levels in CNS stem/progenitor cells from transgenic mice were comparable to those observed within brain tumors, but we cannot rule out the possibility that further increases in expression within adult CNS cells might render these cells tumorigenic. Nonetheless, it is not clear whether it is possible to achieve further increases in expression as all transgenic mice with higher transgene copy numbers silenced the transgene. Since prior studies have suggested that Bmi-1 is degraded when unable to bind other polycomb repressor complex 1 components (Ben-Saadon et al., 2006; Hernandez-Munoz et al., 2005), the stoichiometry of other complex components may limit the degree to which Bmi-1 expression and function can be increased.

DISCUSSION

In this study, we generated *Nestin-Bmi-1-GFP* transgenic mice to study the effect of Bmi-1 overexpression in neural stem/progenitor cells on CNS development and tumorigenesis. Bmi-1 overexpression in CNS stem/progenitor cells *in vitro* was sufficient to significantly increase stem cell self-renewal, overall proliferation, and neuronal differentiation (Figure 3.7). In contrast, Bmi-1 overexpression *in vivo* had little effect on SVZ proliferation, adult olfactory bulb neurogenesis, or neurogenesis/gliogenesis during development (Figure 3.9-11). Bmi-1 transgenic mice showed only a mild increase in

neural stem cell frequency (<2-fold; Figure 3.7A) with no increase in the total number of neural stem cells per mouse (Figure 3.7B). They also exhibited no evidence of tumorigenesis, even when aged for more than 20 months (Figure 3.13E). These data demonstrate that *Bmi-1* overexpression has much more profound effects on CNS stem cell function in culture than *in vivo*.

The increased effect of *Bmi-1* overexpression in culture correlated with its ability to reduce $p16^{Ink4a}$ and $p19^{Arf}$ expression in culture. Although $p16^{Ink4a}$ and $p19^{Arf}$ are not detectably expressed by neural stem/progenitor cells in developing or young adult mice (Bruggeman et al., 2007; Bruggeman et al., 2005; Molofsky et al., 2005; Molofsky et al., 2003; Nishino et al., 2008) (Figure 3.6C, D), $p16^{Ink4a}$ and $p19^{Arf}$ are induced in culture in neural stem cells (Molofsky et al., 2003) in response to the stress associated with adaptation to the nonphysiological culture environment (Lowe and Sherr, 2003; Sherr and DePinho, 2000). Since $p16^{Ink4a}$ and $p19^{Arf}$ were not detectably expressed by neural stem/progenitors cells *in vivo*, *Bmi-1* overexpression had no effect on $p16^{Ink4a}$ and $p19^{Arf}$ expression *in vivo*. In contrast, *Bmi-1* overexpression did reduce $p16^{Ink4a}$ and $p19^{Arf}$ expression in culture (Figure 3.6B). This suggested that the increased effects of *Bmi-1* overexpression in culture were caused by its ability to reduce $p16^{Ink4a}$ and $p19^{Arf}$ expression in culture. Consistent with this, *Bmi-1* overexpression no longer enhanced self-renewal, proliferation, or neurogenesis in *Ink4a-Arf* deficient neural stem cells in culture (Figure 3.12). These data demonstrate that caution must be exercised when inferring *in vivo* functions for Bmi-1 based on observations collected in culture because the increased expression of $p16^{Ink4a}$ and $p19^{Arf}$ in culture increases the reliance of cells

upon Bmi-1 and makes cells respond to Bmi-1 overexpression in a way that is not observed *in vivo*.

In *Bmi-1* deficient mice *in vivo*, neural stem cells require Bmi-1 postnatally, but not during fetal development, for self-renewal. Fetal *Bmi-1* deficient mice do not exhibit detectable $p16^{Ink4a}$ and $p19^{Arf}$ expression in neural tissue *in vivo* and are born with normal numbers of neural stem cells (Molofsky et al., 2003). In contrast, postnatal *Bmi-1* deficient mice exhibit elevated $p16^{Ink4a}$ and $p19^{Arf}$ expression in neural tissues *in vivo* and neural stem cells become increasingly depleted with time (Molofsky et al., 2003). This depletion of neural stem cells can be largely, but not completely, rescued by *Ink4a* and/or *Arf* deficiency (Bruggeman et al., 2005; Molofsky et al., 2005; Molofsky et al., 2003). These data suggest that the primary physiological role for Bmi-1 in the nervous system is to repress *Ink4a-Arf* in postnatal stem cells and to promote the maintenance of these cells throughout adulthood (Bruggeman et al., 2005; Molofsky et al., 2005; Molofsky et al., 2003). Nonetheless, a recent study found that shRNA knockdown of *Bmi-1*, primarily in cultured fetal neural stem cells, resulted in a self-renewal defect (Fasano et al., 2007b). These authors speculated that acute knockdown of *Bmi-1* revealed a physiological role for Bmi-1 in fetal neural stem cells that was not evident in germline knockout mice. One possibility is that unknown mechanisms in germline *Bmi-1* knockout mice compensate for the loss of *Bmi-1* during fetal development. Another possibility is that shRNA knockdown of *Bmi-1* in cultured fetal neural stem cells reflected a function for Bmi-1 that is not required *in vivo* because these cells express $p16^{Ink4a}$ and $p19^{Arf}$ in culture in a way that does not occur *in vivo*. To distinguish between these possibilities it will be necessary

to study *Bmi-1*^{floxed} mice to determine whether conditional deletion of *Bmi-1 in vivo* leads to neurodevelopmental defects during fetal development.

Consistent with other recent studies (Bruggeman et al., 2007; Leung et al., 2004), we observed elevated levels of Bmi-1 expression in many brain tumors as compared to normal brain tissue, irrespective of whether the tumors were low or high grade (Figure 3.1). Indeed, *Bmi-1* is required for the growth of gliomas and for glioma stem cell function, through *Ink4a-Arf* dependent and independent mechanisms (Bruggeman et al., 2007). However, our data demonstrate that the degree of Bmi-1 overexpression that can be achieved in transgenic mice does not promote tumorigenesis in the CNS. Thus, increased Bmi-1 expression is not likely to be an initiating event in the formation of brain tumors. Rather, Bmi-1 may be required to cooperate with other mutations, such as to reduce the extent to which oncogenic stimuli induce $p16^{Ink4a}$ and $p19^{Arf}$ expression. In medulloblastomas, elevated Bmi-1 expression may reflect mutations that activate sonic hedgehog signaling (Leung et al., 2004). Elevated Bmi-1 expression in brain tumors may be the consequence of other mutations, or may confer a selective advantage in the context of mutations, but is not likely to reflect a primary role for increased Bmi-1 expression in the initiation of tumorigenesis.

MATERIALS AND METHODS

Generation of *Nestin-Bmi-1-HA-GFP* transgenic mice

Full-length mouse *Bmi-1* cDNA was PCR amplified from total mouse embryo cDNA and HA-tagged, then inserted into the pMIG vector immediately upstream of the

IRES site. The *Bmi-1-IRES-GFP* fragment was then isolated by NotI digestion and inserted into NotI digested *nes1852tk/lacZ* plasmid (kindly provided by Dr. Urban Lendahl). This *nes1852tk/lacZ* plasmid carried the *Nestin* second intronic enhancer that has previously been shown to drive transgene expression in CNS stem and progenitor cells (Kawaguchi et al., 2001) as well as the thymidine kinase minimal promoter (Lothian and Lendahl, 1997). The entire sequence (~7600 bp) was then linearized with ScaI and microinjected into mouse zygotes (Hogan et al., 1994). Founder males were bred to wild-type C57Bl/6 females. Offspring were screened by GFP phenotyping of the brain in neonatal pups, and by genotyping using PCR at later ages using the primer set: 5'-TGGACACAAAGACCTCTGTG-3' and 5'-GGTTGTTCGATGCATTTCTGC-3'.

Isolation of CNS progenitors and flow cytometry analysis

Adult lateral ventricle subventricular zone (SVZ) cells from 2-4 month old wild type or transgenic mice were obtained by micro-dissecting the lateral walls of the lateral ventricles, then dissociating for 20 min at 37 °C in 0.025% trypsin/0.5 mM EDTA (Calbiochem; San Diego, CA) plus 0.001% DNaseI (Roche; Indiannapolis, IN). After quenching the enzymatic dissociation with staining medium (L15 medium (Invitrogen; Carlsbad, CA) supplemented with 1 mg/ml BSA (Sigma; St. Louis, MO), 10 mM HEPES (pH 7.4) and 1% penicillin/streptomycin (Invitrogen)) containing 0.014% soybean trypsin inhibitor (Sigma) and 0.001% DNase1, the cells were washed and resuspended in staining medium, triturated, filtered through nylon screen (45 μm, Sefar America; Depew, NY), counted by haemocytometer, and plated.

For flow-cytometric analysis of GFP expression in transgenic mouse brain tissue, freshly dissociated single cell suspensions from neonatal mouse cerebral cortex and

cerebellum, or adult SVZ were analyzed by a FACS VantageSE flow-cytometer (Becton-Dickinson; San Jose, CA). Dead cells were excluded from analysis by DAPI staining.

Neural stem cell culture, differentiation, cell proliferation and self-renewal assays

For neurosphere culture, dissociated SVZ cells were plated at clonal density (1.3 cells/μl of culture medium) onto ultra-low binding plates (Corning, Lowell, MA). The culture medium (self-renewal medium) was based on a 5:3 mixture of DMEM-low glucose: neurobasal medium (Invitrogen) supplemented with 20 ng/ml human bFGF (R&D Systems, Minneapolis, MN), 20 ng/ml EGF (R&D Systems), 1% N2 supplement (Invitrogen), 2% B27 supplement (Invitrogen), 50 μM 2-mercaptoethanol (Sigma), 1% pen/strep (Invitrogen) and 10% chick embryo extract (prepared as described (Stemple and Anderson, 1992)). All cultures were maintained at 37˚C in 6% CO_2/balance air. Neurosphere numbers and diameters were determined on the tenth day of culture.

For neurosphere culture from single cells, P5 wild type and transgenic mouse SVZ cells were dissociated as described above. To enrich neural stem cells, the dissociated SVZ cells were stained with anti-CD24 (BD Biosciences, San Jose, CA) and anti-CD15 (clone MMA) antibodies, and single $CD24^{-}CD15^{hi}$ cells were sorted into each well of 96 well ultra-low binding plates. Single cell sorting was confirmed in control plates stained with DAPI. Cultures were maintained at 37˚C in 6% CO_2/balance air. Neurospheres were measured and subcloned for self-renewal quantification on the tenth day of culture.

To assess the differentiation of primary neurospheres, individual neurospheres were replated onto Poly-D-Lysine (PDL, Biomedical technology, Stoughton, MN) and fibronectin (Biomedical technology) coated 48-well plates and cultured adherently in

differentiation medium for 7 days before being fixed and stained for markers of neurons, oligodendrocytes, and astrocytes as previously described (Molofsky et al., 2003). Differentiation medium was the same as self-renewal medium except that it contained no EGF, and reduced concentrations of chick embryo extract (1%) and FGF (10 ng/ml).

For cell proliferation assays, dissociated adult SVZ cells were plated onto PDL and laminin (Invitrogen) coated tissue culture plates at clonal density (0.7 cells/μl) and cultured for 6 days, then pulse-labeled with 10 μM BrdU for 1 hour at 37°C before being fixed and stained with an antibody against BrdU as described (Molofsky et al., 2003). Only stem cell colonies (identified by large compact colony morphology) were included in this analysis.

To assess the self-renewal potential of cultured neural stem cells, individual primary neurospheres were mechanically dissociated by trituration and then replated at clonal density (1.3 cells/μl) into non-adherent cultures. Secondary neurospheres were counted 10 days later and differentiated in the same manner as described above. Self-renewal is reported as the number of multipotent secondary neurospheres that arose per subcloned primary neurosphere.

Generation of Bmi-1-GFP-MSCV virus and infection of neural stem cells

Bmi-1 bearing retrovirus was made using a mouse stem cell virus (MSCV) vector (pMIG) which contains an internal ribosome entry site (IRES) followed by GFP (Van Parijs et al., 1999). Full length mouse Bmi-1 cDNA was PCR amplified from perinatal mouse lateral ventricle SVZ cDNA. Hpa1 and Bgl2 sites were added to either end and the sequence was inserted into the MSCV vector 5' to the IRES GFP. Preparation of high-titer virus was carried out by calcium phosphate transfection of BOSC packaging cells

(Pear et al., 1993) with the Bmi-MSCV vector. Vesicular stomatitis virus G protein (VSV-G) plasmid was added during transfection to increase the infectivity of the packaged virus (Lee et al., 2001). Cells were allowed to produce virus for 24-48 hours, then cell supernatants were collected, 0.2 micron filtered, and stored at –80°C or used fresh to infect cultured neural stem/progenitor cells.

Neonatal lateral ventricular zone (VZ) tissue from wild type or *Ink4a-Arf* deficient mice was dissected, dissociated, and cultured as described above. Cells were plated adherently at high density (20,000 cells per well of a six-well plate). After 24-48 hours of culture, viral supernatant was added for 12-24 hours. Then the culture medium was replaced for 24-48 hours, and cells were briefly trypsinized and replated at clonal density (0.7 cells/µl of media). Viral titers allowed infection of 25 to 90% of colonies.

Immunohistochemistry of tissue sections

Immunohistochemical staining of Bmi-1 on normal human brain tissue and brain tumor samples was performed on the DAKO Autostainer (DAKO, Carpinteria, CA) using DAKO Envision+ and diaminobenzadine (DAB) as the chromogen. De-paraffinized sections of formalin fixed tissue at 5µm thickness were labeled with mouse monoclonal anti-Bmi-1 (1:400, Clone F6, Upstate Chemicals, Pickens, SC) for 60 minutes, after microwave citric acid epitope retrieval. Appropriate negative (no primary antibody) and positive controls (high grade brain tumor) were stained in parallel with each set of tumors studied. The immunoreactivity was scored by a three-tier (negative, low (+) and high (++) positive) grading scheme.

For immunofluorescence staining of mouse brain sections, whole embryos or postnatal brains were fixed in 4% paraformaldehyde overnight, then cryoprotected in

30% sucrose, embedded in OCT (Sakura Finetek, Torrance, CA) and flash frozen. Twelve micron sections were cut on a Leica cryostat and air dried over night. Tissue sections were first blocked in PG/HN (5% horse serum, 5% goat serum, 1% BSA, 0.05% sodium azide and 0.05% Triton X-100 in 1x PBS) for 1 hour at room temperature (RT). Primary antibodies were diluted in PG/HN and incubated with the sections for 1 hour at RT, followed by washing then secondary antibody incubation for 1 hour at RT. Antibodies included mouse monoclonal anti-GFAP (1:500, Clone G-A-5, Sigma); mouse monoclonal anti-b-III-Tubulin (1:500, Clone TUJ1, Covance); rat monoclonal anti-myelin basic protein (MBP, 1:100, Millipore, Temecula, CA), rabbit polyclonal anti-BFABP (1:2000, gift from T. Muller, Max-Delbruck-Center, Berlin, Germany), mouse monoclonal anti-Reelin (1:1000, Clone G10, Abcam), rabbit polyclonal anti-FoxP2 (1:500, Abcam) and Alexa 488 conjugated rabbit polyclonal anti-GFP (1:400, Invitrogen). Alexa Fluor conjugated secondary antibodies were purchased from Invitrogen and used at 1:500 dilution. Nuclei were visualized using DAPI (2μg/ml, Sigma) and slides were mounted with Prolong antifade solution (Invitrogen). Images were collected on a Leica TCS SP5 laser scanning confocal microscope, and multi-channel overlays were assembled in Adobe Photoshop.

For immunohistochemical staining of Bmi-1 on E15 telecephalon, 12 μm frozen sections of E15 wild type and transgenic mouse telencephalon were first treated with 3% H_2O_2/0.1% NaN_3 for 1h at RT to quench endogenous peroxidase activity, then blocked with PG/HN before being labeled with mouse monoclonal anti-Bmi-1 (1:400, Clone F6, Upstate Chemicals) for 60 minutes at room temperature. The staining were then visualized using DAKO Envision+ and diaminobenzadine (DAB) as the chromogen.

To quantify adult SVZ proliferation, mice were injected with 100 mg/kg of 5-bromo-2-deoxyuridine (BrdU, Sigma), and sacrificed 2 hour later. Brains were fixed and embedded as described above. Twelve micron thick coronal sections were cut on a Leica cryostat. For detection of BrdU, DNA was first denatured in 2N HCl for 45 min at RT and neutralized with 0.1M Sodium Borate for 10 minutes. Sections were then pre-blocked in PG/HN for 1 hour at RT and stained with primary rat anti-BrdU antibody (1:500, Accurate Chemical, Westbury, NY) diluted in PG/HN for 1 hour at room temperature, followed by biotinylated goat-anti-rat IgG (Jackson Immunoresearch) for 30 minutes at RT. BrdU staining were then visualized with Alexa594-conjugated streptavidin (Invitrogen) and nuclei were counter-stained with DAPI. Slides were mounted using ProLong antifade solution (Invitrogen) and imaged on a Leica TCS SP5 laser scanning confocal microscope using a 63x oil immersion objective (NA=1.4).

To assess proliferation in E14.5 telencephalon, timed pregnant females were injected with a single dose of 100mg/ml BrdU 15 minutes prior to euthanization. Tissue processing and BrdU staining were then performed in a similar manner as described for adult tissue.

To quantify olfactory bulb neurogenesis, 1-2 month old mice were given a single injection of 100mg/kg of BrdU and kept on BrdU-containing drinking water (1mg/ml) for the next 7 days. They were switched to regular water for an additional 4 weeks before being sacrificed. Brains were fixed and embedded as described. Ten micron coronal sections of the olfactory bulb were cut on a Leica cryostat. Tissue sections were blocked with PG/HN, stained with anti-NeuN (1:100, Clone A60, Millipore), re-fixed with 4% PFA then stained for BrdU as described above. NeuN staining was visualized with

Alexa555-conjugated goat-anti-mouse IgG_1 secondary antibody (Invitrogen). BrdU staining was visualized with biotinylated goat-anti-rat IgG secondary antibody and Alexa594 conjugated streptavidin. Nuclei were counter-stained with DAPI. Slides were mounted in Prolong antifade (Molecular Probes), and imaged on a Leica TCS SP5 laser scanning confocal microscope using a 63x oil immersion objective (NA=1.4). Twenty five random fields of view (each containing 300-500 cells) spanning the full thickness of the olfactory bulb were counted in ImageJ software.

Neuron birth dates were determined by injecting timed pregnant females with a single dose of 100mg/ml 5-chloro-2-deoxyuridine (CldU, Sigma) at E17. Pups were sacrificed at P20, brains were fixed and embedded as described, and 40μm-thick floating sections were cut on a Leica cryostat. CldU staining was performed in a similar manner as described for BrdU, using CldU-specific (1:500, Clone BU1/75, Accurate Chemical) antibody (Kiel et al., 2007); Cux-1 was stained using a rabbit polyclonal anti-Cux1 antibody (1:50, Santa Cruz Biotechnology; Santa Cruz, CA). CldU staining was visualized by biotinylated goat-anti-rat IgG secondary antibody and Alexa594 conjugated streptavidin, and Cux-1 staining was visualized using Alexa555 conjugated goat-anti-rabbit IgG secondary antibody.

MRI analysis

All mice analyzed were anesthetized with 2% isoflurane/air mixture throughout MRI. Mice lay prone, head first in a 7.0T Varian MR scanner (183-mm horizontal bore, Varian, Palo Alto, CA), with the body temperature maintained at 37ºC using circulated heated air. A double-tuned volume radio frequency coil was used to scan the head region of the mice. Axial T_2-weighted images were acquired using a fast spin-echo sequence

with the following parameters: repetition time (TR)/effective echo time (TE), 4000/47.456 ms; field of view (FOV), 30x30 mm; matrix, 256x128; slice thickness, 0.5 mm; slice spacing, 0 mm; number of slices, 25; and number of scans, 1 (total scan time ~1 min).

Southern blots

Southern blotting was performed to determine the number of transgene insertion sites and number of transgene copies that inserted into the genome of various lines of *Nestin-Bmi-1-GFP* transgenic mice. Purified mouse tail genomic DNA from each line was digested with EcoRV or ScaI, which both cut only once within the transgene. Digestion products were separated on a 0.8% agarose gel and blotted following standard methods, using a probe against the GFP sequence in the transgene. Copy number standards from linearized plasmid were run simultaneously, and band intensities were used to approximate copy number in each of the transgenic founders. For our experiments, two independent transgenic founders were selected that each had one to 10 copies of the transgene at a single point in the genome (Figure 3.3).

Western blots and quantitative RT-PCR

Western blotting was performed as previously described (Molofsky et al., 2005). Mouse tissues and cultured neurospheres were harvested as described in the paper, primary human glioma samples were obtained from the frozen tumor bank of University of Michigan Comprehensive Cancer Center Tissue Core, xenografted human glioma cells were passaged at least twice in NOD-SCID mice before being harvested, normal human brain and cerebral cortex total protein extract were purchased from Biochain, Hayward,

CA. For sample preparation, tissues were homogenized in ice-cold RIPA buffer supplemented with protease inhibitor cocktail (complete mini tablet, Roche) by brief sonication using a Virsonic-100 ultrasonic cell disruptor (VirTis; Gardiner, NY). The cell homogenates were then spun down for 20 minutes at 4°C at 16,000g and the supernatant was quantified colorimetrically (BioRad protein assay; Bio-Rad, Hercules, CA). 10-50 µg of protein per lane were separated on a 4-20% gradient Tris-glycine denaturing SDS-PAGE gels (Invitrogen) or a NuPAGE 10% Bis-Tris gel and transferred for 1-2 hours to PVDF membranes (Bio-Rad) at 4°C. The membranes were blocked in Tris buffered saline with 0.1% tween-20 (TBST) and 5% skim milk, then incubated with primary and secondary antibodies, and washed following standard procedures. Horseradish peroxidase conjugated secondary antibodies were visualized by chemiluminescence (ECL Plus, Amersham-Pharmacia, Piscataway, NJ; or SuperSignal West Femto, Thermo Scientific, Waltham, Ma). Primary antibodies were mouse monoclonal anti-ß-actin (1:2000, Clone AC-15; Sigma), rat monoclonal anti-$p19^{Arf}$ (1:500, Clone 5-C3-1, Upstate Chemicals, Lake Placid, NY), mouse monoclonal anti Bmi-1 (1:500, Clone F6, Upstate Chemicals), mouse monoclonal anti-HA (1:1000, Clone HA-7, Sigma), rat monoclonal anti-HA (1:2000, Clone 3F10, R&D), and rabbit polyclonal anti-$p16^{Ink4a}$ (1:1000, M-156; Santa Cruz Biotechnology).

Quantitative (real-time) RT-PCR was performed as described previously (Molofsky et al., 2003). Primers used to amplify *Bmi-1* were 5'-CCAATGGCTCCAATGAAGACC -3' and 5'-TTGCTGCTGGGCATCGTAAG -3'. Primers for *b-actin* were 5'-GTCAGGATACCTCTCTTGCTCTGG-3' and 5'-CAGGGTGTGATGGTGGGAATG-3'.

Neurosphere clonality assay

To assess the clonality of neurospheres, a 1:1 mixture of dissociated adult SVZ cells from UBC-GFP (Jackson laboratory, Bar Harbor, Maine) and ROSA-26 mice were plated at indicated cell densities (0.7 cells/μl or 1.3 cells/μl). After 10 days in culture, individual neurospheres were replated onto PDL and fibronectin coated 96-well plate and imaged for GFP fluorescence. The day after neurosphere attachment, cultures were fixed with 0.5% glutaraldehyde in 1x PBS for 10min at RT, then stained with X-gal to visualize LacZ expression. The frequencies of GFP-only, X-gal-only and mixed colonies were scored to estimate the rate of neurosphere fusion. All neurospheres were GFP+, LacZ+, or both.

Histology

Mouse brains used for H&E staining were fixed in 4% PFA or 10% neutral buffered formalin (NBF) for 24-48 hours at 4ºC; then dehydrated through an ethanol gradient and embedded in paraffin. Five micron coronal sections were cut on a Leica microtome and stained with hematoxylin and eosin. Images were taken on an Olympus BX-51 microscope using a 4x objective and assembled using Adobe Photoshop. For Nissl staining of perinatal mouse brain sections, 40 μm brain cryosections were stained with 0.1% cresyl violet for 3 minutes, rinsed in distilled water and differentiated in 95% ethyl alcohol. Slides were then dehydrated and mounted in Vectamount (Vector Laboratories, Burlingame, CA). Images were taken on an Olympus BX-51 microscope using 4x or 10x objectives, and assembled with Adobe Photoshop.

ACKNOWLEDGEMENTS

This work was supported by the McDonnell Foundation and the Howard Hughes Medical Institute. Thanks to David Adams, Martin White, and Ann Marie Deslaurier of the University of Michigan (UM) Flow-Cytometry Core Facility. Flow-cytometry was supported in part by the UM Comprehensive Cancer Center NIH CA46592, and the UM Multipurpose Arthritis Center NIH AR20557. Thanks to Amanda Welton and the UM Center for Molecular Imaging for help with MRI analysis. Thanks to Galina Gavrilina and Thom Saunders of the UM Transgenic Animal Core Facility for generating *Nestin-Bmi-1-HA-GFP* transgenic mice with partial financial support from the UM Comprehensive Cancer Center NIH CA46592, the UM Center for Organogenesis, and the Michigan Economic Development Corporation (grant 085P1000815). Thanks to Daisuke Nakada for technical assistance with Southern and western blotting.

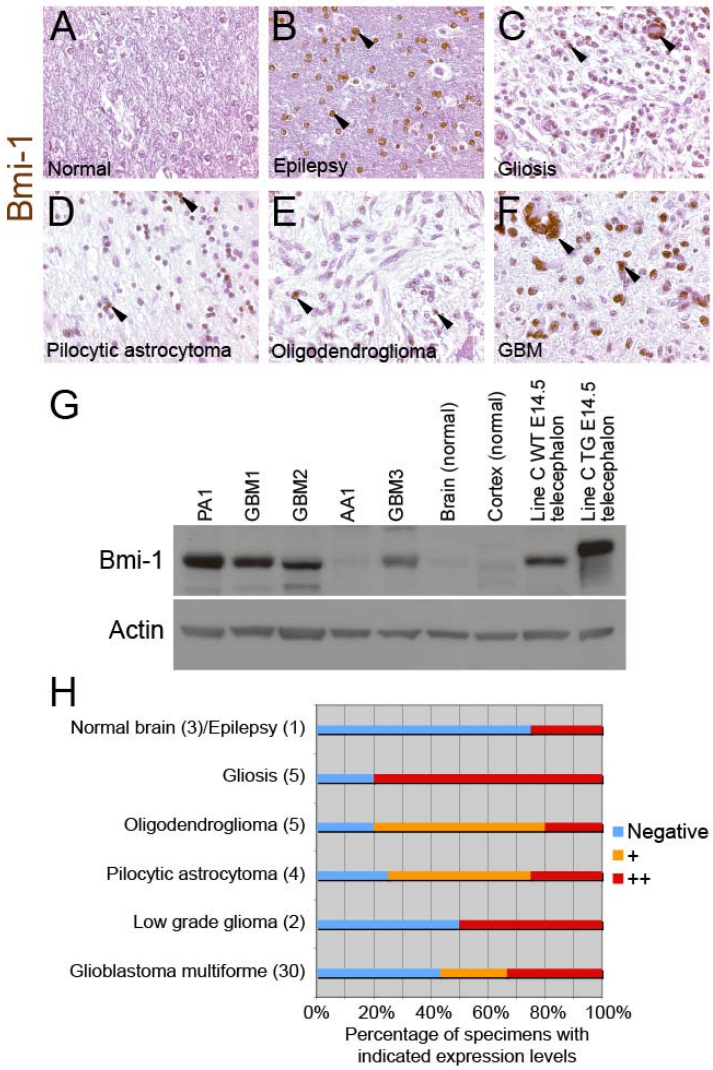

Figure 3.1: Bmi-1 expression was elevated in human brain tumors.
A-F) Immunohistochemistry for Bmi-1 in representative sections from normal human brain tissue and various types of brain tumors. Bmi-1 (brown, arrowheads) was not detected in uninjured normal human brain tissue (A), but was detected in white matter after an epileptic seizure (B), in gliosis (C), pilocytic astrocytoma (D), oligodendroglioma (E) and glioblastoma (F). Sections are counterstained with hematoxylin. G) Western blotting showed Bmi-1 was faintly detected in normal human brain and cerebral cortex (brain, cortex) but it was elevated to various degrees in human glioma specimens obtained directly from patients (AA1, GBM3) as well as from mouse xenografts (PA1, GBM1,GBM2). In comparison, telencephalon cells from Bmi-1 transgenic mice showed the highest level of Bmi-1 expression. AA1: anaplastic astrocytoma (grade 3); PA1: pilocytic astrocytoma (grade 1); GBM1, GBM2, GBM3: glioblastoma multiforme (grade 4). H) Comparison of Bmi-1 expression between normal human brain tissues and various brain tumors. A three-tier grading system was used to evaluate Bmi-1 expression levels: strong Bmi-1 expression in many cells (red, ++); variable Bmi-1 expression in some cells (orange, +), no Bmi-1 expression above background (blue, -). Numbers in parentheses indicate the number of specimens examined for each category.

Figure 3.2: Transgene expression in Nestin-Bmi-1-GFP transgenic mice.
A). Schematic representation of the *Nestin-Bmi-1-GFP* transgene. B). GFP epifluorescence shows transgene expression throughout the CNS in an E14.5 transgenic embryo but not in non-neural tissues or in a wild type control embryo (to the left of the transgenic embryo). C) The transgene was still widely expressed in most regions of the P0 transgenic brain, with nerve fiber bundles (ac, cc) and the wall of the ventricular system (aq) expressing the highest levels of GFP (left, whole brain overview; right, sagittal view from the midline). D-F). GFP expression became more restricted in the adult transgenic mouse brain (D) and concentrated in regions enriched for neural stem/progenitor cells, such as the SVZ of the lateral ventricle (E) and the subgranular layer of the dentate gyrus (F). All photos are from line C transgenic mice, but are also representative of line B mice. Flow-cytometry of cells from line B mice confirmed the presence of GFP+ cells in the ventricular zone, the cortex, and the cerebellum of neonatal transgenic mice (green histograms; G) but not in control littermates (unshaded histograms; G), as well as in the adult SVZ (H). I-J). The vast majority of neurospheres formed by neonatal VZ, cerebral cortex, and cerebellum (I) as well as adult SVZ (J) derived from the GFP+ fraction of cells. Data represent mean±s.d. from 3 independent experiments using line B transgenic mice. K). Many *Bmi-1* transgenic neurospheres were capable of undergoing multilineage differentiation into astrocytes (GFAP+, green), neurons (Tuj-1+, red) and oligodendrocytes (O4+, black). ac, anterior commissure; aq, aqueduct; cbl, cerebellum; cc, corpus callosum; ctx, cerebral cortex; DG, dentate gyrus; LV, lateral ventricle; ob, olfactory bulb; str, striaum.

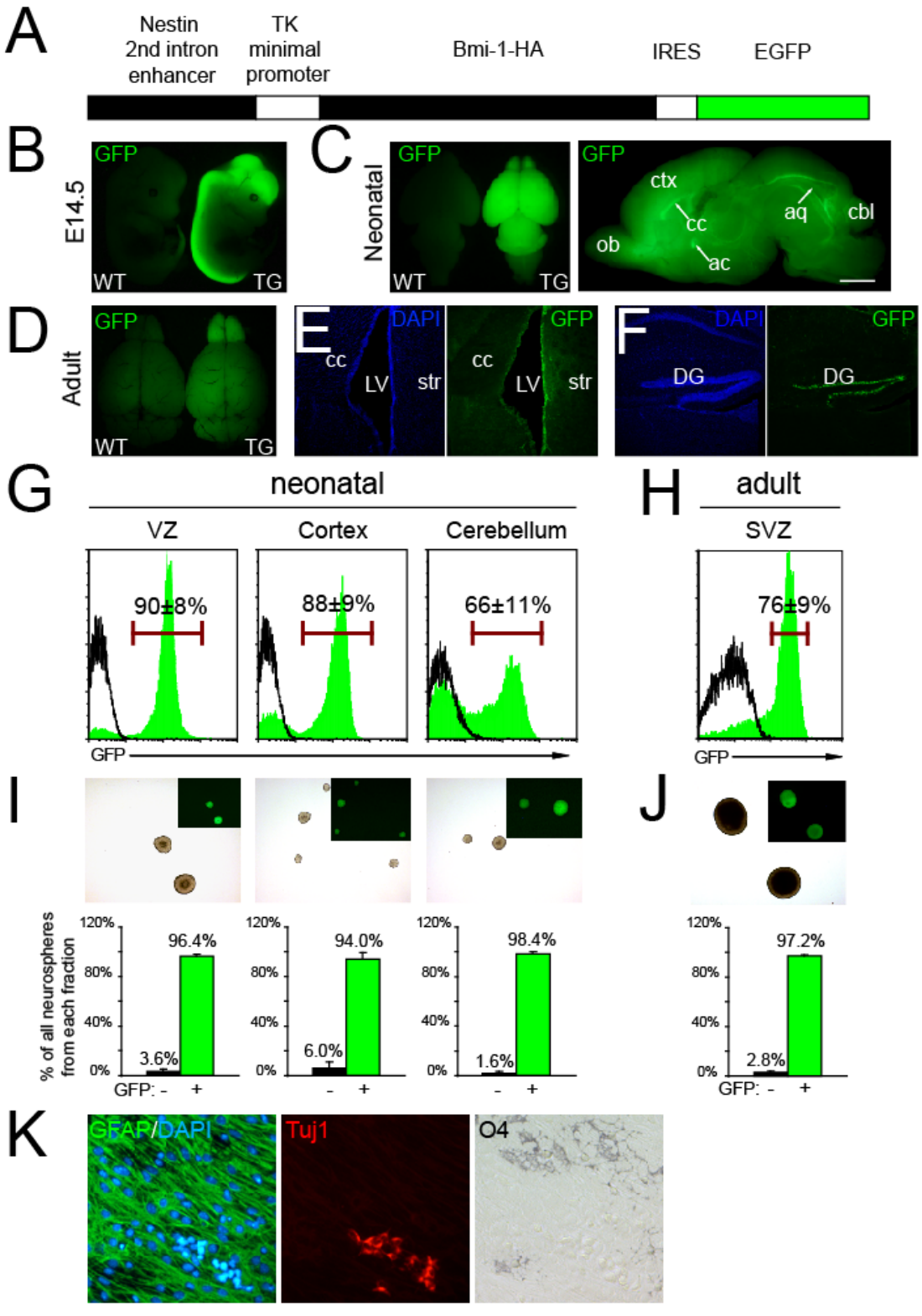
A
Nestin 2nd intron enhancer
TK minimal promoter
Bmi-1-HA
IRES
EGFP
B
E14.5
GFP
WT
TG
C
Neonatal
GFP
WT
TG
GFP
ctx
cc
aq
cbl
ob
ac
D
Adult
GFP
WT
TG
E
DAPI
cc
LV
str
GFP
cc
LV
str
F
DAPI
DG
GFP
DG
G
neonatal
VZ
Cortex
Cerebellum
90±8%
88±9%
66±11%
GFP
H
adult
SVZ
76±9%
GFP
I
% of all neurospheres from each fraction
120%
80%
40%
0%
96.4%
3.6%
GFP: - +
120%
80%
40%
0%
94.0%
6.0%
- +
120%
80%
40%
0%
98.4%
1.6%
- +
J
120%
80%
40%
0%
97.2%
2.8%
GFP: - +
K
GFAP/DAPI
Tuj1
O4

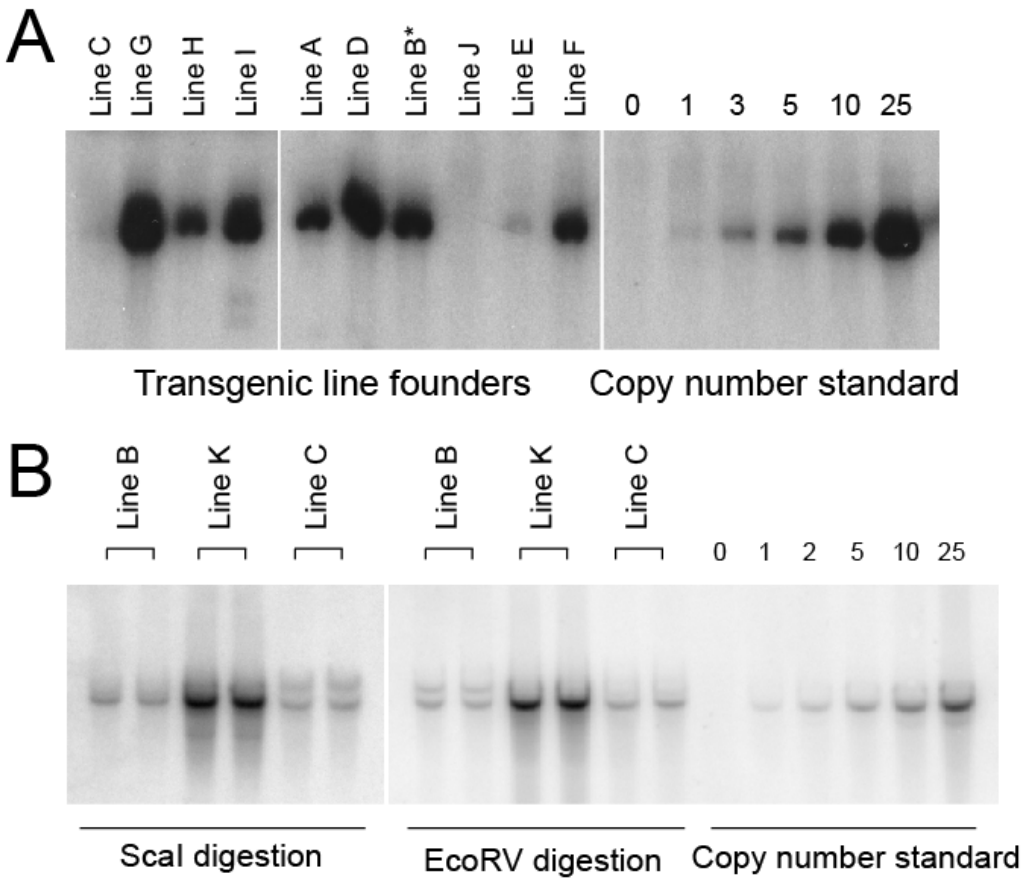

Figure 3.3: Southern blot analysis of transgene copy number and insertion site in transgenic founders.
A). Southern blots of genomic DNA from the ten transgenic founders showed variable transgene copy numbers. ScaI linearized transgene was used for copy number standards. Five lines (B*, C, D, E, G) gave germ line transmission. B). Genomic DNA from lines B, K, and C were digested with ScaI or EcoRV (which each cut at single sites within the transgene) and analyzed by Southern blot using an internal probe against the transgene. Line B and Line K mice were both derived from the original line B* founder; however, they had different transgene copy numbers and different transgene integration sites. Note that the presence of only 1 or 2 bands indicates a single chromosome integration site. Line C samples were included for transgene copy number comparison. All experiments were performed on line B and C mice, which had approximately 5 copies of the transgene inserted at a single integration site.

A Characterization of GFP transgene expression in all surviving transgenic lines

	Line K		Line B		Line C		Line D		Line E		Line G	
	P0	P30	P0	P30	P0	P30	P0	P30	P0	P30	P0	P30
VZ/SVZ	0%	0%	90±8%	76±9%	95%	69±14%	0%	0%	0.2%	0%	0.4%	0%
cortex			88±9%	4.2%	63%	3±0%						0%
cerebellum			66±11%	2.9%	50%	3±2%						0%
olfactory bulb				3.5%		23±11%						
Bone marrow				0.0±0.0%		0.0±0.0%						

B

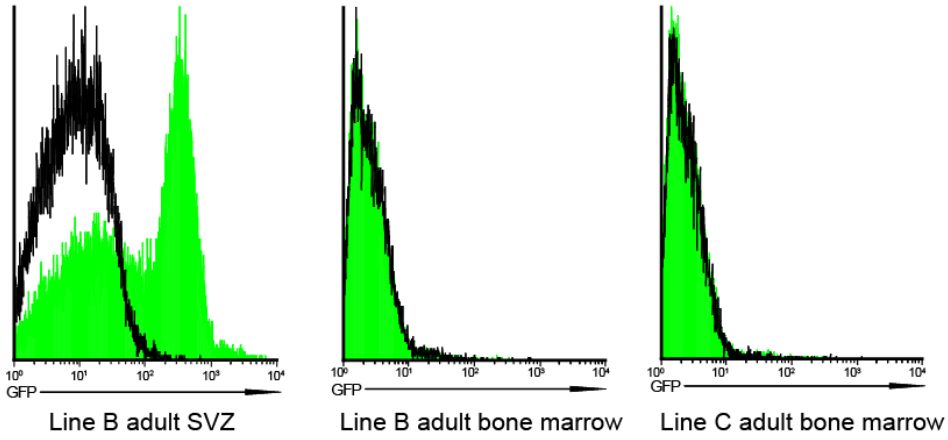

Line B adult SVZ | Line B adult bone marrow | Line C adult bone marrow

Figure 3.4: Characterization of transgene expression in lines that gave germline transmission.
A). GFP expression in transgenic mice was examined at P0 and P30 by analyzing dissociated cells by flow-cytometry. Only two transgenic lines with low copy numbers of the transgene (lines B and C) showed GFP expression in the CNS at both time points examined, while the other lines showed no appreciable expression at either developmental stage. GFP expression was not detected in tissues outside of the nervous system such as in bone marrow hematopoietic cells. B). Representative flow-cytometry histograms show the absence of GFP expression in transgenic mouse bone marrow cells (black open histograms show littermate control cells; green solid histograms show transgenic cells). Line B adult SVZ cells were included as a positive control for GFP expression.

A

		Observed	Expected	p-value
Line B	WT	65	55	0.06
	TG	45	55	
Line C	WT	135	128	0.38
	TG	121	128	

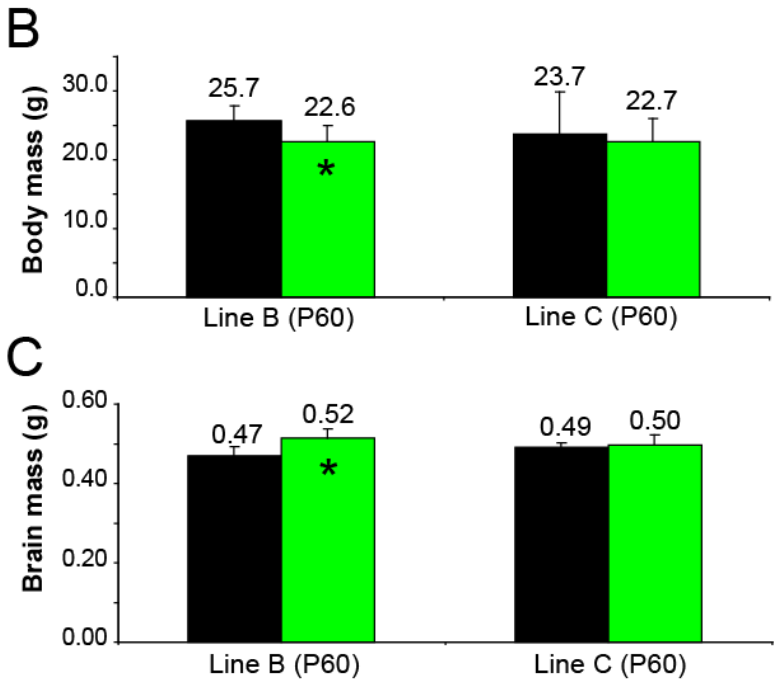

Figure 3.5: *Bmi-1* transgenic mice were born at expected Mendelian frequency and showed no substantial growth defects.
A) *Bmi-1* transgenic mice from both lines were born at Mendelian frequency and showed no increased mortality relative to control littermates within the first month after birth. Numbers of surviving wild type and transgenic mice were counted at P30. B, C) Bmi-1 transgenic mice from both lines exhibited similar brain and body masses as control littermates at P60, though a subset (~25%) of transgenic mice that developed hydrocephalus in early adulthood tended to exhibit increased brain mass and decreased body mass. Since line B mice tended to develop hydrocephalus earlier than line C mice, these effects led to line B mice exhibiting slightly but significantly lower body masses and slightly but significantly higher brain masses than littermate controls (n=3 independent experiments, with 6 mice per genotype; *, $p<0.05$, error bars represent s.d.).

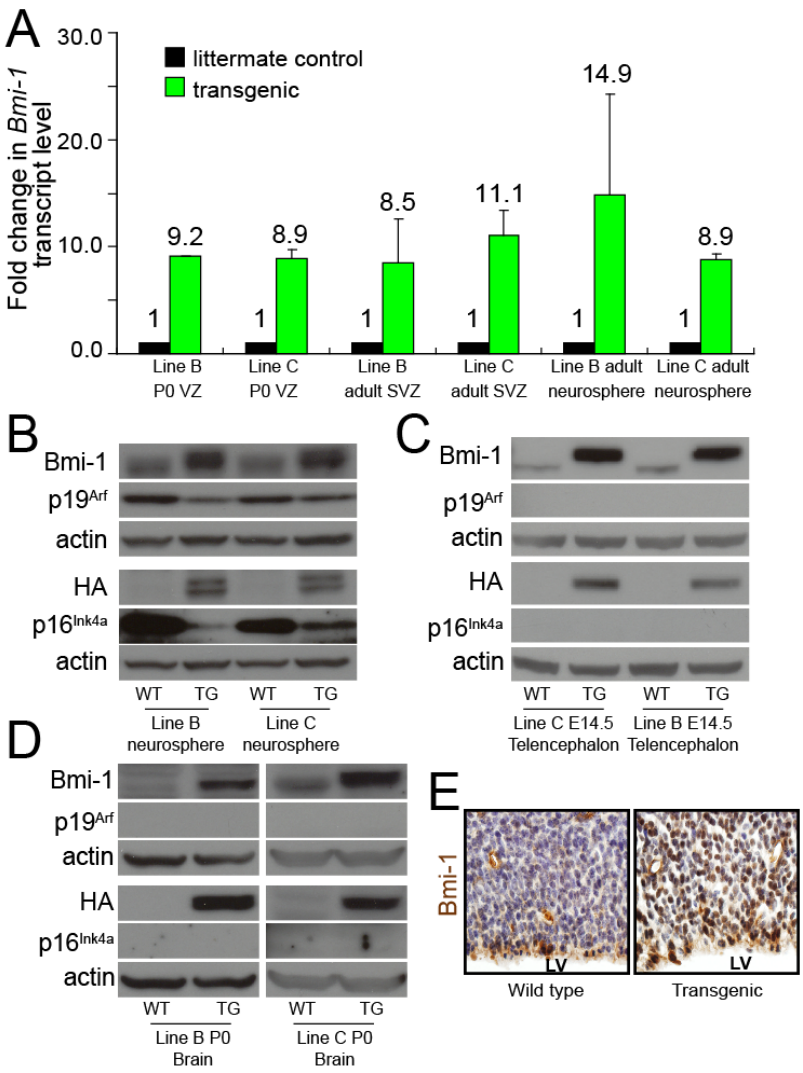

Figure 3.6: Bmi-1 expression was elevated in transgenic neural stem/progenitor cells.

A). qRT-PCR showed that *Bmi-1* transcript expression was markedly increased in uncultured transgenic P0 VZ and adult SVZ cells as well as in neurospheres cultured from adult transgenic SVZ cells as compared to littermate control cells. Fold change is presented (mean±s.d. from 3-5 independent experiments) relative to control cells, which were set to 1. Total cDNA levels in each pair of samples were normalized based on ß-actin expression. B) Western blotting showed the expression of HA tag, as well as increased Bmi-1 and decreased $p16^{Ink4a}$ and $p19^{Arf}$ in transgenic as compared to control neurospheres from lines B and C. Western blotting showed the expression of HA tag and increased Bmi-1 levels in E14.5 telecephalon (C) and P0 brain (D) from transgenic as compared to control mice. Note that $p16^{Ink4a}$ and $p19^{Arf}$ were not detected in E14.5 telecephalon (C) or P0 brain (D) from either transgenic or control mice, as expected. E). Representative immunohistochemical staining of Bmi-1 on coronal sections of E15 wild type and line B transgenic telencephalon. Bmi-1 staining was nuclear, LV is lateral ventricle.

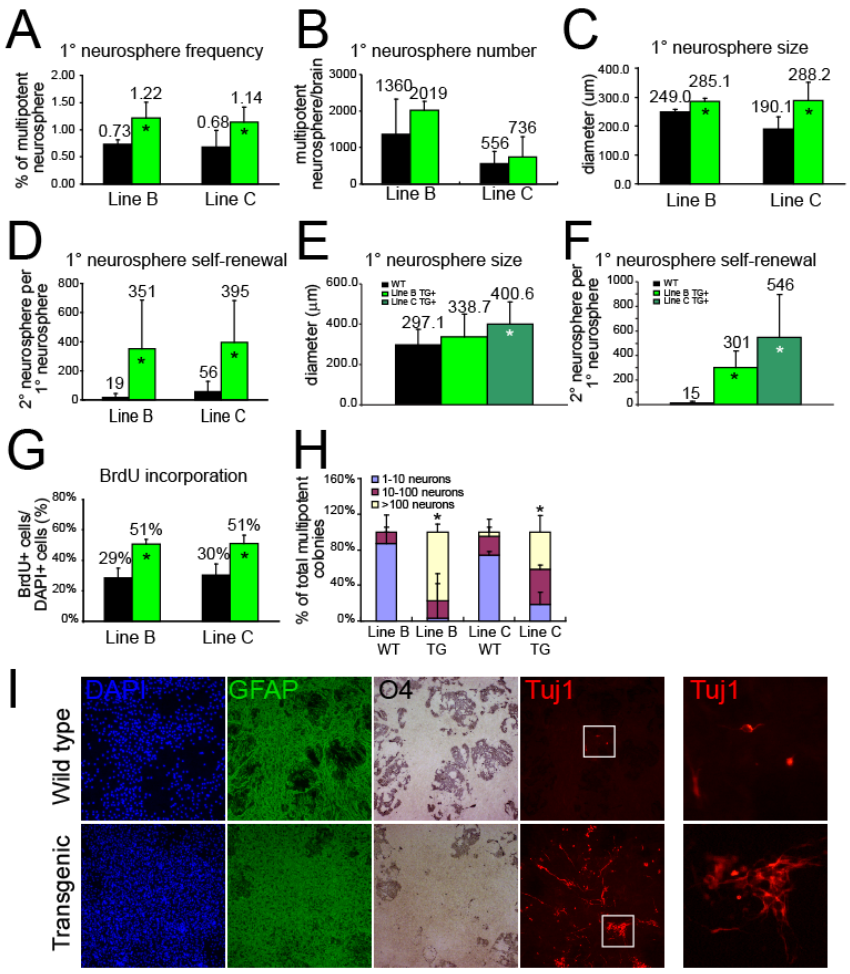

Figure 3.7: Bmi-1 overexpression increased the self-renewal and neuronal differentiation of neural stem/progenitor cells in culture.
A) A significantly higher percentage of freshly isolated SVZ cells from 2-3 month old transgenic mice gave rise to multipotent neurospheres than littermate control cells. (*, $p<0.05$); however, the total number of multipotent neurospheres formed per transgenic SVZ (from both brain hemispheres) was not significantly different from control SVZ (B, $p=0.31$ for line B and $p=0.55$ for line C). Transgenic neurospheres were significantly larger than control neurospheres (C; *, $p<0.01$) and gave rise to significantly more multipotent secondary neurospheres upon subcloning (D; *, $p<0.05$). E, F) Single CD15+CD24- SVZ cells from P5 wild type and transgenic mice were sorted per well of 96 well plates. The transgenic single cell-derived neurospheres were larger than controls (E; *, $p<0.01$) and generated significantly more multipotent secondary neurospheres upon subcloning (F; *, $p<0.01$). G) Adherent Bmi-1 transgenic neural stem cell colonies showed a significantly higher frequency of BrdU+ cells as compared to control colonies after a 1 hour pulse with BrdU (*, $p<0.01$). H, I) Transgenic neurospheres were capable of multilineage differentiation and gave rise to larger numbers of neurons as compared to control colonies. Significantly more transgenic colonies contained large numbers of neurons (>100) as compared to control colonies ($p<0.01$ for line B and $p<0.05$ for line C). Data represent mean±s.d. from 3-5 independent experiments.

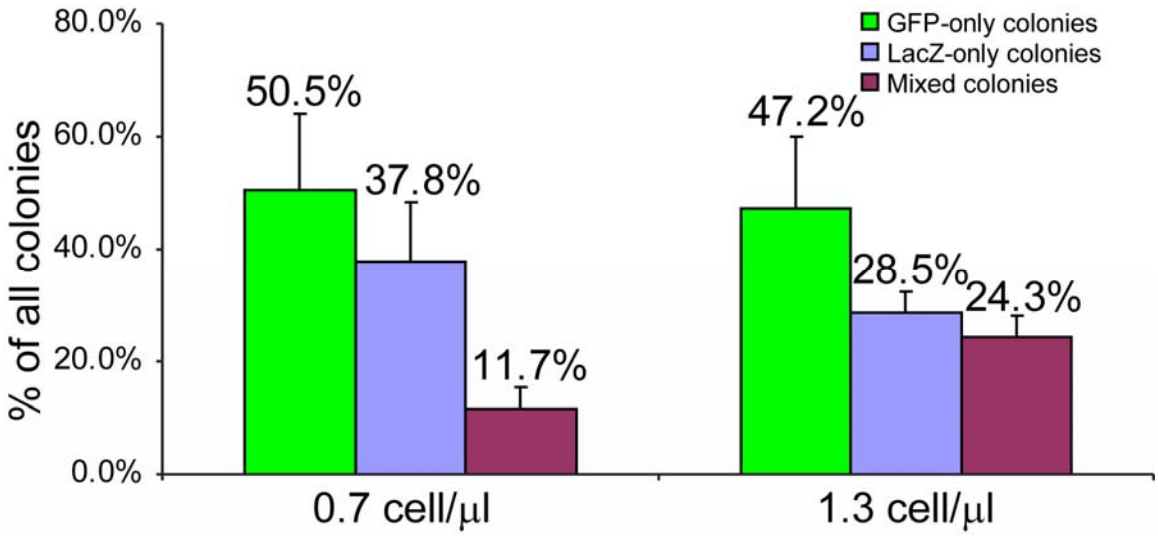

Figure 3.8: Most neurospheres grown under our culture conditions were clonal. A 1:1 mixture of freshly isolated adult SVZ cells from UBC-GFP and ROSA-26 mice were plated at the indicated total cell density in non-adherent cultures, and neurospheres were allowed to form. After 10 days in culture spheres were scored for GFP and LacZ expression. While most neurospheres appeared to be clonally derived (containing GFP+ cells or LacZ+ cells but not both), a small fraction of neurospheres contained both GFP+ and LacZ+ cells suggestive of sphere-fusion (red bar) (Singec et al., 2006). Data represent mean±s.d. from 3 experiments.

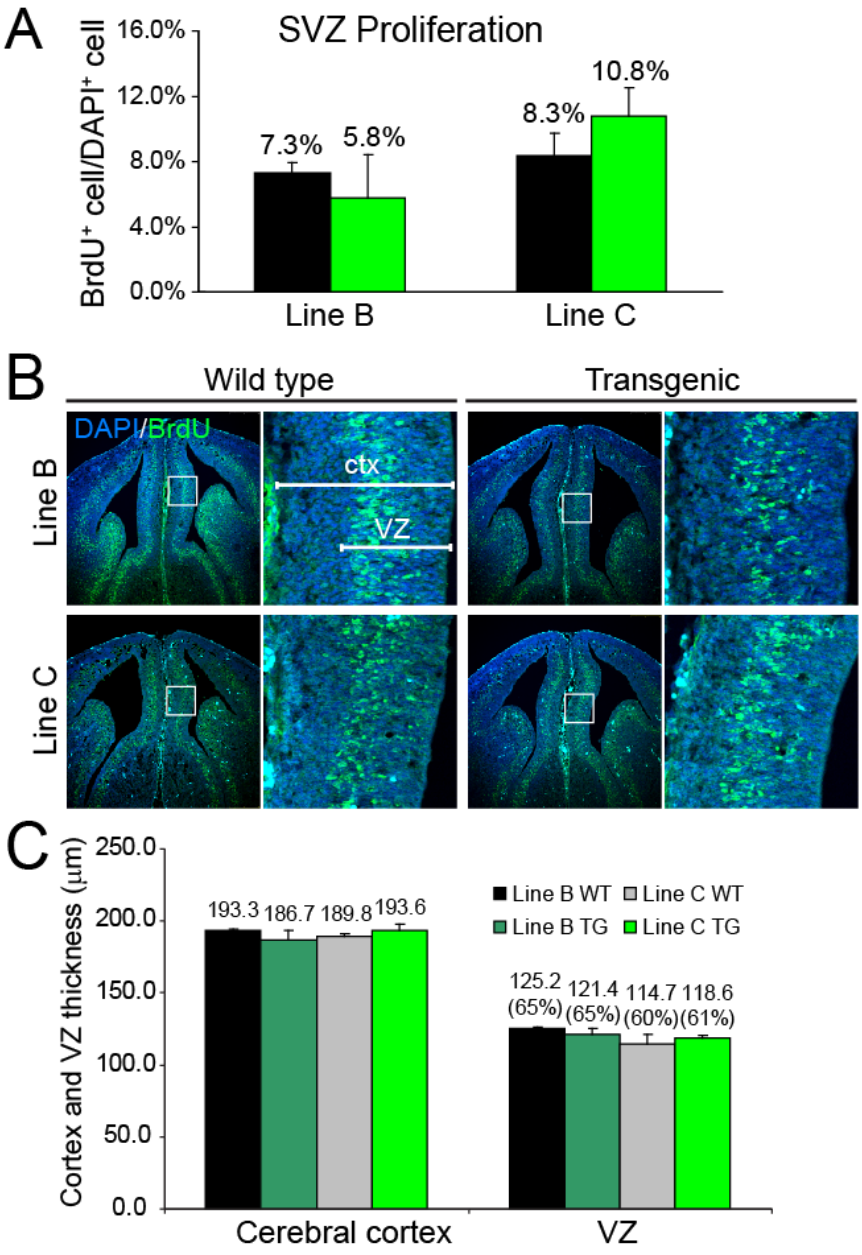

Figure 3.9: Bmi-1 overexpression had little effect on fetal or adult neural stem/progenitor cell proliferation *in vivo*.
A) The rate of BrdU incorporation by SVZ cells was comparable between transgenic and control mice after a 2 hour pulse of BrdU (p=0.31 for line B and p=0.08 for line C; data represent mean±s.d. from 4 independent experiments). B) Representative confocal images showing BrdU+ cell distribution in wild type and transgenic E14.5 telencephalon after a 15 minute pulse of BrdU. No differences in the gross distribution or frequency of BrdU+ cells were noted between wild type and transgenic embryos. C). No differences in the thickness of the cerebral cortex or VZ (as indicated in B) were found between transgenic and control embryos. Numbers in parenthesis indicate VZ thickness as a fraction of total cortex thickness.

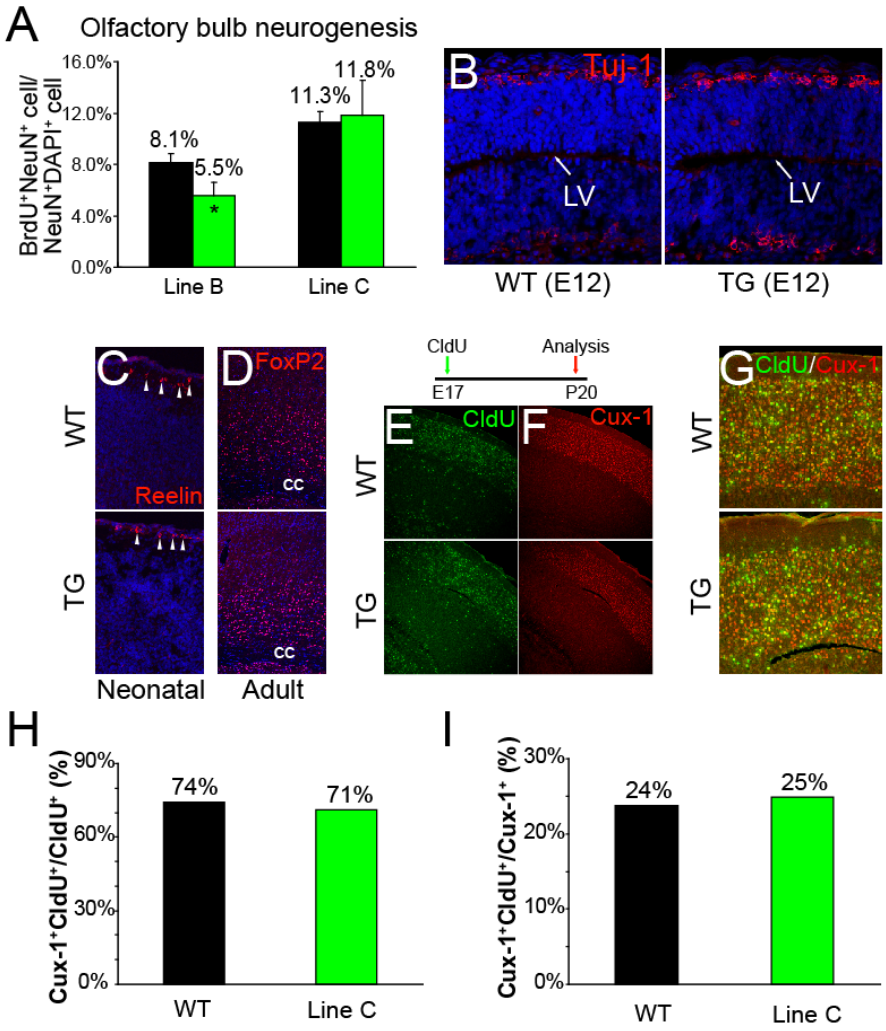

Figure 3.10: Bmi-1 overexpression had little effect on fetal or adult neurogenesis. A) One month old transgenic and control mice were pulsed with BrdU for one week. Four weeks later, the frequency of $BrdU^+NeuN^+$ neurons in the olfactory bulb was significantly reduced among line B transgenics (p=0.02) but was not affected in line C (p=0.74; data represent mean±s.d. from 3-4 independent experiments). B-F) Representative images from line C transgenic mice show normal cortical neurogenesis in Bmi-1 transgenic mice. B) At E12, the frequency and localization of $Tuj1^+$ neurons in the cerebral cortex was similar between transgenic and control littermates. C, D) Cortical layer organization appeared to be normal in the postnatal transgenic mouse brain. Reelin labels Cajal-Retzius neurons in layer I of the neonatal cortex (C) and FoxP2 labels layer VI neurons (D). E, F) Bmi-1 transgenics and littermate controls were pulsed with a single injection of CldU at E17 and analyzed at P20: no difference was observed in the frequency or localization of $CldU^+$ neurons. Cux-1 labels upper layer (II-IV) neurons. G) High magnification confocal images of the same tissue sections as shown in (E,F). Cux-1 staining is shown in red while CldU staining is shown in green (double stained cells are yellow). The frequency of $CldU^+Cux\text{-}1^+$ neurons as compared to total $CldU^+$ cells (H) and as compared to total $Cux\text{-}1^+$ neurons (I) was normal in transgenic mice.

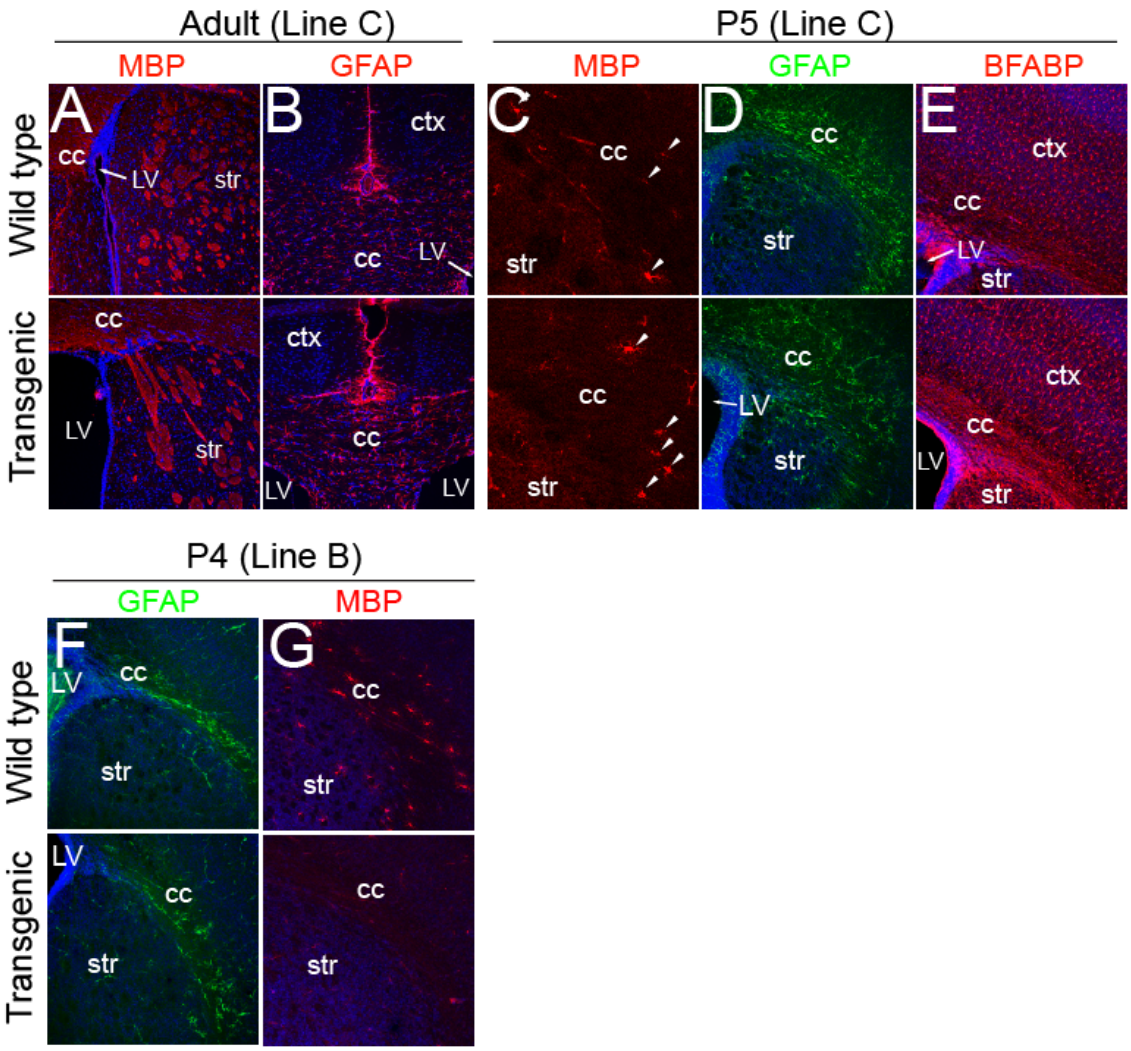

Figure 3.11: Bmi-1 overexpression had little effect on gliogenesis *in vivo*.
A-E) We did not detect any effect of Bmi-1 overexpression on postnatal gliogenesis in line C transgenic mice, as indicated by the normal number and distribution of MBP^+ oligodendrocytes (A) and $GFAP^+$ astrocytes (B) in the adult transgenic brain as well as the normal timing of early postnatal gliogenesis (C-E). F,G) While no difference was observed in the frequency of $GFAP^+$ astrocytes in P4 line B wild type and transgenic mouse brains (F); the frequency of MBP^+ oligodendrocytes was transiently reduced as compared to littermate controls at P4 (G). As with line C, adult line B transgenic mice exhibited no difference relative to control mice in terms of the frequency of GFAP+ astrocytes or MBP+ oligodendrocytes (data not shown).

Figure 3.12: Bmi-1 overexpression increased proliferation, self-renewal, and neurogenesis by wild-type but not *Ink4a-Arf* deficient neural stem/progenitor cells in culture.

Wild type and *Ink4a-Arf* deficient neural stem cells were infected with either a *Bmi1*-encoding retrovirus (MSCV-Bmi1-IRES-GFP) or control retrovirus (MSCV-GFP). A) qRT-PCR confirmed a 4 to 5.5-fold increase in *Bmi-1* expression in MSCV-Bmi-1 infected neurospheres as compared to neurospheres infected with control virus. B) Wild type neurospheres infected with MSCV-Bmi1 were significantly larger than those infected with control virus or uninfected neurospheres ($p<0.01$). In contrast, MSCV-Bmi1 infection did not affect the size of *Ink4a-Arf* deficient neurospheres ($p=0.57$). Data represent mean±s.d. from 3-4 independent experiments. C) Wild type neurospheres infected with MSCV-Bmi1 virus exhibited significantly increased self-renewal as compared to neurospheres infected with control virus or uninfected neurospheres ($p<0.05$). In contrast, MSCV-Bmi1 infection did not affect the self-renewal of *Ink4a-Arf* deficient neurospheres ($p=0.45$). Data represent mean±s.d. for 3-5 independent experiments. D). MSCV-Bmi1 infection increased neuronal differentiation within wild-type (*, $p<0.05$ relative to WT no virus) but not *Ink4a-Arf* deficient neural stem cell colonies. Data represent mean±s.d. from 3-4 independent experiments. E-I) Bmi-1 transgenic mice (*Bmi-1*$^{TG+}$) were also mated with *Ink4a-Arf* deficient mice. E) Freshly dissociated SVZ cells showed that *Bmi-1*$^{TG+}$*Ink4a-Arf*$^{-/-}$ mice expressed the transgene *in vivo* (green filled histogram), while *Ink4a-Arf*-/- mice (black open histogram) did not. F). qRT-PCR analysis showed that Bmi-1 expression was increased in the SVZ of *Bmi-1*$^{TG+}$*Ink4a-Arf*$^{-/-}$ mice. G). The frequency of multipotent neurospheres that arose in culture from *Bmi-1*$^{TG+}$*Ink4a-Arf*$^{-/-}$ SVZ cells was not significantly different from *Ink4a-Arf*$^{-/-}$ SVZ. H,I). *Bmi-1*$^{TG+}$*Ink4a-Arf*$^{-/-}$ neurospheres did not show increased diameter or self-renewal potential as compared with *Ink4a-Arf*$^{-/-}$ neurospheres.

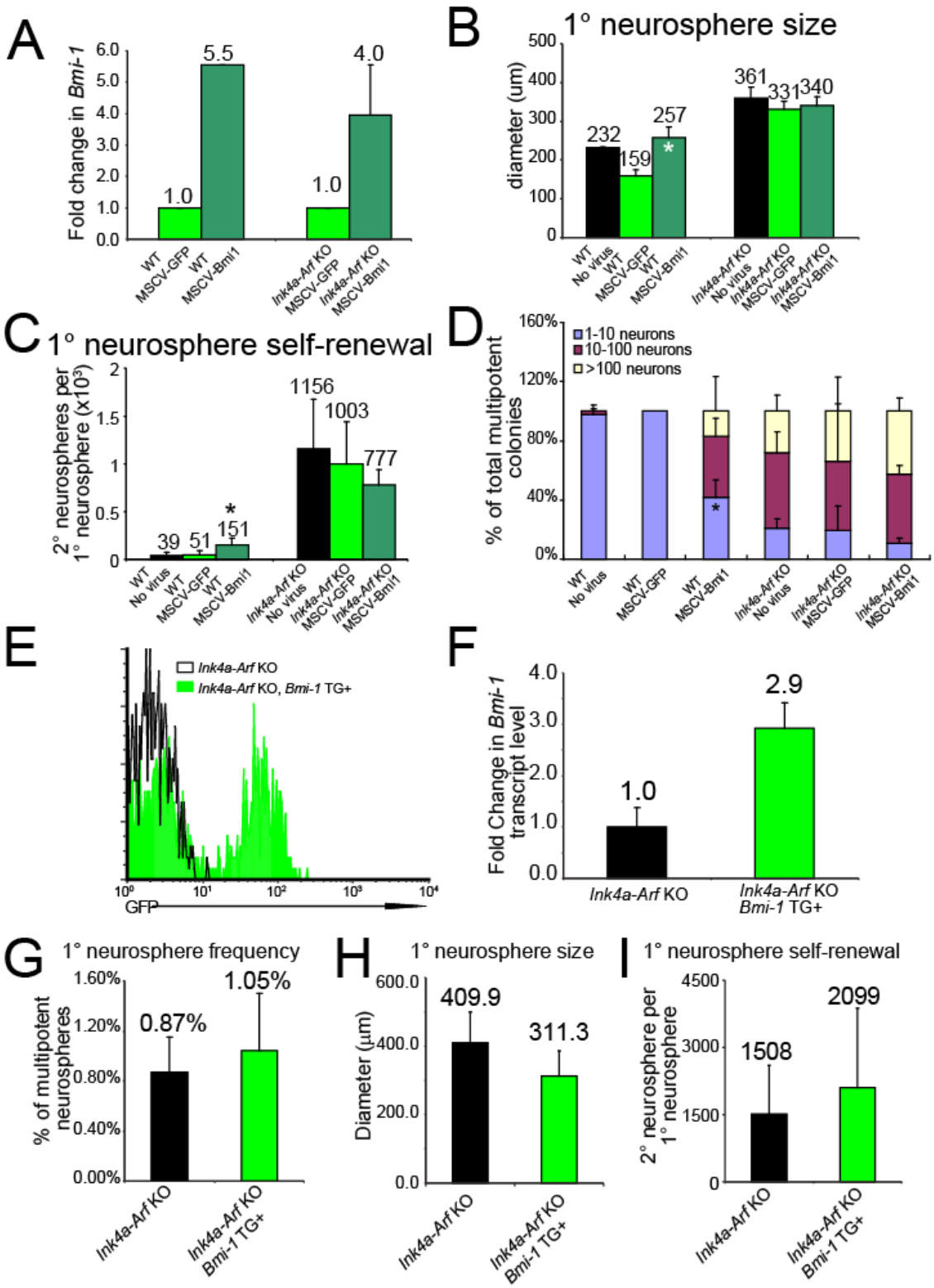
A
Fold change in Bmi-1
6.0
5.0
4.0
3.0
2.0
1.0
0.0
1.0
5.5
1.0
4.0
WT MSCV-GFP
WT MSCV-Bmi1
Ink4a-Arf KO MSCV-GFP
Ink4a-Arf KO MSCV-Bmi1
B
1° neurosphere size
diameter (um)
500
400
300
200
100
0
232
159
257
*
361
331
340
WT No virus
WT MSCV-GFP
WT MSCV-Bmi1
Ink4a-Arf KO No virus
Ink4a-Arf KO MSCV-GFP
Ink4a-Arf KO MSCV-Bmi1
C
1° neurosphere self-renewal
2° neurospheres per 1° neurosphere (x10³)
2
1.5
1
0.5
0
39
51
*
151
1156
1003
777
WT No virus
WT MSCV-GFP
WT MSCV-Bmi1
Ink4a-Arf KO No virus
Ink4a-Arf KO MSCV-GFP
Ink4a-Arf KO MSCV-Bmi1
D
% of total multipotent colonies
160%
120%
80%
40%
0%
1-10 neurons
10-100 neurons
>100 neurons
*
WT No virus
WT MSCV-GFP
WT MSCV-Bmi1
Ink4a-Arf KO No virus
Ink4a-Arf KO MSCV-GFP
Ink4a-Arf KO MSCV-Bmi1
E
Ink4a-Arf KO
Ink4a-Arf KO, Bmi-1 TG+
10⁰
10¹
10²
10³
10⁴
GFP
F
Fold Change in Bmi-1 transcript level
4.0
3.0
2.0
1.0
0.0
1.0
2.9
Ink4a-Arf KO
Ink4a-Arf KO Bmi-1 TG+
G
1° neurosphere frequency
% of multipotent neurospheres
1.60%
1.20%
0.80%
0.40%
0.00%
0.87%
1.05%
Ink4a-Arf KO
Ink4a-Arf KO Bmi-1 TG+
H
1° neurosphere size
Diameter (μm)
600.0
400.0
200.0
0.0
409.9
311.3
Ink4a-Arf KO
Ink4a-Arf KO Bmi-1 TG+
I
1° neurosphere self-renewal
2° neurosphere per 1° neurosphere
4500
3000
1500
0
1508
2099
Ink4a-Arf KO
Ink4a-Arf KO Bmi-1 TG+

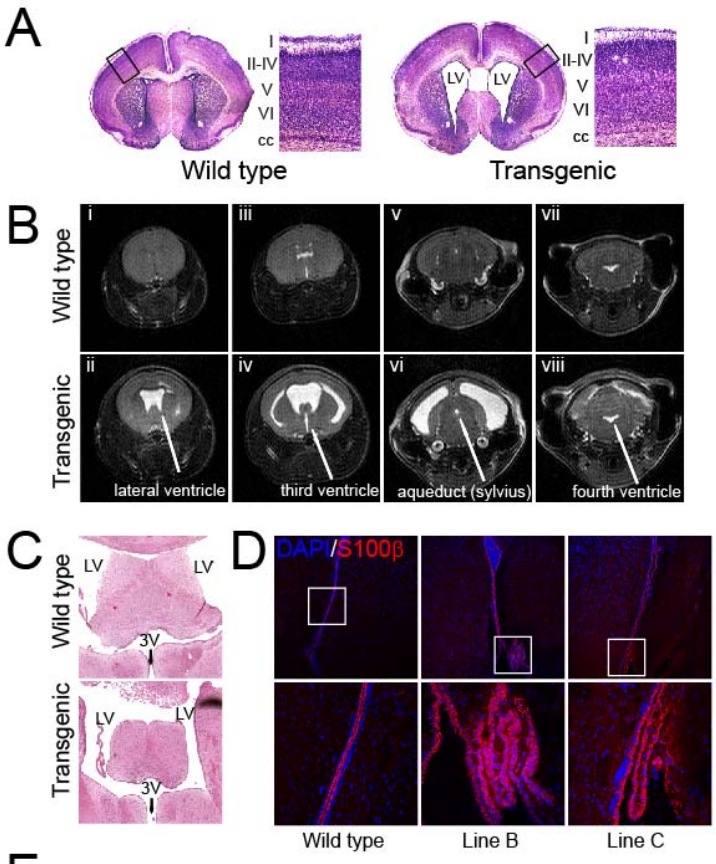

E

Tumor incidence in Bmi-1 transgenic mice

		Age (month)	Brains analyzed: Histology/ IHC	Brains analyzed: Gross examination	Neoplasm: CNS	Neoplasm: Hematopoietic	Neoplasm: Other
Line B	WT	1-4	5	>50	0	0	0
		15-24	0	1	0	1	0
	TG	1-4	5	>50	0	0	0
		15-24	2	0	0	0	0
Line C	WT	1-4	8	>50	0	0	0
		15-24	1	1	0	0	0
	TG	1-4	16	>50	0	0	1
		15-24	3	3	0	3	1

Figure 3.13: A minority of Bmi-1 transgenic mice developed idiopathic hydrocephalus but showed no sign of brain tumors.
A) Representative nissl stains of P5 line C and littermate control brain sections showed enlarged lateral ventricles (LV) in the transgenic brain but a normal laminar organization of the cortex. B) MRI images showed hydrocephalus in adult line C mice: lateral ventricles were enlarged, while the third and fourth ventricles as well as the sylvius aqueduct were relatively normal. C) No physical block was detected between the lateral and third ventricles in H&E stained serial brain sections. D) The ependymal cell layer (S100ß+ cells) in the transgenic mouse brain was abnormally folded in places. E) Bmi-1 over-expressing mice did not develop brain tumors, even when aged for approximately two years. Brains in the "gross examination" column are in addition to those examined by histology. Mice that did not develop hydrocephalus showed no sign of premature death relative to control mice.

BIBLIOGRAPHY

Almqvist, P. M., Mah, R., Lendahl, U., Jacobsson, B., Hendson, G., 2002. Immunohistochemical detection of nestin in pediatric brain tumors. J Histochem Cytochem. 50**,** 147-58.

Bea, S., Tort, F., Pinyol, M., Puig, X., Hernandez, L., Hernandez, S., Fernandez, P. L., van Lohuizen, M., Colomer, D., Campo, E., 2001. BMI-1 gene amplification and overexpression in hematological malignancies occur mainly in mantle cell lymphomas. Cancer Res. 61**,** 2409-12.

Ben-Saadon, R., Zaaroor, D., Ziv, T., Ciechanover, A., 2006. The polycomb protein Ring1B generates self atypical mixed ubiquitin chains required for its in vitro histone H2A ligase activity. Mol Cell. 24**,** 701-11.

Bracken, A. P., Kleine-Kohlbrecher, D., Dietrich, N., Pasini, D., Gargiulo, G., Beekman, C., Theilgaard-Monch, K., Minucci, S., Porse, B. T., Marine, J. C., Hansen, K. H., Helin, K., 2007. The Polycomb group proteins bind throughout the INK4A-ARF locus and are disassociated in senescent cells. Genes Dev. 21**,** 525-30.

Bruggeman, S. W., Hulsman, D., Tanger, E., Buckle, T., Blom, M., Zevenhoven, J., van Tellingen, O., van Lohuizen, M., 2007. Bmi1 controls tumor development in an Ink4a/Arf-independent manner in a mouse model for glioma. Cancer Cell. 12**,** 328-41.

Bruggeman, S. W., Valk-Lingbeek, M. E., van der Stoop, P. P., Jacobs, J. J., Kieboom, K., Tanger, E., Hulsman, D., Leung, C., Arsenijevic, Y., Marino, S., van Lohuizen, M., 2005. Ink4a and Arf differentially affect cell proliferation and neural stem cell self-renewal in Bmi1-deficient mice. Genes Dev. 19**,** 1438-43.

Capela, A., Temple, S., 2002. LeX/ssea-1 is expressed by adult mouse CNS stem cells, identifying them as nonependymal. Neuron. 35**,** 865-875.

Chagraoui, J., Niessen, S. L., Lessard, J., Girard, S., Coulombe, P., Sauvageau, M., Meloche, S., Sauvageau, G., 2006. E4F1: a novel candidate factor for mediating BMI1 function in primitive hematopoietic cells. Genes Dev. 20**,** 2110-20.

Dahlstrand, J., Collins, V. P., Lendahl, U., 1992a. Expression of the class VI intermediate filament nestin in human central nervous system tumors. Cancer Res. 52**,** 5334-41.

Dahlstrand, J., Zimmerman, L. B., McKay, R. D., Lendahl, U., 1992b. Characterization of the human nestin gene reveals a close evolutionary relationship to neurofilaments. J Cell Sci. 103 (Pt 2)**,** 589-97.

Fasano, C. A., Dimos, J. T., Ivanova, N. B., Lowry, N., Lemischka, I. R., Temple, S., 2007. shRNA knockdown of Bmi-1 reveals a critical role for p21-Rb pathway in NSC self-renewal during development. Cell Stem Cell. 1**,** 87-99.

Ferland, R. J., Cherry, T. J., Preware, P. O., Morrisey, E. E., Walsh, C. A., 2003. Characterization of Foxp2 and Foxp1 mRNA and protein in the developing and mature brain. J Comp Neurol. 460**,** 266-79.

Hatten, M. E., 1999. Central nervous system neuronal migration. Annu Rev Neurosci. 22**,** 511-39.

Haupt, Y., Bath, M. L., Harris, A. W., Adams, J. M., 1993. BMI-1 transgene induces lymphomas and collaborates with Myc in tumorigenesis. Oncogene. 8**,** 3161-3164.

Hernandez-Munoz, I., Lund, A. H., van der Stoop, P., Boutsma, E., Muijrers, I., Verhoeven, E., Nusinow, D. A., Panning, B., Marahrens, Y., van Lohuizen, M., 2005. Stable X chromosome inactivation involves the PRC1 Polycomb complex and requires histone MACROH2A1 and the CULLIN3/SPOP ubiquitin E3 ligase. Proc Natl Acad Sci U S A. 102**,** 7635-40.

Hogan, B., Beddington, R., Costantini, F., Lacy, E., Production of transgenic mice. Manipulating the Mouse Embryo: A Laboratory Manual. Cold Spring Harbor Press, Plainview, New York, 1994, pp. 218-252.

Iwama, A., Oguro, H., Negishi, M., Kato, Y., Morita, Y., Tsukui, H., Ema, H., Kamijo, T., Katoh-Fukui, Y., Koseki, H., van Lohuizen, M., Nakauchi, H., 2004. Enhanced self-renewal of hematopoietic stem cells mediated by the polycomb gene product Bmi-1. Immunity. 21**,** 843-51.

Jacobs, J. J., Kieboom, K., Marino, S., DePinho, R. A., van Lohuizen, M., 1999a. The oncogene and Polycomb-group gene bmi-1 regulates cell proliferation and senescence through the ink4a locus. Nature. 397**,** 164-8.

Jacobs, J. J. L., Scheijen, B., Voncken, J.-W., Kieboom, K., Berns, A., von Lohuizen, M., 1999b. Bmi-1 collaborates with c-Myc in tumorigenesis by inhibiting c-Myc-induced apoptosis via INK4a/ARF. Genes and Development. 13**,** 2678-2690.

Kawaguchi, A., Miyata, T., Sawamoto, K., Takashita, N., Murayama, A., Akamatsu, W., Ogawa, M., Okabe, M., Tano, Y., Goldman, S. A., Okano, H., 2001. Nestin-EGFP transgenic mice: visualization of the self-renewal and multipotency of CNS stem cells. Molecular and Cellular Neuroscience. 17**,** 259-273.

Kiel, M. J., He, S., Ashkenazi, R., Gentry, S. N., Teta, M., Kushner, J. A., Jackson, T. L., Morrison, S. J., 2007. Haematopoietic stem cells do not asymmetrically segregate chromosomes or retain BrdU. Nature. 449**,** 238-42.

Lee, H., Song, J. J., Kim, E., Yun, C. O., Choi, J., Lee, B., Kim, J., Chang, J. W., Kim, J. H., 2001. Efficient gene transfer of VSV-G pseudotyped retroviral vector to human brain tumor. Gene Ther. 8**,** 268-73.

Lessard, J., Sauvageau, G., 2003. Bmi-1 determines the proliferative capacity of normal and leukaemic stem cells. Nature. 423**,** 255-60.

Leung, C., Lingbeek, M., Shakhova, O., Liu, J., Tanger, E., Saremaslani, P., Van Lohuizen, M., Marino, S., 2004. Bmi1 is essential for cerebellar development and is overexpressed in human medulloblastomas. Nature. 428**,** 337-41.

Lothian, C., Lendahl, U., 1997. An evolutionarily conserved region in the second intron of the human nestin gene directs gene expression to CNS progenitor cells and to early neural crest cells. Eur J Neurosci. 9**,** 452-62.

Lowe, S. W., Sherr, C. J., 2003. Tumor suppression by Ink4a-Arf: progress and puzzles. Current Opinion in Genetics & Development. 13**,** 77-83.

Molofsky, A. V., He, S., Bydon, M., Morrison, S. J., Pardal, R., 2005. Bmi-1 promotes neural stem cell self-renewal and neural development but not mouse growth and survival by repressing the p16Ink4a and p19Arf senescence pathways. Genes Dev. 19**,** 1432-7.

Molofsky, A. V., Pardal, R., Iwashita, T., Park, I. K., Clarke, M. F., Morrison, S. J., 2003. Bmi-1 dependence distinguishes neural stem cell self-renewal from progenitor proliferation. Nature. 425**,** 962-7.

Nieto, M., Monuki, E. S., Tang, H., Imitola, J., Haubst, N., Khoury, S. J., Cunningham, J., Gotz, M., Walsh, C. A., 2004. Expression of Cux-1 and Cux-2 in the subventricular zone and upper layers II-IV of the cerebral cortex. J Comp Neurol. 479**,** 168-80.

Nishino, J., Kim, I., Chada, K., Morrison, S. J., 2008. Hmga2 promotes neural stem cell self-renewal in young but not old mice by reducing p16Ink4a and p19Arf Expression. Cell. 135**,** 227-39.

Park, I. K., Qian, D., Kiel, M., Becker, M. W., Pihalja, M., Weissman, I. L., Morrison, S. J., Clarke, M. F., 2003. Bmi-1 is required for maintenance of adult self-renewing haematopoietic stem cells. Nature. 423**,** 302-5.

Pear, W. S., Nolan, G. P., Scott, M. L., Baltimore, D., 1993. Production of high-titer helper-free retroviruses by transient transfection. Proc. Natl. Acad. Sci. U.S.A. 90**,** 8392-8396.

Polleux, F., Dehay, C., Kennedy, H., 1997. The timetable of laminar neurogenesis contributes to the specification of cortical areas in mouse isocortex. J Comp Neurol. 385**,** 95-116.

Rutka, J. T., Ivanchuk, S., Mondal, S., Taylor, M., Sakai, K., Dirks, P., Jun, P., Jung, S., Becker, L. E., Ackerley, C., 1999. Co-expression of nestin and vimentin intermediate filaments in invasive human astrocytoma cells. Int J Dev Neurosci. 17**,** 503-15.

Sherr, C. J., DePinho, R. A., 2000. Cellular senescence: mitotic clock or culture shock? Cell. 102**,** 407-10.

Singec, I., Knoth, R., Meyer, R. P., Maciaczyk, J., Volk, B., Nikkhah, G., Frotscher, M., Snyder, E. Y., 2006. Defining the actual sensitivity and specificity of the neurosphere assay in stem cell biology. Nat Methods. 3**,** 801-6.

Song, L. B., Zeng, M. S., Liao, W. T., Zhang, L., Mo, H. Y., Liu, W. L., Shao, J. Y., Wu, Q. L., Li, M. Z., Xia, Y. F., Fu, L. W., Huang, W. L., Dimri, G. P., Band, V., Zeng, Y. X., 2006. Bmi-1 is a novel molecular marker of nasopharyngeal carcinoma progression and immortalizes primary human nasopharyngeal epithelial cells. Cancer Res. 66**,** 6225-32.

Soriano, E., Del Rio, J. A., 2005. The cells of cajal-retzius: still a mystery one century after. Neuron. 46**,** 389-94.

Stemple, D. L., Anderson, D. J., 1992. Isolation of a stem cell for neurons and glia from the mammalian neural crest. Cell. 71**,** 973-85.

Tateishi, K., Ohta, M., Kanai, F., Guleng, B., Tanaka, Y., Asaoka, Y., Tada, M., Seto, M., Jazag, A., Lianjie, L., Okamoto, M., Isayama, H., Yoshida, H., Kawabe, T., Omata, M., 2006. Dysregulated expression of stem cell factor Bmi1 in precancerous lesions of the gastrointestinal tract. Clin Cancer Res. 12**,** 6960-6.

Valk-Lingbeek, M. E., Bruggeman, S. W., van Lohuizen, M., 2004. Stem cells and cancer; the polycomb connection. Cell. 118**,** 409-18.

van der Lugt, N. M., Domen, J., Linders, K., van Roon, M., Robanus-Maandag, E., te Riele, H., van der Valk, M., Deschamps, J., Sofroniew, M., van Lohuizen, M., et al., 1994. Posterior transformation, neurological abnormalities, and severe hematopoietic defects in mice with a targeted deletion of the bmi-1 proto-oncogene. Genes Dev. 8**,** 757-69.

van Lohuizen, M., Verbeek, S., Scheijen, B., Wientjens, E., van der Gulden, H., Berns, A., 1991. Identification of cooperating oncogenes in E mu-myc transgenic mice by provirus tagging. Cell. 65**,** 737-52.

Van Parijs, L., Refaeli, Y., Lord, J. D., Nelson, B. H., Abbas, A. K., Baltimore, D., 1999. Uncoupling IL-2 signals that regulate T cell proliferation, survival, and Fas-mediated activation-induced cell death. Immunity. 11**,** 281-8.

Vonlanthen, S., Heighway, J., Altermatt, H. J., Gugger, M., Kappeler, A., Borner, M. M., van Lohuizen, M., Betticher, D. C., 2001. The bmi-1 oncoprotein is differentially expressed in non-small cell lung cancer and correlates with INK4A-ARF locus expression. Br J Cancer. 84**,** 1372-6.

Wang, H., Pan, K., Zhang, H. K., Weng, D. S., Zhou, J., Li, J. J., Huang, W., Song, H. F., Chen, M. S., Xia, J. C., 2007. Increased polycomb-group oncogene Bmi-1 expression correlates with poor prognosis in hepatocellular carcinoma. J Cancer Res Clin Oncol.

Zencak, D., Lingbeek, M., Kostic, C., Tekaya, M., Tanger, E., Hornfeld, D., Jaquet, M., Munier, F. L., Schorderet, D. F., van Lohuizen, M., Arsenijevic, Y., 2005. Bmi1 loss produces an increase in astroglial cells and a decrease in neural stem cell population and proliferation. J Neurosci. 25**,** 5774-83.

CHAPTER 4

SOX17 IS SUFFICIENT TO CONFER SELF-RENEWAL POTENTIAL AND FETAL CHARACTERISTICS TO ADULT HEMATOPOIETIC PROGENITOR CELLS[1]

SUMMARY

Fetal liver hematopoiesis represents a unique stage of hematopoietic system development that is dominated by definitive erythropoiesis and myelopoiesis. Correspondingly, fetal liver hematopoietic stem cells (HSCs) are distinct from adult bone marrow HSCs in their gene expression, surface marker expression, developmental potential, and self-renewal capacity. While a number of genes have been identified to date to be specifically required for fetal HSC formation and/or maintenance but not adult HSCs; no gene has yet been found to define the unique characteristics of fetal liver HSCs or fetal hematopoiesis. Here we report that *Sox17*, a gene previously shown by us to be specifically expressed by fetal and neonatal HSCs but not adult HSCs, and essential for the maintenance of fetal HSCs, is sufficient to confer fetal properties and stem cell properties upon adult hematopoietic progenitor cells, including enhanced self-renewal potential and fetal gene expression. Furthermore, the hematopoietic reconstitution pattern of *Sox17*-over-expressing adult bone marrow cells exhibited a striking resemblance to fetal liver hematopoiesis, including augmented erythropoiesis and myelopoiesis and diminished lymphoid cell production. Thus, our findings have identified *Sox17* as the

[1] Manuscript in preparation with authors listed as **He, S**., Lim, M.S., Kim, I. and Morrison, S.J.

only gene identified to date that is not only essential for fetal liver HSC maintenance but is also sufficient to confer fetal HSC features to adult cells.

INTRODUCTION

Mammalian hematopoiesis undergoes significant developmental changes during ontogeny. In the developing mouse embryo, two distinct waves of blood cell production occur (Mikkola and Orkin, 2006; Orkin and Zon, 2008). The first wave of blood formation ("primitive hematopoiesis") takes place in the yolk sac of E7 embryos, and is characterized by the production of large, nucleated primitive erythrocytes which express embryonic globin proteins. Primitive hematopoiesis is transient and rapidly replaced by adult ("definitive") hematopoiesis, which originates in the Aorta-Gonad-Mesonephros (AGM) region of the E8.5 mouse embryo. Shortly after, the HSCs that arise in the AGM migrate into the fetal liver, the major site of hematopoiesis within the developing embryo. Fetal liver hematopoiesis differs from both primitive hematopoiesis and adult bone marrow hematopoiesis by the predominant production of definitive erythrocytes (enucleated red cells expressing adult type hemoglobin) and the unbalanced production of myeloid vs. lymphoid cells. During late embryonic to early postnatal development, adult hematopoiesis is established by the migration of hematopoietic stem and progenitor cells from fetal liver to bone marrow. Adult hematopoiesis is characterized by balanced erythroid, myeloid and lymphoid cell production.

Parallel to the changes that occur in hematopoiesis during the fetal to adult transition, fetal liver hematopoietic stem cells (HSCs) are distinct from adult HSCs in gene expression (Ivanova et al., 2002; Kiel et al., 2005a; Phillips et al., 2000), surface

marker expression (Jordan and Lemischka, 1990; Kim et al., 2005; Morrison et al., 1995), developmental potential (Bowie et al., 2007; Ikuta et al., 1990; Kantor et al., 1992) as well as self-renewal capability (Bowie et al., 2007; Harrison et al., 1997; Morrison et al., 1995). A number of genes have been identified that differentially regulate the function and/or maintenance of fetal and adult HSCs. *Scl* (Mikkola et al., 2003; Porcher et al., 1996; Robb et al., 1996; Shivdasani et al., 1995), *Aml-1/Runx1* (Ichikawa et al., 2004; Okuda et al., 1996a; Wang et al., 1996) and *Sox17* (Kim et al., 2007) are required for the formation and/or maintenance of fetal liver HSCs but are dispensable for the function of adult HSCs. In contrast, several transcriptional regulators including *Gfi-1*(Hock et al., 2004a), *Tel/Etv6* (Hock et al., 2004a), and *Bmi-1*(Park et al., 2003b) maintain adult but not fetal HSCs. However to our knowledge, no gene has yet been shown to be sufficient to determine HSC identity. Such gene(s), if they exist, should meet three criteria: their expression should be restricted to HSCs at a certain stage of development, they should be required for the function/maintenance of HSCs at a certain stage of development, and when overexpressed they should be sufficient to confer developmental stage-specific HSC properties. Using these criteria, we report that *Sox17* is a critical determinant of fetal HSC identity.

Sox17 is a member of sub-group F of the Sry-related high mobility group box (Sox) transcription factors, and was originally considered a marker of endodermal identity (Yasunaga et al., 2005). It is required for the formation and maintenance of definitive endoderm (Hudson et al., 1997; Kanai-Azuma et al., 2002; Niakan et al., 2010) and vascular endothelium (Matsui et al., 2006) *in vivo*. We have previously shown that within the hematopoietic system *Sox17* expression is temporally restricted to fetal and

neonatal, but not adult, HSCs (Kim et al., 2007); Sox17 expression correlates with fetal HSC characteristics during their transition from fetal to adult HSCs in terms of both immunophenotype and cell cycle status. Germline loss of *Sox17* leads to severe defects in definitive hematopoiesis in the fetal liver, including a complete absence of definitive HSCs, while conditional deletion of *Sox17* leads to the loss of fetal and neonatal but not adult HSCs (Kim et al., 2007). This indicates *Sox17* is essential for the function/maintenance of fetal but not adult HSCs.

To test whether re-introducing Sox17 expression into adult mouse hematopoietic cells is sufficient to confer fetal HSC identity, including enhanced self-renewal potential and fetal specific gene expression, we overexpressed *Sox17* in adult mouse hematopoietic cells by retroviral infection and followed their fate after transplantation into lethally irradiated recipients. *Sox17* overexpression was sufficient to enhance the long-term reconstituting potential of adult bone marrow progenitors and to confer self-renewal capacity to certain types of early hematopoietic progenitors. In addition, *Sox17*-over-expressing adult progenitors expressed several fetal specific cell surface markers and exhibited global upregulation of fetal HSC genes. Meanwhile, *Sox17*-over-expressing hematopoietic cells exhibited biased differentiation characterized by augmented erythroid and myeloid production at the expense of lymphoid cells, and produced platelet and myeloid cells with fetal characteristics. Together, our data identify *Sox17* as the only gene known to date that is sufficient to control the developmental identity of HSCs.

RESULTS

Sox17 expression levels decline with fetal development and differentiation

To better understand the role of *Sox17* in regulating fetal liver hematopoiesis, we examined the detailed expression pattern of *Sox17* in HSCs and various types of hematopoietic progenitors at embryonic day (E)13.5 and at birth (P0) using *Sox17-GFP* knock-in mice (Kim et al., 2007). In this mouse, endogenous *Sox17* coding sequence was replaced by an enhanced green fluorescence protein (EGFP), which can be used to track the endogenous level of *Sox17* expression during development. Similar to what we reported previously (Kim et al., 2007), Sox17-GFP expression is restricted to fetal liver HSCs and early hematopoietic progenitors as no GFP expression was observed in lineage positive cells or in adult HSCs or progenitor cells (data not shown). Interestingly the Sox17-GFP expression level was highest in $CD150^{+}CD48^{-}CD41^{-}Lin^{-}Sca\text{-}1^{+}cKit^{+}$ ($LSK150^{+}48^{-}41^{-}$) HSCs and $CD150^{-}CD48^{-}CD41^{-}Lin^{-}Sca1^{+}cKit^{+}$ ($LSK150^{-}48^{-}41^{-}$) cells at both developmental stages examined. As HSCs differentiated toward the myeloid lineage ($Lin^{-}Sca^{-}1\text{-}cKit^{+}$), Sox17-GFP expression progressively decreased (Figure 4.1). On the other hand, Sox17-GFP expression by P0 fetal liver HSCs and hematopoietic progenitors was significantly lower than by their E13.5 counterparts, such that Sox17-GFP expression could only be detected on the more immature LSK cells at P0 but no longer on the myeloid progenitors (Figure 4.1). Together, these data indicate that *Sox17* expression is tightly correlated with both the fetal state and the undifferentiated stem cell state, raising the possibility that *Sox17* is not only essential for fetal liver HSC maintenance but is also essential to specify fetal characteristics. To test this, we decided to examine whether *Sox17* overexpression confers fetal or stem cell characteristics to adult hematopoietic progenitors.

Overexpression of *Sox17* in adult bone marrow cells enhances their long-term reconstituting potential, and biases lineage differentiation

To directly test whether re-introducing *Sox17* expression in adult hematopoietic cells is sufficient to confer fetal characteristics, we used retrovirus to over-express *Sox17* in adult hematopoietic cells and followed their fate after transplantation. Two *Sox17*-expressing retrovirus vectors were constructed by inserting full length or C-terminal his-tagged *Sox17* cDNA into the murine stem cell virus (MSCV) based pMIG (MSCV-GFP) vector (Van Parijs et al., 1999) immediately upstream of the internal ribosomal entry site (IRES) followed by EGFP. This allowed for the tracking of viral infected cells and their progeny *in vivo*. Western blotting of control (MSCV-GFP) and Sox17 virus (MSCV-Sox17 and MSCV-Sox17his) infected 3T3 cells confirmed the presence of ectopic Sox17 protein expression (Figure 4.2A). Quantitative RT-PCR comparing Sox17 virus infected primary hematopoietic cells with E16.5 fetal liver HSCs showed 800 to 950 fold *Sox17* expression over the endogenous level at this developmental stage (Figure 4.2B).

One million control (MSCV-GFP) or Sox17 (MSCV-Sox17 and MSCV-Sox17his) retrovirus infected CD45.1 whole bone marrow cells from 8 week-old young adult mice were transplanted into lethally irradiated CD45.1 recipients along with 200,000 recipient cells for radioprotection, and peripheral blood chimerism was monitored for up to 16 weeks post transplantation (Figure 4.3A-F). Peripheral blood leukocytes, erythrocytes and platelets derived from virus infected donor cells could be reliably identified using flow cytometry, based on EGFP expression (Figure 4.4). Compared with control virus infected cells, bone marrow cells infected with *Sox17* virus generated significantly higher levels of peripheral blood myeloid, erythroid, and platelet

reconstitution at 16 week post transplantation (Figure 4.3, A, B, E, F). And more recipients that received *Sox17*-overexpressing cells showed long-term myeloid (9 of 9 for MSCV-Sox17 and 8 of 9 for MSCV-Sox17his) and erythroid (9 of 9 for MSCV-Sox17 and 9 of 9 for MSCV-Sox17his) reconstitution than controls (5 of 14 for myeloid and 9 of 14 for erythroid only) (Figure 4.3G). These results indicate that *Sox17* overexpression significantly enhanced the long-term reconstitution potential of adult bone marrow cells.

In contrast to the augmented myeloerythroid reconstitution by *Sox17*-overexpressing cells, lymphoid reconstitution by *Sox17*-overexpressing cells generally did not significantly differ from the control virus infected cells (Figure 4.3C, D), suggesting *Sox17* overexpression may bias the balance between lymphoid and myeloid cells in the peripheral blood. Indeed, the ratio of GFP^+ donor-derived peripheral blood lymphoid versus myeloid cells was significantly reduced in the recipients of *Sox17*-overexpresing bone marrow cells at both 4 and 16 weeks after transplantation (Figure 4.3H), indicating *Sox17* overexpression may either enhance the production or survival of myeloid cells or suppress the production or survival of lymphoid cells. Intriguingly, despite the robust contribution of *Sox17*-overexpressing cells to the platelet compartment in the peripheral blood, the overall platelet counts were significantly reduced in all primary recipients of *Sox17* virus infected cells (Figure 4.5A). This was accompanied by the appearance of large reticulated platelets in the peripheral blood (Figure 4.5B), resembling platelets derived from fetal liver megakaryocytes (Tober et al., 2007). Meanwhile, the number of reticulocytes was also elevated in the peripheral blood of *Sox17*-overexpressing cell recipients, indicative of augmented erythropoiesis (Figure 4.5B). Together, these data indicated that *Sox17* overexpression was shifting adult

hematopoiesis to a more fetal phenotype, including augmented myeloerythropoiesis, suppressed lymphopoiesis and production of platelets with fetal characteristics. On the other hand, we did not observe a dramatic increase in circulating nucleated erythrocyte numbers, indicating *Sox17* overexpression did not seem to revert definitive erythropoiesis to primitive erythropoiesis.

To understand what mechanisms might contribute to the observed changes in the peripheral blood reconstitution pattern after *Sox17* overexpression, we analyzed the hematopoietic tissues of primary recipients at 16 weeks post transplantation. In comparison to control recipients, the spleen of the primary recipients reconstituted with *Sox17*-overexpressing cells were significantly enlarged (Figure 4.6 A, B), while the thymus was decreased (Figure 4.6A). This translated into a mild but not significant increase in spleen cellularity and a decrease in thymus cellularity (Figure 4.6C). GFP^+ donor cell chimerism was highly variable in primary recipients, with a statistically insignificant increase in the recipients of *Sox17*-overexpressing cells (Figure 4.7A). A detailed analysis of the lineage compositions of GFP^+ donor cells in the bone marrow and spleen of primary recipients showed that the frequency of Mac-1^+ immature myeloid cells generated by *Sox17*-overexpressing cells was not significantly different from controls (Figure 4.6D, H, I). However, Gr-1 expression on the myeloid cells was significantly reduced (Figure 4.6D), similar to what was found on Mac-1^+ myeloid cells in E12 fetal liver (Figure 4.7B). The frequency of $CD41^+$ megakaryocytic cells in GFP^+ donor-derived cells was significantly increased in both bone marrow and spleen as a result of *Sox17* overexpression, and CD41 expression showed a inverse correlation with ckit (Figure 4.6D), similar to what had been observed on E12 fetal liver $CD41^+$

megakaryocytic cells (Figure 4.7B). The frequency of Ter119$^+$ erythroid cells did not differ between control and *Sox17*-overexpressing donor derived GFP$^+$ cells in the bone marrow (Figure 4.6H), however, it was significantly increased in the spleen of primary recipients that received *Sox17*-overexpressing cells (Figure 4.6E, I), indicating augmented extramedullary erythropoiesis. On the other hand, we did not detect a significant increase in the transcription of embryonic hemoglobins in the *Sox17*-overexpressing erythroid progenitor cells (data not shown), further supporting the conclusion that *Sox17* overexpression did not promote primitive erythropoiesis. In contrast to the normal level or augmented myeloerythroid cell production by *Sox17*-overexpressing cells, the frequencies of B220$^+$ B-cells and CD4$^+$ or CD8$^+$ T-cells produced by *Sox17*-overexpressing cells in both bone marrow and spleen of the primary recipients were significantly reduced as compared to controls (Figure 4.6F-I), indicating suppressed lymphopoiesis as a result of *Sox17* overexpression.

To independently confirm these findings, we also analyzed a strain of *Sox17* transgenic mice (Otet-Sox17/Rosa-rtTA) in which ectopic *Sox17* expression in all tissues can be induced by administration of doxycycline (Park et al., 2006). For unknown reasons, all *Sox17* transgenic mice died within 7 days after Doxycycline administration, restricting the analysis of hematopoietic cells to only short-term *Sox17* overexpression. Nevertheless, within 6 days after the induction of transgene expression, we observed a progressive and significant decrease in thymus weight and cellularity (Figure 4.8A, B), a progressive increase in peripheral blood neutrophil count (Figure 4.8C) and a significantly decrease in peripheral blood platelet count (Figure 4.8C). As a result, the peripheral blood lymphoid vs. myeloid cell ratio was significantly reduced starting from

4 days after transgene induction (Figure 4.8D). A detailed analysis of the lineage composition of the transgenic mouse bone marrow, spleen and thymus at 2, 4 and 6 days after transgene induction revealed a significant increase in Mac-1^+ myeloid cell frequency in the bone marrow and spleen and progressive downregulation of Gr-1 expression on the Mac-1^+ cells in bone marrow (compare the frequency of Mac-1^+ cells with Mac-1^+Gr-1^+ cells; Figure 4.8E, F). In contrast, the frequency of $B220^+$ B cells in bone marrow was significantly reduced after transgene expression with reductions of both mature ($B220^+sIgM^+$) and immature B-cells ($B220^+sIgM^-$). Development of T-cells was also affected as the frequency of $CD4^+CD8^+$ double positive cells in the thymus was significantly reduced after 6 days of transgene induction while the corresponding single positive T-cell frequency was relatively increased (Figure 4.8G). All of these findings are similar to the phenotypes observed in the primary recipients reconstituted with *Sox17*-overexpressing hematopoietic cells (Figure 4.3&4.6). On the other hand, we failed to observe any consistent increase in erythroid or megakaryocytic cell frequency in the hematopoietic tissues of the *Sox17* transgenic mice (Figure 4.8. E, F). This is most likely due to the very short time of transgene expression by which time the expansion of erythroid and megakaryocytic cells may not yet be apparent. Similarly, the short period of transgene induction may also explain the absence of reduced lymphocyte frequency in the spleen due to their long overall life span.

Together, these data indicate that *Sox17* overexpression leads to an expansion of myeloerythroid cells in primary recipients at the cost of lymphoid differentiation, which shares striking similarity to normal fetal liver hematopoiesis. In addition, *Sox17* overexpression appears to be able to modify the surface phenotype and/or differentiation

pattern of myeloid and megakaryocytic cells, leading to the production of platelets and myeloid cells possessing certain fetal-like characteristics.

Sox17 overexpression confers fetal characteristics to adult HSPCs

To test the direct effects of *Sox17* overexpression on hematopopoietic stem and/or progenitor cells (HSPCs), we analyzed the frequency and surface phenotype of donor derived GFP^+ HSCs ($Lineage^-Sca1^+cKit^+CD150^+CD48^-CD41^-$) and the HSPC-enriched $lineage^-cKit^+Sca1^+CD41^-$ ($LSK41^-$) cells in primary recipients 16 weeks after transplantation. In comparison to controls, *Sox17* overexpression led to a significant expansion of $LSK41^-$ cells in the bone marrow and spleen of primary recipients of MSCV-Sox17 virus infected bone marrow cells (Figure 4.9A, B). A similar expansion of $LSK41^-$ cells was also observed in the spleen but not bone marrow of recipients reconstituted with MSCV-Sox17his virus infected bone marrow cells (Figure 4.9B). Intriguingly, detailed examination of the *Sox17*-overexpressing $LSK41^-$ cells revealed that they were predominantly $CD48^+$. As a result, the frequency of cells with an HSC surface marker phenotype was actually depleted in both bone marrow and spleen of recipients of *Sox17*-overexpressing cells as compared to control recipients (Figure 4.9A, B). This observation may either indicate a loss of functional HSCs or reflect a change in HSC surface marker expression. Similarly, we observed a significant increase in $LSK41^-$ cell frequency in both bone marrow and spleen of Otet-*Sox17*/Rosa-rtTA mice after 6 days of transgene expression; however the frequency of cells with HSC surface marker phenotype in these mice remained unchanged at this time (Figure 4.8H). It is so far unclear whether the absence of HSC depletion in *Sox17* transgenic mice was due to the

short period of transgene expression (6 days vs. 16-weeks), or due to different levels of *Sox17* overexpression between these two systems.

Interestingly, *Sox17*-overexpressing LSK41$^-$ cells expressed higher levels of the HSC specific markers Tie-2 and ESAM as compared to the control LSK41$^-$ cells (Figure 4.9C), and they re-expressed the fetal HSC specific markers VE-cadherin and CD93 (AA4.1) (Figure 4.9C), indicating *Sox17* overexpression was sufficient to upregulate certain fetal and/or HSC specific markers on adult hematopoietic progenitor cells.

To directly address the question of whether the expanded LSK48$^+$41$^-$ cell population in *Sox17*-overexpressing cell recipients contained HSC activity, we transplanted 200,000 control or *Sox17*-overexpressing whole bone marrow cells or 50 purified GFP$^+$ *Sox17*-overexpressing LSK48$^+$41$^-$ cells from primary recipients into lethally irradiated secondary recipients together with 200,000 cells for radioprotection. The vast majority of recipients that received 50 GFP$^+$ *Sox17*-overexpressing LSK48$^+$41$^-$ cells contained variable levels of long-term myeloid (14/15 recipients) and/or erythroid (14/15 recipients) donor cell reconstitution at 16- week post transplantation (Figure 4.10B, C), suggesting the *Sox17*-overexpressing LSK48$^+$41$^-$ cells possessed long-term reconstituting potential. This result raised two possibilities. One was that *Sox17* overexpression was sufficient to confer self-renewal potential to adult bone marrow LSK48$^+$41$^-$ cells. The other suggested *Sox17*-overexpressing bone marrow HSCs might simply have changed their surface phenotype to express CD48.

Overexpression of *Sox17* in purified short-term adult hematopoietic progenitors is sufficient to confer long-term self-renewal potential

To test whether overexpression of *Sox17* in purified adult bone marrow short-term hematopoietic progenitor cells can directly confer long-term self-renewal potential, we infected adult bone marrow multipotent progenitors (MPPs, $Lin^-Sca\text{-}1^+cKit^+CD150^-CD48^-CD41^-$), LSKCD48$^+$CD41$^-$ cells (LSK48$^+$41$^-$), granulocyte-monocyte progenitors (GMPs, $Lin^-Sca\text{-}1^-cKit^+CD41^-Fc\gamma R^+$) and megakaryocytic-erythroid progenitors (Pre-MegEs, $Lin^-Sca\text{-}1^-cKit^+CD41^-CD150^+CD105^-$) with MSCV-GFP or MSCV-Sox17 virus and tested their self-renewal potential in long-term reconstitution assays. Bone marrow HSCs were also infected in parallel to serve as a positive control (see Figure 4.11 for sorting strategy and the rate of retroviral infection for each population). HSCs, MPPs and LSK48$^+$41$^-$ cells together comprise the undifferentiated LSK cell population. We have previously shown that MPPs are capable of short-term (up to 8 week) multilineage reconstitution but lack HSC activity (Kiel et al., 2005b; Kiel et al., 2008).

In this study, we experimentally determined the developmental potential of adult bone marrow LSK48$^+$41$^-$ cells by transplanting 100, 500 or 2500 double sorted cells from UBC-GFP mice (CD45.2) into 600rad sublethally irradiated CD45.1 recipients and monitoring their peripheral blood reconstitution for up to 16 weeks. On the population level, adult LSK48$^+$41$^-$ cells were capable of multilineage reconstitution similar to MPPs, however their myeloid and platelet reconstitution only lasted for 3 weeks, indicating they were less primitive than, and likely downstream of, MPPs (Figure 4.12). GMPs and pre-MegEs are both bi-potent short-term progenitors downstream of LSK cells, which are

specific for the monocytic-granulocytic and megakaryocytic-erythroid lineage respectively (Akashi et al., 2000; Pronk et al., 2007).

Transplantation of 500 to 2000 control virus infected MPPs or LSK48^{+}41^{-} cells failed to generate significant myeloid reconstitution in any recipients at 16 weeks post transplantation (0 of 13 and 0 of 20 respectively, Figure 4.13 A-C). Similarly, only one recipient of control virus infected MPPs showed a low level of long-term erythroid reconstitution (1 of 13, Figure 4.13B, C) while control virus infected LSK48^{+}41^{-} cells gave no long-term erythroid reconstitution (0 of 20, Figure 4.13A, C). In contrast, 5 of 15 recipients of Sox17 virus infected MPPs and 3 of 22 recipients of Sox17 virus infected LSK48^{+}41^{-} cells showed variable levels of myeloid reconstitution at 16 weeks post transplantation, and 6 of 15 recipients of Sox17 virus infected MPPs and 9 of 22 recipients of Sox17-virus infected LSK48^{+}41^{-} cells exhibited robust long-term erythroid reconstitution (Figure 4.13A-C). These data indicated that *Sox17* overexpression in some types of short-term progenitors such as MPPs and LSK48^{+}41^{-} cells could indeed confer long-term reconstitution potential. On the other hand, we have so far been unable to confer long-term reconstitution potential to more differentiated progenitors, such as GMPs and Pre-MegEs by overexpression of *Sox17* (Figure 4.14B, C). One possibility is that there are intrinsic differences among different progenitors that determine whether they can be affected by *Sox17* overexpression; another possibility is that the culture conditions used during viral infection are suboptimal for these progenitors such that they rapidly differentiate into mature progeny before sufficient numbers of progenitors get infected.

To test whether Sox17 virus infected HSCs, MPPs and LSK48^{+}41^{-} cells resulted in a similar or different hematopoietic reconstitution pattern in primary recipients, we sacrificed a subset of recipient mice from each group 16 weeks post transplantation and examined the lineage composition of donor derived GFP^{+} cells in bone marrow and spleen. Similar to what had been observed in the recipients of Sox17 virus infected whole bone marrow cells, we saw a similar expansion of CD41^{+} megakaryocytic cells in the bone marrow and spleen, decreased Gr-1 expression on Mac-1^{+} myeloid cells, and a global depletion of B and T lymphoid cells (Figure 4.15A and data not shown). More importantly, we saw a similar expansion of LSK48^{+}41^{-} cells and the depletion of cells with adult HSC phenotype in the recipients of all three populations (Figure 4.15B). These data indicated that irrespective of the starting population, *Sox17* overexpression appeared to be able to convert multipotent hematopoietic progenitors into a common type of progenitor with fetal characteristics and the capacity to give long-term reconstitution.

Sox17 overexpression upregulates genes associated with stem cell and fetal characteristics.

To understand what molecular changes took place in the hematopoietic stem and/or progenitor cells after *Sox17* overexpression, we performed microarray analysis to compare the whole genome transcriptome of freshly isolated adult bone marrow LSK48^{+}41^{-} cells with *Sox17*-overexpressing LSK48^{+}41^{-} cells isolated from reconstituted primary recipients at 16 weeks post transplantation.

We first performed gene set enrichment analysis (GSEA) to compare *Sox17*-overexpressing and control bone marrow LSK48^{+}41^{-} cells using customized gene sets that are specific to adult HSCs (genes that are upregulated at least 2-fold in HSCs as

compared to adult bone marrow LSK48^{+}41^{-} cells, $p<0.05$), differentiating progenitors (genes that are upregulated at least 2-fold in adult LSK48^{+}41^{-} cells as compared to HSCs, $p<0.05$), or fetal liver HSCs (genes that are upregulated at least 2 fold in E16.5 fetal liver HSCs as compared to adult HSCs), to see whether *Sox17* overexpression could lead to global changes in gene expression that resemble adult or fetal HSCs. We observed a strong correlation between genes that were upregulated after *Sox17* overexpression with genes that were HSC-specific (Figure 4.16A), as well as a strong correlation between genes that were downregulated after *Sox17* overexpression with genes that were upregulated during HSC differentiation (Figure 4.16B). We also observed a statistically significant correlation between genes upregulated by *Sox17* overexpression with genes that were preferentially expressed by fetal but not adult HSCs (Figure 4.16C). These results were supported by repeating the GSEA profiling using independent gene sets retrieved from the Broad Institute web site (Figure 4.17A), as well as by detailed analysis of the significantly changed genes (fold change>2, $p<0.05$) after *Sox17* overexpression (described below).

In total, we found 376 and 264 genes which were significantly upregulated and downregulated as the result of *Sox17* overexpression. Within the 376 upregulated genes, 88 were significantly upregulated in adult HSCs as compared to normal LSK48^{+}41^{-} cells, compared to only 7 genes that exhibited the opposite expression pattern (Figure 4.16D). On the other hand, while about equal numbers of genes in the upregulated list were preferentially expressed by fetal or adult HSCs (27/376 and 31/376 respectively, Figure 4.16D), detailed examination reveals that the most upregulated genes (fold change >5, 78 total) tended to be more enriched in fetal HSCs (16/78, Figure 4.16D) rather than adult

HSCs (4/78, Figure 4.16D). These highly upregulated genes included the known fetal HSC specific marker VE-cadherin (Figure 4.16E). Within the 264 significantly down regulated genes, 112 genes were downregulated in HSCs as compared with LSK48^{+}41^{-} cells while only 12 genes were preferentially expressed by HSCs. Meanwhile, of the 33 top downregulated genes (fold change >5), more were enriched in adult HSCs (12/33) as compared to fetal HSCs (4/33, Figure 4.16D). Together, these data indicate that *Sox17* overexpression upregulated stem cell and fetal specific gene expression, while suppressing genes that are associated with differentiation. However, it is important to note that *Sox17* overexpression did not fully convert adult progenitor cells into HSCs, or completely convert adult progenitors into a fetal phenotype. GSEA profiling comparing *Sox17*-overexpressing LSK48^{+}41^{-} cells with adult HSCs showed that *Sox17*-overexpressing LSK48^{+}41^{-} cells still expressed overall higher levels of differentiation-associated genes (Figure 4.17B), and lower levels of HSC specific genes (Figure 4.17B) than bone marrow HSCs. This was also supported by principle component analysis comparing *Sox17*-overexpressing LSK48^{+}41^{-} cells to wild type fetal and adult HSCs or LSK48^{+}41^{-} cells.

In order to identify which gene(s) may be contributing to the observed phenotype after *Sox17* overexpression, we screened the significantly changed gene list for known regulators of HSCs function or lineage differentiation. Expression of *Mpl*, *Evi-1*, *Gata-2*, *Pbx-1*, *Egr-1* and *Mllt-3* were found to be significantly elevated after *Sox17* overexpression by both microarray and qRT-PCR (Figure 4.16E), all of which are known to be essential positive regulators of HSC maintenance (Alexander et al., 1996; Dobson et al., 1999; Ficara et al., 2008; Goyama et al., 2008; Kimura et al., 1998; Min et al., 2008;

Pina et al., 2008; Tsai et al., 1994). Therefore the upregulation of these genes may explain the enhanced self-renewal potential of *Sox17*-overexpressing cells. In contrast, many significantly downregulated genes after *Sox17* overexpression, including *Rag1*, *Rag2*, *Dntt*, *Ltb*, *Blnk* and *Satb1* (Alimzhanov et al., 1997; Alvarez et al., 2000; Gilfillan et al., 1993; Jumaa et al., 1999; Komori et al., 1993; Koni et al., 1997; Mombaerts et al., 1992; Pappu et al., 1999; Shinkai et al., 1992), are essential for lymphoid differentiation. This may explain the defective lymphopoiesis by *Sox17*-overexpressing cells.

Long-term *Sox17* overexpression leads to development of non-lymphoid leukemia

Given the ability of *Sox17* to enhance the self-renewal potential of HSCs and confer long-term reconstituting potential to MPPs and LSk48^{+}41^{-} cells, we wanted to test whether long-term overexpression of *Sox17* would lead to the development of hematopoietic neoplasms. All primary recipients of MSCV-Sox17 and MSCV-Sox17his virus infected whole bone marrow cells died between 28 and 374 days with features of leukemia (see below), with a median survival time of 171 days after transplantation for MSCV-Sox17 virus recipients, and 303 days after transplantation for MSCV-Sox17his recipients (Figure 4.18A). In contrast, none of the recipients reconstituted with control virus infected bone marrow cells died from leukemia up to 490 days after transplantation. Importantly, when we transplanted whole bone marrow cells isolated from moribund *Sox17*-overexpressing primary recipients into lethally irradiated secondary recipients, all secondary recipients died between 23 and 99 days after transplantation, with a median survival of 59 days for MSCV-Sox17 secondary recipients and 41 days for MSCV-Sox17his secondary recipients, showing a greatly accelerated onset of the disease (Figure 4.18B).

In order to identify what type of hematopoietic neoplasm developed after long-term *Sox17* overexpression, we performed hematological and pathological evaluation of hematopoietic tissues isolated from moribund primary recipients. At the onset of the disease, all affected primary recipients exhibited thrombocytopenia, anemia and/or leukocytosis in peripheral blood, as well as pronounced splenomegaly and/or hepatomegaly. Extensive infiltration of undifferentiated blast cells could be identified in bone marrow, spleen, and liver of the affected mice and sometimes also in lung and lymph nodes, resulting in complete disruption of normal tissue architecture (Figure 4.18C, E). Immunohistochemical staining of paraffin embedded tissue sections showed the blast cells did not expresses the myeloid cell marker Mac-1 or the lymphoid marker CD3 (data not shown), but expressed the megakaryocyte lineage marker Von Willebrand factor (Vwf+, Figure 4.18D). No blast cells were found to express the erythroid marker Ter119 (data not shown), the total amount of erythroid cells at various stages of differentiation identifiable by histology were nonetheless greatly increased in spleen and liver tissue sections, indicating an expansion of erythroid cells in these tissues (Figure 4.18C). Consistent with these findings, flow cytometry revealed the frequency of $CD41^+$ megakaryocytes and/or $Ter119^+$ erythroid cells were greatly expanded in the bone marrow, spleen and/or liver of the affected animals despite (data not shown). In addition, freshly isolated GFP^+CD41^+ cells showed similar morphology to the blast cells, and expressed Vwf (Figure 4.18E, F), indicating they are likely the observed leukemic blast cells found in both tissue sections and cytospin samples.

Together, these data suggested the pathological conditions developed after long-term *Sox17* overexpression were most consistent with the features of nonlymphoid

leukemia with features of megakaryocytic and/or erythroid differentiation as defined in the Bethesda proposals for classification of murine hematopoietic neoplasms (Kogan et al., 2002). This indicates that *Sox17*, like many self-renewal genes, can act as an oncogene when overexpressed in adult hematopoietic cells.

DISCUSSION

In this study, we have shown that *Sox17* expression is restricted to fetal liver HSC and early hematopoietic progenitors during mouse hematopoietic system development, and its expression declines with differentiation and with developmental time (Figure 4.1). Using a retroviral overexpression system, we examined the effect of *Sox17* overexpression on adult bone marrow hematopoietic cells. *Sox17* overexpression was sufficient to enhance the long-term reconstitution potential of adult bone marrow cells (Figure 4.3) which acted at least partially by enhancing the self-renewal potential of HSCs and conferring self-renewal capacity to certain early hematopoietic progenitors (Figure 4.13 and Figure 4.14). *Sox17* also altered their lineage differentiation pattern, which was characterized by augmented erythroid, megakaryocytic and/or myeloid cell production at the expense of lymphoid differentiation (Figure 4.6), and production of myeloid cells and platelets possessing fetal characteristics (Figure 4.5&4.7). Overall, *Sox17* overexpression caused a striking resemblance to fetal liver hematopoiesis. In addition, phenotypic and global gene expression analysis of *Sox17*-overexpressing hematopoietic progenitors revealed upregulation of fetal HSCs specific gene expression (Figure 4.9 and Figure 4.16), indicating *Sox17* overexpression was sufficient to confer at least some fetal characteristics to adult hematopoietic cells. Together, our data suggest

Sox17 is a critical regulator of HSC temporal identity, making it the only gene known to date that controls the distinction between fetal and adult HSC identity.

Interestingly, long-term overexpression of *Sox17* in adult hematopoietic progenitor cells led to the development of lethal, transplantable, nonlymphoid leukemias, emphasizing the importance of terminating the fetal transcriptional program during adult development, as well as pointing to *Sox17* as a potential oncogene involved in hematopoietic neoplasm development.

The observation that endogenous *Sox17* expression in fetal liver HSCs declines with age is intriguing, as it suggests intrinsic changes may already take places in fetal liver HSCs before their transition into adult HSCs between 3 to 4 weeks of age after birth (Bowie et al., 2007; Bowie et al., 2006). This suggests that either the reduction of *Sox17* expression in fetal liver HSCs does not result in any functional consequences, or there are more changes in fetal liver HSCs during late embryonic development than we currently appreciate. Interestingly, one study has shown that certain functional changes already take place in HSCs before 3 weeks of age, which modifies their ability to generate certain types of B cells (Kikuchi and Kondo, 2006). Therefore, it will be interesting to test whether the relative changes in *Sox17* expression level in fetal HSCs could actually control their progressive maturation into adult HSCs.

Although *Sox17* overexpression was capable of conferring certain fetal HSC identities including enhanced self-renewal capacity and expression of fetal-specific gene and surface markers to adult hematopoietic progenitor cells, it was certainly not sufficient to completely convert adult hematopoietic progenitor cells into normal fetal or adult HSCs. This was supported by comparing the global gene expression signature between

Sox17-overexpressing LSK48^{+}41^{-} cells with wild type fetal/adult HSCs or LSK48^{+}41^{-} cells, as *Sox17*-overexpressing cells expressed a combination of fetal and adult HSC-specific genes (Figure 4.16). These results indicated *Sox17* is not the only gene that controls the distinction between fetal and adult HSCs or the differences between fetal and adult hematopoiesis. By studying the subset of HSC-specific or fetal HSC-specific genes that failed to upregulate after *Sox17* overexpression in adult hematopoietic progenitor cells, we may gain more insights into the molecular regulation of fetal and/or HSC identity. Alternatively, it is also possible that adult hematopoietic stem/progenitor cells cannot be fully converted back to their fetal counterparts as limited by epigenetic modifications.

Due to the uncontrolled, ubiquitous expression pattern intrinsic to the retroviral overexpression system, it is so far unclear whether the skewed lineage differentiation phenotype observed after *Sox17* overexpression was due to biased HSC differentiation, or changes in the relative proliferation and/or survival of lineage restricted progenitors or terminally differentiated cells. It is also unclear whether any of the observed phenotypes require continuous *Sox17* overexpression in these cells. To answer these questions, we need to develop tools to specifically overexpress *Sox17* in selected cell populations in a temporally controllable fashion.

Lastly, we observed the development of a rare type of lethal and transplantable nonlymphoid leukemia characterized by accumulation of erythroid cells and CD41^{+}Vwf^{+} undifferentiated blast cells in all major hematopoietic organs after long-term *Sox17* overexpression. This resembled human megakaryoblastic leukemia and erythroid leukemia. Interestingly, the lineage composition of the donor-derived hematopoietic cells

isolated from recipients with leukemia shared strong similarities to donor cells isolated from healthy recipients shortly after transplantation, only with a further expansion of $Ter119^+$ erythroid and/or $CD41^+$ megakaryocytes. This raised the question of whether the appearance of leukemia was just a result of further elevated donor cell reconstitution which failed to maintain normal hematopoiesis, or it actually involved secondary genetic mutations. Another related question is whether the *Sox17* -induced leukemia was dependent on continuous *Sox17* expression. It will also be interesting to test whether dysregulated *Sox17* expression is involved in human megakaryocytic or erythroid leukemia development.

MATERIALS AND METHODS

Mice

C57BL/Ka-Thy-1.1 (CD45.2) and C57BL/Ka-Thy-1.2 (CD45.1) mice were housed in the Unit for Laboratory Animal Medicine at the University of Michigan and all experiments were performed in accordance with protocols approved by the University Committee on the Use and Care of Animals. $(tetO)_7$CMVSox17-IRES-NucEGFP mice (Otet-Sox17 mice) on an FVB background were kindly provided by Dr. Whitsett at Cincinnati Children's Hospital Medical Center. B6.Cg-*Gt(ROSA)26Sor*$^{tm1(rtTA*M2)Jae}$/J mice (Rosa-rtTA mice) and C57BL/6-Tg(UBC-GFP)30Scha/J mice (UBC-GFP mice) were purchased from Jackson laboratory.

Otet-Sox17 mice were crossed with ROSA-rtTA mice to generate doxycycline-inducible double transgenic mice (Otet-Sox17/Rosa-rtA). Transgene expression was

induced by giving 2mg/ml of doxycycline in drinking water starting at 8 week of age. Treated mice were analyzed at 2, 4 and 6 days after transgene induction.

Antibodies and flow cytometry

All primary antibodies used for flow cytometry were purchased from ebiosciences (San Diego, CA), Biolegend (San Diego, CA) or BD biosciences (San Jose, CA) unless otherwise indicated. Alexafluor 700 and PE-TexasRed conjugated streptavidin was purchased from Invitrogen (Carlsbad, CA), FITC-conjugated streptavidin was purchased from Jackson ImmunoResearch Laboratories (West Grove, PA). All flow cytometry was performed on a customized FACSAria II three laser, ten color flow cytometer (Becton-Dickinson, San Jose, California).

For isolating HSCs and hematopoietic progenitor cells from adult mouse bone marrow, bone marrow cells were obtained from both hind limbs, pelvis and vertebrae by crushing the bones with a mortar and pestle, then resuspended in ice-cold staining medium (1x Hank's buffered salt solution without calcium or magnesium, supplemented with 2% heat-inactivated calf serum (Invitrogen)) and filtered through 40μm nylon mesh (Sefar, Depew, NY). Unfractionated bone marrow cells were first enriched by staining with APC-Efluor780 conjugated anti-ckit (2B8), followed by incubation with anti-APC magnetic beads and magnetic selection by autoMACS (Miltenyi, Auburn, CA). The ckit enriched cells were then stained with PE conjugated monoclonal antibodies against CD41 (ebioMWReg30) and lineage markers (CD2, RM2-5; CD3e, 145-2c11; CD5, 53-7.3; CD8a, 53-6.7; B220, RA3-6B2; Gr-1, RB6-8C5; Ter-119 and CD127, A7R34), PE-Cy5 conjugated anti-CD150 (TC15-12F12.2, Biolegend), PE-Cy7 conjugated anti-Sca-1 (E13-161.7), Alexafluor 700 conjugated anti-CD16/32 (93), biotin conjugated anti-

CD105(MJ7/18) and APC-conjugated anti-CD48 (HM48-1). CD105 staining was developed with FITC conjugated streptavidin. HSCs and hematopoietic progenitor cells were sorted using following phenotypes: HSCs (Lineage$^-$cKit$^+$Sca-1$^+$CD150$^+$CD48$^-$ CD41$^-$), multipotent progenitors (MPPs; Lineage$^-$Sca-1$^-$cKit$^+$CD150$^-$CD48$^-$CD41$^-$)(Kiel et al., 2005b), LSK48$^+$41$^-$ cells (Lineage$^-$Sca-1$^+$cKit$^+$CD48$^+$CD41$^-$), granulocyte/macrophage progenitors (GMPs; Lineage$^-$cKit$^+$Sca-1$^-$CD41$^-$CD16/32$^+$) and megakaryocyte/erythroid progenitors (Pre-MegE; Lineage$^-$cKit$^+$Sca-1$^-$CD41$^-$CD16/32$^-$ CD150$^+$CD105$^-$) (Pronk et al., 2007). Cells were resuspended in 2 μg/ml DAPI to discriminate live from dead cells by flow-cytometry.

To assess the lineage differentiation potential of GFP$^+$ donor-derived cells in primary and secondary recipients, a single cell suspension of flushed bone marrow cells, splenocytes and thymocytes was prepared as previously described (Yilmaz et al., 2006). Unfractionated cells were stained with antibodies specific for myeloid cells (Mac-1 (M1/70-APC), Gr-1 (RB6-8C5-PE/Cy7) and CD41 (eBioMWReg30-PE)), erythroid cells ((Ter119-APC and CD71 (R17217-PE)), B cells (B220, (RA3-6B2-PE/Cy5), CD43 (S7-PE) and sIgM (ll/41-APC)), or T cells (CD3e (145-2c11-APC), CD4 (GK1.5-PE/Cy7) and CD8 (53-6.7-PE), together with APC/efluor780 conjugated anti-CD45.1 (A20) and alexafluor 700 conjugated anti-CD45.2 (104) to distinguish donor from recipient cells. To analyze the frequency of HSCs and LSK41$^-$ cells in the GFP$^+$ fraction of recipient bone marrow and spleen cells, unfractionated cells were stained with PE conjugated antibodies against lineage markers as described above, and antibodies against CD150 (TC15-12F12.2-PE/Cy5), CD48 (HM48-1-PE/Cy7), ckit (2B8-PE/Alexafluor 610) and Sca-1 (E13-161.7-APC/Cy7); APC conjugated anti-CD93 (AA4.1), APC conjugated anti-

ESAM (1G8), or Alexafluor 647 conjugated anti-CD144 (eBioBV13) were sometimes included to confirm the increased expression of these markers on *Sox17*-over-expressing cells.

Generation of MSCV-Sox17 and MSCV-Sox17his virus

To generate C-terminal 6xhis tagged mouse Sox17, full length mouse Sox17 cDNA was PCR amplified from mouse brain cDNA. AseI and XhoI sites were added to either end and the sequence was inserted into NdeI/XhoI digested pET23b vector (EMD chemicals, Gibbstown, NJ) to generate the pET23-mSox17-6xhis vector. Sox17-6xhis fragment was then isolated using FspI/BsaAI double digestion and inserted into HpaI digested mouse stem cell virus (MSCV) based pMIG (MSCV-GFP) vector (Van Parijs et al., 1999), immediately upstream of the internal ribosome entry site (IRES) to generate the MSCV-Sox17his vector. The MSCV-Sox17 vector was generated similarly except a short linker containing an in-frame stop codon and a FspI site was inserted into pET-23-mSox17-6xhis vector before the 6xhis tag to generate pET23-mSox17STOP, and a FspI fragment containing Sox17 was then inserted into HpaI digested pMIG to generate the MSCV-Sox17 vector.

Preparation of high-titer virus was carried out by transfecting 293T cells with control (MSCV-GFP) or Sox17-encoding MSCV vector together with the pCL-Eco packaging vector (Naviaux et al., 1996) using standard calcium phosphate methods as previously described (He et al., 2009). Cells were allowed to produce virus for 24-48 hours, then viral supernatants were collected, 0.45 micron filtered, and stored at –80°C. Virus titer was determined by infecting $2x10^5$ 3T3 cells using 1, 10 or 100 µl of viral supernatant. A viral titer of $2\text{-}5x10^6$/ml was routinely obtained.

Viral infection of whole bone marrow and purified hematopoietic progenitor cells

For adult whole bone marrow cell infection, 3-5 donor mice (CD45.1) were treated with a single injection of 150mg/kg 5-fluorouracil, and bone marrow cells from both hind limbs and pelvis bones were harvested on day 4 by flushing. Pooled bone marrow cells were first treated with ammonium-chloride potassium red cell lysis buffer to enrich for mononuclear cells, then resuspended in pre-stimulation cytokine cocktail (1x DMEM supplemented with 15% fetal bovine serum (FBS), 1% penicillin/streptomycin (Pen/strep), 100ng/ml stem cell factor (SCF), 10ng/ml interleukin-3 (IL-3), 10ng/ml interleukin-6 (IL-6) and 50μM 2-mercaptoethanol (2-ME) at a concentration of $5x10^6$ cells/ml, and incubated in a 37°C incubator, with 6% CO2 for about 24 hours. Two spin infections were performed at 24 and 36 hours post stimulation by adding retrovirus supernatant (MOI=2) and 4ng/ml of polybrene to the cell suspension and spinning at 1300 xg for 90 minutes at room temperature (RT). Cells were harvested 5 hours after the second spin, counted and transplanted into lethally irradiated mice at the indicated cell dose.

For infection of purified adult hematopoietic progenitor cells, 500 or 2000 HSCs, MPPs, $LSK48^+41^-$ cells, GMPs or Pre-MegEs were double sorted from untreated adult donor mice and deposited into a 96-well round bottom plate containing 100μl of pre-stimulation cytokine cocktails (base medium: 1x α-MEM + 1% FBS + 1% Pen/strep; cytokine supplements for HSC: 50ng/ml SCF + 50ng/ml thrombopoietin (TPO); MPP: 50ng/ml SCF + 50ng/ml Flt3-ligand + 50ng/ml TPO + 10ng/ml IL-3; $LSK48^+41^-$ cells and GMPs: 100ng/ml SCF + 10ng/ml IL-3 + 10ng/ml IL-6; pre-MegE: 100ng/ml SCF + 10ng/ml IL-3 + 10ng/ml IL-6 + 2U/ml erythropoietin(EPO)). Viral supernatant was

added at 0 and 12 hours (For LSK48^{+}41^{-} cells, GMPs and Pre-MegEs) or 24 and 36 hours (for HSCs and MPPs) after culture initiation at MOI=200. Cells from each well were harvested 12hours after the second round of viral infection and transplanted into lethally irradiated recipients together with 200,000 recipient cells for radioprotection. Viral infection efficiency was determined by analyzing cells infected in parallel at 48 hours after the second round of viral infection.

Long-term reconstitution assay

Two to four month old adult recipient mice were irradiated with a Gammacell 40 Exactor Cesium137 γ-ray source (MDS Nordia, ON, Canada) delivering approximately 110 rad/min. Lethal irradiation was done by giving two doses of 540 rad, delivered at least 2 hr apart, and sublethal irradiation was performed by giving a single dose of 600 rad.

For transplantation of virus-infected whole bone marrow or hematopoietic stem/progenitor cells (HSPC) into lethally irradiated primary recipients, test cells (CD45.1) together with 200,000 (CD45.2) radioprotective whole bone marrow cells were resuspended in 100μl of staining medium and injected into the retroorbital venous sinus of individual lethally irradiated recipient mice.

To test the long-term reconstituting potential of *Sox17*-overexpressing hematopoietic progenitors isolated from primary recipients, 50 GFP^{+} donor LSK48^{+}41^{-} cells were double sorted into individual wells of a 96-well plate containing 200,000 recipient whole bone marrow cells in staining medium. The contents of individual wells were injected into individual lethally irradiated secondary recipients by retroorbital injection.

To test the reconstituting potential of wild type adult bone marrow LSK48^{+}41^{-} cells, 100, 500 and 2,500 double sorted LSK48^{+}41^{-} cells from 8-week old UBC-GFP mice (CD45.2) were transplanted into sublethally irradiated (600 rads) CD45.1 recipients. The use of sublethally irradiated recipients allows monitoring of donor cell engraftment as early as one week post transplantation.

To monitor donor cell engraftment, blood was obtained from the tail veins of recipient mice every 1 to 4 weeks for at least 16 weeks after transplantation, blood cells were subjected to ammonium-chloride potassium red cell lysis (Morrison and Weissman, 1994), and stained with directly conjugated antibodies to CD45.2 (104-Alexafluor 700), CD45.1 (A20-APC/Efluor 780), B220 (RA3-6B2-PE/Cy5), Mac-1 (M1/70-PE), CD3e (145-2c11-APC) and Gr-1 (RB6-8C5-PE/Cy7) to examine GFP^{+} donor cell chimerism.

Cytology, histology and immunohistochemistry

For Wright-Giemsa staining of blood smears, bone marrow, spleen, and liver cells, freshly prepared blood smears and cytospun slides were air-dried, fixed in methanol for 5 min, stained in Wright-Giemsa staining solution (Sigma, St. Louis, MO) for 2 minutes, developed in 8.3mM phosphate buffer (pH=6.8) for 2-5 min, dipped 10 times in deionized water, dehydrated through an ethanol gradient and mounted in Permount (Fisher Scientific, Waltham MA). For peripheral blood reticulocyte staining, fresh whole blood was mixed with reticulocyte staining solution (Sigma, St. Louis, MO) at a 1:1 ratio and smeared onto microscope slides following standard procedures. Slides were air-dried and subjected to Wright-Giemsa staining as described above.

For histological analysis of hematopoietic tissues from control and *Sox17*-overexpressing bone marrow cell recipients, spleen, liver, lung and lymph node samples

were fixed in 10% neutral buffered formalin and paraffin embedded. Tibia or sternum samples were fixed with 10% neutral buffered formalin, decalcified in 0.5M EDTA/1xPBS for 7 days at 4˚C and paraffin embedded. Five micron sections were cut on a Leica microtome and stained with hematoxylin and eosin following standard protocols. Immunohistochemical staining for Von Willebrand's Factor (Vwf) on tissue sections was performed using a DAKO Autostainer (DAKO, Carpinteria, CA) using DAKO Envision+ and diaminobenzadine (DAB) as the chromogen. De-paraffinized sections of formalin fixed tissue at 5μm thickness were labeled with rabbit polyclonal anti-Vwf (1:500, DAKO) for 60 minutes, after microwave citric acid epitope retrieval. Immunofluorescent staining of Vwf on sorted $GFP^{+}CD41^{+}$ cells was performed by fixing the sorted cells in 4% paraformaldehyde in 1x phosphate buffered saline (PBS) for 10 min on ice, followed by washing three time with 1x PBS and cytospinning onto microscope slides. Rehydrated slides were blocked/permeabilized with 1xPBS containing 1% Triton X-100 and 10% goat serum. Slides were stained with anti-Vwf (1:500) at 4°C overnight. After washing, slides were incubated with secondary antibodies conjugated with AlexaFluor 555 (Invitrogen) together with DAPI for 1 hour at room temperature. All images were collected using an Olympus BX-71 inverted microscope with 20x and 40x dry objectives. Histological slides were analyzed by a hematopathologist and classified according to the Bethesda protocols for the classification of hematopoietic neoplasms in mice (Kogan et al., 2002; Morse et al., 2002).

Microarray

Total RNA (~5ng) from 3 independent, freshly isolated aliquots of 10,000 E16.5 fetal liver HSCs, 10,000 fetal liver $LSK48^{+}41^{-}$ cells, 10,000 adult bone marrow HSCs,

10,000 adult bone marrow LSK48^{+}41^{-} cells or 10,000 *Sox17*-overexpressing LSK48^{+}41^{-} cells (Sox17 LSK48^{+}41^{-}) isolated from primary recipients 12 weeks post transplantation of Sox17 virus infected bone marrow cells were extracted using Trizol with 25µg/ml linear acrylamide (Ambion, Austin, TX). The extracted RNA (10µl volume) was treated with 2 Units of RNase-free recombinant DNase I (Ambion) for 15 min at 25˚C, followed by 15 min at 37˚C to remove any contaminating genomic DNA. The DNA-free RNA samples were purified using the RNA Clean & Concentrator™-5 from Zymo Research (Orange, CA) and eluted in 10µl of nuclease-free water. Purified RNA was reverse transcribed and amplified using the WT-Ovation™ Pico RNA Amplification system (NuGEN Technologies, San Carlos, CA) following the manufacturer's instructions. Sense strand cDNA was generated using WT-Ovation™ Exon Module (NuGEN), and fragmented and labeled using the FL-Ovation™ cDNA Biotin Module V2 (NuGEN). 2.5µg of labeled cDNA were hybridized to Affymetrix Mouse Gene ST 1.0 microarrays. The chips were hybridized and scanned according to the manufacturer's instructions. Expression values for all genes were calculated using the robust multi-array average (RMA) method (Irizarry et al., 2003).

For the identification of genes with differential expression levels between groups, the raw expression data were analyzed using Expander v5.1 software (Shamir et al., 2005), and genes with fold changes greater than 2 and p-values less than 0.05 (t-test, using log2 transformed expression values) between sample groups were considered to be significantly changed.

For Gene Set Enrichment Analysis (GSEA), normalized expression data were assessed by GSEA 2.0.6 software as described (Mootha et al., 2003; Subramanian et al.,

2005). Gene expression profiles of *Sox17*-overexpressing LSK48^{+}41^{-} cells and control LSK48^{+}41^{-} cells were used as the background data set and the following gene sets were used as the foreground: C2-curated gene sets from the Broad Institute, HSC or short-term progenitor (LSK48^{+}41^{-} cells) specific gene sets we constructed by comparing adult bone marrow HSCs versus bone marrow LSK48^{+}41^{-} cells ($p<0.05$, fold change >2) and a fetal liver HSC specific gene set we constructed by comparing fetal liver HSCs versus adult bone marrow HSCs ($p<0.05$, fold change >2).

Quantitative RT-PCR

Quantitative (real-time) RT-PCR was performed as described previously (Molofsky et al., 2003). Three replicates of 10,000 *Sox17*-overexpressing LSK48^{+}41^{-} cells from reconstituted primary recipients and control bone marrow LSK48^{+}41^{-} cells were sorted into Trizol. RNA was isolated using chloroform extraction and isopropanol precipitation. cDNA was made with random primers and SuperScript III reverse transcriptase (Invitrogen). Quantitative PCR was performed with cDNA from 100 cell equivalents using a SYBR Green Kit and a LightCycler 480 (Roche Applied Science).

Statistics

All experiments were performed at least three times and all data are expressed as mean ± s.d. Statistical comparisons between samples were performed in Excel using Student's t-test. Unless otherwise indicated, a p-value less than 0.05 was considered statistically significant. The survival analysis of primary and secondary recipients was performed in Graphpad Prism 5 software, and the p-values for log-rank test between individual curves are presented.

ACKNOWLEDGEMENTS

This work was supported by the Howard Hughes Medical Institute. Thanks to Tina Levanthal for the initial construction of the MSCV-Sox17 and MSCV-Sox17his retroviral vector. Thanks to Dr. Jeffery Whitsett at Cincinnati Children's Hospital Medical Center for providing the Otet-*Sox17* mice. Thanks to David Adams, Martin White, and Ann Marie Deslaurier of the University of Michigan (UM) Flow-Cytometry Core Facility. Flow-cytometry was supported in part by the UM Comprehensive Cancer Center NIH CA46592, and the UM Multipurpose Arthritis Center NIH AR20557. Thanks to the histology cores at the UM Microscopy and Image analysis Laboratory and the UM Comprehensive Cancer Center for histology service.

AUTHOR CONTRIBUTIONS

S.H. performed all experiments and participated in the design and interpretation of experiments. I.K generated the original *Sox17-GFP* knockin mice used in this study. M.S.L. analyzed mouse pathology with help from S.H. S.J.M. participated in the design and interpretation of all experiments and wrote the manuscript with S.H.

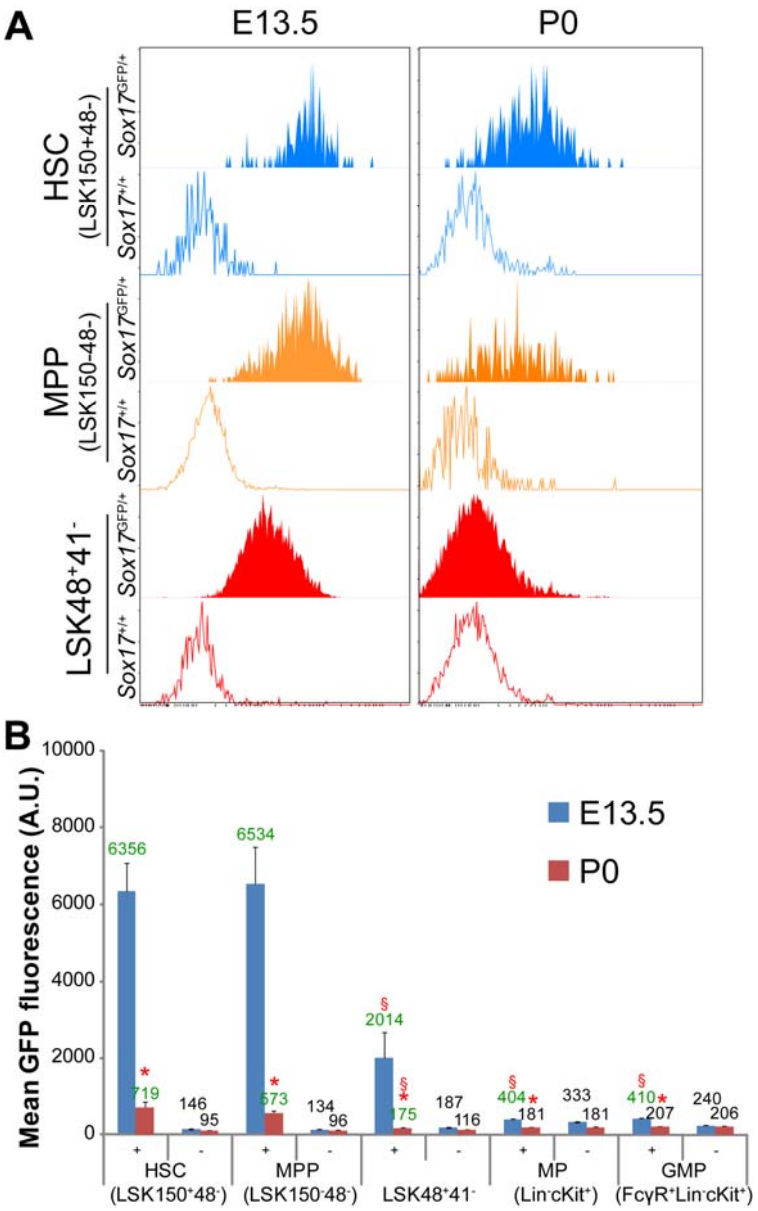

Figure 4.1: *Sox17* expression in hematopoietic stem and progenitor cells decreased with fetal development and lineage commitment.
A) A representative histogram showing the *Sox17* expression level based on GFP fluorescence in $Sox17^{GFP/+}$ knockin mice at E13.5 and P0 in fetal liver HSCs, LSK150$^-$48$^-$41$^-$ cells, and LSK48$^+$41$^-$ cells. B) Quantification of *Sox17* expression level in fetal liver hematopoietic stem and progenitor cells during development. *Sox17* expression decreased both with age as well as with degree of differentiation. Green label indicates GFP expression was significantly above $Sox17^{+/+}$ littermate controls; *, significantly reduced ($p<0.05$) when compared with E13.5 counterparts; §, significantly reduced ($p<0.05$) when compared with HSCs from same developmental stage; +, Sox17-GFP knock-in; -, control littermates; A.U. arbitrary units.

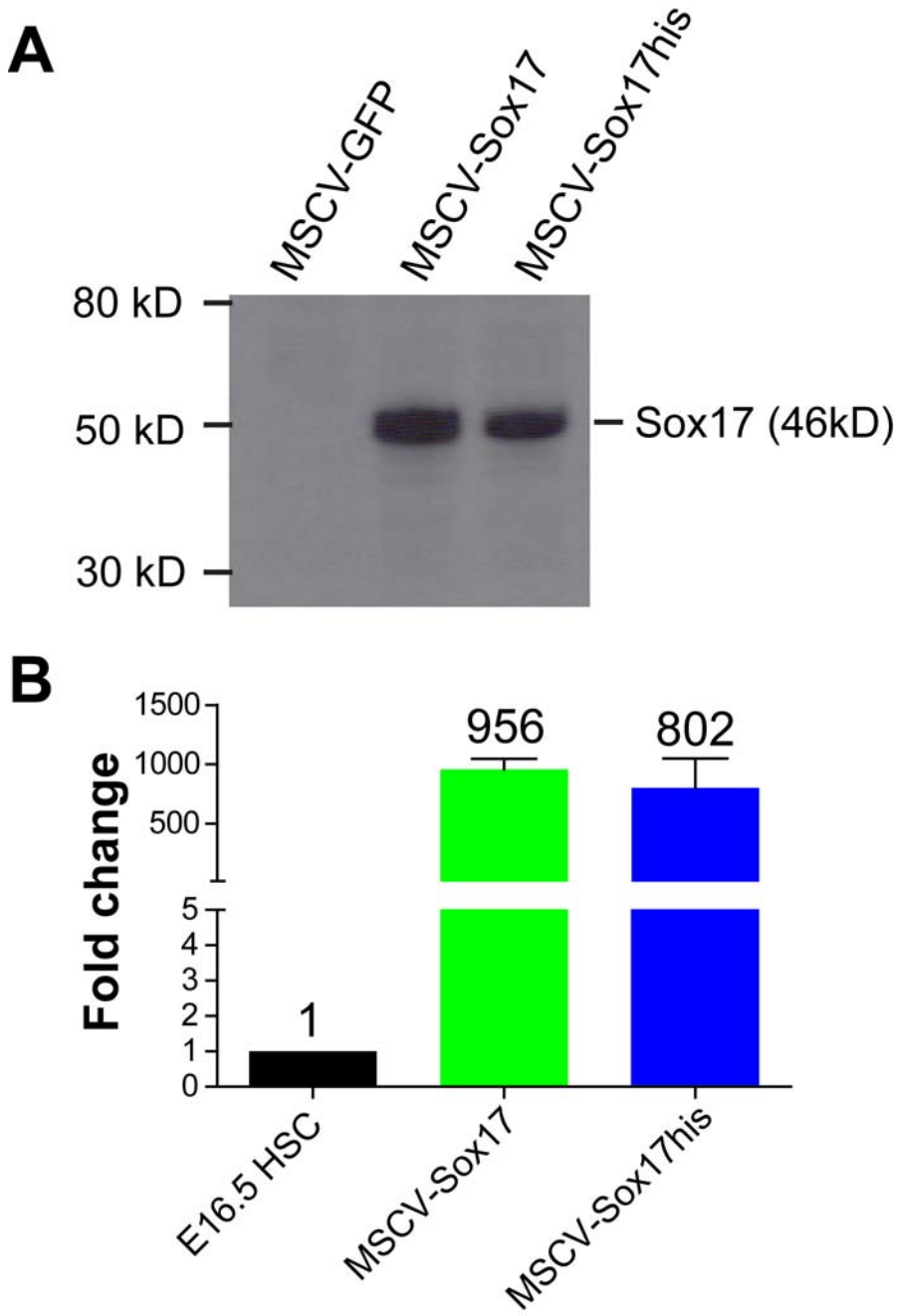

Figure 4.2: Level of *Sox17* overexpression from retroviral infection
A). Western blotting for Sox17 protein comparing MSCV-GFP, MSCV-Sox17 and MSCV-Sox17his virus infected 3T3 cells. Ectopic Sox17 protein expression (46KD) was only observed in Sox17 virus infected cells. B). qRT-PCR comparison of Sox17 expression level in E16.5 fetal liver HSCs versus GFP+ bone marrow cells isolated from primary recipients of Sox17 virus infected cells. Sox17 retrovirus infection led to 800 to 950-fold overexpression of *Sox17* mRNA above endogenous levels in E16.5 fetal liver HSCs.

Figure 4.3: *Sox17* overexpression enhanced the long-term reconstitution potential of adult bone marrow cells and biased their lymphoid versus myeloid lineage output in peripheral blood.
1 million control (MSCV-GFP) or Sox17 (MSCV-Sox17 or MSCV-Sox17his) virus infected adult bone marrow cells (CD45.1) were transplanted into 8-week old lethally irradiated CD45.2 recipients together with 200,000 CD45.2 bone marrow cells. A-F) At 16-weeks post transplantation, *Sox17*-overexpressing bone marrow cells gave rise to significantly higher levels of peripheral blood myeloid (Mac-1+ or Gr-1^+, A,B), erythroid (Ter119^+, E) and platelet (CD41^+, F) reconstitution as compared to control virus infected cells. MSCV-Sox17 but not MSCV-Sox17his virus infected cells also exhibited significantly enhanced B-cell (B220^+) reconstitution (C). No differences were observed in T-cell (CD3^+) reconstitution between control or Sox17 virus infected cells (D). N=3 experiments; n=9-14 recipients per treatment; *, $p<0.05$; **, $p<0.01$. G) Quantification of primary recipient peripheral blood reconstitution at 16-weeks post-transplantation; 89% to 100% of recipients of *Sox17*-overexpressing cells exhibited long-term myeloid and/or erythroid reconstitution, compared to only 36% or 64% of recipients of control virus infected cells showed long-term myeloid or erythroid reconstitution. H) *Sox17* overexpression reduced the lymphoid (B220^+ or CD3^+) versus myeloid (Mac-1^+Gr-1^+) ratio of donor derived GFP^+ peripheral blood cells at both 4 and 16 weeks post transplantation (*, $p<0.05$; **, $p<0.01$).

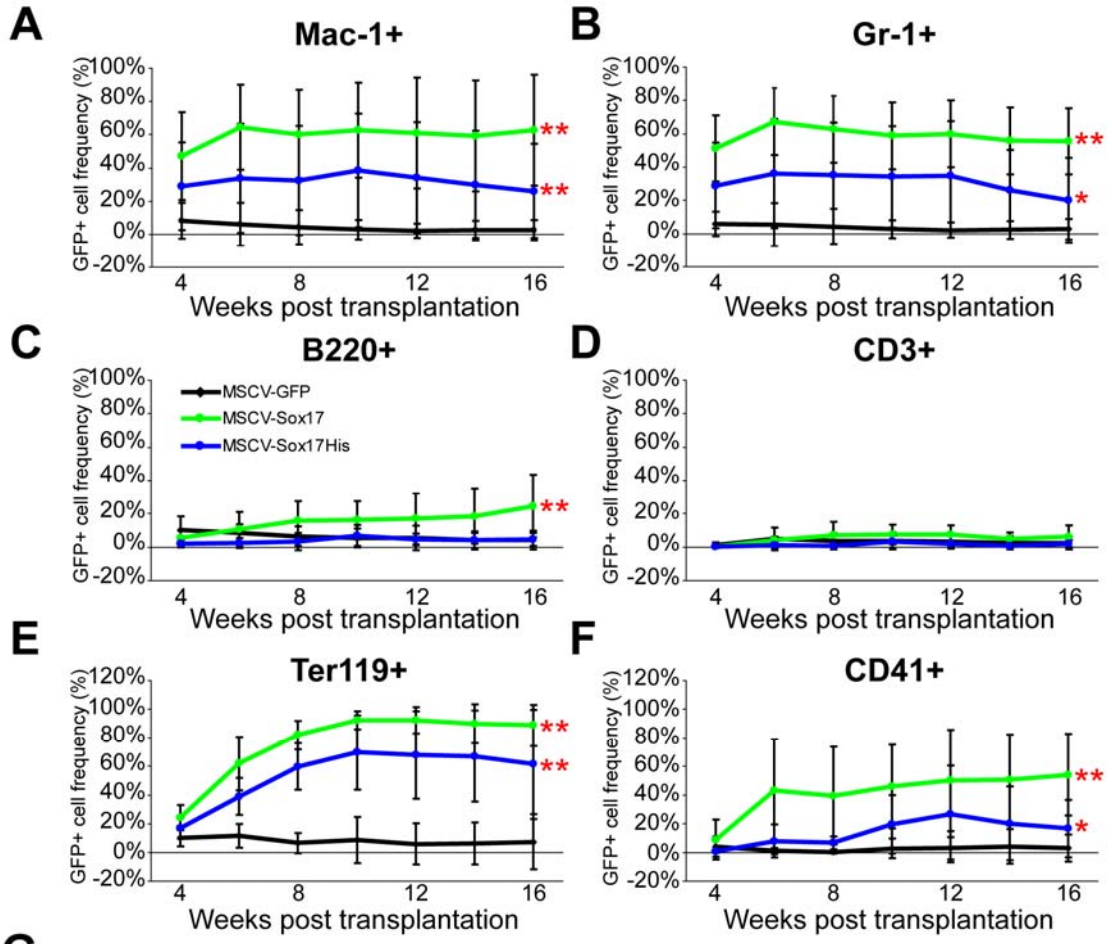

G

	M/E/B/T/Plt	M/E/B/T	M/E/T/Plt	E/Plt	B/E	B/T	Total	Contain long-term erythroid #	Contain long-term erythroid %	Contain long-term myeloid #	Contain long-term myeloid %	B/T only #	B/T only %	Any type #	Any type %
MSCV-GFP	4	1			4	3	14	9	64%	5	36%	3	21%	12	86%
MSCV-Sox17	9						9	9	100%	9	100%	0	0%	9	100%
MSCV-Sox17his	7		1	1			9	9	100%	8	89%	0	0%	9	100%

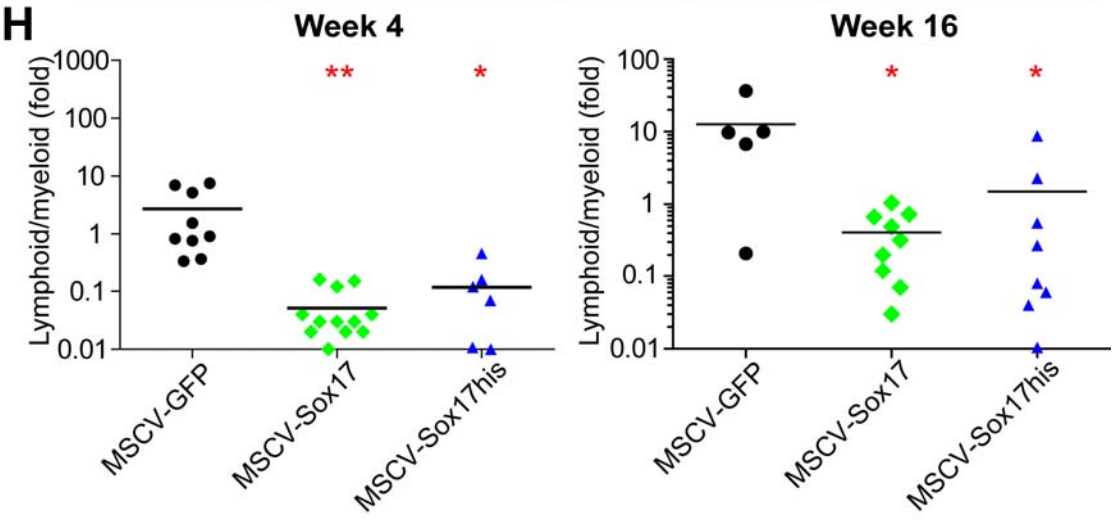

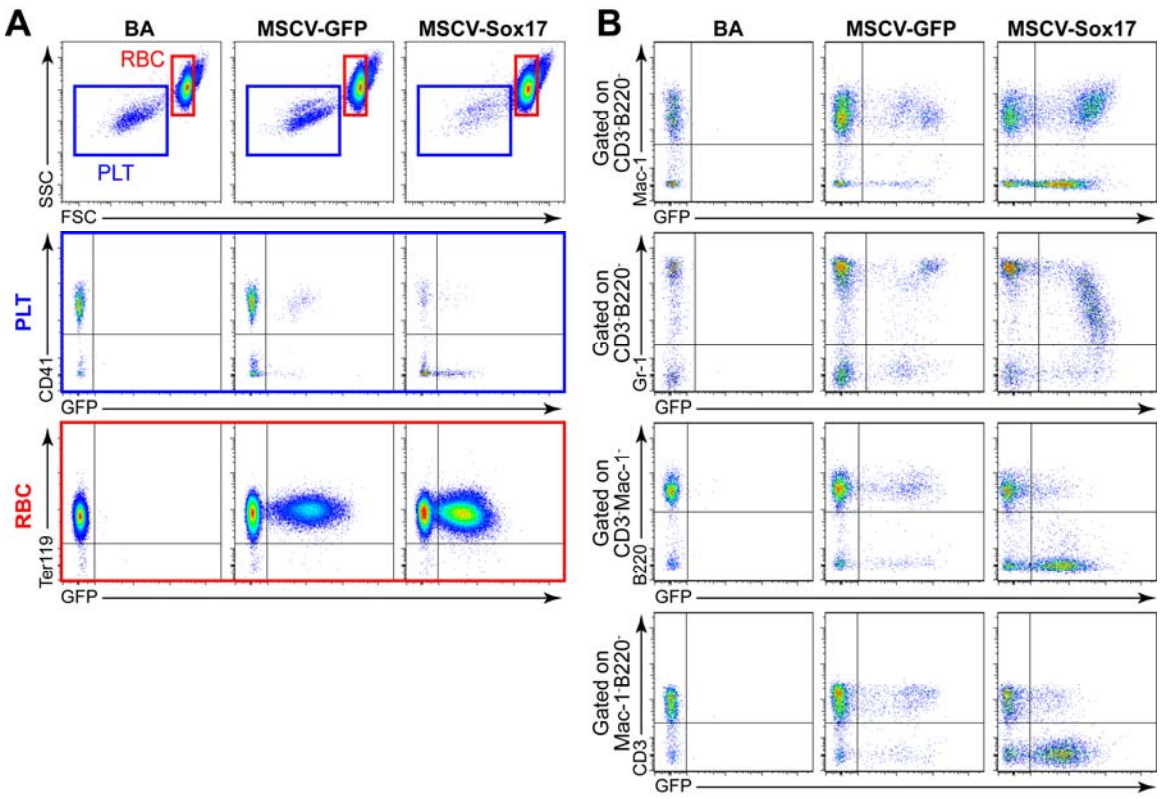

Figure 4.4: Representative flow cytometry plots of primary recipient peripheral blood reconstitution at 16 weeks after transplantation.
A) Representative flow cytometry plots showing GFP^+ peripheral blood erythrocytes and platelets in control mice or mice reconstituted by *Sox17*-overexpressing bone marrow cells. B) Representative flow cytometry plots showing GFP^+ peripheral blood myeloid and lymphoid cells in control mice or mice reconstituted by *Sox17*-overexpressing bone marrow cells. Note the decreased Gr-1 expression by *Sox17*-overexpressing myeloid cells and the overall lower expression of GFP by *Sox17*-overexpressing lymphoid cells. Background level was set using untransplanted recipient cells.

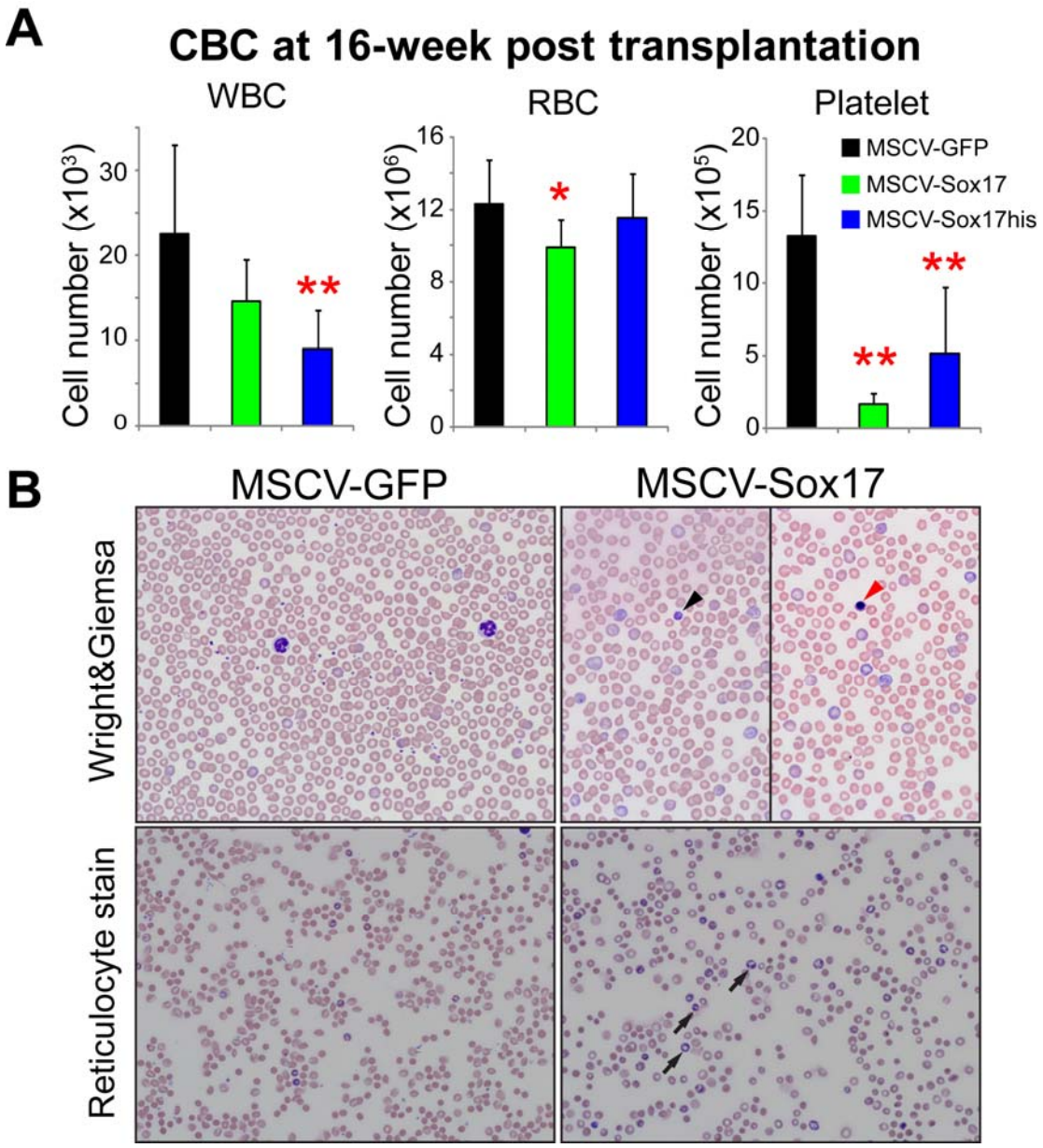

Figure 4.5: *Sox17* overexpression leads to thrombocytopenia and increased peripheral blood reticulocyte count.
A) CBC analysis of control mice or mice reconstituted by *Sox17*-overexpressing bone marrow cells at 16 weeks post transplantation. Recipients of *Sox17*-overexpressing cells showed a mild reduction in white blood cell (WBC) and erythrocyte (RBC) counts and a significant reduction in platelet counts (*, $p<0.05$; **, $p<0.01$, n=3 experiments with 8-9 mice per treatment). B) Representative peripheral blood smears stained with wright-giemsa or reticulocyte staining showed an increase in reticulocyte counts and a reduction of platelet numbers. Note the presence of large reticulated platelets in the *Sox17*-overexpressing samples. Black arrow, reticulocytes, black arrowhead, nucleated red blood cells; red arrowhead, large platelet

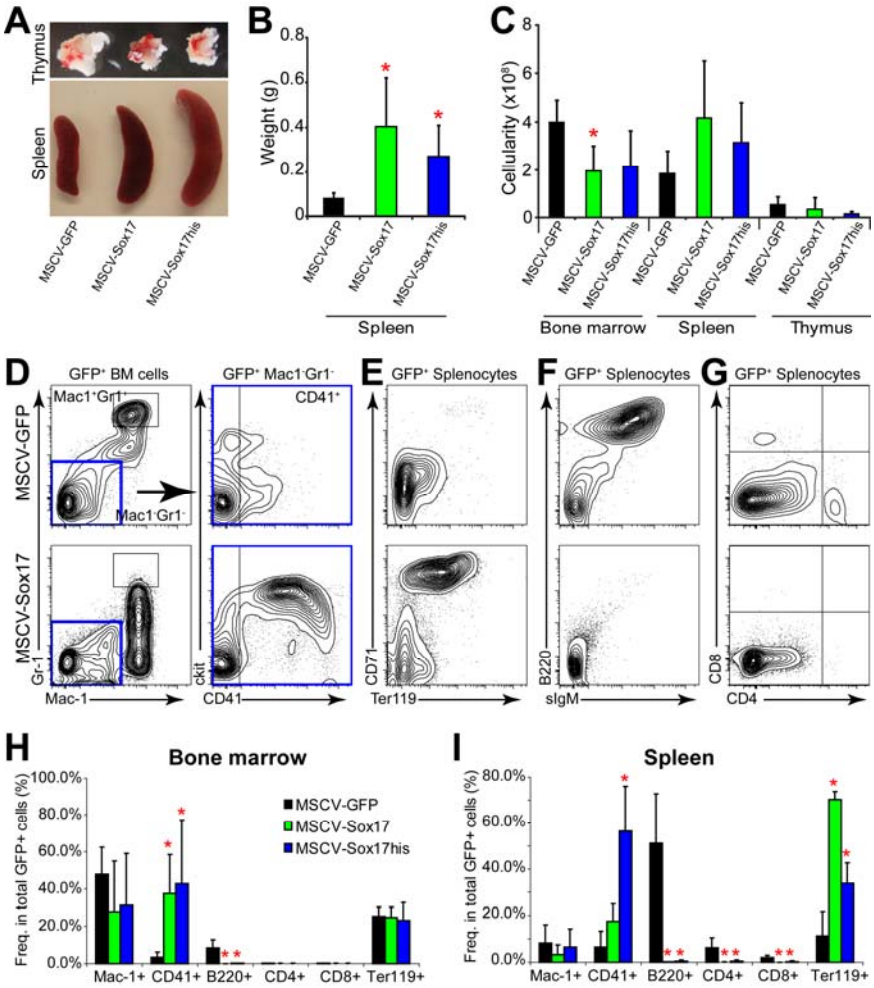

Figure 4.6: *Sox17* overexpression biased hematopoiesis in bone marrow and spleen. A) Representative image of spleen and thymus from primary recipients reconstituted with control or Sox17 virus infected bone marrow cells at 16-weeks post transplantation. *Sox17* overexpression led to increased spleen size and decreased thymus size. B) Recipients of *Sox17*-overexpressing cells showed significantly increased spleen weight. C) *Sox17* overexpression led to slightly decreased bone marrow cellularity (*, $p<0.05$ for MSCV-Sox17 recipients), and a trend toward increased spleen cellularity that was not statistically significant. D-G) Representative flow cytometry plots showing the lineage composition of GFP^+ donor-derived cells in the bone marrow and/or spleen of mice reconstituted by control or Sox17 virus infected cells. *Sox17* overexpression led to decreased Gr-1 expression on bone marrow myeloid cells, increased $CD41^+$ cell frequency in bone marrow (D), increased erythroid cell frequency in spleen (E) and decreased spleen B and T cell frequency (F, G). H, I) Quantification of lineage composition of GFP^+ bone marrow and spleen cells in primary recipients. *Sox17* overexpression led to significantly increased $CD41^+$ cells in bone marrow and/or spleen, significantly increased erythroid cells ($Ter119^+$) in spleen and a global depletion of lymphoid cells in both tissues (N=4 experiments; n=4-6 mice per treatment; *, $p<0.05$; **, $p<0.01$).

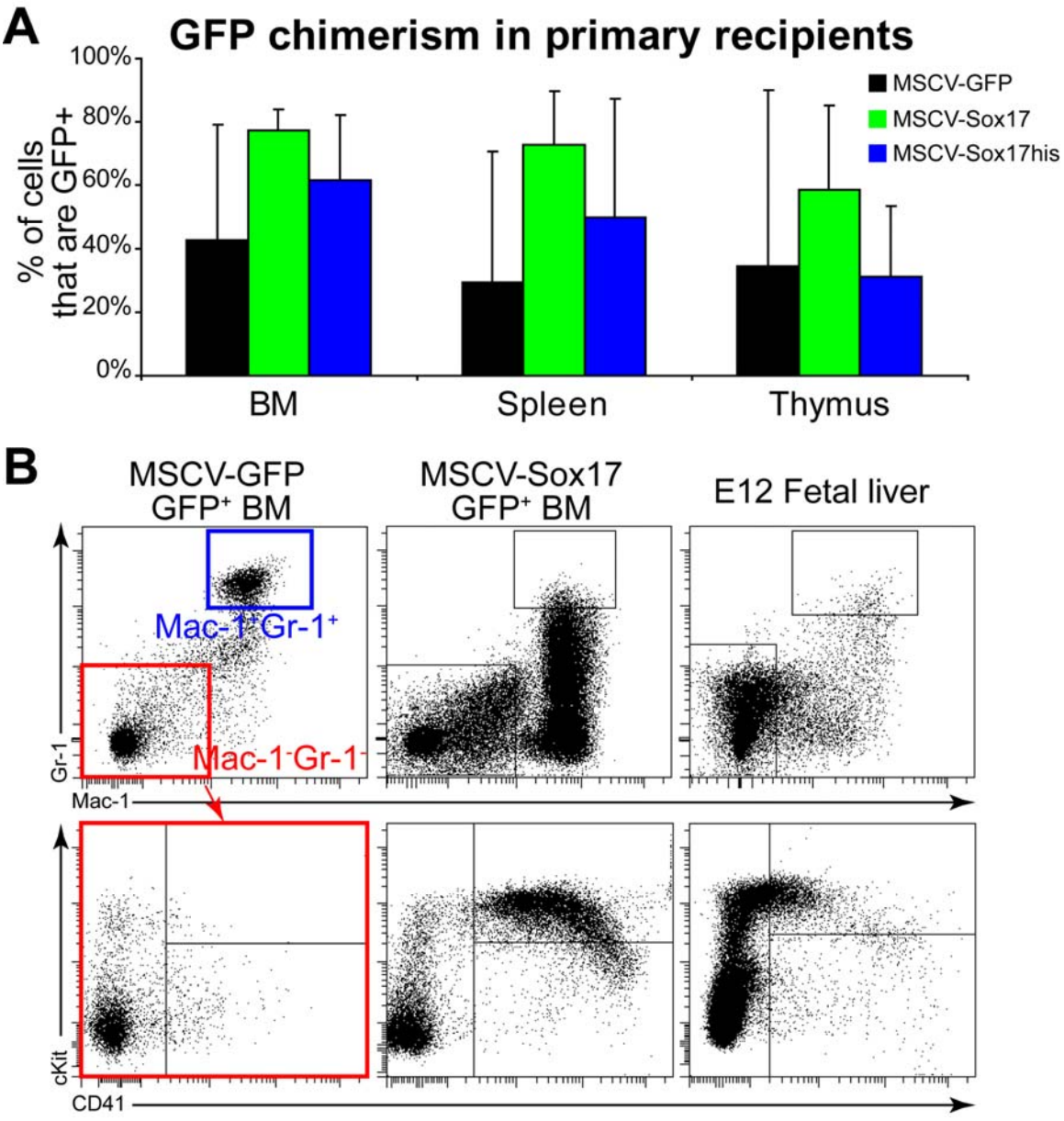

Figure 4.7: *Sox17* overexpression led to changes in bone marrow myeloid and megakaryocyte phenotypes that resembled their fetal liver counterparts.
A) Overall GFP$^+$ donor cell chimerism was comparable between control mice and mice reconstituted by *Sox17*-overexpressing cells, with a trend towards higher reconstitution level by the *Sox17*-overexpressing cells. B) *Sox17* overexpression led to downregulation of Gr-1 expression on bone marrow myeloid cells, and expansion of ckit$^+$CD41$^+$ megakaryocyte lineage cells, both of which showed a striking similarity to their counterparts in E12 fetal liver.

Figure 4.8: *Sox17* transgene expression led to a similar phenotype as observed in recipients of Sox17 virus infected bone marrow cells.
A) Thymus cellularity in *Sox17*-transgenic mice was significantly reduced after 4 days of doxycycline administration as compared to littermate controls. In contrast, bone marrow and spleen cellularities were not significantly affected. B) Induction of *Sox17* transgene expression led to a progressive reduction of thymus and spleen weight in *Sox17* transgenic mice. C) Peripheral blood neurophil counts were significantly increased as a result of transgene expression, and platelet number was significantly reduced. As a result, the peripheral blood lymphocyte versus myeloid cell ratio was significantly reduced (D). E, F) *Sox17* transgene expression led to a progressive increase of myeloid cells in the bone marrow and spleen, and depletion of both mature and immature B cells in the bone marrow. No consistent changes in the frequency of bone marrow and/or spleen erythroid, megakaryocyte or T-lymphoid cells were observed at the three time points tested so far. G) *Sox17* transgene expression led to depletion of thymic $CD4^{+}CD8^{+}$ double positive T-cells and increases in the relative frequency of single positive T cells 6 days after induction. H) The frequency of $LSK41^{-}$ cells but not HSCs was significantly increased in the bone marrow and spleen of *Sox17* transgenic mice after transgene induction. *, $p<0.05$, n=3-5 mice per treatment.

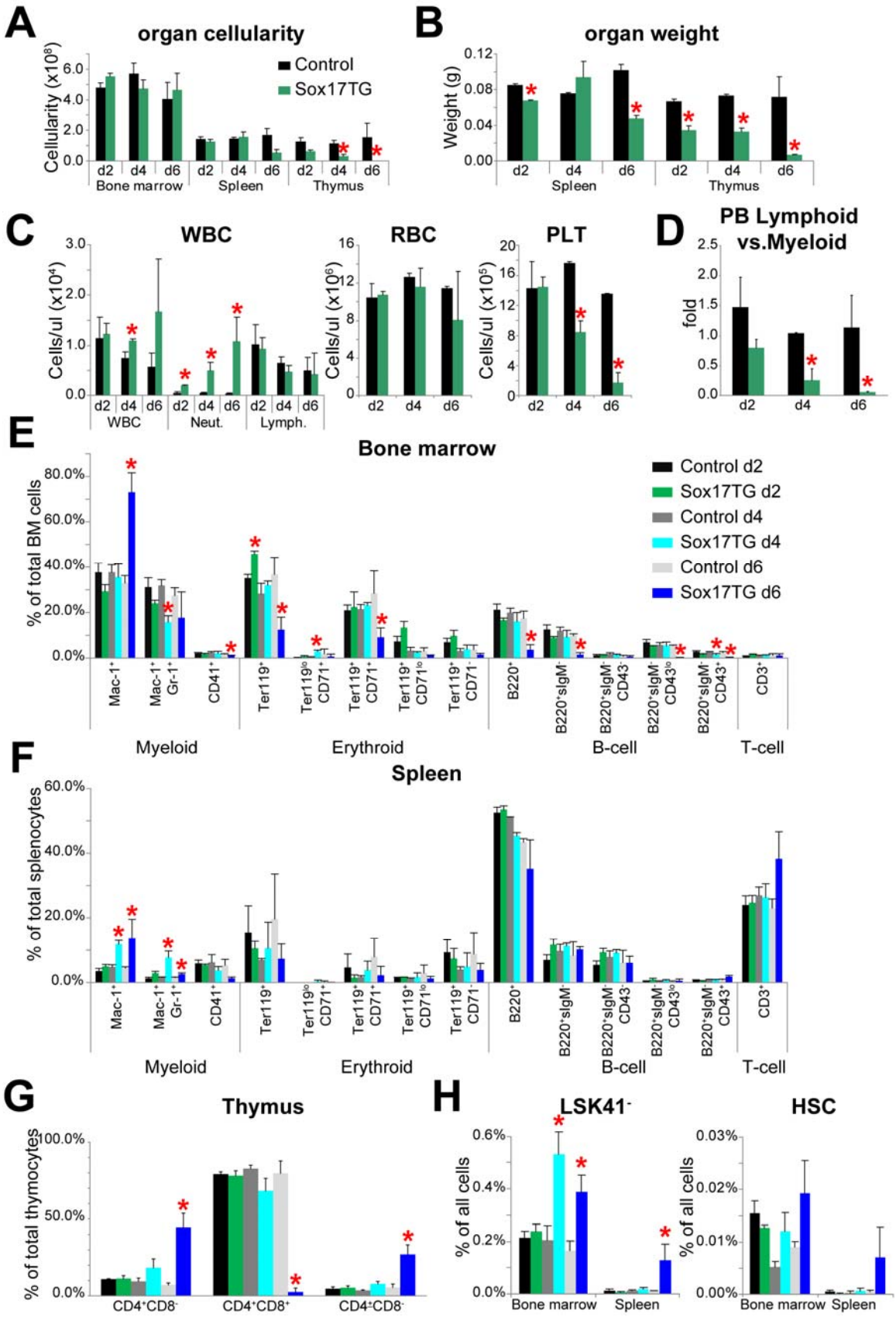
A
organ cellularity
Cellularity (x10^8)
Control
Sox17TG
d2 d4 d6 d2 d4 d6 d2 d4 d6
Bone marrow
Spleen
Thymus
B
organ weight
Weight (g)
d2 d4 d6 d2 d4 d6
Spleen
Thymus
C
WBC
RBC
PLT
Cells/ul (x10^4)
Cells/ul (x10^6)
Cells/ul (x10^5)
WBC
Neut.
Lymph.
D
PB Lymphoid vs.Myeloid
fold
E
Bone marrow
% of total BM cells
Control d2
Sox17TG d2
Control d4
Sox17TG d4
Control d6
Sox17TG d6
Mac-1+
Mac-1+ Gr-1+
CD41+
Ter119+
Ter119lo CD71+
Ter119+ CD71+
Ter119+ CD71lo
Ter119+ CD71-
B220+
B220+sIgM-
B220+sIgM- CD43+
B220+sIgM- CD43lo
B220+sIgM- CD43-
CD3+
Myeloid
Erythroid
B-cell
T-cell
F
Spleen
% of total splenocytes
G
Thymus
% of total thymocytes
CD4+CD8-
CD4+CD8+
CD4-CD8-
H
LSK41-
HSC
% of all cells
Bone marrow
Spleen

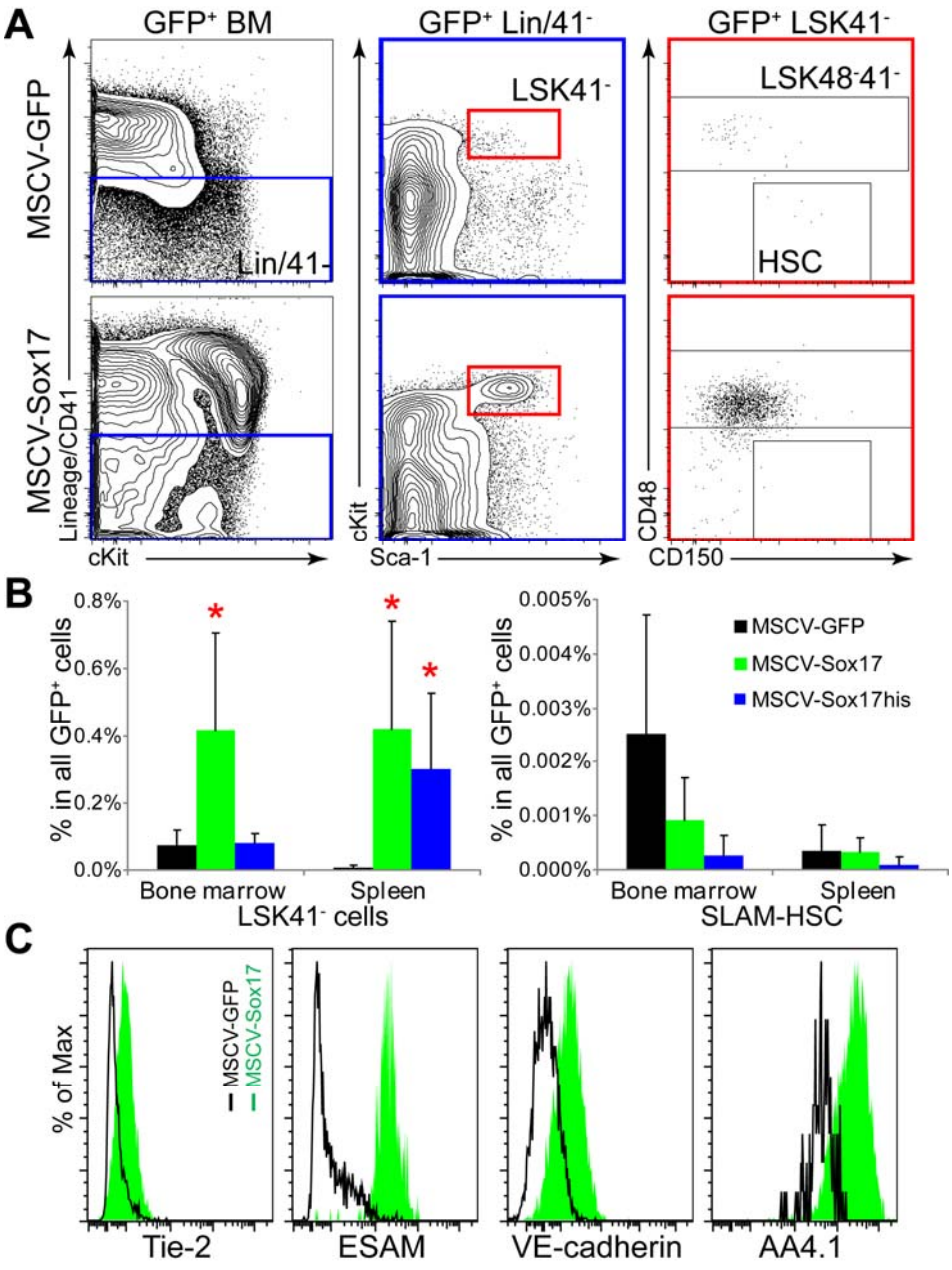

Figure 4.9: *Sox17* overexpression led to expansion of hematopoietic progenitor cells and fetal HSC specific marker expression.
A). Representative flow cytometry plots of GFP^+ donor-derived bone marrow cells in primary recipients showing expansion of $LSK41^-$ hematopoietic progenitors and depletion of HSCs as the result of *Sox17* overexpression. B) The frequency of GFP^+LSK41^- cells was significantly increased in the bone marrow and/or spleen of recipients of *Sox17*-overexpressing cells, while GFP^+ HSC frequency was reduced. *, $p<0.05$; N=5-7 experiments. C) *Sox17*-overexpressing $LSK41^-$ cells upregulated the expression of HSC markers Tie2 and Esam, and the fetal HSC markers VE-cadherin and AA4.1.

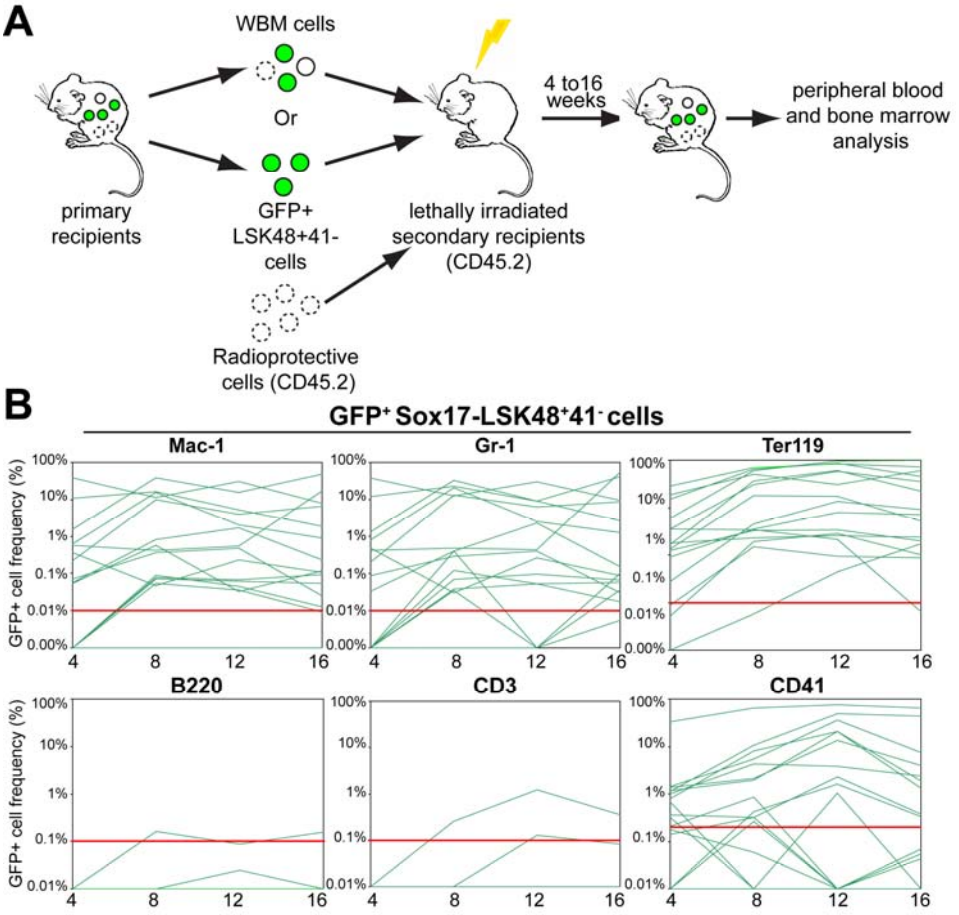

C

		Types of reconstitution (week 16)								long-term erythroid		long-term myeloid		any type	
		E/M/B/T/Plt	E/M/B/T	E/M/T/Plt	E/M/Plt	E/M	E/Plt	M/Plt	Total	#	%	#	%	#	%
MSCV-Sox17	WBM	6		4			1		11	11	100%	10	91%	11	100%
	LSK48+41-	1			7	6		1	15	14	93%	15	100%	15	100%
MSCV-GFP	WBM	3	1						4	4	100%	4	100%	4	100%

Figure 4.10: *Sox17*-overexpressing LSK48$^+$41$^-$ cells from primary recipients were capable of long-term erythroid and/or myeloid reconstitution.
A). Schema for secondary transplantation of Sox17-overexpressing whole bone marrow or GFP$^+$LSK48$^+$41$^-$ cells. B). 50 GFP$^+$LSK48$^+$41$^-$ cells from primary recipients of *Sox17* virus infected bone marrow cells were transplanted into lethally irradiated secondary recipients together with 200,000 radioprotective recipient cells. At 16 weeks post transplantation, GFP$^+$ myeloid (Mac-1$^+$ or Gr-1$^+$), erythroid (Ter119$^+$) and platelet (CD41$^+$) reconstitution were detected in the peripheral blood of 15/15, 14/15, and 9/15 of secondary recipients, respectively (see panel B). In contrast, only 1 recipient showed clear long-term lymphoid reconstitution. C) Quantification of peripheral blood reconstitution at 16 weeks post transplantation of either 50 *Sox17*-overexpressing GFP$^+$LSK48$^+$41$^-$ cells or 200,000 control or *Sox17*-overexpressing whole bone marrow cells from primary recipients.

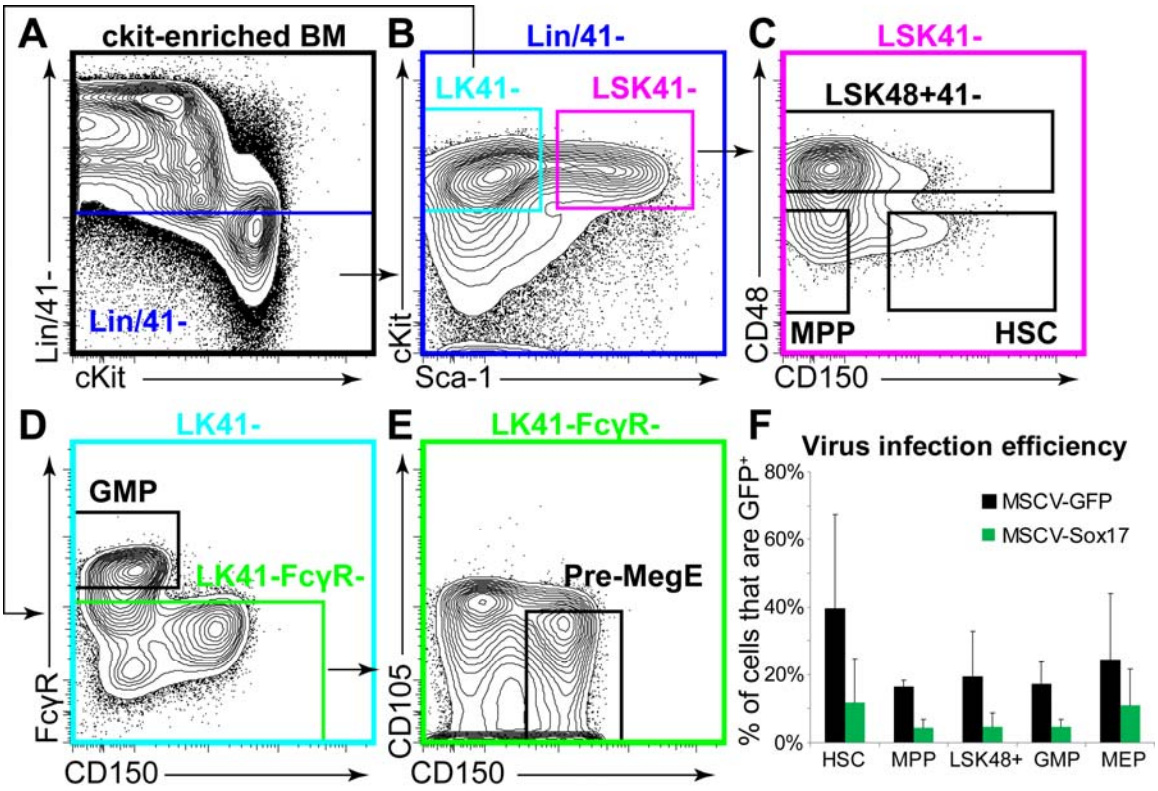

Figure 4.11: Sorting strategy for isolation of adult hematopoietic stem and progenitor cells for virus infection and viral infection efficiency.
A-E) Sorting strategy for isolation of adult bone marrow HSCs, MPPs, LSK48^{+}41^{-} cells, GMPs and Pre-MegE cells. B) Viral infection efficiency of cultured adult hematopoietic stem and progenitor cells determined at 48 hours after infection.

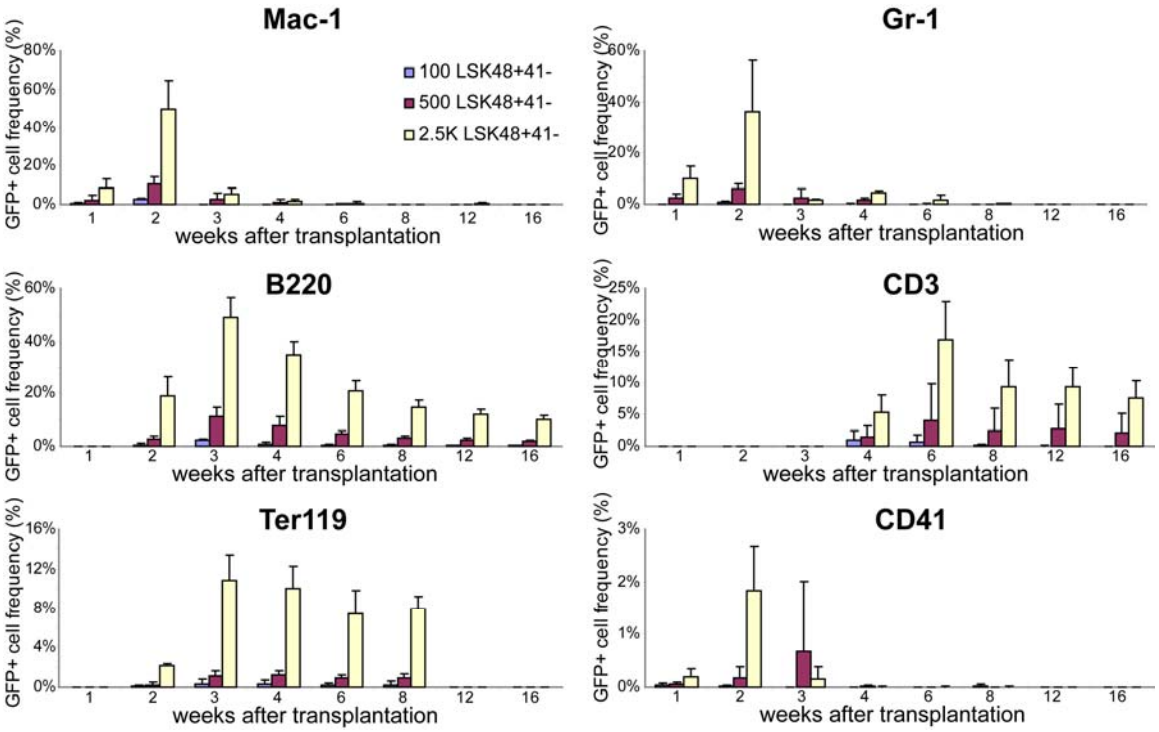

Figure 4.12: Adult bone marrow LSK48^{+}41^{-} cells possessed only short-term multilineage reconstituting potential.
100, 500 or 2000 adult bone marrow LSK48^{+}41^{-} cells from UBC-GFP mice were transplanted into 600 rad sublethally irradiated recipients, and peripheral blood GFP^{+} cell chimerism was monitored up to 16 weeks. Adult LSK48^{+}41^{-} cells were only capable of transient myeloid (peaks at week 2, disappears after week 4), erythroid (peaks at week 3, disappears after week 8) and platelet (peaks at week 2, disappears after week 4) reconstitution similar to MPPs, but were more temporally limited.

Figure 4.13: Overexpression of *Sox17* in transiently-reconstituting adult hematopoietic progenitors conferred long-term reconstituting potential.
A) Schema for transplantation of control or Sox17 virus infected purified adult HSCs and progenitor cells. B) 500 or 2000 LSK48^{+}41^{-} adult bone marrow cells were infected with MSCV-GFP or MSCV-Sox17 virus, and transplanted into irradiated recipients together with 200,000 recipient cells for radioprotection. At 16 weeks post transplantation, 3 of 22 and 9 of 22 recipients of Sox17 virus infected cells exhibited long-term myeloid and erythroid reconstitution, respectively. In contrast, no recipients of control virus infected cells exhibited any type of long-term reconstitution. C). 500 adult bone marrow MPPs (LSK150^{-}48^{-}41^{-}) were infected with control or Sox17 virus and transplanted into lethally irradiated recipients with 200,000 recipient cells. At 16 weeks post transplantation, 5 of 15 and 6 of 15 recipients of Sox17 virus infected cells exhibited long-term myeloid and erythroid reconstitution, respectively, while only 1 recipient of control virus infected cell had long-term erythroid reconstitution. D) Peripheral blood reconstitution patterns at 16 weeks post transplantation of control or Sox17 virus infected adult hematopoietic stem or progenitor cells.

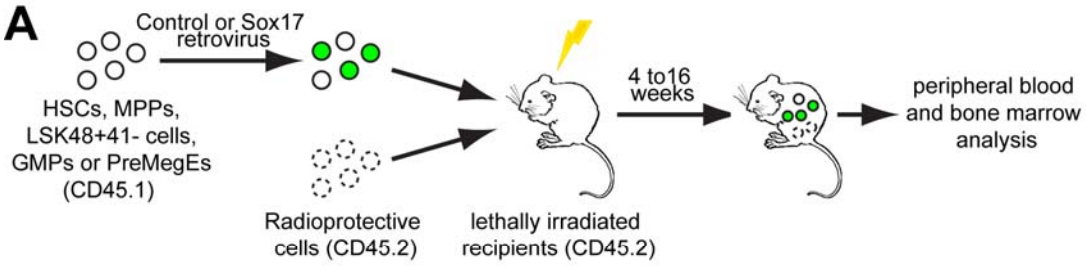

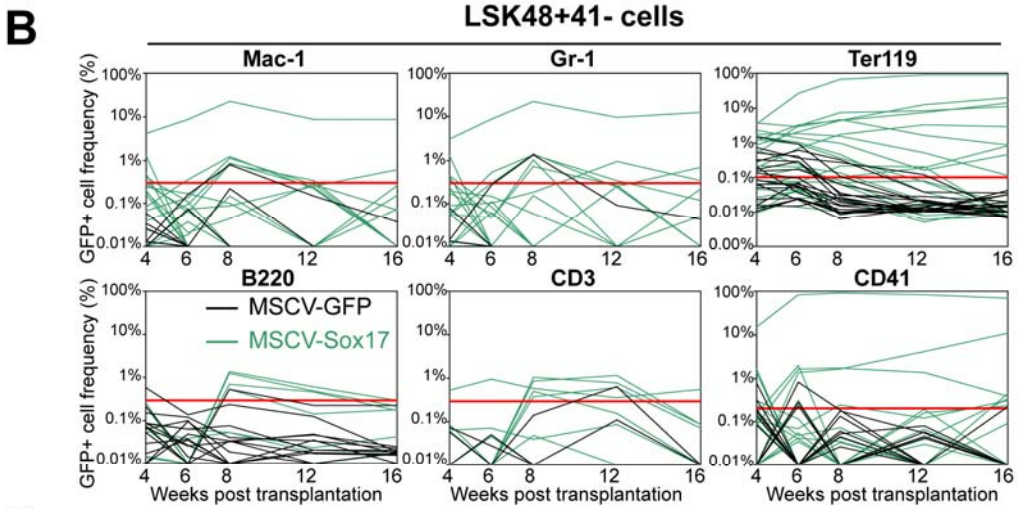

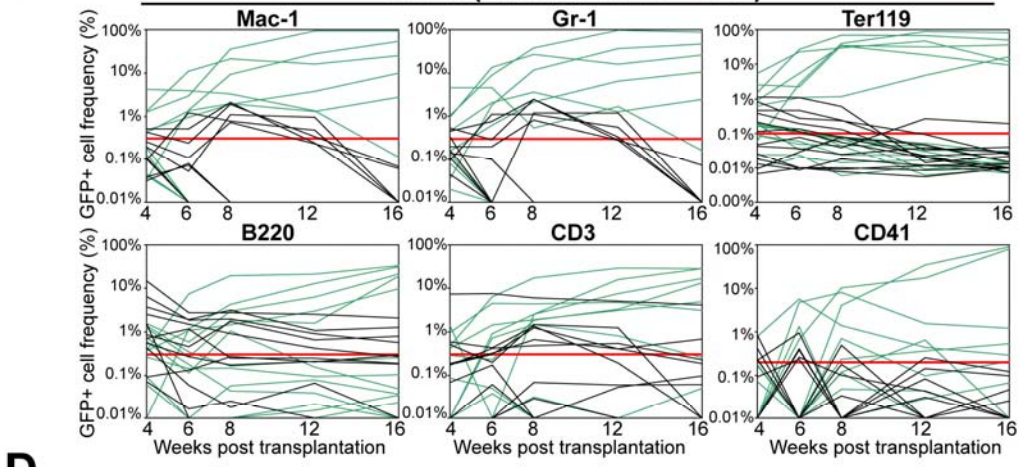

D

		Types of reconstitution (week 16)											Contain long-term erythroid		Contain long-term myeloid		T and/or B only		Any type	
		E/Plt/M/B/T	E/M/B/T	E/M/Plt	E/T/M	E/Plt	E/B/T	E	Plt	B	T	Total	#	%	#	%	#	%	#	%
MSCV-Sox17	HSC	9		2		1		2	1			16	14	88%	11	69%	0	0%	15	94%
	MPP	4	1			1			1		1	15	6	40%	5	33%	1	7%	8	53%
	LSK48+			2	1	4		2	1			22	9	41%	3	14%	0	0%	10	45%
	PreMegE											12	0	0%	0	0%	0	0%	0	0%
	GMP											13	0	0%	0	0%	0	0%	0	0%
MSCV-GFP	HSC						4				1	19	4	21%	0	0%	1	5%	5	26%
	MPP						1			3	1	13	1	8%	0	0%	4	31%	5	38%
	LSK48+											20	0	0%	0	0%	0	0%	0	0%
	PreMegE											12	0	0%	0	0%	0	0%	0	0%
	GMP											14	0	0%	0	0%	0	0%	0	0%

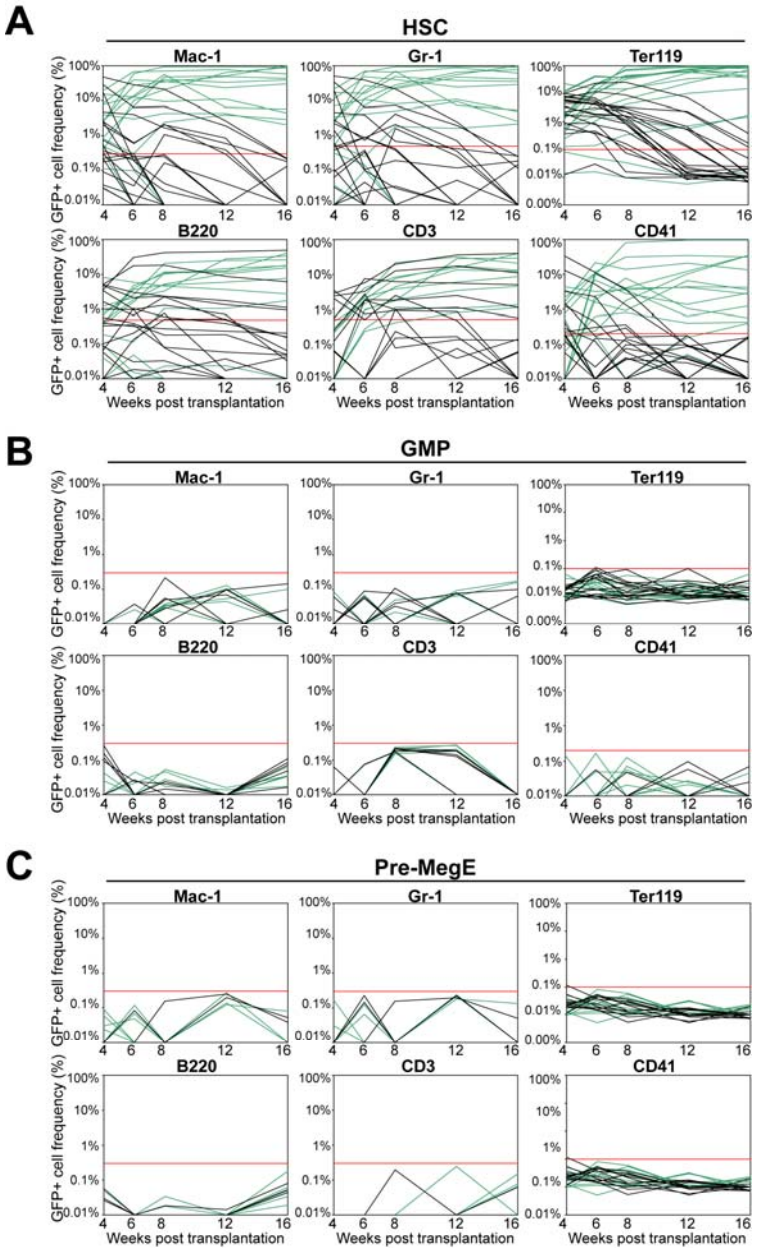

Figure 4.14: *Sox17* overexpression did not enhance the long-term reconstituting potential of adult GMPs or Pre-MegE progenitors.
A) 500 control or Sox17 virus infected bone marrow HSCs were transplanted into lethally irradiated recipients together with 200,000 recipient cells. *Sox17*-overexpressing HSCs showed significantly enhanced long-term erythroid and myeloid reconstitution as compared to control virus infected cells, which only exhibited significant levels of lymphoid reconstitution at 16 weeks post transplantation. B, C) 500 control or Sox17 virus infected bone marrow GMPs or Pre-MegE progenitors were transplanted into lethally irradiated recipients together with 200,000 recipient cells. Neither control nor Sox17 virus infected cells gave any level of peripheral blood reconstitution between 4 and 16 weeks post transplantation.

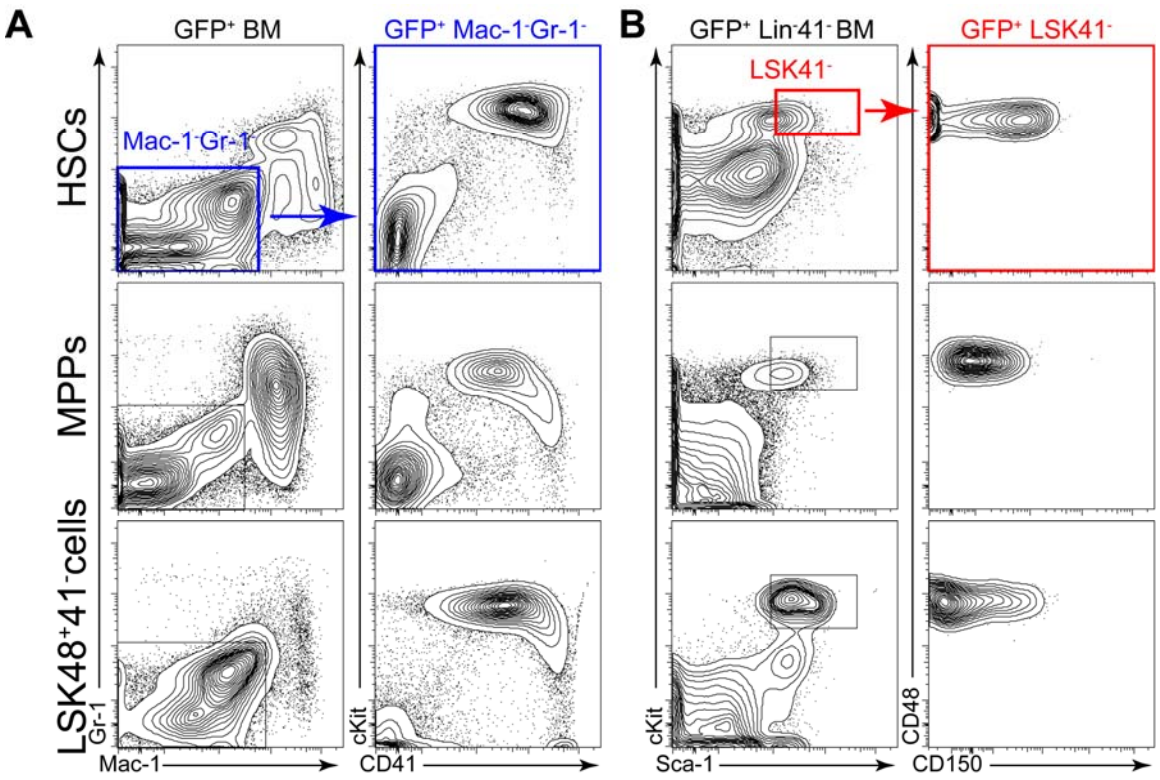

Figure 4.15: *Sox17* overexpression in purified adult bone marrow HSCs, MPPs and LSK48^{+}41^{-} cells resulted in a similar bone marrow reconstitution pattern after transplantation.

A) A similar expansion of donor-derived GFP^{+}CD41^{+} megakaryocytic cells and downregulation of Gr-1 on donor derived GFP^{+} myeloid cells were observed in the primary recipients of Sox17 virus infected adult HSCs, MPPs or LSk48^{+}41^{-} cells. B) Transplantation of Sox17 virus infected adult HSCs, MPPs or LSk48^{+}41^{-} cells led to a similar expansion of donor derived GFP^{+} LSK41^{-} cells and depletion of cells with an HSC phenotype.

Figure 4.16: *Sox17* overexpression increased the expression of genes associated with stem cell and fetal characteristics.
A-C) Gene set enrichment analysis (GSEA) comparing *Sox17*-overexpressing (red) versus control bone marrow (blue) $LSK48^{+}41^{-}$ cells. *Sox17*-overexpressing $LSK48^{+}41^{-}$ cells showed significantly increased expression of HSC-specific (compared to BM $LSK48^{+}41^{-}$ cells) and fetal HSC-specific (compared to BM HSCs) genes (A, C), and downregulation of differentiation-associated ($LSK48^{+}41^{-}$ cell specific, compared to HSCs) genes (B). NES means normailized enrichment score. D) Comparison of the gene expression profiles of *Sox17*-overexpressing and control bone marrow $LSK48^{+}41^{-}$ cells revealed 376 significantly upregulated and 264 significantly down-regulated genes in the Sox17-overexpressing cells (fold change >2 and $p<0.05$). Eighty-eight of the 376 upregulated genes were preferentially expressed by HSCs (compared to BM $LSK48^{+}41^{-}$ cells, fold >2, $p<0.05$), while 112 of the 264 downregulated genes were preferentially expressed by transiently reconstituting $LSK48^{+}41^{-}$ cells (compared to HSCs, fold >2, $p<0.05$). This suggests *Sox17* overexpression was associated with increased expression of genes preferentially expressed by HSCs and decreased expression of genes associated with differentiation/lineage restriction. Sixteen of the 78 highest up-regulated genes (fold>5) were preferentially expressed by fetal HSCs (compared to BM HSCs, fold >2, $p<0.05$) while only 4 of the 78 genes were preferentially expressed by adult HSCs (compared to fetal HSCs, fold>2, $p<0.05$); indicating *Sox17* overexpression increased the expression of certain fetal HSC genes. (*, numbers in parenthesis are number of significantly changed genes when using fold change >5 in the Sox17 vs. control $LSK48^{+}41^{-}$ cell comparison). E) qRT-PCR verification of selected genes from *Sox17*-overexpressing vs. control $LSK48^{+}41^{-}$ cell microarray. Red text indicates fold change was estimated using 35 cycles as the detection limit for transcripts that are not detected.

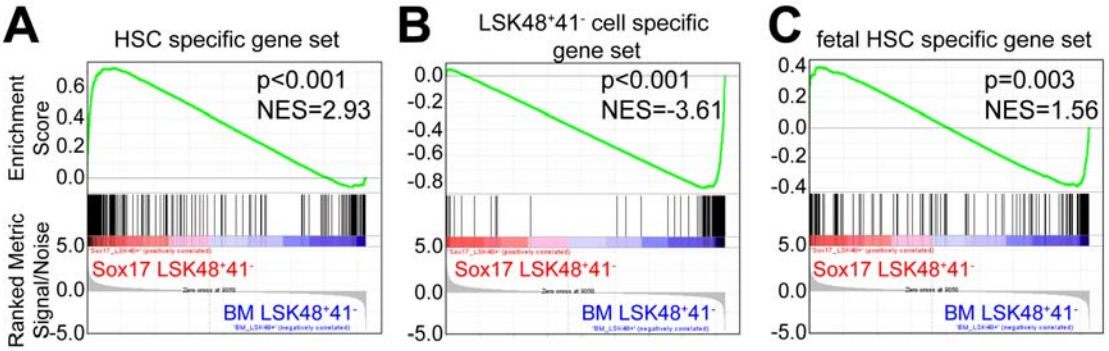

D

	# of genes						
	Total	HSC vs. LSK48+41-			FL HSC vs. BM HSC		
		UP	DOWN	N.C.	UP	DOWN	N.C.
Genes upregulated in Sox17-LSK48+41- cells (Fold >2; p<0.05)	376(78*)	88	7	281	27(16*)	31(4*)	318(58*)
	(100%)	23%	2%	75%	7%	8%	85%
Genes downregulated in Sox17-LSK48+41- cells (Fold>2; p<0.05)	264(33*)	12	112	140	31(4*)	36(12*)	197(17*)
	(100%)	5%	42%	53%	12%	14%	75%

E

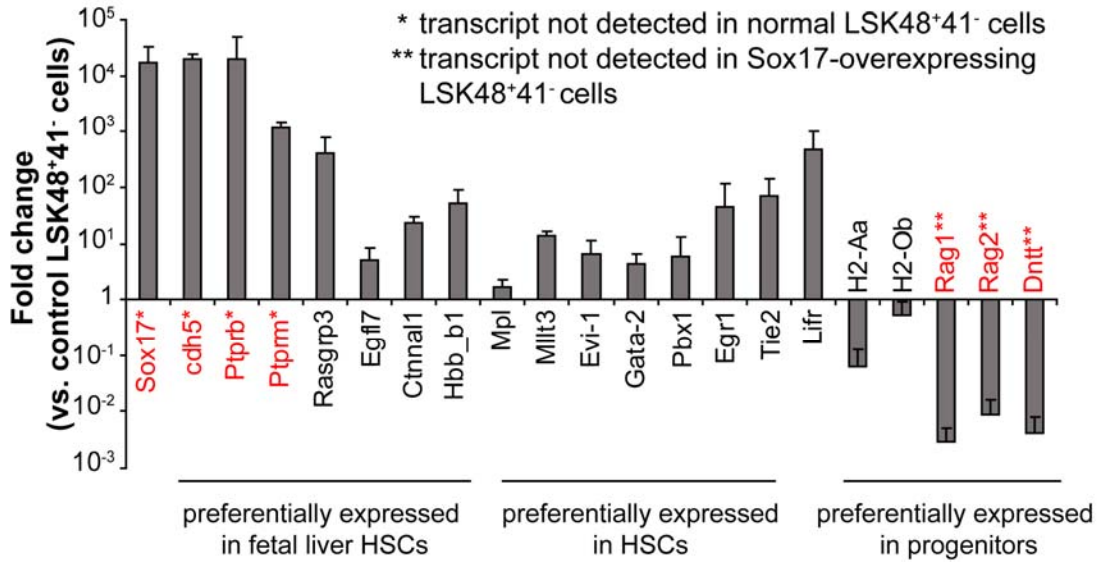

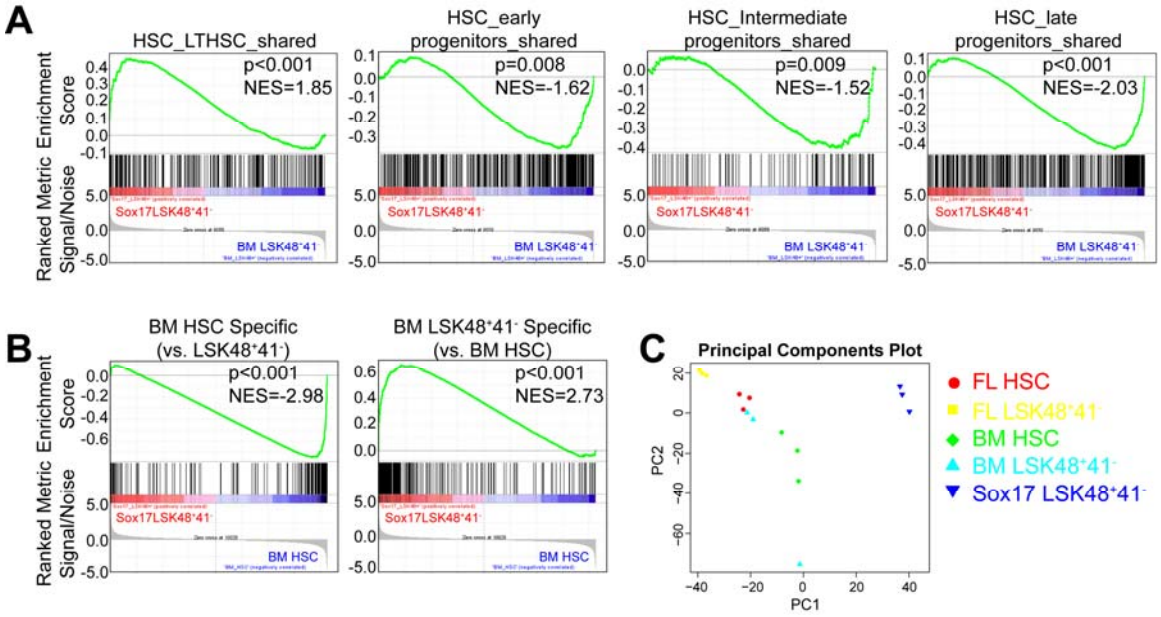

Figure 4.17: *Sox17* overexpression in LSK48^{+}41^{-} cells upregulated HSC specific genes and downregulated genes associated with lineage commitment/differentiation. A) GSEA profiles comparing *Sox17*-overexpressing (red) with control bone marrow (blue) LSK48^{+}41^{-} cells using C2-curated gene sets from the Broad Institute. *Sox17*-overexpressing LSK48^{+}41^{-} cells showed significant enrichment of LT-HSC specific genes and depletion of genes expressed by short-term hematopoietic progenitors at various stages of differentiation. B). GSEA profiles comparing *Sox17*-overexpressing LSK48^{+}41^{-} cells (red) with control bone marrow HSCs (blue) using customized gene sets containing genes preferentially expressed by bone marrow HSCs or LSK48^{+}41^{-} cells. *Sox17* overexpression did not fully convert LSK48^{+}41^{-} cells to HSCs as some genes that are preferentially expressed by HSCs were not upregulated by Sox17-overexpressing LSK48^{+}41^{-} cells. C) Principle components analysis of fetal liver HSCs, fetal liver LSK48^{+}41^{-} cells, bone marrow HSCs, bone marrow LSK48^{+}41^{-} cells and *Sox17*-overexpressing LSK48^{+}41^{-} cells. NES means normalized enrichment score.

Figure 4.18: Long-term *Sox17* overexpression induces nonlymphoid leukemias. A) Kaplan-Meier survival curve of primary recipients that received 1 million control or Sox17 virus infected whole bone marrow cells together with 200,000 cells for radioprotection (*, $p<0.01$ versus control, n=15-22 mice per group). B) Kaplan-Meier survival curve of secondary recipients that received three million whole bone marrow cells from control primary recipients or Sox17 primary recipients that developed nonlymphoid leukemia (*, $p<0.01$ vs. control, n=8-27 mice per group). C). H&E staining of representative tissue sections from control primary recipients and primary recipients that developed nonlymphoid leukemia. Infiltration of blast cells could be seen in spleen, liver and lung, resulting in the disruption of normal tissue architecture. Increased numbers of erythroid cells at various stages of differentiation could also be seen in the spleen of *Sox17*-overexpressing cell recipients (inset). D). The infiltrating blast cells in the spleen of *Sox17*-overexpressing bone marrow cell recipients stained positively for Von Willebrand factor (Vwf+, brown), suggesting megakaryocyte lineage origin. Only resident megakaryoctes and platelets stained positively for Vwf in control spleen sections. E) Wright-Giemsa staining of bone marrow, spleen, and/or liver cell cytospin samples from *Sox17*-overexpressing cell recipients showed the presence of leukemic blast cells and expanded erythroid cells. F) *Sox17*-overexpressing GFP^+CD41^+ cells had a morphology similar to the leukemia blast cells, and are also Vwf+.

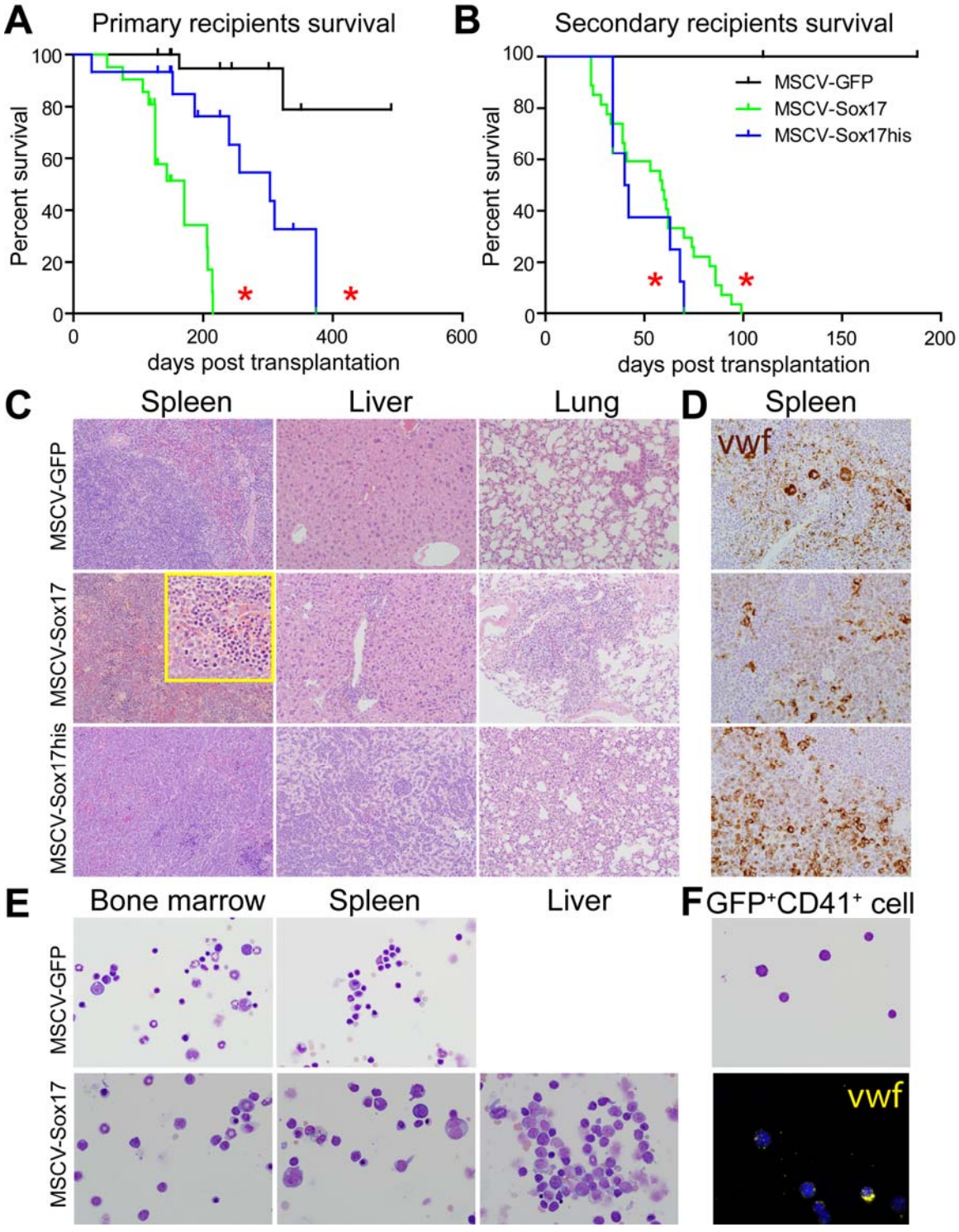
A
Primary recipients survival
Percent survival
days post transplantation
B
Secondary recipients survival
MSCV-GFP
MSCV-Sox17
MSCV-Sox17his
C
Spleen
Liver
Lung
MSCV-GFP
MSCV-Sox17
MSCV-Sox17his
D
Spleen
vwf
E
Bone marrow
Spleen
Liver
F
GFP+CD41+ cell
vwf

BIBLIOGRAPHY

Akashi, K., Traver, D., Miyamoto, T., and Weissman, I.L. (2000). A clonogenic common myeloid progenitor that gives rise to all myeloid lineages. Nature *404*, 193-197.

Alexander, W.S., Roberts, A.W., Nicola, N.A., Li, R., and Metcalf, D. (1996). Deficiencies in progenitor cells of multiple hematopoietic lineages and defective megakaryocytopoiesis in mice lacking the thrombopoietic receptor c-Mpl. Blood *87*, 2162-2170.

Alimzhanov, M.B., Kuprash, D.V., Kosco-Vilbois, M.H., Luz, A., Turetskaya, R.L., Tarakhovsky, A., Rajewsky, K., Nedospasov, S.A., and Pfeffer, K. (1997). Abnormal development of secondary lymphoid tissues in lymphotoxin beta-deficient mice. Proc Natl Acad Sci U S A *94*, 9302-9307.

Alvarez, J.D., Yasui, D.H., Niida, H., Joh, T., Loh, D.Y., and Kohwi-Shigematsu, T. (2000). The MAR-binding protein SATB1 orchestrates temporal and spatial expression of multiple genes during T-cell development. Genes Dev *14*, 521-535.

Bowie, M.B., Kent, D.G., Dykstra, B., McKnight, K.D., McCaffrey, L., Hoodless, P.A., and Eaves, C.J. (2007). Identification of a new intrinsically timed developmental checkpoint that reprograms key hematopoietic stem cell properties. Proc Natl Acad Sci U S A *104*, 5878-5882.

Bowie, M.B., McKnight, K.D., Kent, D.G., McCaffrey, L., Hoodless, P.A., and Eaves, C.J. (2006). Hematopoietic stem cells proliferate until after birth and show a reversible phase-specific engraftment defect. J Clin Invest *116*, 2808-2816.

Dobson, C.L., Warren, A.J., Pannell, R., Forster, A., Lavenir, I., Corral, J., Smith, A.J., and Rabbitts, T.H. (1999). The mll-AF9 gene fusion in mice controls myeloproliferation and specifies acute myeloid leukaemogenesis. Embo J *18*, 3564-3574.

Ficara, F., Murphy, M.J., Lin, M., and Cleary, M.L. (2008). Pbx1 regulates self-renewal of long-term hematopoietic stem cells by maintaining their quiescence. Cell Stem Cell *2*, 484-496.

Gilfillan, S., Dierich, A., Lemeur, M., Benoist, C., and Mathis, D. (1993). Mice lacking TdT: mature animals with an immature lymphocyte repertoire. Science (New York, NY *261*, 1175-1178.

Goyama, S., Yamamoto, G., Shimabe, M., Sato, T., Ichikawa, M., Ogawa, S., Chiba, S., and Kurokawa, M. (2008). Evi-1 is a critical regulator for hematopoietic stem cells and transformed leukemic cells. Cell Stem Cell *3*, 207-220.

Harrison, D.E., Zhong, R.K., Jordan, C.T., Lemischka, I.R., and Astle, C.M. (1997). Relative to adult marrow, fetal liver repopulates nearly five times more effectively long-term than short-term. Exp Hematol *25*, 293-297.

He, S., Iwashita, T., Buchstaller, J., Molofsky, A.V., Thomas, D., and Morrison, S.J. (2009). Bmi-1 overexpression in neural stem/progenitor cells increases proliferation and neurogenesis in culture but has little effect on these functions in vivo. Dev Biol *328*, 257-272.

Hock, H., Hamblen, M.J., Rooke, H.M., Schindler, J.W., Saleque, S., Fujiwara, Y., and Orkin, S.H. (2004). Gfi-1 restricts proliferation and preserves functional integrity of haematopoietic stem cells. Nature *431*, 1002-1007.

Hudson, C., Clements, D., Friday, R.V., Stott, D., and Woodland, H.R. (1997). Xsox17alpha and -beta mediate endoderm formation in Xenopus. Cell *91*, 397-405.

Ichikawa, M., Asai, T., Saito, T., Yamamoto, G., Seo, S., Yamazaki, I., Yamagata, T., Mitani, K., Chiba, S., Hirai, H., *et al.* (2004). AML-1 is required for megakaryocytic maturation and lymphocytic differentiation, but not for maintenance of hematopoietic stem cells in adult hematopoiesis. Nat Med *10*, 299-304.

Ikuta, K., Kina, T., Macneil, I., Uchida, N., Peault, B., Chien, Y.H., and Weissman, I.L. (1990). A developmental switch in thymic lymphocyte maturation potential occurs at the level of hematopoietic stem cells. Cell *62*, 863-874.

Irizarry, R.A., Hobbs, B., Collin, F., Beazer-Barclay, Y.D., Antonellis, K.J., Scherf, U., and Speed, T.P. (2003). Exploration, normalization, and summaries of high density oligonucleotide array probe level data. Biostatistics *4*, 249-264.

Ivanova, N.B., Dimos, J.T., Schaniel, C., Hackney, J.A., Moore, K.A., and Lemischka, I.R. (2002). A stem cell molecular signature. Science (New York, NY *298*, 601-604.

Jordan, C.T., and Lemischka, I.R. (1990). Clonal and systemic analysis of long-term hematopoiesis in the mouse. Genes and Development *4*, 220-232.

Jumaa, H., Wollscheid, B., Mitterer, M., Wienands, J., Reth, M., and Nielsen, P.J. (1999). Abnormal development and function of B lymphocytes in mice deficient for the signaling adaptor protein SLP-65. Immunity *11*, 547-554.

Kanai-Azuma, M., Kanai, Y., Gad, J.M., Tajima, Y., Taya, C., Kurohmaru, M., Sanai, Y., Yonekawa, H., Yazaki, K., Tam, P.P., *et al.* (2002). Depletion of definitive gut endoderm in Sox17-null mutant mice. Development *129*, 2367-2379.

Kantor, A.B., Stall, A.M., Adams, S., Herzenberg, L.A., and Herzenberg, L.A. (1992). Differential development of progenitor activity for three B-cell lineages. Proceedings of the National Academy of Sciences USA *89*, 3320-3324.

Kiel, M.J., Iwashita, T., Yilmaz, O.H., and Morrison, S.J. (2005a). Spatial differences in hematopoiesis but not in stem cells indicate a lack of regional patterning in definitive hematopoietic stem cells. Dev Biol *283*, 29-39.

Kiel, M.J., Yilmaz, O.H., Iwashita, T., Terhorst, C., and Morrison, S.J. (2005b). SLAM Family Receptors Distinguish Hematopoietic Stem and Progenitor Cells and Reveal Endothelial Niches for Stem Cells. Cell *121*, 1109-1121.

Kiel, M.J., Yilmaz, O.H., and Morrison, S.J. (2008). CD150- cells are transiently reconstituting multipotent progenitors with little or no stem cell activity. Blood *111*, 4413-4414.

Kikuchi, K., and Kondo, M. (2006). Developmental switch of mouse hematopoietic stem cells from fetal to adult type occurs in bone marrow after birth. Proc Natl Acad Sci U S A *103*, 17852-17857.

Kim, I., Saunders, T.L., and Morrison, S.J. (2007). Sox17 dependence distinguishes the transcriptional regulation of fetal from adult hematopoietic stem cells. Cell *130*, 470-483.

Kim, I., Yilmaz, O.H., and Morrison, S.J. (2005). CD144 (VE-cadherin) is transiently expressed by fetal liver hematopoietic stem cells. Blood *106*, 903-905.

Kimura, S., Roberts, A.W., Metcalf, D., and Alexander, W.S. (1998). Hematopoietic stem cell deficiencies in mice lacking c-Mpl, the receptor for thrombopoietin. Proc Natl Acad Sci U S A *95*, 1195-1200.

Kogan, S.C., Ward, J.M., Anver, M.R., Berman, J.J., Brayton, C., Cardiff, R.D., Carter, J.S., deCoronado, S., Downing, J.R., Fredrickson, T.N.*, et al.* (2002). Bethesda proposals for classification of nonlymphoid hematopoietic neoplasms in mice. Blood *100*, 238-245.

Komori, T., Okada, A., Stewart, V., and Alt, F.W. (1993). Lack of N regions in antigen receptor variable region genes of TdT-deficient lymphocytes. Science (New York, NY *261*, 1171-1175.

Koni, P.A., Sacca, R., Lawton, P., Browning, J.L., Ruddle, N.H., and Flavell, R.A. (1997). Distinct roles in lymphoid organogenesis for lymphotoxins alpha and beta revealed in lymphotoxin beta-deficient mice. Immunity *6*, 491-500.

Matsui, T., Kanai-Azuma, M., Hara, K., Matoba, S., Hiramatsu, R., Kawakami, H., Kurohmaru, M., Koopman, P., and Kanai, Y. (2006). Redundant roles of Sox17 and Sox18 in postnatal angiogenesis in mice. J Cell Sci *119*, 3513-3526.

Mikkola, H.K., Klintman, J., Yang, H., Hock, H., Schlaeger, T.M., Fujiwara, Y., and Orkin, S.H. (2003). Haematopoietic stem cells retain long-term repopulating activity and multipotency in the absence of stem-cell leukaemia SCL/tal-1 gene. Nature *421*, 547-551.

Mikkola, H.K., and Orkin, S.H. (2006). The journey of developing hematopoietic stem cells. Development *133*, 3733-3744.

Min, I.M., Pietramaggiori, G., Kim, F.S., Passegue, E., Stevenson, K.E., and Wagers, A.J. (2008). The transcription factor EGR1 controls both the proliferation and localization of hematopoietic stem cells. Cell Stem Cell *2*, 380-391.

Molofsky, A.V., Pardal, R., Iwashita, T., Park, I.K., Clarke, M.F., and Morrison, S.J. (2003). Bmi-1 dependence distinguishes neural stem cell self-renewal from progenitor proliferation. Nature *425*, 962-967.

Mombaerts, P., Iacomini, J., Johnson, R.S., Herrup, K., Tonegawa, S., and Papaioannou, V.E. (1992). RAG-1-deficient mice have no mature B and T lymphocytes. Cell *68*, 869-877.

Mootha, V.K., Lindgren, C.M., Eriksson, K.F., Subramanian, A., Sihag, S., Lehar, J., Puigserver, P., Carlsson, E., Ridderstrale, M., Laurila, E.*, et al.* (2003). PGC-1 alpha-responsive genes involved in oxidative phosphorylation are coordinately downregulated in human diabetes. Nature Genetics *34*, 267-273.

Morrison, S.J., Hemmati, H.D., Wandycz, A.M., and Weissman, I.L. (1995). The purification and characterization of fetal liver hematopoietic stem cells. Proc Natl Acad Sci U S A *92*, 10302-10306.

Morse, H.C., Anver, M.R., Fredrickson, T.N., Haines, D.C., Harris, A.W., Harris, N.L., Jaffe, E.S., Kogan, S.C., MacLennan, I.C.M., Pattengale, P.K.*, et al.* (2002). Bethesda proposals for classification of lymphoid neoplasms in mice. Blood *100*, 246-258.

Naviaux, R.K., Costanzi, E., Haas, M., and Verma, I.M. (1996). The pCL vector system: rapid production of helper-free, high-titer, recombinant retroviruses. J Virol *70*, 5701-5705.

Niakan, K.K., Ji, H., Maehr, R., Vokes, S.A., Rodolfa, K.T., Sherwood, R.I., Yamaki, M., Dimos, J.T., Chen, A.E., Melton, D.A.*, et al.* (2010). Sox17 promotes differentiation in mouse embryonic stem cells by directly regulating extraembryonic gene expression and indirectly antagonizing self-renewal. Genes Dev *24*, 312-326.

Okuda, T., Deursen, J.v., Hiebert, S.W., Grosveld, G., and Downing, J.R. (1996). AML1, the target of multiple chromosomal translocations in human leukemia, is essential for normal fetal liver hematopoiesis. Cell *84*, 321-330.

Orkin, S.H., and Zon, L.I. (2008). Hematopoiesis: an evolving paradigm for stem cell biology. Cell *132*, 631-644.

Pappu, R., Cheng, A.M., Li, B., Gong, Q., Chiu, C., Griffin, N., White, M., Sleckman, B.P., and Chan, A.C. (1999). Requirement for B cell linker protein (BLNK) in B cell development. Science (New York, NY *286*, 1949-1954.

Park, I.K., Qian, D., Kiel, M., Becker, M.W., Pihalja, M., Weissman, I.L., Morrison, S.J., and Clarke, M.F. (2003). Bmi-1 is required for maintenance of adult self-renewing haematopoietic stem cells. Nature *423*, 302-305.

Park, K.S., Wells, J.M., Zorn, A.M., Wert, S.E., and Whitsett, J.A. (2006). Sox17 influences the differentiation of respiratory epithelial cells. Dev Biol *294*, 192-202.

Phillips, R.L., Ernst, R.E., Brunk, B., Ivanova, N., Mahan, M.A., Deanehan, J.K., Moore, K.A., Overton, G.C., and Lemischka, I.R. (2000). The genetic program of hematopoietic stem cells. Science (New York, NY *288*, 1635-1640.

Pina, C., May, G., Soneji, S., Hong, D., and Enver, T. (2008). MLLT3 regulates early human erythroid and megakaryocytic cell fate. Cell Stem Cell *2*, 264-273.

Porcher, C., Swat, W., Rockwell, K., Fujiwara, Y., Alt, F.W., and Orkin, S.H. (1996). The T cell leukemia oncoprotein SCL/tal-1 is essential for development of all hematopoietic lineages. Cell *86*, 47-57.

Pronk, C.J.H., Rossi, D.J., Mansson, R., Attema, J.L., Norddahl, G.L., Chan, C.K.F., Sigvardsson, M., Weissman, I.L., and Bryder, D. (2007). Elucidation of the phenotypic, functional, and molecular topography of a myeloerythroid progenitor cell hierarchy. Cell Stem Cell *1*, 428-442.

Robb, L., Elwood, N., Elefanty, A., Kontgen, F., Li, R., Barnett, L., and Begley, C. (1996). The scl gene is required for the generation of all hematopoietic lineages in the adult mouse. EMBO Journal *15*, 4123-4129.

Shamir, R., Maron-Katz, A., Tanay, A., Linhart, C., Steinfeld, I., Sharan, R., Shiloh, Y., and Elkon, R. (2005). EXPANDER--an integrative program suite for microarray data analysis. BMC Bioinformatics *6*, 232.

Shinkai, Y., Rathbun, G., Lam, K.P., Oltz, E.M., Stewart, V., Mendelsohn, M., Charron, J., Datta, M., Young, F., Stall, A.M.*, et al.* (1992). RAG-2-deficient mice lack mature lymphocytes owing to inability to initiate V(D)J rearrangement. Cell *68*, 855-867.

Shivdasani, R.A., Mayer, E.L., and Orkin, S.H. (1995). Absence of blood formation in mice lacking the T-cell leukaemia oncoprotein tal-1/SCL. Nature *373*, 432-434.

Subramanian, A., Tamayo, P., Mootha, V.K., Mukherjee, S., Ebert, B.L., Gillette, M.A., Paulovich, A., Pomeroy, S.L., Golub, T.R., Lander, E.S.*, et al.* (2005). Gene set enrichment analysis: A knowledge-based approach for interpreting genome-wide expression profiles. Proc Natl Acad Sci U S A *102*, 15545-15550.

Tober, J., Koniski, A., McGrath, K.E., Vemishetti, R., Emerson, R., de Mesy-Bentley, K.K., Waugh, R., and Palis, J. (2007). The megakaryocyte lineage originates from hemangioblast precursors and is an integral component both of primitive and of definitive hematopoiesis. Blood *109*, 1433-1441.

Tsai, F.-Y., Keller, G., Kuo, F.C., Weiss, M., Chen, J., Rosenblatt, M., Alt, F.W., and Orkin, S.H. (1994). An early haematopoietic defect in mice lacking the transcription factor GATA-2. Nature *371*, 221-226.

Van Parijs, L., Refaeli, Y., Lord, J.D., Nelson, B.H., Abbas, A.K., and Baltimore, D. (1999). Uncoupling IL-2 signals that regulate T cell proliferation, survival, and Fas-mediated activation-induced cell death. Immunity *11*, 281-288.

Wang, Q., Stacy, T., Binder, M., Marin-Padilla, M., Sharpe, A.H., and Speck, N.A. (1996). Disruption of the Cbfa2 gene causes necrosis and hemorrhaging in the central nervous system and blocks definitive hematopoiesis. Proc Natl Acad Sci U S A *93*, 3444-3449.

Yasunaga, M., Tada, S., Torikai-Nishikawa, S., Nakano, Y., Okada, M., Jakt, L.M., Nishikawa, S., Chiba, T., and Era, T. (2005). Induction and monitoring of definitive and visceral endoderm differentiation of mouse ES cells. Nat Biotechnol *23*, 1542-1550.

Yilmaz, O.H., Valdez, R., Theisen, B.K., Guo, W., Ferguson, D.O., Wu, H., and Morrison, S.J. (2006). Pten dependence distinguishes haematopoietic stem cells from leukaemia-initiating cells. Nature *441*, 475-482.

CHAPTER 5

HEMATOPOIETIC STEM CELLS DO NOT ASYMMETRICALLY SEGREGATE CHROMOSOMES OR RETAIN BROMO-DEOXYURIDINE[1]

SUMMARY

Stem cells are proposed to asymmetrically segregate chromosomes during self-renewing divisions such that older ('immortal') DNA strands are retained in daughter stem cells while newly-synthesized strands segregate to differentiating cells (Cairns, 1975; Conboy et al., 2007; Karpowicz et al., 2005; Potten et al., 1978; Shinin et al., 2006; Smith, 2005). Stem cells are also proposed to retain DNA labels, like bromo-deoxyuridine (BrdU), either because they segregate chromosomes asymmetrically or because they divide slowly (Cotsarelis et al., 1990; Shinin et al., 2006; Tumbar et al., 2004; Zhang et al., 2003). However, the purity of stem cells among BrdU label-retaining cells has not been documented in any tissue and the 'immortal strand hypothesis' has not been tested in a system with definitive stem cell markers. We tested these hypotheses in hematopoietic stem cells (HSCs), which can be highly purified using well-characterized markers. We administered BrdU to newborn, cyclophosphamide/G-CSF mobilized, and normal adult mice for 4 to 10 days, followed by 70-days without BrdU. In each case, less than 6% of HSCs retained BrdU and less than 0.5% of all BrdU-retaining hematopoietic

---

[1] Originally published in *Nature. 2007; 449:238-42* with authors listed as Kiel., M.J., **He, S.**, Ashkenazi, R., Gentry, S.N., Teta, M., Kushner, J.A., Jackson, T.L. and Morrison, S.J.

cells were HSCs, revealing poor specificity and poor sensitivity as an HSC marker. Sequential administration of chloro-deoxyuridine (CldU) and iodo-deoxyuridine (IdU) suggested that all HSCs segregate their chromosomes randomly. Division of individual HSCs in culture revealed no asymmetric segregation of label. HSCs therefore cannot be identified based on BrdU label-retention and do not retain older DNA strands during division, indicating these are not general properties of stem cells.

INTRODUCTION

The 'immortal strand hypothesis' was proposed as a mechanism by which stem cells could avoid accumulating mutations that arise during DNA replication (Cairns, 1975). While most cells segregate their chromosomes randomly (Armakolas and Klar, 2006; Potten et al., 1978), it was argued that adult stem cells in steady-state tissues might retain older strands during asymmetric self-renewing divisions, segregating newly-synthesized strands to daughters fated to differentiate (Figure 5.1a). Evidence has supported this model in some epithelial stem cells (Potten et al., 1978), neural stem cells (Karpowicz et al., 2005), mammary epithelial progenitors (Smith, 2005), and muscle satellite cells (Conboy et al., 2007; Shinin et al., 2006). A related idea is that adult stem cells in steady-state tissues might consistently retain DNA labels, either because chromosomes segregate randomly but stem cells divide more infrequently than other cells (Figure 5.1b) or because the older DNA strand is labeled and segregated asymmetrically (Figure 5.1c). Tritiated thymidine (Cotsarelis et al., 1990) or histone (Tumbar et al., 2004) label-retaining cells from the hair follicle are enriched for epithelial stem cells, though purity remains uncertain. Label-retaining cells have also been identified in the

hematopoietic system (Arai et al., 2004; Zhang et al., 2003), in mammary epithelium (Welm et al., 2002), in intestinal epithelium (Potten et al., 1978; Potten et al., 2002), and in the heart (Urbanek et al., 2006), but the purity of stem cells among these label-retaining cells has not been tested. As a result, it remains uncertain whether label-retention can identify stem cells with specificity or sensitivity.

Under steady-state conditions in adult bone marrow, all HSCs divide regularly but infrequently (Cheshier et al., 1999a) to sustain hematopoiesis as well as to maintain nearly constant numbers of HSCs. As a result of this observation, as well as the observation that HSC divisions yield asymmetric outcomes in culture (Takano et al., 2004), it has been proposed that adult HSCs divide asymmetrically (Takano et al., 2004), though the rarity of HSCs *in vivo* and their relative quiescence has made it impossible to confirm this directly. Nonetheless, if BrdU label-retention and/or asymmetric chromosome segregation are general properties of adult stem cells, then either or both of these characteristics should be evident in HSCs, depending on experimental conditions.

RESULTS AND DISCUSSION

To test the rate at which HSCs go into cycle we administered BrdU to mice for 1, 4, or 10 days, then sorted HSCs onto microscope slides and stained with an anti-BrdU antibody. HSCs were sorted as $CD150^{+}CD48^{-}CD41^{-}lineage^{-}Sca\text{-}1^{+}c\text{-}kit^{+}$ cells (Figure 5.2a). This population contains all of the detectable HSC activity in bone marrow and 47% of single cells from this population give long-term multilineage reconstitution in irradiated mice (Kiel et al., 2005b). After 1 to 10 days of BrdU, 51 to 94% of whole bone marrow cells and 6.5 to 46% of $CD150^{+}CD48^{-}CD41^{-}lineage^{-}Sca\text{-}1^{+}c\text{-}kit^{+}$ HSCs became

$BrdU^+$ (Figure 5.2c,d). We calculated the rate at which HSCs went into cycle (Cheshier et al., 1999a) as 6.0% per day (Figure 5.2e). Consistent with this, only 3.2% of $CD150^+CD48^-CD41^-lineage^-Sca\text{-}1^+c\text{-}kit^+$ cells were in S/G2/M phase of the cell cycle at any one time (Figure 5.3). These results are similar to a prior study that identified HSCs with somewhat different markers (Cheshier et al., 1999a).

The linearity of BrdU incorporation over time (Figure 5.2e) suggests that most HSCs divide at a similar rate. If a minority of HSCs divided more rapidly, significantly more than 6.0% of HSCs should have incorporated BrdU after one day; however, we did not observe this (Figure 5.2d). If a minority of HSCs were more deeply quiescent than most other HSCs, these HSCs should remain BrdU negative even after long periods of BrdU. This also has not been observed as more than 99% of HSCs are labeled after six months of BrdU (Cheshier et al., 1999a). Therefore, there is no evidence for more rapidly dividing or more slowly dividing subsets of long-term self-renewing HSCs under steady-state conditions, though we cannot exclude the possibility that a minority of HSCs divide somewhat more slowly than 6% per day.

To evaluate BrdU label-retention, we administered BrdU for 10 days, followed by a 70 day chase without BrdU, similar to prior studies in the hematopoietic system (Arai et al., 2004; Zhang et al., 2003). Given that 6.0% of HSCs entered cycle each day and 46% of HSCs were labeled after 10 days of BrdU (Figure 5.2d), we modeled the fraction of HSCs that would be expected to retain BrdU over time (Figure 5.4a; see Materials and Methods for explanation).

If HSCs follow the immortal strand model they should lose their BrdU only one division after BrdU is discontinued as the labeled chromosomes are segregated to

differentiating daughter cells (Figure 5.1a), and only 0.6% of HSCs would be expected to retain BrdU after 70 days without BrdU (Figure 5.4a). If HSCs segregate chromosomes randomly, then BrdU would be lost stochastically over time and the fraction of $BrdU^+$ HSCs after a 70 day chase would depend upon the threshold of BrdU required for detection. If the threshold is equivalent to 0.5N labeled chromosomes (one quarter of the genome), this level of BrdU dilution could be achieved in cells that had divided 1 or 2 times after BrdU was discontinued (depending on whether they had divided once or twice in the presence of BrdU), and only 1.4% of HSCs would be expected to retain BrdU after the 70 day chase (Figure 5.4a). In contrast, if the threshold of detection is equivalent to 0.0625N labeled chromosomes, this could be achieved on average in cells that had divided 4 or 5 times after BrdU was discontinued, and 19.8% of HSCs would be expected to retain BrdU after the 70 day chase (Figure 5.4a). These calculations thus predict that few (<20%) HSCs should retain BrdU after a 70-day chase, irrespective of how chromosomes are segregated.

To test this we administered BrdU for 10 days then stained whole bone marrow cells and $CD150^+CD48^-CD41^-lineage^-Sca\text{-}1^+c\text{-}kit^+$ HSCs after 40, 70, and 120 days of chase. After 70 days of chase, 0.4±0.1% of bone marrow cells and 4.6±0.9% of HSCs were $BrdU^+$ (Figure 5.4c). This demonstrates, as predicted (Figure 5.4a), that few HSCs retain BrdU. Moreover, only 2.0±1.0% of HSCs were $BrdU^+$ after 120 days of chase, demonstrating that the frequency of BrdU-retaining HSCs continues to decline over time rather than identifying a deeply quiescent subset of HSCs that retains BrdU indefinitely. Although BrdU label-retaining cells were 10-fold enriched in the HSCs, the rarity of HSCs means that only 0.08% of $BrdU^+$ bone marrow cells were HSCs (0.0066% x

4.6%/0.4%). BrdU label-retention is therefore a very insensitive and non-specific marker of HSCs as the vast majority of HSCs did not retain detectable BrdU, and only rare BrdU label-retaining cells were HSCs. Very similar results were obtained when we used flow-cytometry to detect BrdU incorporation (Figure 5.5) or when HSCs were isolated using different surface markers (c-kit$^+$Flk-2$^-$lineage$^-$Sca-1$^+$ cells; Figure 5.6). These data are most consistent with random chromosome segregation by HSCs and the failure to detect BrdU after approximately 3 divisions in the absence of BrdU (Figure 5.4a).

According to the immortal strand model, stem cells can incorporate BrdU into DNA strands that become the 'older' strands during symmetric cell divisions and these labeled DNA strands would be retained indefinitely by stem cells that resume asymmetric divisions (Figure 5.1c). To test this, we administered BrdU to newborn mice for 10 days or to cyclophosphamide/G-CSF treated mice for 4 days. The absolute number of HSCs expands dramatically in both newborn (Bowie et al., 2006) and cyclophosphamide/G-CSF mobilized mice (Morrison et al., 1997b) (indicating symmetric divisions), before stabilizing to steady-state levels as mice enter adulthood or G-CSF is discontinued. After 10 days of BrdU in neonatal mice, 93±3.7% of bone marrow cells and 80±11% of CD150$^+$CD48$^-$CD41$^-$lineage$^-$Sca-1$^+$c-kit$^+$ HSCs were BrdU$^+$. Seventy days later, 0.1% of bone marrow cells and 6.4±2.5% of CD150$^+$CD48$^-$CD41$^-$lineage$^-$Sca-1$^+$c-kit$^+$ HSCs were BrdU$^+$ (Figure 5.4d). After 4 days of BrdU in mobilized mice, 94±3% of CD150$^+$CD48$^-$CD41$^-$lineage$^-$Sca-1$^+$c-kit$^+$ HSCs were BrdU$^+$. Seventy days later, 0.1% of bone marrow cells and 2.1±1.1% of CD150$^+$CD48$^-$CD41$^-$lineage$^-$Sca-1$^+$c-kit$^+$ HSCs were BrdU$^+$ (Figure 5.4d). Thus even when BrdU was administered to symmetrically dividing HSCs, only 2 to 6% of HSCs retained the label and only 0.2% to 0.4% of BrdU-retaining bone

marrow cells were HSCs. We were unable to identify any context in which BrdU label-retention identified HSCs with sensitivity or specificity, and none of these results were consistent with the immortal strand hypothesis.

To address the possibility that the HSCs in the above experiments might have continued to divide symmetrically after BrdU was discontinued we also administered BrdU to mice from 20 to 29 days postnatally. HSCs are thought to transition from rapidly dividing cells with a fetal phenotype to relatively quiescent cells with an adult phenotype between 21 and 28 days postnatally (Bowie et al., 2006). We obtained similar results with only 6.5±1.1% of HSCs retaining BrdU after a 70-day chase. There was therefore no period during neonatal development when BrdU could be administered in a way that resulted in retention within significant numbers of HSCs.

To test the immortal strand model directly, we treated mice with 10 days of CldU then 10 days of IdU. If HSCs segregate older and younger DNA strands asymmetrically, then HSCs should rarely incorporate both CldU and IdU under steady-state conditions because newly synthesized (labeled) DNA strands should be segregated to differentiating daughter cells after each division (Figure 5.7a). In contrast, if HSCs segregate older and younger DNA strands randomly then CldU-labeled HSCs should have the same chance of incorporating IdU as unlabeled cells and approximately 25% (50% x 50%) of HSCs should be double labeled (Figure 5.7b).

After 10 days of CldU followed by 10 to 11 days of IdU we observed that 14% of HSCs incorporated only CldU, 32% of HSCs incorporated only IdU, and 27% of HSCs incorporated both CldU and IdU (Figure 5.7c; Figure 5.8). The frequency of $CldU^+IdU^+$ cells (27%) was therefore similar to the product of the frequencies of total $CldU^+$ cells

and total IdU^+ cells (41% x 59%=24%) indicating that $CldU^+$ cells had a similar probability of incorporating IdU as other cells. We repeated this experiment by administering CldU to mice for 60 days followed by 15 days of IdU, and found the frequency of $CldU^+IdU^+$ cells (63%) was again similar to the product of the frequencies of total $CldU^+$ cells and total IdU^+ cells (73% x 84%=61%). These results were not significantly affected by a slow clearance of CldU from mice, as CldU was cleared in less than 1 day after being discontinued from the drinking water (Figure 5.9). These observations directly contradict a key prediction made by the immortal strand hypothesis but are as would be expected by random chromosome segregation.

The foregoing experiments left the formal possibility that if HSCs divide by a combination of symmetric and asymmetric divisions *in vivo* we might underestimate the frequency of HSCs that retain older DNA strands. To address this we examined the division of individual HSCs in culture that were isolated from mice treated for 10 days with BrdU. Single $CD150^+CD48^-CD41^-lineage^-Sca\text{-}1^+c\text{-}kit^+$ HSCs were sorted into cultures under conditions in which half of HSC divisions give asymmetric outcomes (daughter cells with different developmental potentials) (Takano et al., 2004). After 2 to 3 days of culture we observed a total of 346 colonies in which HSCs had divided once (2 daughter cells) or twice (3 or 4 daughter cells). Either all daughter cells were $BrdU^+$ (162 colonies; 46%) or all daughter cells were $BrdU^-$ (184 colonies) (Figure 5.7f) as would be expected by random chromosome segregation given that 46% of HSCs incorporate BrdU *in vivo* after 10 days (Figure 5.2d). We observed no colonies after 1 or 2 rounds of division that contained a mixture of $BrdU^+$ and $BrdU^-$ cells. These *in vitro* experiments

on individual HSCs thus failed to detect any asymmetric segregation of labeled chromosomes.

Our results were not confounded by effects of BrdU/CldU/IdU on HSC proliferation, survival, or DNA repair. The cell cycle status (Figure 5.3) and frequency (data not shown) of HSCs was not affected by these treatments. BrdU/CldU/IdU incorporation from DNA repair was not detectable (Figure 5.3).

Our results indicate that BrdU label-retention is neither a sensitive nor a specific marker of HSCs. Nonetheless BrdU label-retention could be a better marker of stem cells in other tissues. Moreover, histone-GFP (Tumbar et al., 2004) may do a better job of marking stem cells, including HSCs, because it can be selectively expressed in subsets of progenitors and may be retained with different kinetics than BrdU. Our data demonstrate the need to test the sensitivity and specificity of BrdU and other label-retention markers before assuming they mark stem cells with fidelity.

Our data also demonstrate that the immortal strand model (Cairns, 1975) does not apply to HSCs and cannot be considered a general model of stem cell division. Our data do not address whether stem cells from other tissues asymmetrically segregate chromosomes or whether HSCs segregate a limited number of chromosomes asymmetrically (Armakolas and Klar, 2006). Nonetheless, asymmetric chromosome segregation cannot be a mechanism by which HSCs avoid accumulating mutations over time.

MATERIALS AND METHORDS

BrdU/CldU/IdU administration

All experiments employed C57BL/Ka-CD45.2:Thy-1.1 mice. For experiments in adult mice, BrdU (Sigma, St. Louis, MO) was administered when the mice were 8 to 10 weeks of age. Mice were given an intraperitoneal injection of 100 mg of BrdU/kg of body mass in Dulbecco's phosphate buffered saline (DPBS; Gibco, Carlsbad, CA) and maintained on 1 mg/ml of BrdU in the drinking water for 1 to 10 days. Amber bottles containing BrdU water were changed every 1 to 3 days. For retention studies, BrdU water was replaced with regular water and the mice were maintained for 40 to 120 days before analysis.

BrdU injections into neonatal mice were performed as described (Taylor et al., 2000). Beginning within 3 days after birth, neonatal mice were injected subcutaneously with 50 mg BrdU/kg body weight twice daily for 10 days. Mice were weighed every two days and the dose of BrdU was adjusted.

To assess BrdU retention following cytokine mobilization, adult mice were injected with cyclophosphamide (200 mg/kg; Bristol-Myers Squibb, New York) and then on each of 4 subsequent days with 250 μg/kg per day of human G-CSF (Amgen, Thousand Oaks, CA)(Morrison et al., 1997b). On the fourth day of G-CSF injection, a single intraperitoneal injection of 100 mg BrdU/kg of body mass was given and the mice were put on 1 mg/ml BrdU water for 4 additional days. The mice were then returned to regular water for 70 days before analysis.

For 5-chloro-2-deoxyuridine (CldU) and 5-iodo-2-deoxyuridine (IdU) experiments, mice were given an intraperitoneal injection of 100 mg of CldU/kg of body

mass in DPBS and maintained on 1 mg/ml of CldU (Sigma) in the drinking water for 10 days. Mice were then given an intraperitoneal injection of 100 mg of IdU/kg of body mass in DPBS, and switched to 1 mg/ml of IdU (Sigma) in the drinking water for 10 to 11 days before being sacrificed.

For details related to the flow-cytometric isolation of HSCs and CldU/IdU/BrdU staining see Supplementary Materials.

BrdU segregation in cultured HSCs

Single $CD150^{+}CD48^{-}CD41^{-}lineage^{-}Sca\text{-}1^{+}c\text{-}kit^{+}$ HSCs were sorted from BrdU-treated mice into a V-bottom 96-well plate containing Stempro-34 medium (Invitrogen) supplemented with 2 mM L-glutamine, 50 μM 2-mercaptoethanol (Sigma), murine IL-3 (10 ng/ml), murine SCF (100 ng/ml) and murine Tpo (100 ng/ml; all cytokines from R&D Systems) with 10% charcoal absorbed fetal bovine serum (Cocalico Biologicals, Inc., Reamstown, PA) and cultured for 2 to 3 days in low oxygen chambers (Morrison et al., 2000). For analysis, plates were centrifuged at 500xg for 10 minutes, then cells from each colony were pipetted onto individual wells of Teflon printed glass slides and allowed to dry overnight prior to staining for BrdU and DAPI.

Flow-cytometric isolation of HSCs

Bone marrow cells were flushed from the long bones (tibias and femurs) with Hank's buffered salt solution without calcium or magnesium, supplemented with 2% heat-inactivated calf serum (GIBCO, Grand Island, NY; $HBSS^{+}$). Cells were triturated and filtered through nylon screen (45 um, Sefar America, Kansas City, MO) to obtain a single cell suspension. For isolation of $Flk2^{-}lineage^{-}Sca\text{-}1^{+}c\text{-}kit^{+}$ HSCs, whole bone

marrow cells were incubated with PE-conjugated monoclonal antibodies against lineage markers including B220 (6B2), CD3 (KT31.1), CD4 (GK1.5), CD8 (53-6.7), Gr-1 (8C5), Mac-1 (M1/70), Flk-2 (A2F10.1), Ter119, and IgM in addition to FITC-conjugated anti-Sca-1 (Ly6A/E) and biotin-conjugated anti-c-kit (2B8) antibodies, followed by streptavidin APC-Cy7. For isolation of $CD150^{+}CD48^{-}CD41^{-}lineage^{-}Sca\text{-}1^{+}c\text{-}kit^{+}$ HSCs, whole bone marrow cells were incubated with PE-conjugated anti-CD150 (TC15-12F12.2; BioLegend, San Diego, California), FITC-conjugated anti-CD48 (HM48-1; BioLegend), FITC-conjugated anti-CD41 (MWReg30; BD Pharmingen, San Diego, California), APC-conjugated anti-Sca-1 (E13-6.7), and biotin-conjugated anti-c-kit (2B8) antibody, in addition to FITC-conjugated antibodies against Ter119, B220 (6B2), Gr-1 (8C5) and CD2 (RM2-5). HSCs were frequently pre-enriched by selecting $c\text{-}kit^{+}$ cells using paramagnetic microbeads and autoMACS (Miltenyi Biotec, Auburn, CA). All flow-cytometry was performed on a FACSVantage SE-dual laser, three-line flow-cytometer (Becton-Dickinson).

BrdU staining

Staining for BrdU on slides was performed as previously described using an anti-BrdU antibody (clone BU1/75, Accurate Chemical and Scientific Corp, Westbury, NY)(Cheshier et al., 1999a). HSCs were sorted and then resorted (to ensure purity) onto glass slides in 25 to 100 cell spots, allowed to dry for 1 hour and stored at $-80^{o}C$ for up to 4 weeks. Slides were thawed at room temperature for 15 minutes, fixed in 70% ethanol at –20°C for 30 minutes, rinsed in 0.1M phosphate buffer (PB) twice, incubated in 2N HCl with 0.8% Triton in PB for 30 minutes, incubated in 0.1M Sodium Borate (pH 8.5) for 15 minutes, then rinsed in 0.1M PB at room temperature, at $37^{o}C$, and at room temperature

again. The slides were then incubated with 0.3% Triton in 0.1M PB supplemented with 5% Goat Serum for 1 hour at 4°C. Slides were incubated at 4°C overnight with the primary anti-BrdU antibody that specifically recognizes BrdU and CldU but does not recognize IdU (clone BU1/75, Accurate Chemical and Scientific Corp.). Slides were then rinsed in 0.1M PB twice and incubated with Alexa488-conjugated goat anti-rat IgG (Invitrogen-Molecular Probes, Carlsbad, California) for 2 hours at room temperature. Slides were rinsed in 0.1M PB twice and incubated with DAPI for 1 hour at room temperature. Finally, slides were rinsed three times in 0.1M PB, the excess buffer was shaken off and the slides were mounted in 70% glycerol in PBS. Images were gathered using an Olympus BX-51 florescence microscope equipped with a Cooke Pixelfly CCD camera.

In some experiments, BrdU incorporation was measured by flow-cytometry using an antibody directly conjugated to allophycocyanin (APC; APC BrdU flow kit, BD Pharmingen). Sorted samples were fixed and permeablized according to manufacturer's instructions, incubated in 2N HCl for 30 minutes at room temperature, neutralized in 0.1M Sodium Borate (pH 8.5), washed in 0.5% Triton in DPBS, stained with anti-BrdU APC and resuspended in DAPI (10 μg/ml) prior to FACS analysis. All flow-cytometry was performed on a FACSVantage SE-dual laser, three-line flow-cytometer (Becton-Dickinson).

CldU and IdU double-labeling

Slides were processed as for BrdU analysis with the addition of a subsequent set of staining steps using a second anti-IdU antibody (clone B44, BD Pharmingen) that does not recognize CldU. Slides were incubated at room temperature in anti-IdU antibody for

2 to 3 hours. Immunofluorescence was developed using a Cy3-conjugated anti-mouse IgG secondary antibody with minimal cross reactivity to rat IgG (Jackson Immunoresearch). Cells isolated from mice that had only received CldU, or only received IdU, or neither were processed in parallel with experimental samples, and demonstrated no cross-reactivity or background staining from primary or secondary antibodies.

Analysis of cell cycle distribution and cell death in HSCs

Cell cycle distribution was analyzed by Hoechst 33342 (Invitrogen-Molecular Probes, Carlsbad, California) staining. $CD150^{+}CD48^{-}CD41^{-}lineage^{-}Sca\text{-}1^{+}c\text{-}kit^{+}$ HSCs were sorted and resorted into ice-cold 70% ethanol and stored at –20^{o}C overnight. Cells were resuspended in PBS containing 0.02 mg/ml Hoechst 33342, incubated for 30 minutes and analyzed by flow-cytometry using a UV laser.

For activated caspase-3 staining, frozen slides bearing sorted $CD150^{+}CD48^{-}CD41^{-}lineage^{-}Sca\text{-}1^{+}c\text{-}kit^{+}$ HSCs or sections through E11 mouse forebrain were thawed at room temperature for 10 minutes, fixed at room temperature in 10% buffered neutral formalin (VWR, West Chester, Pennsylvania) for 10 minutes, rinsed in 0.1M PB twice, and blocked with 0.3% Triton in 0.1M PB supplemented with 5% Goat Serum for 1 hour at 4°C. Slides were then incubated with anti-activated caspase-3 antibody (BD Pharmingen, San Diego, California) at room temperature for 2 hours. Slides were then rinsed in 0.1M PB twice and incubated with Alexa488-conjugated goat anti-rabbit IgG (Invitrogen-Molecular Probes, Carlsbad, California) for 1 hour at room temperature. Slides were rinsed in 0.1M PB twice and incubated with DAPI for 30 minutes at room temperature. Finally, slides were rinsed three times in 0.1M PB, the excess buffer was

shaken off and the slides were mounted in 70% glycerol in PBS. Images were collected using a florescence microscope.

To test for the incorporation of BrdU due to DNA repair, BrdU was administered to adult mice for 12 hours followed by irradiation with 100 rad from a Gammacell40 Extractor (MDS Nordion, Ottawa, ON, Canada) followed by 48 hours of further BrdU administration. $CD150^{+}CD48^{-}CD41^{-}lineage^{-}Sca\text{-}1^{+}c\text{-}kit^{+}$ HSCs were then sorted onto slides and stained for BrdU as described above.

Mathematical models of BrdU uptake and retention

To model the uptake and retention of BrdU in a population of stem cells we assumed that for days 0 through T the stem cells are exposed to adequate BrdU so that cells incorporate BrdU when they divide. Based on our data a random 6.0% of HSCs enter cycle each day. At day T, the BrdU supply is removed and the level of BrdU incorporated into the chromosomes decreases for every cell division after day T. The rate at which BrdU is diluted from cells during this chase period depends upon how the cells segregate their chromosomes. If chromosomes segregate randomly, then irrespective of whether stem cells divide asymmetrically or symmetrically with respect to daughter cell fate, BrdU labeled chromosomes will stochastically become diluted over time: on average the BrdU label will be diluted by half during each round of division and multiple divisions will be required to dilute the BrdU label to the point that it is no longer detectable by immunohistochemistry. This is modeled as case 1 below for asymmetrically dividing cells. In contrast, according to the immortal strand model (Cairns, 1975), stem cells divide asymmetrically under steady-state conditions and BrdU is preferentially incorporated into newly synthesized DNA strands that are asymmetrically segregated into

differentiating daughter cells with each round of division. Under these assumptions, modeled as case 2 below, stem cells retain only the unlabeled older DNA strands once BrdU is withdrawn.

Case 1: Random segregation of chromosomes (see Figure 5.1b)

BrdU Incorporation: When chromosomes are allowed to segregate randomly, BrdU could be incorporated into one or two DNA strands within each chromosome, depending on the number of times a stem cell divides during the period of BrdU incorporation and the way in which the chromosomes segregate. To model the rate of BrdU incorporation:

y_0 = fraction of cells without BrdU

y_1 = fraction of cells with one strand $BrdU^+$ after only one division

y_2 = fraction of cells with both strands $BrdU^+$ after two or more divisions

α = the proliferation rate of stem cells (we observed 6.0% of HSCs enter cycle per day)

Note as well that cell death was not incorporated into this model because we did not observe significant cell death or changes in HSC frequency during the experiments.

The equations for uptake:

$$\frac{dy_0}{dt} = -\alpha y_0$$

$$\frac{dy_1}{dt} = -\alpha y_1 + \alpha y_0$$

$$\frac{dy_2}{dt} = \alpha y_1$$

Equation 1: Cells leave the y_0 population when they divide.
Equation 2: Cells from the y_0 population are added into the y_1 population through the incorporation of BrdU into one of the DNA strands. Cells leave the y_1 population when they divide.
Equation 3: Cells from the y_1 population are added into the y_2 population through further incorporation of BrdU through cell division.

To determine the frequency of $BrdU^+$ stem cells at any time after the addition of BrdU we solve the system of ordinary differential equations with all HSCs initially being unlabeled prior to BrdU administration. Note that similar equations have previously been used to model BrdU incorporation and depletion from other cells (Bonhoeffer et al., 2000).

The process by which cells lose the BrdU label: At day T (when BrdU is removed), we determine the total number of $BrdU^+$ stem cells by adding the y_1 and y_2 populations. Cells in the y_1 population have a BrdU level of 1, whereas y_2 cells have a BrdU level of up to 2. To model the rate at which these cells lose BrdU during subsequent divisions after removing BrdU:

y_{10} = fraction of cells, initially with one labeled DNA strand that undergo 0 divisions after day T

y_{11} = fraction of cells, initially with one labeled DNA strand that undergo 1 division after day T

…

y_{1N} = fraction of cells, initially with one labeled DNA strand that undergo N divisions after day T

y_{20} = fraction of cells, initially with two labeled DNA strands that undergo 0 divisions after day T

y_{21} = fraction of cells, initially with two labeled DNA strands that undergo 1 division after day T

…

y_{2N}=fraction of cells, initially with two labeled DNA strands that undergo N divisions after day T

Cells move from $y_{1(k-1)}$ to y_{1k} at the proliferation rate α (cells move in y_{2k} similarly). The equations for dilution of the BrdU label are:

$$\frac{dy_{10}}{dt} = -\alpha y_{10}$$
$$\frac{dy_{11}}{dt} = -\alpha y_{11} + \alpha y_{10}$$
...
$$\frac{dy_{1N}}{dt} = \alpha y_{1(N-1)}$$
$$\frac{dy_{20}}{dt} = -\alpha y_{20}$$
$$\frac{dy_{21}}{dt} = -\alpha y_{21} + \alpha y_{20}$$
...
$$\frac{dy_{2N}}{dt} = \alpha y_{2(N-1)}$$

With each cell division, the cell's BrdU level is decreased by half. For instance, cells in y_{10} have BrdU level 1, cells in y_{11} have half as much BrdU on average, cells in y_{12} have one quarter as much BrdU on average, etc. Similarly, cells in y_{20} have BrdU level 2, cells in y_{21} have BrdU level 1, cells in y_{22} have BrdU level 0.5, etc. We can determine the total fraction of cells that have a BrdU level that is above a minimum detection level (which can be set at any desired level in the simulations) by adding all relevant populations at any time after day T.

This set of ordinary differential equations is solved for initial conditions that are determined by the observed results of the BrdU incorporation at time T. In this way, it is possible to plot the frequency of $BrdU^+$ HSCs over time, depending on whether it takes 1, 2, 3, or 4 rounds of division to dilute BrdU to the point at which it is no longer detectable (Figure 5.4a). Note that 1 round of division corresponds to a 2-fold dilution of BrdU while 4 rounds of division correspond to 16-fold dilution. Our empirical data suggest that approximately 3 rounds of division are required to dilute BrdU to the point that it is no longer detectable in HSCs.

Case 2: Asymmetric chromosome segregation (immortal strand model; see Figure 5.1a)

BrdU Incorporation: Under this model, only one strand of DNA within each chromosome in stem cells can contain BrdU irrespective of how long BrdU is administered (though the proportion of labeled stem cells will increase over time).

The equations for Case 2 are:

y_0 = fraction of cells without BrdU

y_1 = fraction of cells with one strand $BrdU^+$ (after one or more divisions)

α = proliferation rate of stem cells

The equations for uptake:

$$\frac{dy_0}{dt} = -\alpha y_0$$

Equation 4: Cells leave the y_0 population when they divide.

$$\frac{dy_1}{dt} = \alpha y_0$$

Equation 5: Cells from the y_0 population are added into the y_1 population through the incorporation of BrdU into one of the DNA strands.

As before, in order to determine the proportion of cells within each population at the end of day T we solve the system of ordinary differential equations with initial conditions corresponding to the case where initially all HCSs are unlabeled prior to BrdU administration. Cells in population y_0 do not contain any BrdU, while those in y_1 have a BrdU level of 1.

The process by which cells lose BrdU label: We take all cells containing BrdU at day T (all cells in population y_1 and monitor BrdU loss through cell division in the absence of BrdU). In this case, the asymmetric segregation of chromosomes means that all dividing

stem cells will lose all of the BrdU label in a single division in the absence of BrdU. Therefore, the fraction of stem cells that remain $BrdU^+$ at time T, simplifies to the fraction of $BrdU^+$ HSCs that do not divide after removing BrdU:

y_{10} = fraction of cells, initially with one labeled strand that undergo 0 divisions after day T

Cells move from y_{10} (and lose their Brdu label) at the proliferation rate α. The equations for loss of BrdU label:

$$\frac{dy_{10}}{dt} = -\alpha y_{10}$$

This differential equation with initial condition $y_{10}(0) = y_1(T)$ determines the fraction of HSCs that retain BrdU over time, according to the immortal strand hypothesis.

ACKNOWLEDGEMENTS

This work was supported by the Howard Hughes Medical Institute and the U.S. Army Research Laboratory/Office under grant number DAAD19-03-1-0168. Flow-cytometry was partially supported by the UM-Comprehensive Cancer Center NIH CA46592, and the UM-Multipurpose Arthritis Center NIH AR20557. Antibody production was partially supported by the Rheumatic Core Disease Center (1 P30 AR48310). MJK was supported by a University of Michigan Cancer Biology Training Grant. Thanks to David Adams and Martin White for flow-cytometry and to Elizabeth Smith (Hybridoma Core Facility) for antibody production.

AUTHOR CONTRIBUTION STATEMENT

MJK performed all experiments and interpreted results. SH helped to design and interpret many experiments and helped to perform some experiments. RA, SNG, and TLJ generated the mathematical model of BrdU retention over time (Figure 5.4a). MT and JAK developed the protocol for double labeling cells with CldU and IdU. SJM participated in the design and interpretation of experiments, and wrote the paper with MJK and SH.

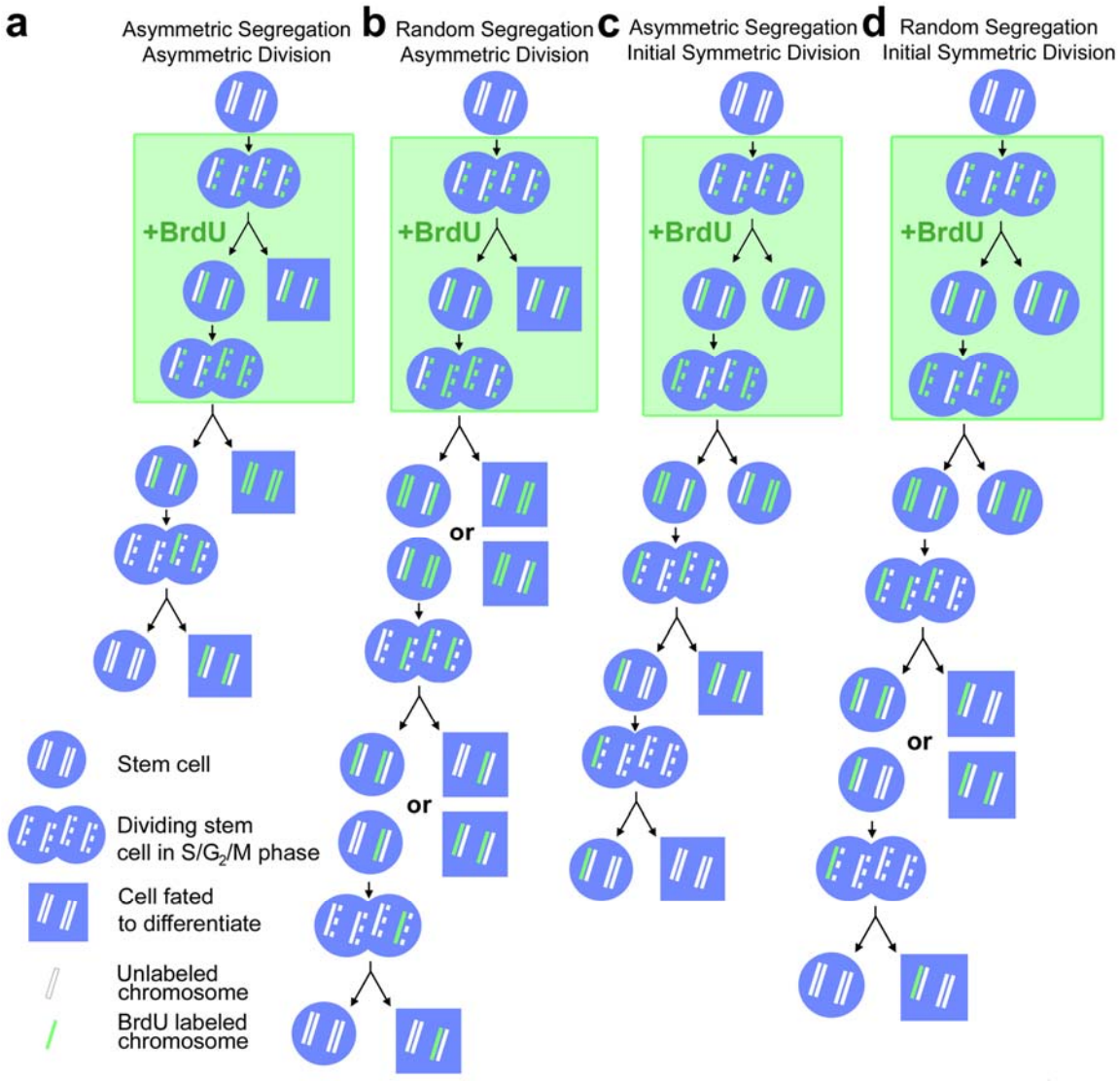

Figure 5.1: Contrasting predictions regarding stem cell labeling based on the immortal strand model versus random chromosome segregation.
a) According to the immortal strand model (Cairns, 1975), stem cells divide asymmetrically under steady-state conditions and BrdU is incorporated into newly-synthesized DNA strands that are asymmetrically segregated into differentiating daughter cells with each round of division, such that stem cells retain only the unlabeled older DNA strands. b) In contrast, if chromosomes segregate randomly, then BrdU labeled chromosomes will be stochastically diluted over multiple rounds of divisions. c) By the immortal strand model, if stem cells divide symmetrically then BrdU can be incorporated into DNA strands that become the 'older' strands once stem cells resume asymmetric division. Under these circumstances the $BrdU^+$ older strands would be retained indefinitely in stem cells. d) In contrast, if chromosome segregation is random then $BrdU^+$ chromosomes are stochastically diluted over time after BrdU is discontinued.

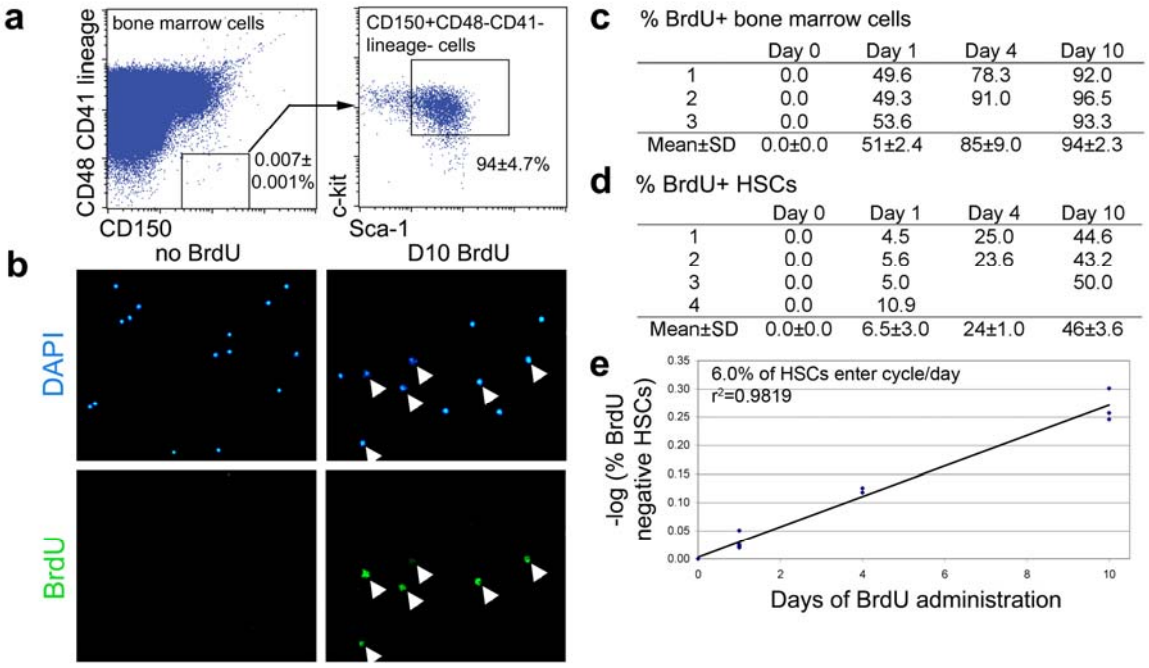

	Day 0	Day 1	Day 4	Day 10
1	0.0	49.6	78.3	92.0
2	0.0	49.3	91.0	96.5
3	0.0	53.6		93.3
Mean±SD	0.0±0.0	51±2.4	85±9.0	94±2.3

	Day 0	Day 1	Day 4	Day 10
1	0.0	4.5	25.0	44.6
2	0.0	5.6	23.6	43.2
3	0.0	5.0		50.0
4	0.0	10.9		
Mean±SD	0.0±0.0	6.5±3.0	24±1.0	46±3.6

Figure 5.2: 6.0% of HSCs stochastically enter cell cycle each day.
a) HSCs can be isolated by flow-cytometry as $CD150^{+}CD48^{-}CD41^{-}lineage^{-}Sca\text{-}1^{+}c\text{-}kit^{+}$ cells that represent only 0.0066±0.0003% (0.007% x 94%) of bone marrow cells but which contain all detectable HSC activity and which are very highly enriched for HSCs (nearly 50% of single cells give long-term multilineage reconstitution in irradiated mice(Kiel et al., 2005b)). b) BrdU incorporation into HSCs evaluated by immunofluorescence after sorting HSCs onto microscope slides (DAPI is a nuclear stain). The percentage of $BrdU^{+}$ bone marrow cells (c) and $CD150^{+}CD48^{-}CD41^{-}lineage^{-}Sca\text{-}1^{+}c\text{-}kit^{+}$ HSCs (d) after various periods of BrdU administration (3 independent experiments with 3 to 4 mice per experiment and 200 to 400 bone marrow cells or 100 to 400 HSCs counted per mouse). e) The percentage of HSCs that enter cycle each day (6.0%) can be derived by plotting the negative logarithm of the percentage of HSCs that were $BrdU^{-}$ over time (Cheshier et al., 1999a).

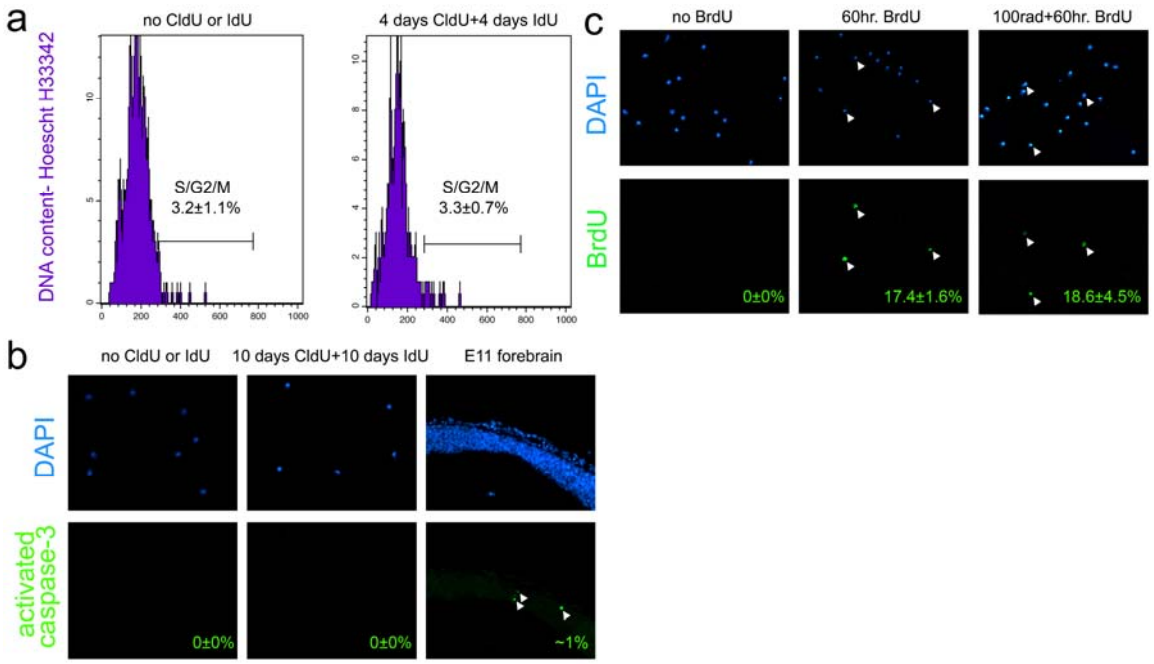

Figure 5.3: Administration of CldU and IdU does not affect HSC proliferation or cell death and BrdU incorporation during DNA repair is negligible.
a) Cell cycle distribution (based on DNA content) of $CD150^{+}CD48^{-}CD41^{-}lineage^{-}Sca\text{-}1^{+}c\text{-}kit^{+}$ HSCs isolated from a mouse that did not receive CldU or IdU (left) or from a mouse that received 4 days of CldU followed by 4 days of IdU (right) (two independent experiments). b) Activated caspase-3 staining of $CD150^{+}CD48^{-}CD41^{-}lineage^{-}Sca\text{-}1^{+}c\text{-}kit^{+}$ HSCs sorted onto a microscope slide following 10 days of CldU administration and 10 days of IdU administration. Arrowheads identify activated caspase-3^{+} cells in a section through embryonic day 11 mouse forebrain (positive control), but no activated caspase-3^{+} HSCs were detected in either CldU/IdU-treated or control mice (200 to 300 HSCs examined per treatment; two independent experiments). c) BrdU was administered for 12 hours followed by gamma irradiation with 100 rad and then 48 hours of further BrdU administration. No $BrdU^{+}$ HSCs were detected in negative control mice (no BrdU). Among mice treated with BrdU for 60 hours, 17.4±1.6% of HSCs from non-irradiated mice were $BrdU^{+}$ and 18.6±4.5% of HSCs from irradiated mice were $BrdU^{+}$ (250 to 600 HSCs analyzed per treatment; 3 independent experiments). Since DNA damage would be expected in all cells that receive this dose of irradiation(Taniguchi et al., 1993), this demonstrates that the amount of BrdU that is incorporated as a result of DNA damage repair is negligible and cannot be detected by immunofluorescence in these assays. Our failure to detect BrdU incorporation from DNA repair is consistent with prior studies that found that nucleotide incorporation as a result of DNA repair is negligible relative to DNA replication, even over many years (Spalding et al., 2005).

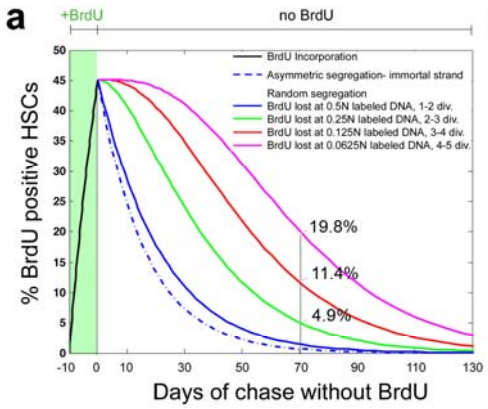

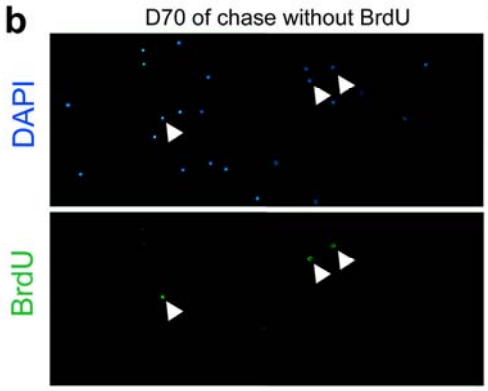

c % BrdU+ cells from adult mice

		chase D40	chase D70	chase D120
bone marrow cells	1	0.3	0.4	0.3
	2	0.6	0.3	0.4
	3		0.5	0.1
	Mean±SD	0.4±0.2	0.4±0.1	0.3±0.1
		chase D40	chase D70	chase D120
HSCs	1	7.4	4.0	1.5
	2	14.5	5.7	1.4
	3	8.3	3.4	3.1
	4	6.9	5.0	
	5		4.8	
	Mean±SD	9.3±3.5	4.6±0.9	2.0±1.0

d % BrdU+ cells from neonatal or mobilized mice

		chase D70 neonate	chase D120 neonate	chase D70 mobilized
bone marrow cells	1	0.0	0.1	0.0
	2	0.2	0.1	0.0
	3	0.2	0.0	0.2
	Mean±SD	0.1±0.1	0.1±0.1	0.1±0.1
		chase D70 neonate	chase D120 neonate	chase D70 mobilized
HSCs	1	6.1	2.5	2.8
	2	5.6	0.8	2.6
	3	4.3	2.1	0.9
	4	10.8		
	5	5.3		
	Mean±SD	6.4±2.5	1.8±0.9	2.1±1.1

Figure 5.4: Few HSCs retain BrdU and the vast majority of BrdU-retaining bone marrow cells are not HSCs.

a) Model predicting the fraction of HSCs that retain BrdU over time after administering BrdU 10 days, depending on whether chromosomes segregate asymmetrically or randomly and on the threshold of BrdU that can be detected by immunofluorescence (0.5N, 0.25N, 0.125N, or 0.0625N labeled DNA). b) $CD150^{+}CD48^{-}CD41^{-}lineage^{-}Sca\text{-}1^{+}c\text{-}kit^{+}$ HSCs sorted onto a microscope slide following 10 days BrdU administration and 70 days chase (without BrdU). Arrowheads identify $BrdU^{+}$ cells. c) The frequency of $BrdU^{+}$ bone marrow cells and HSCs after 10 days BrdU administration and 40, 70, or 120 days chase. d) The frequency of $BrdU^{+}$ bone marrow cells and HSCs after 10 days BrdU administration to neonatal mice followed by 70 or 120 days chase; or after 4 days BrdU administration to cyclophosphamide/G-CSF treated mice followed by 70 days chase. All data are based on 3 to 5 independent experiments with 3 mice per experiment and 400 to 700 bone marrow cells or 300 to 400 HSCs counted per mouse.

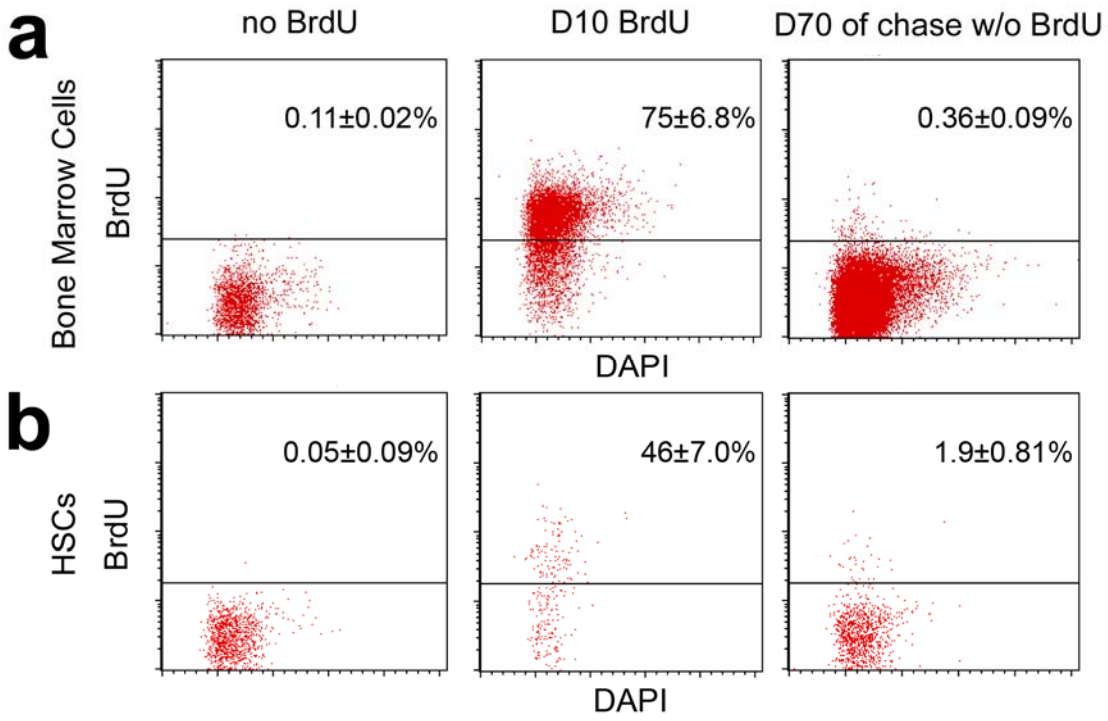

Figure 5.5: Few HSCs retain BrdU, and the vast majority of BrdU label-retaining bone marrow cells are not HSCs even when BrdU incorporation is measured by flow-cytometry.

In case flow-cytometric detection of BrdU was more sensitive than immunofluorescence microscopy, we repeated all of the experiments using this approach. The percentage of $BrdU^+$ whole bone marrow cells (a) or $CD150^+CD48^-CD41^-lineage^-$ HSCs (b) in negative control mice (no BrdU), or after 10 days of BrdU administration, or after an additional 70 days of chase (without BrdU). Note that fewer HSC markers were used to free up a fluorescence channel to detect BrdU by flow-cytometry; however, this should not introduce significant impurities as 45% of $CD150^+CD48^-CD41^-$ cells give long-term multilineage reconstitution in irradiated mice (Kiel et al., 2005b). Only 1.9% of HSCs detectably retained BrdU after 70 days chase and less than 0.04% of $BrdU^+$ bone marrow cells were HSCs (0.0066% x 1.9%/0.36%). The data are based on 3 independent experiments in which 6,000 to 60,000 bone marrow cells or 400 to 1200 HSCs were analyzed per experiment.

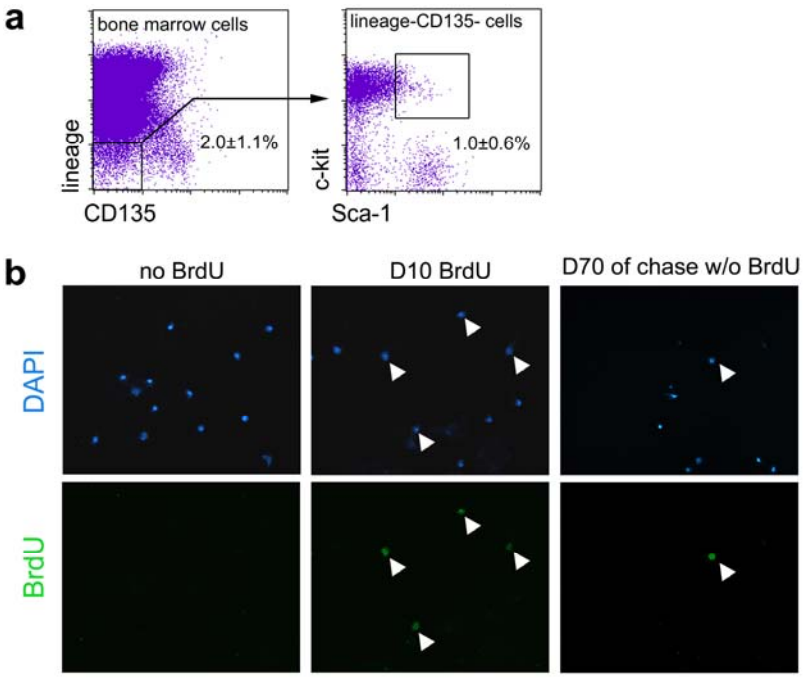

c % BrdU+ HSCs

	D0 of BrdU adult	D10 of BrdU adult	D70 of chase adult	D70 of chase neonate	D70 of chase mobilized
1	0.3	53.3	3.9	8.2	4.4
2	0.0	31.5	4.6	4.6	2.4
3	0.0	46.4			
Mean±SD	0.1±0.2	44±11	4.3±0.5	6.3±2.7	3.4±1.4

Figure 5.6: HSCs identified as c-kit$^+$Flk-2$^-$lineage$^-$Sca-1$^+$ cells also cannot be reliably identified based on BrdU label-retention.

a) In case the isolation of HSCs using different markers would identify a population that is more consistently marked by BrdU label-retention, we isolated c-kit$^+$Flk-2$^-$lineage$^-$Sca-1$^+$ cells, which represent around 0.02% of bone marrow cells (2.0% x 1.0%; a), and which are highly enriched for HSCs (Christensen and Weissman, 2001). b) c-kit$^+$Flk-2$^-$lineage$^-$Sca-1$^+$ cells were isolated from mice that had been administered BrdU for 10 days followed by a 70 day chase without BrdU. Cells were sorted onto microscope slides and stained with DAPI (to identify nuclei) and BrdU. c) The frequency of BrdU$^+$ c-kit$^+$Flk-2$^-$lineage$^-$Sca-1$^+$ cells after 10 days of BrdU administration or after an additional 70 days of chase in normal young adult mice or neonatal mice was very similar to what we observed when HSCs were isolated as CD150$^+$CD48$^-$CD41$^-$lineage$^-$Sca-1$^+$c-kit$^+$ cells (Figure 5.4c, d). The frequency of BrdU$^+$ c-kit$^+$Flk-2$^-$lineage$^-$Sca-1$^+$ cells after 4 days of BrdU administration followed by 70 days of chase in cyclophosphamide/G-CSF treated mice was also similar to what we observed in CD150$^+$CD48$^-$CD41$^-$lineage$^-$Sca-1$^+$c-kit$^+$ HSCs (Figure 5.4d). Note that these cells were isolated from some of the same mice analyzed in Figure 5.4c, d, so the frequency of BrdU$^+$ bone marrow cells from the same mice are presented in Figure 5.4c, d. These results were based on two independent experiments in which 6 mice and 200 to 300 cells per mouse were analyzed per experiment.

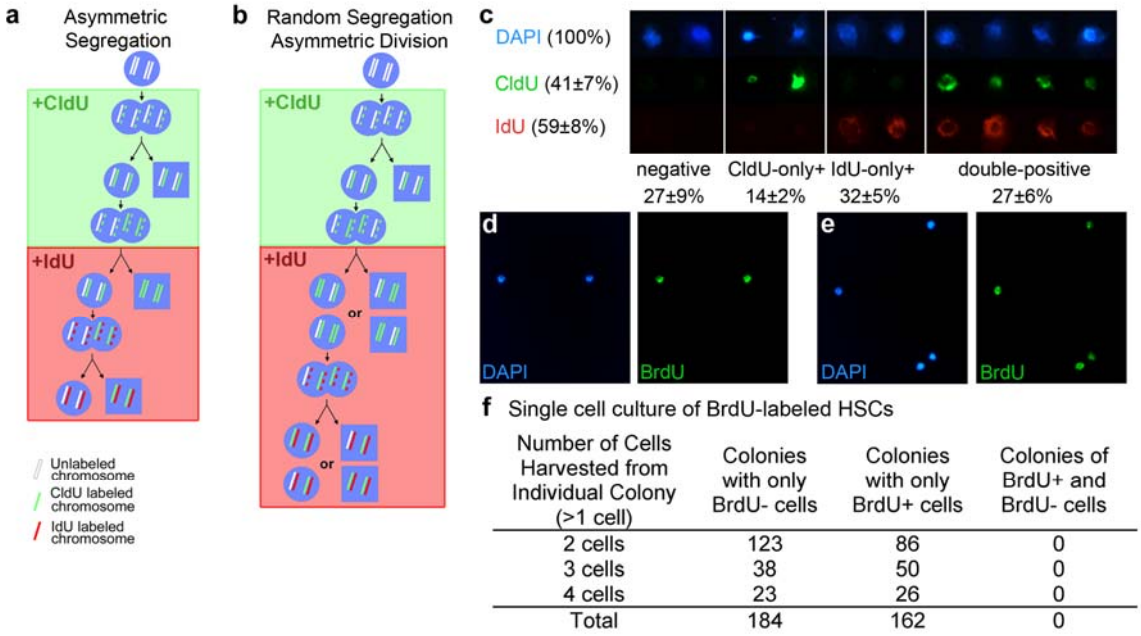

f Single cell culture of BrdU-labeled HSCs

Number of Cells Harvested from Individual Colony (>1 cell)	Colonies with only BrdU- cells	Colonies with only BrdU+ cells	Colonies of BrdU+ and BrdU- cells
2 cells	123	86	0
3 cells	38	50	0
4 cells	23	26	0
Total	184	162	0

Figure 5.7: HSCs segregate chromosomes randomly in vivo and in vitro.
a) By the immortal strand model, stem cells sequentially exposed to CldU (10 days) then IdU (10 days) would not incorporate both labels, with the exception of rare cells in S/G2/M phase of their first division after switching from CldU into IdU (expected frequency <<3%). b) In contrast, if chromosome segregation is random then $CldU^+$ stem cells would have the same probability of incorporating IdU as unlabeled cells (expected frequency of $CldU^+IdU^+$ HSCs approximately 25%). c) CldU was administered to mice for 10 days followed by IdU for 10 to 11 days and $CD150^+CD48^-CD41^-lineage^-Sca\text{-}1^+c\text{-}kit^+$ HSCs were stained. d) Examples of HSCs that incorporated neither label, only CldU, only IdU, or both labels (data are based on two independent experiments with 2 or 3 mice per experiment and 100 to 250 HSCs per mouse). HSCs from BrdU-treated mice divided once (d) or twice (e) in culture to form daughter cells. f) The progeny of these HSCs were either all $BrdU^+$ or all $BrdU^-$. We detected no clones in which label was asymmetrically segregated to a subset of daughter cells.

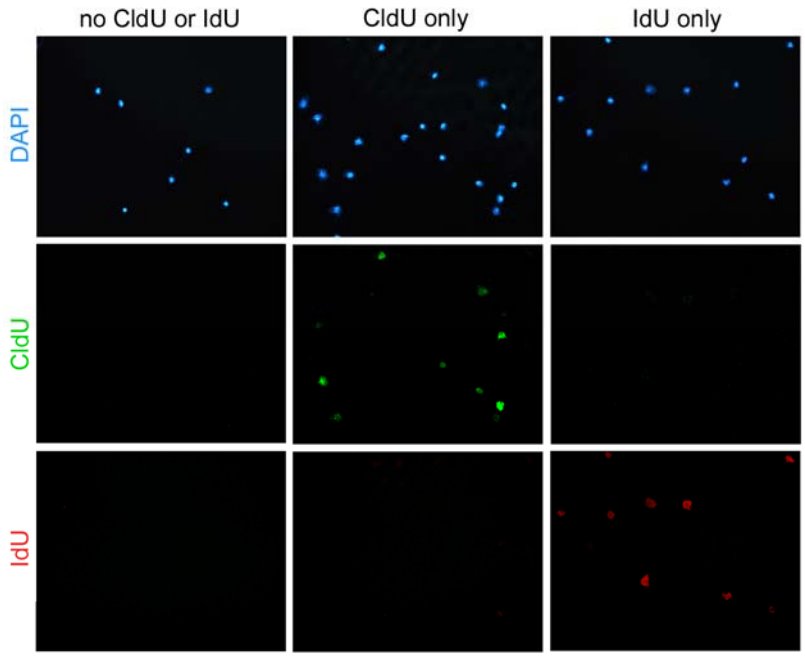

Figure 5.8: CldU$^+$ and IdU$^+$ cells can be distinguished by antibody staining.
CldU and IdU staining of CD150$^+$CD48$^-$CD41$^-$lineage$^-$Sca-1$^+$c-kit$^+$ HSCs from control mice that were administered neither label (left column), only CldU (middle column), or only IdU (right column). These controls were performed side-by-side with all CldU/IdU samples using the same staining conditions. IdU staining was only observed in samples from mice administered IdU and CldU staining was only observed in samples from mice administered CldU.

a

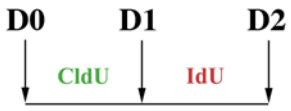

b % HSCs positive for CldU and/or IdU

	CldU-only+	IdU-only+	Total CldU+	Total IdU+	CldU+IdU +
1	11.7	6.2	16.0	10.5	4.3
2	10.2	5.4	13.6	8.8	3.4
3	13.4	6.0	14.8	7.4	1.4
Mean±SD	12±2	6±0.4	15±1	9±2	3±2

Figure 5.9: CldU persists in mice for less than a day after administration is discontinued.

To test whether the CldU/IdU double labeling of HSCs might simply have reflected a slow clearance of CldU from mice after its administration was discontinued (such that dividing HSCs were inadvertently exposed to both CldU and IdU) we sequentially administered CldU and IdU to mice for only 1 day each (a). If significant residual CldU remained in the mice for at least a day during IdU administration, all IdU^+ HSCs should also be $CldU^+$ in this experiment. In contrast, if CldU is cleared from mice within hours of being discontinued, then only a minority of IdU^+ HSCs should also be $CldU^+$. b) The frequency of $CD150^+CD48^-CD41^-lineage^-Sca\text{-}1^+c\text{-}kit^+$ HSCs that stained only with CldU, or only with IdU, the total frequencies of $CldU^+$ or IdU^+ cells, and the frequency of $CldU^+IdU^+$ HSCs. Nearly two-thirds of IdU^+ HSCs (6% IdU-only$^+$ versus 9% total IdU^+) were able to incorporate IdU without incorporating CldU over this brief period of administration, indicating that CldU does not persist in mice for longer than 8 hours after administration. The data are based on 3 separate mice analyzed in two independent experiments with 162 to 238 HSCs analyzed per mouse. The fact that some residual CldU remains in these mice during the first several hours of IdU administration can account for the consistent 2 to 3% increase in the frequency of $CldU^+IdU^+$ HSCs above that predicted by the product of single positive HSCs (27% observed versus 24% predicted with 10 day pulses (Figure 5.7c); 3% observed versus 1.3% predicted based on 1 day pulses (panel b above)).

BIBIOGRAPHY

Arai, F., Hirao, A., Ohmura, M., Sato, H., Matsuoka, S., Takubo, K., Ito, K., Koh, G.Y., and Suda, T. (2004). Tie2/angiopoietin-1 signaling regulates hematopoietic stem cell quiescence in the bone marrow niche. Cell *118*, 149-161.

Armakolas, A., and Klar, A.J. (2006). Cell type regulates selective segregation of mouse chromosome 7 DNA strands in mitosis. Science *311*, 1146-1149.

Bonhoeffer, S., Mohri, H., Ho, D., and Perelson, A.S. (2000). Quantification of cell turnover kinetics using 5-bromo-2'-deoxyuridine. J Immunol *164*, 5049-5054.

Bowie, M.B., McKnight, K.D., Kent, D.G., McCaffrey, L., Hoodless, P.A., and Eaves, C.J. (2006). Hematopoietic stem cells proliferate until after birth and show a reversible phase-specific engraftment defect. J Clin Invest *116*, 2808-2816.

Cairns, J. (1975). Mutation selection and the natural history of cancer. Nature *255*, 197-200.

Cheshier, S., Morrison, S.J., Liao, X., and Weissman, I.L. (1999). In vivo proliferation and cell cycle kinetics of long-term self-renewing hematopoietic stem cells. Proceedings of the National Academy of Sciences USA *96*, 3120-3125.

Christensen, J.L., and Weissman, I.L. (2001). Flk-2 is a marker in hematopoietic stem cell differentiation: a simple method to isolate long-term stem cells. Proc Natl Acad Sci U S A *98*, 14541-14546.

Conboy, M.J., Karasov, A.O., and Rando, T.A. (2007). High incidence of non-random template strand segregation and asymmetric fate determination in dividing stem cells and their progeny. PLoS Biol *5*, e102.

Cotsarelis, G., Sun, T.T., and Lavker, R.M. (1990). Label-retaining cells reside in the bulge area of pilosebaceous unit: implications for follicular stem cells, hair cycle, and skin carcinogenesis. Cell *61*, 1329-1337.

Karpowicz, P., Morshead, C., Kam, A., Jervis, E., Ramunas, J., Cheng, V., and van der Kooy, D. (2005). Support for the immortal strand hypothesis: neural stem cells partition DNA asymmetrically in vitro. J Cell Biol *170*, 721-732.

Kiel, M.J., Yilmaz, O.H., Iwashita, T., Terhorst, C., and Morrison, S.J. (2005). SLAM Family Receptors Distinguish Hematopoietic Stem and Progenitor Cells and Reveal Endothelial Niches for Stem Cells. Cell *121*, 1109-1121.

Morrison, S.J., Csete, M., Groves, A.K., Melega, W., Wold, B., and Anderson, D.J. (2000). Culture in reduced levels of oxygen promotes clonogenic sympathoadrenal differentiation by isolated neural crest stem cells. J Neurosci *20*, 7370-7376.

Morrison, S.J., Wright, D., and Weissman, I.L. (1997). Cyclophosphamide/granulocyte colony-stimulating factor induces hematopoietic stem cells to proliferate prior to mobilization. Proc Natl Acad Sci USA *94*, 1908-1913.

Potten, C.S., Hume, W.J., Reid, P., and Cairns, J. (1978). The segregation of DNA in epithelial stem cells. Cell *15*, 899-906.

Potten, C.S., Owen, G., and Booth, D. (2002). Intestinal stem cells protect their genome by selective segregation of template DNA strands. J Cell Sci *115*, 2381-2388.

Shinin, V., Gayraud-Morel, B., Gomes, D., and Tajbakhsh, S. (2006). Asymmetric division and cosegregation of template DNA strands in adult muscle satellite cells. Nat Cell Biol *8*, 677-687.

Smith, G.H. (2005). Label-retaining epithelial cells in mouse mammary gland divide asymmetrically and retain their template DNA strands. Development *132*, 681-687.

Spalding, K.L., Bhardwaj, R.D., Buchholz, B.A., Druid, H., and Frisen, J. (2005). Retrospective birth dating of cells in humans. Cell *122*, 133-143.

Takano, H., Ema, H., Sudo, K., and Nakauchi, H. (2004). Asymmetric division and lineage commitment at the level of hematopoietic stem cells: inference from differentiation in daughter cell and granddaughter cell pairs. The Journal of experimental medicine *199*, 295-302.

Taniguchi, S., Hirabayashi, Y., Inoue, T., Kanisawa, M., Sasaki, H., Komatsu, K., and Mori, K.J. (1993). Hemopoietic stem-cell compartment of the SCID mouse: double-exponential survival curve after gamma irradiation. Proc Natl Acad Sci U S A *90*, 4354-4358.

Taylor, G., Lehrer, M.S., Jensen, P.J., Sun, T.T., and Lavker, R.M. (2000). Involvement of follicular stem cells in forming not only the follicle but also the epidermis. Cell *102*, 451-461.

Tumbar, T., Guasch, G., Greco, V., Blanpain, C., Lowry, W.E., Rendl, M., and Fuchs, E. (2004). Defining the epithelial stem cell niche in skin. Science (New York, NY *303*, 359-363.

Urbanek, K., Cesselli, D., Rota, M., Nascimbene, A., De Angelis, A., Hosoda, T., Bearzi, C., Boni, A., Bolli, R., Kajstura, J., *et al.* (2006). Stem cell niches in the adult mouse heart. Proc Natl Acad Sci U S A *103*, 9226-9231.

Welm, B.E., Tepera, S.B., Venezia, T., Graubert, T.A., Rosen, J.M., and Goodell, M.A. (2002). Sca-1(pos) cells in the mouse mammary gland represent an enriched progenitor cell population. Dev Biol *245*, 42-56.

Zhang, J., Niu, C., Ye, L., Huang, H., He, X., Tong, W.G., Ross, J., Haug, J., Johnson, T., Feng, J.Q., *et al.* (2003). Identification of the haematopoietic stem cell niche and control of the niche size. Nature *425*, 836-841.

CHAPTER 6

CONCLUSIONS

Extensive self-renewal potential is a defining feature of stem cells, distinguishing them from transit amplifying and restricted progenitors. Self-renewal is characterized by the cell division that leads to the production of one or two daughter cells that possess a developmental potential similar to the mother stem cell. It is essential for the expansion of stem cells during development and maintenance of stem cells during homeostasis. Regulation of stem cell self-renewal involves precise control of cell cycle progression, suppression of premature lineage determination, as well as maintenance of stem cell genomic integrity; all of which are subject to both cell intrinsic and cell extrinsic regulation. Dysregulation of stem cell self-renewal can result in developmental defects, phenotypes that resemble premature aging, and/or the development of neoplasms.

In my thesis, I have studied the function of two important transcriptional regulators, *Bmi-1* and *Sox17*, in regulating the self-renewal of neural stem cells and hematopoietic stem cells, respectively; using loss-of-function and gain-of-function studies. We have shown that by modulating the activities of factors that regulate stem cell cell cycle progression (e.g. *Bmi-1*) and/or lineage restriction (e.g. *Sox17*), we can modify the self-renewal potential of the respective stem cell population, and/or confer self-renewal capability to short-term progenitor cells under certain conditions. Lastly, by using hematopoietic stem cells as a model, we have shown that immortal strand

segregation is not a universal mechanism through which stem cells preserve their genomic integrity.

BMI-1 MAINTAINS STEM CELL SELF-RENEWAL BY SUPPRESSING *INK4A/ARF*

Bmi-1 is a member of the polycomb family of epigenetic regulators, which suppress target gene expression through histone modification and chromatin remodeling. We and others had previously shown that *Bmi-1* is essential for the postnatal self-renewal of stem cells from diverse tissues including the hematopoietic system (Lessard and Sauvageau, 2003; Park et al., 2003) and the CNS (Molofsky et al., 2003). *Bmi-1* deficient mice exhibit a progressive postnatal depletion of stem cells from these tissues, leading to hematopoietic failure, defects in cerebellum development, neurological abnormalities, and death by early adulthood (Leung et al., 2004; van der Lugt et al., 1994). In Chapter 2, we have shown that the depletion of neural stem cells in the absence of *Bmi-1* is at least partially due to the derepression of the *Ink4* locus, which encodes two important negative cell cycle regulators: $p16^{Ink4a}$ and $p19^{Arf}$. Deletion of *Ink4a* and *Arf* from *Bmi-1* deficient mice partially rescues the self-renewal defects of neural stem cells *in vivo* and *in vitro*; but this is not sufficient to rescue the decreased postnatal survival or growth retardation of these mice. This indicates that *Bmi-1* regulates adult neural stem cell self-renewal mainly by repressing the expression of *Ink4a* and *Arf*; but other mechanisms also contribute to the developmental defects of *Bmi-1* deficient mice (see discussion below). Similar results have also been obtained by others (Bruggeman et al., 2005), and has been observed in the hematopoietic systems (Oguro et al., 2006; Oguro et al., 2010).

Bmi-1 expression is elevated in a wide range of malignances, and *Bmi-1* is necessary for the maintenance of cancer stem cells from acute myeloid leukemias (Lessard and Sauvageau, 2003) as well as gliomas (Bruggeman et al., 2007). This raises the question of whether *Bmi-1* overexpression is sufficient to enhance the self-renewal potential of existing stem cells and/or confer self-renewal ability to non-self-renewing cells, or to induce transformation. Indeed, overexpression of *Bmi-1* has been shown to enhance the long-term reconstitution potential of adult hematopoietic stem cells in some studies (Iwama et al., 2004). In Chapter 3, we tested the consequences of *Bmi-1* overexpression in neural stem cells. *Bmi-1* overexpression was sufficient to significantly increase stem cell self-renewal, overall proliferation, and neuronal differentiation *in vitro*, but had little effect on SVZ proliferation, adult olfactory bulb neurogenesis, or neurogenesis/gliogenesis during development *in vivo*. *Bmi-1* transgenic mice showed only a mild increase in neural stem cell frequency with no increase in the total number of neural stem cells per mouse. They also exhibited no evidence of tumorigenesis, even when aged for more than 20 months. These data demonstrate that *Bmi-1* overexpression has much more profound effects on CNS stem cell function in culture than *in vivo*; and that *Bmi-1* overexpression alone is not sufficient to induce tumorigenesis in the CNS.

The different ability of *Bmi-1* to promote neural stem cell self-renewal *in vitro* versus *in vivo* is at least partially explained by the differential expression of $p16^{Ink4a}$ and $p19^{Arf}$ under these two different conditions. $p16^{Ink4a}$ and $p19^{Arf}$ are not detectably expressed by neural stem/progenitor cells in developing or young adult mice (Bruggeman et al., 2007; Bruggeman et al., 2005; Molofsky et al., 2005; Molofsky et al., 2003; Nishino et al., 2008), but are induced in culture in neural stem cells (Molofsky et al.,

2003) in response to the stress associated with adaptation to the unphysiological culture environment (Lowe and Sherr, 2003; Sherr and DePinho, 2000). Therefore, *Bmi-1* overexpression is able to repress the nonphysiological upregulation of $p16^{Ink4a}$ and $p19^{Arf}$ induced by suboptimal culture condition to enhance neural stem cell self-renewal *in vitro*, but has little effect in *vivo* since $p16^{Ink4a}$ and $p19^{Arf}$ are not normally expressed *in vivo*. This is supported by the observation that *Bmi-1* overexpression no longer enhanced self-renewal, proliferation, or neurogenesis in *Ink4a-Arf* deficient neural stem cells in culture (Chapter 3).

Together, our data emphasize the importance of precise cell cycle regulation in controlling stem cell self-renewal during development and under pathological conditions. Our data also point out differences in stem cell self-renewal mechanisms may exist between *in vivo* and *in vitro* culture systems and that extra caution must be exercised when inferring *in vivo* mechanisms for stem cell self-renewal regulation based on observations collected in culture.

Our data also leave many questions that remain to be answered. One important question concerns the mechanisms through which $p16^{Ink4a}$ and $p19^{Arf}$ suppress stem cell self-renewal after the loss of *Bmi-1*. While our data demonstrate that the upregulation of $p16^{Ink4a}$ and $p19^{Arf}$ in the absence of *Bmi-1* plays a major role in limiting the self-renewal potential of *Bmi-1*-deficient neural stem cells, how this is achieved is still unclear. The simplest explanation would be that up-regulation of $p16^{Ink4a}$ and $p19^{Arf}$ in stem cells induces cellular senescence or apoptosis which depletes functional stem cells. However, we did not observed increased endogenous β-galactosidase staining (indicative of cellular senescence) or activated caspase 3 staining (indicative of apoptosis) in the SVZ of *Bmi-1*

deficient animals ((Molofsky et al., 2006) and unpublished observation). It is possible that the senescent/apoptotic cells are rapidly cleared by macrophages *in vivo*, which prevent the reliable assessment of these processes in germ-line *Bmi-1* deficient animals. To overcome this issue, it may be necessary to examine the level of cellular senescence and/or apoptosis in the SVZ of *Bmi-1* conditional knockout mice shortly after deletion to see whether increased apoptosis or senescence can be observed after acute loss of *Bmi-1*. Alternatively, cellular senescence/apoptosis may not play a major role mediating the depletion of functional neural stem cells after *Bmi-1* deletion.

Another possibility is that neural stem cells may prematurely differentiate in response to elevated $p16^{Ink4a}$ and/or $p19^{Arf}$ expression. Differentiation of many stem cells is associated with a progressive lengthening of the cell cycle, especially the G_1 phase and lengthening of G_1 has been proposed to be a cause rather than a consequence of differentiation (Orford and Scadden, 2008). In the case of neural stem cells, it has been shown that when the G_1 phase of the cell cycle is modified by modulating cyclins or CDKs, neural stem cells change their behavior with respect to self-renewal versus differentiation (reviewed in (Salomoni and Calegari, 2010)). Therefore, it is conceivable that upregulation of $p16^{Ink4a}$ and/or $p19^{Arf}$ after *Bmi-1* loss would have a similar impact on cell cycle progression, which could in turn induce premature differentiation and exhaustion of neural stem cells. Future experiments should examine whether acute gain of function of $p16^{Ink4a}$ and/or $p19^{Arf}$ could indeed cause premature differentiation of neural stem cells *in vivo*. For these experiments, a conditional *Ink4a/Arf*-overexpressing transgenic mouse model (LoxP-STOP-LoxP upstream of *Ink4a* and/or *Arf*) will be necessary. This mouse strain should then be crossed with Nestin-CreER and LoxP-EYFP

reporter mice and at different time points after tamoxifen administration, the cell type composition of $EYFP^+$ cells in the brain of control and transgenic mice should be compared to assay for changes in the timing or pattern of neural stem cell differentiation *in vivo*.

Another important question would be what other target genes beyond *Ink4a* and *Arf* may act downstream of *Bmi-1* to regulate stem cell maintenance. In Chapter 2, we have shown that loss of *Ink4a* and *Arf* could only partially rescue the self-renewal defects of *Bmi-1* deficient neural stem cells, which has been confirmed by other groups as well as in the hematopoietic system (Bruggeman et al., 2005; Oguro et al., 2006). On the other hand, *Bmi-1* transgenic mice developed idiopathic hydrocephalus postnatally, while a similar phenotype was never observed in *Ink4a* and *Arf* single and double mutant mice (Chapter 3). All of these data indicate that other genes must act downstream of *Bmi-1*, independent of *Ink4a* and *Arf*, to regulate stem cell self-renewal and/or mouse development. *Hox* genes are known targets of *Bmi-1* which mediate the skeletal development defects observed in *Bmi-1* deficient mice (van der Lugt et al., 1996), however, it is unclear whether *Hox* genes are responsible for any of the observed stem cell self-renewal defects in the absence of *Bmi-1*.

It has been reported that $p21^{cip1}$ is upregulated in cultured fetal mouse neural stem cells when *Bmi-1* is acutely knocked down using RNAi, and is responsible for self-renewal defects in fetal neural stem cells that are not evident in *Bmi-1* germ line knockout mice (Fasano et al., 2007). Fasano et al. speculated that this was explained by compensation in the *Bmi-1* germline mutant mice and suggested that conditional deletion of *Bmi-1* in vivo might reveal a more profound role during fetal development. We have

now conditionally deleted *Bmi-1* from fetal neural stem cells using *Nestin-Cre* but we still do not observe the defects in neural stem cell function or neural development predicted by Fasano et al. (unpublished data). We did observe an upregulation of $p21^{cip1}$ in the absence of *Bmi-1*; however this increase was normalized after deletion of $p19^{Arf}$, indicating $p21^{cip1}$ acts downstream of $p19^{Arf}$ (Chapter 2). It remains to be tested whether the deletion of $p21^{cip1}$ on top of $p16^{Ink4a}$ and $p19^{Arf}$ is able to further rescue the phenotype of *Bmi-1* deficient neural stem cells.

It has recently been shown that Bmi-1 also regulates mitochondrial function and intracellular reactive oxygen species (ROS) level independent of *Ink4a* and *Arf*. And normalizing ROS levels using the antioxidant N-acetylcysteine (NAC), or disrupting the DNA damage response pathway by *Chk2* deletion partially rescues some of the developmental defects of *Bmi-1*-deficient mice, including growth retardation and reduced survival (Liu et al., 2009), which were not rescued by *Ink4a* and *Arf* deletion. It will be interesting to directly test whether oxidative stress also contributes to the neural stem cell defects in *Bmi-1*-deficient mice. To more systematically identify genes that act downstream of Bmi-1, it will be informative to perform gene expression profile comparisons between wild type, *Bmi-1*-deficient and *Bmi-1*-overexpressing neural stem cells to identify genes consistently up- or down-regulated by *Bmi-1*. In addition, it will be helpful to perform CHIP-on-Chip analysis with Bmi-1 using freshly isolated or cultured neural stem cells in parallel to identify the direct targets of *Bmi-1*, and compare this result with the gene expression analysis.

While *Bmi-1* is essential for the maintenance of neural stem cell proliferation and self-renewal *in vivo* and *in vitro*; it is unclear whether this is solely due to its ability to

regulate cell cycle progression (see discussion above), or whether *Bmi-1* also plays a separate role regulating differentiation. Polycomb complex components have been shown to promote the maintenance of ES cell pluripotency by suppressing the expression of differentiation genes (see detailed discussion in Chapter 1). In the case of *Bmi-1*, it has been reported *Bmi-1* loss causes premature lobuloalveolar differentiation in mammary glands (Pietersen et al., 2008). *Bmi-1* is also essential for maintaining the multipotency of hematopoietic stem cells and multipotent hematopoietic progenitor cells by blocking lymphoid differentiation (Oguro et al., 2010). In neural stem cells, it has been reported that loss of *Bmi-1* results in an increase in astroglial cells (Zencak et al., 2005), and differentiation-associated genes are preferentially silenced by polycomb complexes in neural stem/progenitor cells (Mohn et al., 2008). However, direct evidence proving *Bmi-1* maintains neural stem cell multipotency is lacking, and our analysis on the *Bmi-1* transgenic mouse has so far failed to reveal a link between *Bmi-1* overexpression and changes in neuronal/glial differentiation *in vivo* (Chapter 3).

To examine whether acute loss of *Bmi-1* could lead to neural stem cell premature differentiation *in vivo*, we could cross *Bmi-1* conditional knockout mice with Nestin-CreER and LoxP-EYFP reporter mice, and analyze the cell type composition of $EYFP^+$ cells in the brain of control and transgenic mice at various time points after tamoxifen administration to assess for changes in the timing or pattern of neural stem cell differentiation. Alternatively, wild type, *Bmi-1*-deficient or *Bmi-1*-overeexpressing neural stem cells can be cultured *in vitro*, and monitored for their tendency to spontaneously differentiate. To assess whether the effects of *Bmi-1* on neural stem cell differentiation (if they exist) are dependent on *Ink4a*/*Arf* expression, the above mentioned experiments can

be repeated on an *Ink4a*/*Arf*-deficient background. Lastly, by analyzing the gene expression profiles and CHIP-on-chip data with Bmi-1, we could also gain insight into whether and how Bmi-1 may regulate neural stem cell differentiation.

Despite the fact that *Bmi-1* is overexpressed in many types of cancers and is essential for the maintenance of certain cancer stem cells, we have so far failed to observe any CNS tumorigenesis after *Bmi-1* overexpression in neural stem and progenitor cells cells (Chapter 3). One possible explanation for the lack of tumorigenesis is that the level of Bmi-1 overexpression achieved in our transgenic system is not sufficient to induce de novo tumor formation, however, the observation that our transgene is sufficient to overexpress Bmi-1 to a level similar or even higher than what is observed in some human CNS tumors suggests against this possibility (Figure 3.1). Alternatively, since *Bmi-1* is a member of the polycomb suppressor complex, it is also possible that other polycomb complex components are limiting and must also be overexpressed to achieve a gain of PRC1 function. However, we did observe an increase in the self-renewal potential of cultured neural stem cells after Bmi-1 overexpression, which indicates at least in this particular circumstance, the abundance of other polycomb complex components is not limiting. Another possibility is that since in our transgenic system, ectopic Bmi-1 expression is driven by the human Nestin second intron enhancer, which only expresses in neural stem and progenitor cells but not in mature astrocytes; it is possible that the formation of tumors which would normally arise from differentiated astrocytes is not facilitated by the transgene expression. Lastly, it is possible that Bmi-1 overexpression is not an initiating event for CNS tumorigenesis, but rather acts as a secondary mutation to facilitate the progression of pre-existing neoplasms. Indeed, the fact that we also rarely

observe spontaneous brain tumor formation in *Ink4a* and *Arf* single or double mutant mice (unpublished observations) even though *Ink4a* and/or *Arf* mutations commonly occur in brain tumors, suggests that escaping cell cycle control by *Ink4a* and *Arf* in general may not be an initiating event in brain tumor development. To test whether Bmi-1 overexpression can instead act to facilitate CNS tumorigenesis, *Bmi-1* transgenic mice can be crossed onto genetic backgrounds which are prone to develop brain tumors, such as GFAP-Cre^{+}cis-p53$^{-/+}$NF1$^{fl/+}$ mice or mice that expresses constitutively active EGF receptor, and assessed for the acceleration of tumorigenesis or changes in tumor spectrum.

Although Bmi-1 overexpression does not significantly affect neural stem cell function or neuronal/glial differentiation *in vivo*, and does not induce CNS tumor formation, a subset of Bmi-1 transgenic mice nonetheless developed severe hydrocephalus and premature death. The exact cause of this phenotype is currently unclear. The observation that only the lateral ventricles are affected by hydrocephalus seems to suggest this is likely a form of non-communicating hydrocephalus where a physical obstruction between lateral ventricles and the third ventricle blocks the flow of cerebral spinal fluid (CSF). However, we have failed to detect any obstruction at any level of the ventricular system on histological sections. On the other hand, we did observe abnormal lateral ventricle ependymal cell layer morphology in some mice that developed hydrocephalus. Therefore, it is possible that defects in ependymal cell function may block the circulation of CSF between lateral ventricles and the third ventricle. To definitively test this possibility, it will be necessary to perform dye injection into the ventricular system to track CSF flow, as well as perform electron microscopy to examine the

ultrastructure of ependymal cells and assess their ability to direct CSF flow *in vitro*. Lastly, it is also possible that the observed hydrocephalus is not due to an intrinsic neural development defect, but rather a result of cranial skeletal malformation. It is known that Bmi-1 deficiency causes skeletal development defects (van der Lugt et al., 1996), therefore, it is possible that off-target transgene expression in the skeletal system may cause defects in the cranial skeleton that lead to hydrocephalus.

While germ-line knockout and transgenic systems have been used extensively to study the *in vivo* function of many genes, it has argued that compensation mechanisms may take place under these circumstances due to long-term loss or over-expression of the target genes. Therefore, acute gain or loss of function studies may reveal unexpected phenotypes beyond what was observed from knockout or transgenic mice. In line with this argument, it has been reported that acute knockdown and overexpression of Bmi-1 in neural stem/progenitor cells during mouse embryonic development gives stronger phenotypes than what has been observed in our knockout and transgenic studies (Fasano et al., 2007; Fasano et al., 2009). However, in both of these studies, most experiments were performed *in vitro*; for *in vivo* knockdown or overexpression, in utero electroporation was used to introduce the construction. Given that *Ink4a* and *Arf* are induced by culture stress, and may be upregulated by tissue injury; it is unclear whether part of the observed enhanced phenotype could be the result of nonphysiological induction of these two cell cycle inhibitors by the experimental procedures. To more accurately assess the *in vivo* consequences of acute loss or gain of Bmi-1 expression, it would be necessary to conditionally delete Bmi-1 from fetal neural stem cells *in vivo*. As

noted above, we have recently done this and still do not observe the phenotypes that would be predicted by Fasano et al.

SOX17 CONFERS FETAL LIVER HSC IDENTITY

Sox17 is a member of the *Sry*-related high mobility group transcription factors, and is required for the formation and maintenance of definitive endoderm (Hudson et al., 1997; Kanai-Azuma et al., 2002) and vascular endothelium (Matsui et al., 2006). We have previously shown that *Sox17* expression is developmentally restricted to fetal and neonatal, but not adult, HSCs (Kim et al., 2007) and *Sox17* expression is correlated with fetal HSC characteristics during their transition from fetal to adult HSCs in terms of both surface marker phenotype and cell cycle status. Germline loss of *Sox17* leads to severe defects in definitive hematopoiesis in the fetal liver, including a complete absence of definitive HSCs, while conditional deletion of *Sox17* leads to the loss of fetal and neonatal, but not adult, HSCs (Kim et al., 2007) indicating *Sox17* is essential for the function/maintenance of fetal but not adult HSCs.

In chapter 4, we extended our previous findings by showing that overexpression of *Sox17* in adult hematopoietic progenitors is sufficient to confer certain fetal characteristics, including enhanced self-renewal potential and fetal-specific marker and gene expression. Furthermore, the hematopoietic reconstitution pattern of *Sox17*-overexpressing adult bone marrow cells exhibited a striking resemblance to fetal liver hematopoiesis, including augmented myeloerythropoiesis, diminished lymphopoiesis, and production of platelets and myeloid cells with fetal characteristics. This was achieved at least partially by repressing the expression of lymphoid differentiation-associated genes and increasing the expression of HSC-specific genes by *Sox17*. Together, our data

have identified *Sox17* as the only gene identified to date that is not only essential for fetal liver HSC maintenance but is also sufficient to confer fetal HSC features to adult cells.

Our results raise many interesting questions. The observation that endogenous *Sox17* expression in fetal liver HSCs declines with age and differentiation is intriguing. It suggests that cell intrinsic changes may already take place in fetal liver HSCs during late embryonic development before they fully transition into adult HSCs at approximately 3 weeks after birth (Bowie et al., 2007; Bowie et al., 2006). Indeed, it has been reported that while HSCs isolated from fetal liver and 1 week old bone marrow can generate B cells that are not dependent on IL-7 signaling, bone marrow HSCs isolated from 2 week old mice absolutely require IL-7 signaling for B-lymphopoiesis (Kikuchi and Kondo, 2006). This indicates fetal HSCs do undergo developmental changes with age before their transition into adult HSCs. Similar changes have also been observed in the pattern of fetal liver hematopoiesis, which is initially dominated by definitive erythropoiesis but exhibits a progressive increase in lymphopoiesis during late fetal development. These observations raise the question of whether the change in Sox17 expression in fetal liver HSCs during development is causally related to the changes observed in fetal HSC function and fetal liver hematopoiesis. One way to test this is to compare the gene expression profile and developmental/differentiation potential of fetal liver HSCs isolated at different embryonic ages to see whether consistent changes can be observed that correlate with Sox17 expression. Another way to test it is using the Doxycycline-regulatable *Sox17* transgene to maintain high Sox17 expression in fetal liver HSCs during late embryonic development to see whether sustained Sox17 expression in HSCs results in hematopoiesis resembling earlier stage fetal liver hematopoiesis.

The observation that *Sox17* expression declines with fetal liver HSC differentiation raises the possibility that the *Sox17* expression level defines the identities of HSCs and various progenitor cells. One way to test this is to compare the self-renewal and differentiation potential of each population to see whether either property correlates with *Sox17* expression. One cell population in fetal liver, the LSK150^{-}48^{-}41^{-} cells, which share the same surface marker phenotype as adult bone marrow multipotent progenitors, is particularly interesting as they seem to express the same or even higher levels of Sox17-GFP than fetal liver HSCs (LSK150^{+}48^{-}41^{-}) at all developmental stages examined. It will be interesting to directly test the self-renewal and developmental potential of these cells in comparison to HSCs to see whether Sox17 expression indeed correlates with either of these properties. The next test would be to specifically knockout or over-express *Sox17* in each cell population using mice carrying cell type-specific cre-recombinase or tetracycline transactivator protein to see whether modulating Sox17 expression levels would cause changes in the self-renewal or developmental potential of each cell population. In parallel, it would also be interesting to see whether *Sox17*$^{+/-}$ mice have lower expression of *Sox17* and whether this leads to changes in population frequency or maturation rate of the HSCs from fetal to adult characteristics.

Another important question would be to determine what mechanisms regulate the dynamic expression of Sox17 during development and differentiation. To date, no factors or mechanisms that regulate Sox17 expression in fetal liver HSCs have been reported, however, many possibilities exist. For example, Sox17 expression could be regulated by another yet to be identified fetal liver HSC specific transcriptional factor. We have shown that *Sox17* overexpression is sufficient to increase the expression of some, but not all,

fetal liver HSC-specific genes. It is possible that one or more of the genes whose expression is not increased could control *Sox17* expression. Alternatively, Sox17 expression might be suppressed by certain adult HSC-specific or differentiation-associated genes such that Sox17 expression is terminated when fetal HSCs transit into an adult phenotype or become differentiated. Another possibility is that Sox17 expression is controlled by a cell-extrinsic niche signal that is specific for the fetal liver environment; however, the observation that Sox17 expression persists in bone marrow HSCs for more than 3 weeks postnatally (Kim et al., 2007) argues against this possibility. Lastly, Sox17 expression in fetal liver HSCs may reflect an "endothelial memory" which they inherit from the hemogenic endothelial cells in the form of an epigenetic modification, which gets progressively lost during fetal HSC development. It is possible that all of the above mentioned mechanisms play a role in regulating Sox17 expression, and that a detailed examination of the Sox17 promoter for transcription factor binding sites or DNA or histone modification marks may provide some insights in answering this question.

It is also equally important to determine the direct downstream targets of Sox17. From our microarray comparison of *Sox17*-overexpressing LSK48^{+}41^{-} versus normal adult LSK48^{+}41^{-} cells, we have identified 376 significantly upregulated genes and 264 significantly downregulated genes, many of which are involved in HSC maintenance or differentiation. The next important step would be to confirm the physiological relevance of these genes during normal hematopoietic system development by performing a microarray comparison between wild type and *Sox17* deficient fetal liver HSCs, to see whether any of the genes that are upregulated by Sox17 overexpression are also

downregulated after Sox17 deletetion. After that, it would be important to perform CHIP-on-chip or CHIP-seq analysis to identify which genes are likely to be directly regulated by Sox17. Since protein–partner interaction is a crucial mechanism modulating transcriptional activity of the Sox group-F transcription factors (Francois et al., 2010), which include Sox17, it may also be interesting to perform immunoprecipitation of Sox17 coupled with mass spectrometry in *Sox17*-overexpressing bone marrow cells, in order to identify Sox17 protein binding partners.

Using retroviral overexpression, we have shown that Sox17 overexpression can bias adult hematopoiesis to partially resemble fetal liver hematopoiesis; however, it is unclear whether the observed phenotype is due to Sox17 overexpression in HSCs, progenitor cells or terminally differentiated cells. Technically, Sox17 may bias the lymphoid vs. myeloerythroid differentiation of HSCs or MPPs, or it might differentially affect the survival or proliferation of restricted progenitors or differentiated cells. To distinguish between these possibilities, it will be necessary to overexpress Sox17 in each respective cell type. Similarly, it is also unclear what level of Sox17 overexpression is needed to confer the above phenotypes, or whether a transient overexpression (instead of constitutively activated expression) is sufficient to reprogram adult hematopoietic progenitors to a more fetal-like phenotype. All of these questions would require more detailed studies using temporally and/or dosage controllable *Sox17* overexpression.

While Sox17 overexpression is sufficient to confer certain fetal characteristics to adult hematopoietic progenitors, this reprogramming toward fetal HSCs is clearly incomplete, since *Sox17*-overexpressing LSK48^{+}41^{-} cells still express distinct gene sets as compared to both adult and fetal liver HSCs. Therefore, it will be interesting to

determine what other genes are necessary to fully convert adult hematopoietic progenitors into fetal liver HSCs. To begin, we have identified the genes that are specific for fetal liver HSCs, but are not upregulated after *Sox17* overexpression, and we will functionally test whether the overexpression of any of these genes in combination with Sox17 could further reprogram the adult progenitor cells.

IMMORTAL STRAND SEGREGATION IS NOT A UNIVERSAL MECHANISM BY WHICH STEM CELLS MAINTAIN GENOMIC INTEGRITY

Proposed by Cairns thirty year ago (Cairns, 1975) as a mechanism to protect the genomic integrity of stem cells, the "immortal strand" hypothesis postulates that during cell division, adult stem cells could selectively segregate the older DNA strands to daughter stem cells, and the newly synthesized DNA strands from last round of cell division to daughter cells fated to differentiate, therefore minimizing the accumulation of replication-induced DNA damage (reviewed in (Lansdorp, 2007; Rando, 2007; Tajbakhsh, 2008)). In support of the immortal strand hypothesis, asymmetric segregation of old and young DNA strands has been reported in a subset of cells in the crypt of the small intestine (Potten et al., 2002), in cultured neural stem cells (Karpowicz et al., 2005), in mammary gland epithelial cells (Smith, 2005) as well as in muscle satellite cells (Conboy et al., 2007; Shinin et al., 2006); however, limitations in stem cell specific markers in these systems introduced uncertainty about the identity of the cells that segregated chromosomes asymmetrically and the proportion of stem cells capable of doing this. Using one of the best characterized stem cell systems, the mouse hematopoietic stem cells, as a model, we have shown that asymmetric chromosome

segregation does not occur at a significant frequency in HSCs, in contrast to what would be predicted by the immortal strand hypothesis. This result, together with the subsequent finding that hair follicle stem cells also do not asymmetrically segregate their chromosomes during cell division (Sotiropoulou et al., 2008; Waghmare et al., 2008), suggests "immortal strand" segregation does not seem to be a general feature of stem cells, and it may not function to protect cells from accumulating mutations. However, given that asymmetric DNA strand segregation does appear to occur in a subset of cells, it will be important for future studies to determine the precise identity of the cells in which this phenomenon occurs and the biological consequences.

Another important conclusion derived from our study is that BrdU label retention alone cannot be used as a reliable marker for identifying HSCs in situ. In chapter 5, we have shown that after a 10 day pulse of BrdU followed by 70 day chase without BrdU, an experimental strategy used by several prior studies to identify label retaining cells in the bone marrow (Arai et al., 2004; Zhang et al., 2003), only 4.6±0.9% of HSCs are $BrdU^+$ and only 0.08% $BrdU^+$ bone marrow cells are HSCs. Therefore, BrdU label retention alone is not a specific or sensitive marker for HSCs identification, and the vast majority of HSCs do not retain BrdU after 70 days of chase. On the other hand, we did observe that HSCs retain BrdU label better than whole bone marrow cells (4.6±0.9% of HSCs vs. 0.4±0.1% of bone marrow cells were label-retaining) which is consistent with the slower cell cycle rate of HSCs compared with whole bone marrow cells, and does suggest HSCs are enriched in the label retaining bone marrow fraction. However, this enrichment (~10-fold) is does not come close to the level of enrichment required to purify HSCs (more

than 10,000-fold) and is much less than what can be obtained with many cell surface markers.

Nevertheless, our data did not rule out the possibility that a small subset of HSCs may divide even slower than the rest of the HSCs and can therefore better long-term retain BrdU label. In fact, using a "two-population" model which assumes that the HSCs include two cell populations with different cell cycle kinetics instead of the "single population" model which assume all HSCs are cycling at the same rate, we could better fit our experimental data on BrdU label dilution in HSCs with theoretical prediction (unpublished observations). This suggests HSCs are heterogeneous with respect to cell cycle status. In support of this possibility, two recent studies have reported the identification of a more slowly cycling, "dormant" HSC population within the phenotypic HSCs using more detailed analysis of BrdU label dilution kinetic as well as analysis of histone 2B-GFP label retention in HSCs (Foudi et al., 2008; Wilson et al., 2008). Data from both studies have shown that even after long term of chase, the frequencies of BrdU or H2B-GFP label retaining bone marrow cells (0.31% at 1.5 year in Foudi et al study, and 1.1% at 80 days in Wilson et al study) are still 2 orders of magnitude higher than the known frequency of HSCs (~0.003%) (Foudi et al., 2008; Wilson et al., 2008). Thus the data in these studies are consistent with our conclusion that Brdu label retention has poor sensitivity and poor specificity as an HSC marker. Nonetheless, these studies demonstrate that BrdU label retention can be used on concert with other, more powerful, HSC markers to identify a slowly cycling subpopulation of HSCs. Wilson et al went further and concluded that label retaining cells are highly enriched for HSCs, and that BrdU label retention can be used to identify dormant HSCs in situ together with ckit expression, an

assumption unsupported by experimental results. To address this issue definitively, it will be necessary to perform limit dilution analysis to determine the actual frequency of functional HSCs within the ckit^{+} H2B-GFP label retaining cell fraction.

BIBLIOGRAPHY

Arai, F., Hirao, A., Ohmura, M., Sato, H., Matsuoka, S., Takubo, K., Ito, K., Koh, G.Y., and Suda, T. (2004). Tie2/angiopoietin-1 signaling regulates hematopoietic stem cell quiescence in the bone marrow niche. Cell *118*, 149-161.

Bowie, M.B., Kent, D.G., Dykstra, B., McKnight, K.D., McCaffrey, L., Hoodless, P.A., and Eaves, C.J. (2007). Identification of a new intrinsically timed developmental checkpoint that reprograms key hematopoietic stem cell properties. Proc Natl Acad Sci U S A *104*, 5878-5882.

Bowie, M.B., McKnight, K.D., Kent, D.G., McCaffrey, L., Hoodless, P.A., and Eaves, C.J. (2006). Hematopoietic stem cells proliferate until after birth and show a reversible phase-specific engraftment defect. J Clin Invest *116*, 2808-2816.

Bruggeman, S.W., Hulsman, D., Tanger, E., Buckle, T., Blom, M., Zevenhoven, J., van Tellingen, O., and van Lohuizen, M. (2007). Bmi1 controls tumor development in an Ink4a/Arf-independent manner in a mouse model for glioma. Cancer Cell *12*, 328-341.

Bruggeman, S.W., Valk-Lingbeek, M.E., van der Stoop, P.P., Jacobs, J.J., Kieboom, K., Tanger, E., Hulsman, D., Leung, C., Arsenijevic, Y., Marino, S.*, et al.* (2005). Ink4a and Arf differentially affect cell proliferation and neural stem cell self-renewal in Bmi1-deficient mice. Genes Dev *19*, 1438-1443.

Cairns, J. (1975). Mutation selection and the natural history of cancer. Nature *255*, 197-200.

Conboy, M.J., Karasov, A.O., and Rando, T.A. (2007). High incidence of non-random template strand segregation and asymmetric fate determination in dividing stem cells and their progeny. PLoS Biol *5*, e102.

Fasano, C.A., Dimos, J.T., Ivanova, N.B., Lowry, N., Lemischka, I.R., and Temple, S. (2007). shRNA knockdown of Bmi-1 reveals a critical role for p21-Rb pathway in NSC self-renewal during development. Cell Stem Cell *1*, 87-99.

Fasano, C.A., Phoenix, T.N., Kokovay, E., Lowry, N., Elkabetz, Y., Dimos, J.T., Lemischka, I.R., Studer, L., and Temple, S. (2009). Bmi-1 cooperates with Foxg1 to maintain neural stem cell self-renewal in the forebrain. Genes Dev *23*, 561-574.

Foudi, A., Hochedlinger, K., Van Buren, D., Schindler, J.W., Jaenisch, R., Carey, V., and Hock, H. (2008). Analysis of histone 2B-GFP retention reveals slowly cycling hematopoietic stem cells. Nat Biotechnol.

Francois, M., Koopman, P., and Beltrame, M. (2010). SoxF genes: Key players in the development of the cardio-vascular system. Int J Biochem Cell Biol *42*, 445-448.

Hudson, C., Clements, D., Friday, R.V., Stott, D., and Woodland, H.R. (1997). Xsox17alpha and -beta mediate endoderm formation in Xenopus. Cell *91*, 397-405.

Iwama, A., Oguro, H., Negishi, M., Kato, Y., Morita, Y., Tsukui, H., Ema, H., Kamijo, T., Katoh-Fukui, Y., Koseki, H., *et al.* (2004). Enhanced self-renewal of hematopoietic stem cells mediated by the polycomb gene product Bmi-1. Immunity *21*, 843-851.

Kanai-Azuma, M., Kanai, Y., Gad, J.M., Tajima, Y., Taya, C., Kurohmaru, M., Sanai, Y., Yonekawa, H., Yazaki, K., Tam, P.P., *et al.* (2002). Depletion of definitive gut endoderm in Sox17-null mutant mice. Development *129*, 2367-2379.

Karpowicz, P., Morshead, C., Kam, A., Jervis, E., Ramunas, J., Cheng, V., and van der Kooy, D. (2005). Support for the immortal strand hypothesis: neural stem cells partition DNA asymmetrically in vitro. J Cell Biol *170*, 721-732.

Kikuchi, K., and Kondo, M. (2006). Developmental switch of mouse hematopoietic stem cells from fetal to adult type occurs in bone marrow after birth. Proc Natl Acad Sci U S A *103*, 17852-17857.

Kim, I., Saunders, T.L., and Morrison, S.J. (2007). Sox17 dependence distinguishes the transcriptional regulation of fetal from adult hematopoietic stem cells. Cell *130*, 470-483.

Lansdorp, P.M. (2007). Immortal strands? Give me a break. Cell *129*, 1244-1247.

Lessard, J., and Sauvageau, G. (2003). Bmi-1 determines the proliferative capacity of normal and leukaemic stem cells. Nature *423*, 255-260.

Leung, C., Lingbeek, M., Shakhova, O., Liu, J., Tanger, E., Saremaslani, P., Van Lohuizen, M., and Marino, S. (2004). Bmi1 is essential for cerebellar development and is overexpressed in human medulloblastomas. Nature *428*, 337-341.

Liu, J., Cao, L., Chen, J., Song, S., Lee, I.H., Quijano, C., Liu, H., Keyvanfar, K., Chen, H., Cao, L.Y., *et al.* (2009). Bmi1 regulates mitochondrial function and the DNA damage response pathway. Nature *459*, 387-392.

Lowe, S.W., and Sherr, C.J. (2003). Tumor suppression by Ink4a-Arf: progress and puzzles. Current Opinion in Genetics & Development *13*, 77-83.

Matsui, T., Kanai-Azuma, M., Hara, K., Matoba, S., Hiramatsu, R., Kawakami, H., Kurohmaru, M., Koopman, P., and Kanai, Y. (2006). Redundant roles of Sox17 and Sox18 in postnatal angiogenesis in mice. J Cell Sci *119*, 3513-3526.

Mohn, F., Weber, M., Rebhan, M., Roloff, T.C., Richter, J., Stadler, M.B., Bibel, M., and Schubeler, D. (2008). Lineage-specific polycomb targets and de novo DNA methylation define restriction and potential of neuronal progenitors. Mol Cell *30*, 755-766.

Molofsky, A.V., He, S., Bydon, M., Morrison, S.J., and Pardal, R. (2005). Bmi-1 promotes neural stem cell self-renewal and neural development but not mouse growth

and survival by repressing the p16Ink4a and p19Arf senescence pathways. Genes Dev *19*, 1432-1437.

Molofsky, A.V., Pardal, R., Iwashita, T., Park, I.K., Clarke, M.F., and Morrison, S.J. (2003). Bmi-1 dependence distinguishes neural stem cell self-renewal from progenitor proliferation. Nature *425*, 962-967.

Molofsky, A.V., Slutsky, S.G., Joseph, N.M., He, S., Pardal, R., Krishnamurthy, J., Sharpless, N.E., and Morrison, S.J. (2006). Increasing p16INK4a expression decreases forebrain progenitors and neurogenesis during ageing. Nature *443*, 448-452.

Nishino, J., Kim, I., Chada, K., and Morrison, S.J. (2008). Hmga2 promotes neural stem cell self-renewal in young but not old mice by reducing p16Ink4a and p19Arf Expression. Cell *135*, 227-239.

Oguro, H., Iwama, A., Morita, Y., Kamijo, T., van Lohuizen, M., and Nakauchi, H. (2006). Differential impact of Ink4a and Arf on hematopoietic stem cells and their bone marrow microenvironment in Bmi1-deficient mice. The Journal of experimental medicine *203*, 2247-2253.

Oguro, H., Yuan, J., Ichikawa, H., Ikawa, T., Yamazaki, S., Kawamoto, H., Nakauchi, H., and Iwama, A. (2010). Poised lineage specification in multipotential hematopoietic stem and progenitor cells by the polycomb protein Bmi1. Cell Stem Cell *6*, 279-286.

Orford, K.W., and Scadden, D.T. (2008). Deconstructing stem cell self-renewal: genetic insights into cell-cycle regulation. Nat Rev Genet *9*, 115-128.

Park, I.K., Qian, D., Kiel, M., Becker, M.W., Pihalja, M., Weissman, I.L., Morrison, S.J., and Clarke, M.F. (2003). Bmi-1 is required for maintenance of adult self-renewing haematopoietic stem cells. Nature *423*, 302-305.

Pietersen, A.M., Evers, B., Prasad, A.A., Tanger, E., Cornelissen-Steijger, P., Jonkers, J., and van Lohuizen, M. (2008). Bmi1 regulates stem cells and proliferation and differentiation of committed cells in mammary epithelium. Curr Biol *18*, 1094-1099.

Potten, C.S., Owen, G., and Booth, D. (2002). Intestinal stem cells protect their genome by selective segregation of template DNA strands. J Cell Sci *115*, 2381-2388.

Rando, T.A. (2007). The immortal strand hypothesis: segregation and reconstruction. Cell *129*, 1239-1243.

Salomoni, P., and Calegari, F. (2010). Cell cycle control of mammalian neural stem cells: putting a speed limit on G1. Trends Cell Biol *20*, 233-243.

Sherr, C.J., and DePinho, R.A. (2000). Cellular senescence: mitotic clock or culture shock? Cell *102*, 407-410.

Shinin, V., Gayraud-Morel, B., Gomes, D., and Tajbakhsh, S. (2006). Asymmetric division and cosegregation of template DNA strands in adult muscle satellite cells. Nat Cell Biol *8*, 677-687.

Smith, G.H. (2005). Label-retaining epithelial cells in mouse mammary gland divide asymmetrically and retain their template DNA strands. Development *132*, 681-687.

Sotiropoulou, P.A., Candi, A., and Blanpain, C. (2008). The majority of multipotent epidermal stem cells do not protect their genome by asymmetrical chromosome segregation. Stem Cells *26*, 2964-2973.

Tajbakhsh, S. (2008). Stem cell identity and template DNA strand segregation. Curr Opin Cell Biol *20*, 716-722.

van der Lugt, N.M., Alkema, M., Berns, A., and Deschamps, J. (1996). The Polycomb-group homolog Bmi-1 is a regulator of murine Hox gene expression. Mechanisms of development *58*, 153-164.

van der Lugt, N.M., Domen, J., Linders, K., van Roon, M., Robanus-Maandag, E., te Riele, H., van der Valk, M., Deschamps, J., Sofroniew, M., van Lohuizen, M.*, et al.* (1994). Posterior transformation, neurological abnormalities, and severe hematopoietic defects in mice with a targeted deletion of the bmi-1 proto-oncogene. Genes Dev *8*, 757-769.

Waghmare, S.K., Bansal, R., Lee, J., Zhang, Y.V., McDermitt, D.J., and Tumbar, T. (2008). Quantitative proliferation dynamics and random chromosome segregation of hair follicle stem cells. EMBO J *27*, 1309-1320.

Wilson, A., Laurenti, E., Oser, G., van der Wath, R.C., Blanco-Bose, W., Jaworski, M., Offner, S., Dunant, C.F., Eshkind, L., Bockamp, E.*, et al.* (2008). Hematopoietic Stem Cells Reversibly Switch from Dormancy to Self-Renewal during Homeostasis and Repair. Cell.

Zencak, D., Lingbeek, M., Kostic, C., Tekaya, M., Tanger, E., Hornfeld, D., Jaquet, M., Munier, F.L., Schorderet, D.F., van Lohuizen, M.*, et al.* (2005). Bmi1 loss produces an increase in astroglial cells and a decrease in neural stem cell population and proliferation. J Neurosci *25*, 5774-5783.

Zhang, J., Niu, C., Ye, L., Huang, H., He, X., Tong, W.G., Ross, J., Haug, J., Johnson, T., Feng, J.Q.*, et al.* (2003). Identification of the haematopoietic stem cell niche and control of the niche size. Nature *425*, 836-841.